Understanding Glycans and Glycosidases in Infection and Biofilm Formation as a Route to Novel Antimicrobials

By:

Raphael Peter Galleh

A thesis submitted for the degree of
Doctor of Philosophy

The University of Sheffield
School of Clinical Dentistry
Unit of Oral and Maxillofacial Pathology
(Microbiology and Immunology)

March 2023

Table of Contents

Appendices

II   List of Figures

Acknowledgments

Research Group members and all other PhD students in Room E14 (3rd Floor). You all have made my PhD journey a memorable one.

Dedication

I dedicated this work to the glory of God and to my lovely late Parents Mr. Peter Akku Alogoakho Galleh and Mrs. Lucy Agbumbugu Peter Galleh. Although dead, your spiritual presence and contributions towards making me the man I am today cannot be overemphasised. Thank you so much for all the sacrifices.

Abbreviations

®	Trade mark
α	Alpha
β	Beta
γ	Gamma
μ	Micro
μL	Microlitre
Amp	Ampicillin
BHI	Brain heart infusion
BSA	Bovine serum albumin
BSM	Bovine submaxillary mucin
°C	Centigrade

cDNA	Complementary Deoxyribonucleic Acid
CO2	Carbon dioxide
CPS	Capsular polysaccharide
DANA	2-deoxy-2,3-dehydro-N-acetylneuraminic acid
dH2O	Distilled water
DMEM	Dulbecco's Modified Eagle's Medium
DNA	Deoxyribonucleic acid
FA	Fastidious anaerobe
FBS	Foetal bovine serum
g	Gram (in the context of mass)
Glc	Glucose
GlcNac	N-acetylglucosamine
GCF	Gingival crevicular fluid
IFN	Interferons
IL	Interluekin
LPS	Lipopolysaccharide
L	Litre
M	Molar
ManNac	N-acetylmannosamine
mL	Millilitre
mM	Millimolar
MoI	Multiplicity of Infection
mRNA	Messenger ribonucleic Acid
nM	Nanomolar
NAM	N-acetylmuramic acid
Neu5,9Ac	5-N, 9-O-acetylneuraminic acid
Neu5Ac	5-N-acetylneuraminic acid
NeuGc	N-glycolylneuraminic acid
OD	Optical density
PAGE	Poly acrylamide gel electrophoresis
PAMPs	Pathogen-associated molecular patterns
PBS	Phosphate buffered saline
PCR	Polymerase Chain Reaction
PMNs	Polymorphonuclear cells
qPCR	Quantitative polymerase chain reaction
RNA	Ribonucleic acid
RNase	Ribonuclease
RT-PCR	Reverse transcriptase-Polymerase chain reaction
SOCC	Squamous oral carcinoma cells
SD	Standard Deviation
SDS	Sodium dodecyl sulphate
SFM	Serum free medium
TEMED	Tetramethylethylenediamine
TSB	Tryptic soy broth
TGF-β	Transforming growth factor-beta
TNF	Tumour necrosis factor
TLRs	Toll-like receptors
v/v	Concentration, volume by volume
w/v	Concentration, weight by volume

Abstract

Periodontitis is a chronic bacterially induced disease characterized by inflammation of the gingivae and subsequent destruction of the tissues and supporting structures of the periodontium, which can lead to tooth loss. The red complex pathobionts: *Porphyromonas gingivalis* and *Tannerella forsythia* are mostly associated with periodontitis and are shown to modulate the host's innate immune system. These oral pathogens secrete sialidase enzymes that they use to scavenge sialic acids found at the terminus of host glycoprotein chains for nutrition or to evade host immune responses. Activities of these pathogens, therefore, poses a problem to public health as such, necessitates the need to carry out research aimed at understanding this important enzyme as a route for the development of novel inhibitors of periodontitis and other immune-modulatory diseases.

Over-expressed *P. gingivalis* (SiaPG) and *T. forsythia* (NanH) sialidase enzymes were purified using HisTag low-affinity chromatography, and the sialidase activity was tested using 4-methylumbelliferyl *N*-acetyl-α-D-neuraminic acid sodium salt (MUNANA), as substrate.

Inhibition studies using whole cells and the purified sialidases of *T. forsythia* (NanH) and *P. gingivalis* (SiaPg), showed ECG as the best plant-derived inhibitor, while 2e3aDFNeu5Ac9N3 as the most potent of all the screened compounds. Additionally, Palmatine and Berberine chloride synergistically inhibited almost a 100 % NanH sialidase activity, with mechanisms of action (MOA) showing Palmatine, Berberine chloride, and 2e3aDFNeu5Ac9N3, as non-competitive, uncompetitive and competitive inhibitors of NanH sialidase, respectively.

Furthermore, sialidase promotes the growth of *P. gingivalis* and *T. forsythia*, and supports host-pathogen interactions via adhesion and invasion of oral epithelial cells (H357). In addition, the role of *P. gingivalis* and *T. forsythia* sialidases on host innate immune modulation in the presence or absence of 2e3aDFNeu5Ac9N3 was also assessed using flow cytometry. NanH sialidase of *T. forsythia* appears to upregulate the secretion of pro-inflammatory cytokines such as interleukin-6 (IL-6), IL-8, and IL1-β in the cell supernatants, which was abrogated significantly by 2e3aDFNeu5Ac9N3 with minimal cytotoxic effects on the oral epithelial cells. Also, molecular docking of several inhibitors into the active-site pockets of NanH-apo and SiaPg using AutoDock Vina and PyMol suggested that Oseltamivir, Siastatin B, DANA, and 2e3aDFNeu5Ac9N3 coordinate the arginine triad (Arg423, Arg487, Arg212 and Arg194, Arg213, Arg460), of NanH and SIaPg of *T. forsythia* and *P. gingivalis*, respectively. Also, the nucleophilic dyad tyrosine and glutamate interact with the anomeric carbon as well as the acid/base aspartate residue Asp237/Asp280 interacting with the *N*-acetyl group of respective inhibitors. The superior inhibitory properties of 2e3aDFNeu5Ac9N3 on both the purified and whole cell sialidase activities of *P. gingivalis* and *T. forsythia* make it a promising compound, and can further be developed as a novel immunomodulatory agent of periodontitis or other inflammatory diseases.

Keywords:

Periodontitis, *Tannerella forsythia*, *Porphyromonas gingivalis*, Sialidases, Sialic acid Pro-inflammatory cytokines, 2e3aDFNeu5Ac9N3, Molecular docking, Arginine triad

CHAPTER ONE
Introduction and Literature Review

1.1 Major Diseases of the Oral Cavity

The oral cavity is comprised of six major niches namely; (1) intra-oral, supragingival, and hard surfaces (teeth, prosthesis, implants), (2) subgingival regions adjacent to hard surfaces comprising periodontal or peri-implant pockets, (3) the buccal, palatal epithelium and the epithelium of the floor of the mouth, (4) the tongue dorsum, (5) tonsils, and (6) the saliva. The oral cavity has a diverse ecology with each zone composed of a different microbiome (Xu *et al.*, 2018). There are over 700 bacterial species found in the oral cavity, of which more than halve are yet to be cultivated (Aas *et al.*, 2005; Douglas *et al.*, 2014). Specific oral pathogens have been reported to be linked to several systemic diseases: cardiovascular disease, preterm low birth weight, bacterial endocarditis, diabetes, osteomyelitis, cancer, and aspiration pneumonia (Buduneli *et al.*, 2005).

The main oral diseases affecting humans are discussed in the sub-sections below and these include dental caries, periapical abscesses, root canal infections, reversible gingivitis, and periodontitis, which is irreversible.

1.1.1   Dental Caries

Dental caries are caused by many factors that can lead to the demineralization of teeth, and the creation of cavities in the tooth structure thereby compromising the structure and creating bad oral health (Featherstone, 2008). The Gram-positive facultative anaerobe *Streptococcus mutans* is one of the major contributors to dental caries. This organism ferments carbohydrates found in the mouth thereby producing organic acids that interfere with the tooth surfaces (Featherstone, 2008; Struzycka, 2014 and Lamont and England, 2014).

Dental caries are said to be the most common acute disease among children after the common cold, thereby posing a concern for oral health globally (Krol and Nedley,

2007). Also, it was reported to be the most prevalent condition for the decay of permanent teeth (Pandolfo *et al.*, 2013; WHO, 2017).

Although dental caries are the commonest dental disease, fluoride has been shown to be effective in the prevention of this condition. Fluoride works by improving and remineralizing the early stages of caries and inhibiting demineralization of the tooth as such preventing dental decay (Clark and Slayton, 2014; Ten Cate, 2013).

1.1.2 Gingivitis

Although gingivitis is the inflammation of the gingiva, it is a non-destructive reversible form of dental disease (Wiebe and Putnins, 2000). Plaque-induced gingivitis is the most common form of periodontal disease which occurs in response to factors such as bacterial plaque formed on the tooth surfaces (Paddick *et al.*, 2005. This plaque-induced gum disease has been reported to significantly affect about 15-20% of the world's population (Wiebe and Putnins, 2000; Paddick *et al.*, 2005; Eke *et al.*, 2012).

1.1.3 Periodontitis

Periodontitis is defined as a chronic disease of the periodontium caused mainly by a complex microbial consortium capable of gradual colonization of the tooth surfaces in the gingival cavities (Socransky *et al.*, 1998). Unlike gingivitis which can be reversed, periodontitis is an irreversible bacterially-induced disease that is characterized by inflammation of the gingiva and subsequent destruction of supporting structures surrounding the teeth. The gingivae of patients become swollen, red, and may bleed, surrounding bones may be lost, the periodontium can pull away from the tooth creating periodontal pockets, and the patient may lose his/her teeth (Socransky *et al.*, 1998) (Figure 1.1).

Periodontitis is reported to affect 64.7 million of the U.S. adult population (Eke *et al.*, 2012). Almost half of the adults in the UK are reported to have a degree of periodontitis that is not reversible (UKHSA, 2021). Periodontal disease is more prevalent in adults aged between 20-64 years also amongst smokers, those with lower incomes or less education, and Black and Hispanic adults (Eke and Genco, 2007; Kornman, 2008; Eke *et al.*, 2012 and Sochalska and Potempa, 2017).

2
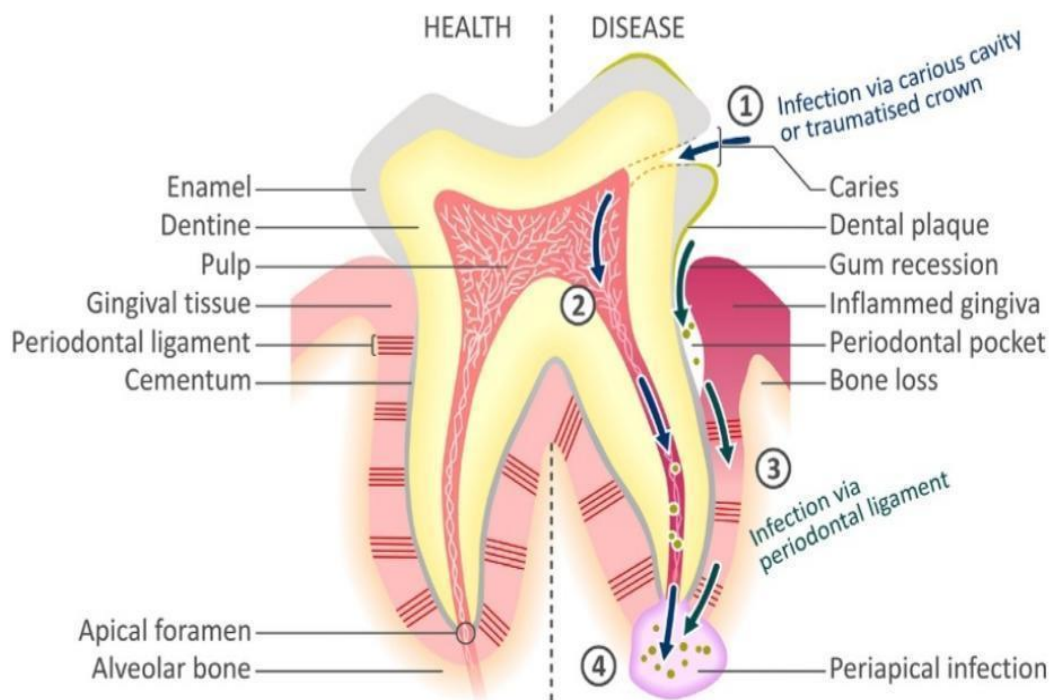
Figure 1.1. Representation of the main features and structures of healthy and diseased teeth

Summary of the main dental diseases: caries, pulp/periapical, and periodontal infections. 1-4 represents the bacterial points of entry and various diseased conditions leading to periapical infection and subsequent alveolar bone loss. 1: Infections via carious cavity, 2: infection via the destruction of pulp tissue, 3: Infection via periodontal ligament and 4: Periapical infection such as root canal. Reproduced from (Douglas et al., 2014) "Advances in Microbial Physiology, Chapter 6: Physiological Adaptations of Key Oral Bacteria" (2014), volume 65, with permission from Elsevier, licence Number 4761330132412.

1.2 Microbial Aetiology of Periodontitis

The characterization of oral microflora, as well as microbial aetiology of periodontal diseases, can be traced back to Antonie Van Leeuwenhoek's famous experiment observed from his own gingival plaque tagged "tiny animalcules" where he saw a community of microorganisms that includes motile rods, needle-like long rods, and cocci (Theilade *et al., 1966*). However, in the mid-1960's, Loe and colleagues demonstrated in their classic study of gingivitis that the bacterial flora shifts from a mostly Gram-positive (healthy mouth) to Gram-negative facultative anaerobes (diseased mouth), illustrating a shift in the oral microbiome that is now termed "dysbiosis" which correlates with periodontitis and gingivitis (Theilade *et al., 1966* and Lamont et al., 2018). Although bacteria are the major causative agents, the host immune response is also shown to be the reason for inflammation in periodontitis (Theilade *et al., 1966* and Cekici *et al., 2014*).

1.2.1   Bacterial Colonisation of the Periodontium

The oral cavity is a dynamic ecosystem with diverse species of microbiota that keep changing due to varying conditions such as temperature, nutrient availability and pH. The periodontium of humans is coated with a plethora of bacteria that are implicated in causing dental diseases such as gingivitis and periodontitis (Aas *et al.*, 2005). More than 700 different bacterial species are reported to reside in the oral cavity, of which over 50 % are yet to be cultured however, techniques such as electron microscopy, 16S rRNA genes sequencing, culture-based methods, qPCR, and other molecular-based diagnostic methods provide a comprehensive overview of how different sites of the periodontium are colonised by different microorganisms (Keijser *et al.*, 2008).

The diverse conditions of the mouth promote the survival of distinct microbial complexes, such as biofilm formation on the supragingival and subgingival region as well as tongue coating. The environmental conditions of each site in the oral cavity determine the microbial occupants of such sites (Socransky *et al.*, 1998). The tooth surfaces are continually coated with salivary protein which leads to the formation of thin films called pellicles in supragingival plaque (Takahashi, 2005). These pellicles support the attachment of Gram-positive cocci, referred to as "the early colonisers" (Takahashi, 2005). As the colonisation progresses, "intermediate colonisers", including

the streptococci are seen to form most parts of the biofilm (Takahashi, 2005). Different positions in the oral cavity were reported to determine the components of the dental biofilm; for instance, the plaque adjacent to the tooth is more anaerobic as compared to the external surfaces due to environmental conditions and microbial activities such as the metabolism of nitrogenous compounds derived from the gingival crevicular fluid (GCF) by asaccharolytic microorganisms which further creates a neutral pH and an anaerobic environment (Takahashi, 2005). Also, changes in environmental conditions have been seen to support the proliferation of "late colonisers", as well as the introduction of pathogenic microorganisms associated with periodontitis (Takahashi, 2005).

In subgingival sites however, microorganisms such as *Fusobacteria, Treponema,* and *Prevotella* utilise compounds found in the gingival crevicular fluid (GCF) thereby creating an anaerobic environment with neutral pH (Mira et al., 2017). This neutral pH environment is favourable for their proteolytic activities and facilitates the colonisation of the periodontium by more periodontopathogenic bacteria such as *Treponema denticola*, *Porphyromonas gingivalis* and *Tannerella forsythia* (previously referred to as *Tannerella forsythensis* and *Bacteroides forsythus*) (Socransky *et al.*, 1998 and Takahashi, 2005).

Investigations such as that conducted by Socransky and colleagues (1998) from a large patient cohort have established six different but closely related bacterial complexes that exist in the subgingival plaque (Figure 1.2) (Socransky *et al.*, 1998). These include the early colonizers are the "Blue complex" consisting of *Actinomyces species*, the "Yellow complex" which are low-risk organisms comprising various *Streptococci*, the "Green complex" comprising *Eiknella corrodens* and *Capnocytophaga species*, and the "Purple complex" comprising *Veillonella parvula* and *Actinomyces odontolyticus*. The late colonizers are the "Orange complex" (moderate risk) comprising *Prevotella, Fusobacterium, Campylobacter*, and other bacteria and lastly, the "Red complex" (high risk) chiefly consisting of *P. gingivalis, T. forsythia,* and *T. denticola* which are associated with chronic periodontitis as a result of dysbiosis (Sukhvinder Singh et al., 2021).

The amount of periodontal microbial complexes in the oral cavity differs between disease and health, with orange and red complex organisms being linked with more

severe dental disease (Socransky *et al.*, 1998). Furthermore, dysbiosis was shown to be linked to oral diseases such as periodontitis and even conditions like inflammatory gastro-intestinal (GI) diseases (Sochalska and Potempa, 2017). Although other factors play roles in modulating microbial shifts and inflammation, dysbiosis and the resulting inflammation is believed to be the major cause of periodontitis (Sochalska and Potempa, 2017).
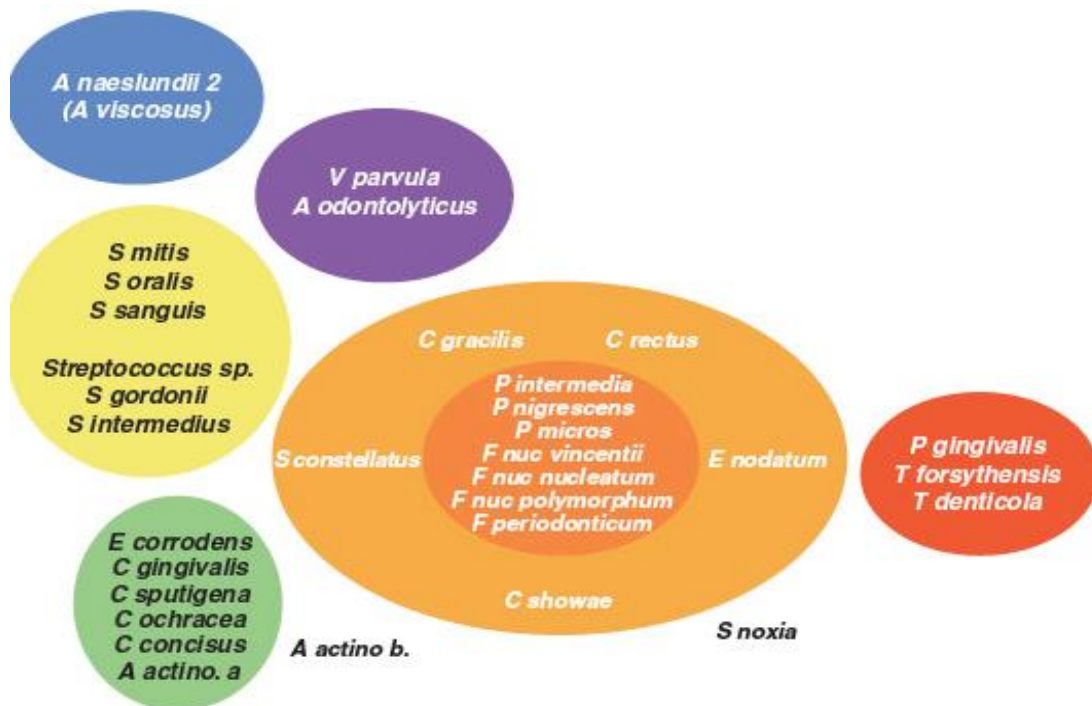
Figure 1.2: Different microbial complexes in the subgingival plaques

Bacterial complexes that exist in the subgingival plaque categorised into "Blue complex", "Yellow complex", "Green complex", "Purple complex", "Orange complex" and the "Red complex", based on their composition and risk level. Proposed by Dwyer DM, Socransky SS. (1968), and reviewed by (Sukhvinder Singh et al., 2021).

1.3 Periodontitis and Systemic Diseases

1.3.1 Atherosclerotic Cardiovascular Diseases

Cardiovascular diseases such as myocardial infarction and atherosclerosis occur in most cases as an outcome of a complex set of environmental and genetic factors (Bourgeois et al., 2019). The environmental risk factors include but are not restricted to; exercise stress, smoking, nonsteroidal anti-inflammatory drugs, type of diet as well as chronic infection. The genetic factors comprise age, hypertension, lipid metabolism, obesity, diabetes, levels, platelet-specific antigen Zwb (P1A2) polymorphism and increased fibrinogen (Li et al., 2000). Periodontal disease is shown to predispose persons to cardiovascular disease, through the involvement of the large number of Gram-negative species involved, the white blood cell (WBC) counts, levels of proinflammatory cytokines present, the association of high peripheral fibrinogen, the heavy immune and inflammatory infiltrates involved (Li *et al.*, 2000).

1.3.2 Rheumatoid Arthritis

This chronic inflammatory autoimmune disease, is characterised by a significant synovial inflammation, which leads to tissue degeneration. (Ellamurugan, 2013 and Sudhakara et al., 2019). Research outcome has shown a strong corelation between the extent and severity of rheumatoid arthritis (RA) and periodontitis (Ellamurugan, 2013). Although this relationship is unlikely to be causal, people living with advanced rheumatoid arthritis experienced periodontal problems more frequently as compared to non-rheumatoid arthritis individuals. Both RA and periodontal diseases manifest due to the imbalance between anti-inflammatory and pro-inflammatory cytokines (Ellamurugan, 2013).

Additionally, previous research using mouse models has shown that periodontopathogens such as *P. gingivalis* influences the progression of rheumatoid arthritis (RA) (Mikuls *et al.*, 2014 and Yamaguchi *et al.*, 2016). In addition, wild type strain of *P. gingivalis* has been shown to mediate citrullination of host fibrinogen protein, which provides a molecular mechanism for generating antigens that drive the autoimmune response in rheumatoid arthritis. An attribute shown to be lacking in mutant strain of *P. gingivalis* (ΔPADs), in which the enzyme peptidylarginine deiminases has been deleted as well as in other oral pathogens (Wegner *et al*., 2010).

1.3.3 Diabetes Mellitus

Diabetes mellitus is a disease condition characterised by hyperglycemia caused by an absolute or decreased sensitivity to insulin (Li et al., 2000). Signs and symptoms of diabetes involve metabolic abnormalities and long-term complications of the kidneys, eyes, nervous system, periodontium and vasculature (Li et al., 2000). Research also revealed that increased severity of type II diabetes mellitus is linked to chronic periodontal disease (Li *et al.*, 2000). In addition, diabetic individuals are more likely to develop periodontitis as compared to the nondiabetic counterparts (Grossi and Genco, 1998 and Li *et al.*, 2000).

1.3.4 Bacterial Pneumonia

Bacterial pneumonia and chronic obstructive pulmonary disease (COPD), have also been reported to be associated with periodontal disease. These infections can be life threatening especially amongst immunocompromised individuals including aged persons (Li *et al.*, 2000 and Kim et al., 2018). Some common pathogens implicated in causing oral diseases such as *Streptococcus mitis*, *Staphylococcus aureus*, *Candida albicans*, *T. forsythia*, *P. gingivalis* and *T. denticola* as well as other pathogens that reside on the oropharyngeal mucosa, like *Haemophilus influenza*, *Aaggregatibacter actinomycetemcomitans*, *Mycoplasma pneumoniae*, *Streptococcus pneumoniae* and even Fusobacterium species can contaminate the lower respiratory epithelium which may lead to COPD (Scannapieco & Genco, 1999).

1.4 Periodontal Pathogens and their Virulence Factors

The direct effects of the virulence factors of periodontal pathogens on host tissues promote the progression of periodontitis and the self-damaging of the host immune responses to the colonising bacteria (Socransky *et al.*, 1998; Sharma, 2010 and Mysak *et al.*, 2014). Of the three red-complex organisms, *P. gingivalis* and *T. forsythia* are the major focus of this research.

1.4.1 *Porphyromonas gingivalis*

P. gingivalis is a non-motile Gram-negative, black-pigmented, asaccharolytic oral anaerobe that requires hemin and vitamin K in its nutrient for growth (How et al., 2016). It is considered one of the most important pathogens associated with periodontitis; a periodontal disease that leads to eventual tooth loss (Bostanci and Belibasakis, 2012).

P. gingivalis has employed both evasive and invasive strategies of harming the host by evading the host's immune responses coupled with its virulence factors such as; capsule, lipopolysaccharide (LPS), fimbriae and gingipains (arginine/lysine proteases). *P. gingivalis* role as a 'keystone pathogen' in leading a host response to inflammatory disease by remodelling a normally benign microbiota into a dysbiotic one has also been reported (Hajishengallis, Darveau and Curtis, 2012).

1.4.1.1 The Lipopolysaccharide (LPS) of *Porphyromonas gingivalis*

The outer membrane of Gram-negative bacteria is made up of large molecules consisting of a lipid and a polysaccharide that are bacterial toxins referred to as Lipopolysaccharides (LPS). Bacterial LPS is composed of an O-antigen, an outer core, and an inner core all joined via a covalent bond (figure 1.3). *P. gingivalis* is known to produce different lipopolysaccharide isoforms with a range of structural variations of their lipid A and O-antigen moieties shown to affect its pro-inflammatory and bone-resorbing ability (Zaric et al., 2017). Additionally, findings on the effect of two isoforms of *P. gingivalis* LPS (PgLPS) tetra- (Pg LPS1435), and penta-acylated (PgLPS 1690) lipid A on the human gingival epithelium, showed that penta-acylated PgLPS 1690 upregulated the secretion of proinflammatory cytokines: IL-1β, IL-6, IL-8 and TNF-α, compared to tetra-acylated PgLPS1435 thereby modulating the innate immune response of the host (Herath et al., 2011).

Holt *et al.,* also reported the interaction between *P. gingivalis* LPS with Toll-like receptor 2 (TLR-2) leading to inflammation and cytokine expression and thereby playing a major role in the pathogenesis of periodontal disease (Holt *et al.*, 1999).
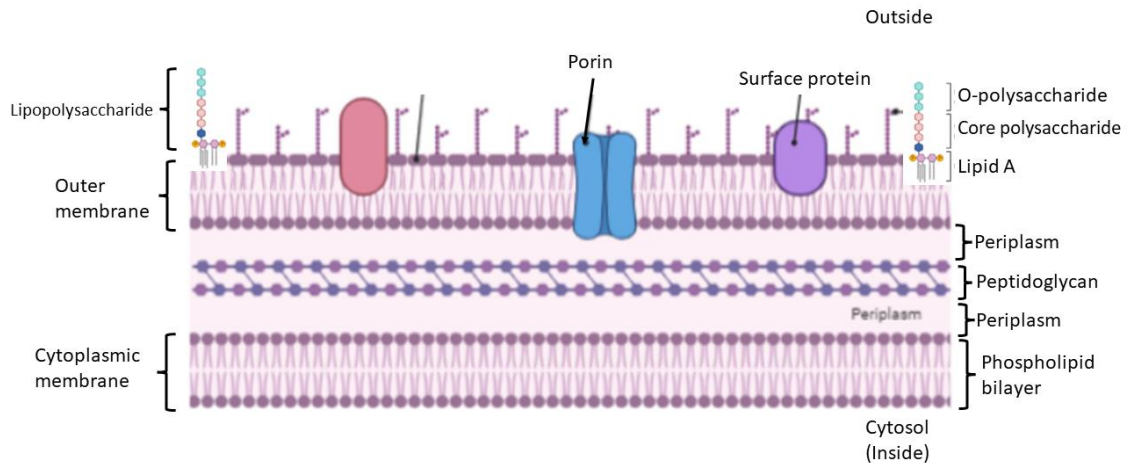
Figure 1.3: Cell surface structure of Gram-negative bacteria (Created in BioRender.com):

The cell wall of a Gram-negative bacteria such as *P. gingivalis* contains several structures such as the lipopolysaccharide (LPS) which comprises lipid A, core (inner/outer) polysaccharide, and the O-antigen (polysaacharide)

1.4.1.2 The Capsule (CPS) of *Porphyromonas gingivalis*

The capsule also known as K-antigen or CPS is considered one of the major virulence factors of *P. gingivalis* functions by 'covering' other surface antigens away from the effect of host adaptive immune response, or complement deposition (Bostanci & Belibasakis, 2012) (figure 1.4).

Non-encapsulated knockout mutant strains of *P. gingivalis* have been observed in a mouse abscess model to be more virulent than the encapsulated strains (Brunner et al., 2010). Also, the non-encapsulated strains were found to be more potent cytokine inducers (IL-1beta, IL-6, IL-8, TNF-α, and IFN-γ) synthesis by human gingival fibroblasts, when compared with the corresponding wild-type strain, signifying the role of capsule in downplaying the innate immune responses (Brunner et al., 2010). This, therefore, suggest that the CPS of *P. gingivalis* acts as an interface between the pathogen and the host which may reduce the host's proinflammatory immune responses. This may be the reason for the high virulence of encapsulated strains which enables the bacteria to elude the host immune system (Brunner *et al.*, 2010).

1.4.1.3 The Fimbriae of *Porphyromonas gingivalis*

Fimbriae (figure 1.4), of Gram-negative organisms like *P. gingivalis* are tiny protrusions supporting its adherence to salivary pellicle-coated tooth surfaces, epithelial mucosa, eukaryotic cells, and bacteria of different or same species thereby participating in the development of polymicrobial biofilm structure (Bostanci and Belibasakis, 2012). Major and minor fimbriae also referred to as long and short are the two main fimbria-molecules known to be expressed by *P. gingivalis*, both of which were shown to mediate bacterial interactions with and invasion of host tissues, thereby promoting the pathogenesis of periodontitis (Jotwani et al., 2010). Additionally, major and minor *P. gingivalis* fimbriae reportedly induce the expression of cytokines such as IL-1α, IL-β, IL-6, and TNF-α, which result in alveolar bone resorption (Enersen et al., 2013). Furthermore, the short fimbria of *P. gingivalis* was shown to strongly interact with TLR2, and CD14 and induced pro-inflammatory cytokine expressions in both human monocytes and mouse macrophages (Hiramine *et al*., 2003 and Enersen et al., 2013).
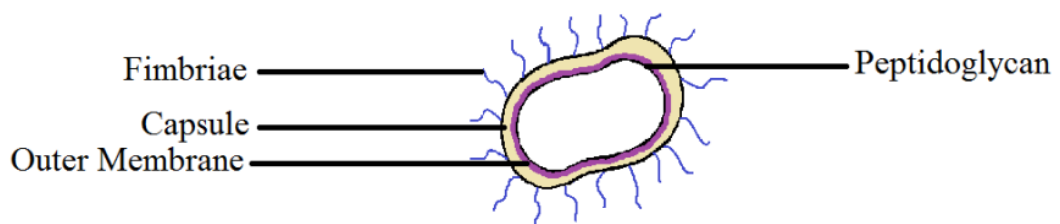
Figure 1.4: Capsule and fimbriae on the bacterial cell surface of Gram-negative bacteria

Gram-negative bacteria like *P. gingivalis* use tiny protrusions called fimbriae to support their adherence to salivary pellicle-coated tooth surfaces, epithelial mucosa, eukaryotic cells, or other bacterial cells of different or same species

1.4.1.4 The Gingipains of *Porphyromonas gingivalis*

Gingipains are defined as a group of trypsin-like cell surface proteolytic enzymes 'cysteine proteinases' either Arginine-specific (RgpA and RgpB) or Lysine-specific (Kgp) expressed by *P. gingivalis* which may also be present in secreted soluble form (Kariu et al., 2017). Thus, gingipains mediate the adherence of the pathogen to different regions of the oral cavity by acting as non-fimbrial adhesions or enabling the assembly of fimbriae and are thought to be important contributors to the virulent nature of *P. gingivalis* (Bostanci and Belibasakis, 2012; Bao *et al.*, 2014; Guo, Nguyen and Potempa, 2010 and Kariu et al., 2017).

Gingipains have also been reported to trigger the production of interleukin-6 (IL-6) in oral epithelial cells, and IL-8 production by gingival fibroblasts, thereby enhancing the host inflammatory responses (Lourbakos *et al.*, 2001 and Oido-Mori *et al.*, 2001). Nonetheless, gingipains can also proteolytically inactivate both anti-inflammatory (IL-4, IL-5) and pro-inflammatory (IL-12, IFN-c) cytokines (Yun, DeCarlo and Hunter, 1999 and Srisatjaluk *et al.*, 2002). Stafford and colleagues also reported in their findings that during invasion, gingipains affect the signalling pathways in oral epithelial cells intracellularly, by degrading the mammalian target of rapamycin (mTOR), thereby seen as the main mechanism to which *P. gingivalis* uses in inducing autophagy or changes to the lifecycle of the host-cell (Stafford *et al.*, 2013).

1.4.1.5 The Sialidase of *Porphyromonas gingivalis* (SiaPg)

P. gingivalis has been reported to express sialidase (neuraminidase), an enzyme used by pathogenic organisms to cleave sialic acid found at the reducing terminus of host glycoprotein chains, thereby contributing to colonisation, persistence and disease progression (Frey et al., 2019). The sialidase encoded by *P. gingivalis* (PG0352) has been shown to improve biofilm formation, capsule biosynthesis and pathogenicity as compared to its sialidase-deficient strain (ΔPG352) which produced less biofilm, less intact capsule and showed less resistance to killing by host complement (Li et al., 2012). Furthermore, sialidase of *P. gingivalis* was reported to support the attachment to and invasion of oral epithelial cells as well as to induce the expression of cytokines such as IL-6 and IL-8 (Frey et al., 2019). Lastly, the sialidase activity of *P. gingivalis* is

suggested to be involved in the regulation of gingipain activity and other virulence factors (Aruni et al., 2011).

1.4.2 *Tannerella forsythia*

T. forsythia formerly called "*Bacteroides forsythus*" (Tanner *et al.*, 2009), is an anaerobic, non-pigmented, Gram-negative oral bacterium belonging to the *Cytophaga–Bacteroides* family which was later reclassified by Sakamoto *et al.,* based on 16S rRNA phylogenetic analysis as *Tannerella forsythia* (Sakamoto *et al.*, 2002). *T. forsythia* is seen more often associating at a later stage with other organisms in various forms of periodontal diseases, such as gingivitis, aggressive and chronic periodontitis, than witnessed in healthy individuals (Tanner and Izard, 2006).

The fastidious growth conditions of *T. forsythia* have made it receive less attention, as such, remained understudied despite several pieces of evidence showing its involvement in the pathogenesis of periodontitis (Ruscitto et al., 2016). However, exogenous *N*-acetylmuramic acid (NAM, one of the two monomer amino sugars in peptidoglycan), was discovered to be a major requirement needed by *T. forsythia* in monoculture growth (Ruscitto et al., 2016). Also, it was shown that sialic acid, sialyllactose and glycolyl sialic acid, which are common sugar moieties on a range of important host glycoproteins, stimulate biofilm growth of *T. forsythia* (Roy *et al.*, 2011 and Stafford *et al.*, 2012).

Previously identified putative virulence factors of *T. forsythia* include: the sialidases SiaH and NanH, a leucine-rich repeat cell-surface-associated and Bacteroides secreted protein (BspA), trypsin-like and PrtH (also called "forsythia detaching factor" (FDF)) proteases, α-D-glucosidase and *N*-acetyl-β-glucosaminidase, a hemagglutinin, components of the bacterial glycosylated surface layer (S-layer) (Sharma *et al.*, 1998; Sabet *et al.*, 2003 and Sharma *et al.*, 2005). Additionally, β-hexosaminidase has been shown to utilise the β-linked glucosamine or galactosamine residue thereby contributing to biofilm formation, an ability reported to be carried out by *T. forsythia* (Roy et al., 2012). Interestingly also, fucose which is often found exposed on various host glycoconjugates has been shown to be cleaved by α-L-fucosidases of *T. forsythia* ATCC 43037 which also promote biofilm formation, adhesion, and invasion of host epithelial cells by this oral pathogen (Megson et al., 2015).

1.4.2.1 Surface-layer Associated Glycoprotein of *T. forsythia*

Many bacteria have an extracellular proteinaceous layer that surrounds their cell wall or cell membranes, often referred to as the S-layer (Tomek et al., 2018). In *T. forsythia,* the surface of the pathogen is densely glycosylated with complex decasaccharide shown to be O-glycosidically linked to its abundant surface layer (S-layer) and other proteins (figure 1.5) (Tomek et al., 2018). Additionally, the S-layer of *T. forsythia* is shown to comprise of a two-dimensional crystalline surface layer having serrated structural subunits (approximately 10 nm wide and 10nm high) in either oblique or tetragonal lattices which lack surface appendages such as fimbriae (Kerosuo *et al.*, 1990 and Posch *et al.*, 2011). The S-layer was reported to consist of at least two high-molecular-weight glycoproteins with *O*-linked oligosaccharides of 220 and 210 kDa encoded by the *tfsA* and *tfsB* genes, respectively (Lee *et al.*, 2006 and Chinthamani *et al.*, 2017). Other specific S-layer glycans seen in the *T. forsythia O*-glycan are α-L-fucose (Fuc), *N*-acetyl mannosaminuronic acid (ManNAcA), and *N*-acetyl mannosaminuronamide (ManNAcCONH$_2$) (Posch et al., 2011) (Figure 1.5).

The strong antigenic S-layer *O*-glycan of this bacterium has been reported to mediate hemagglutination, attachment and invasion of host epithelial cells (Sabet *et al.*, 2003 and Sakakibara et al., 2007), evade recognition by host innate immune system (Sekot et al., 2011), as well as host immune modulation via the action of suppressing T-helper (Th)17 responses (Settem et al., 2013). In addition to its involvement in the above immunological importance, studies have also suggested the involvement of O-glycosylated S-layer of *T. forsythia* in biofilm formation (Honma *et al.*, 2007).

Furthermore, increase in the viability of macrophages which resulted in rapid expression of pro-inflammatory cytokines (IL-1β and TNF-α), was reported in S-layer deficient mutants as compared to the parent strain of *T. forsythia* showing that S-layer has an important role in redirecting or even delaying the innate immune response (Chinthamani et al., 2017).
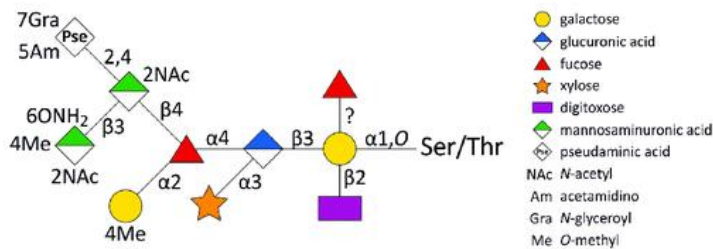
Figure 1.5: Schematic representation of the *T. forsythia* ATCC 34037 S-layer O-glycan structure.

Monosaccharide symbols are shown according to the Symbol Nomenclature for Glycans (SNFG) (Varki et al., 2015; Tomek et al., 2018).

1.4.2.2 Bacteroides Surface Protein A (BspA)

T. forsythia has been reported to possess a surface virulence factor, BspA which is from the leucine-rich repeats (LRRs) family use for adhesion and invasion of epithelial cells and in coaggregation with components of other bacteria and with red complex species (Inagaki, Kuramitsu and Sharma, 2005 and Mishima and Sharma, 2011). The BspA protein contains D1 and D2 regions in the amino-terminal region with 14- and 6-tandem repeats of a 23-amino acid leucine-rich-repeat (LRR) motif, N-terminal, Bacterial immunoglobulin-like (Ig-like) domains, and the catalytic terminal (C-terminal) (Sharma, 2010).

Toll-like receptor (TLR) 2-dependent pathway was shown to be activated by BspA which elicit the release of bone-resorbing proinflammatory cytokines from monocytes and the chemokine IL-8 from gingival epithelial cells (Sharma *et al.*, 2005). In a mouse in vivo model conducted by Sharma *et al.,* (2005), the role of BspA in pathogenesis was evidenced where the BspA-defective mutant showed less potency in comparison to the parent strain in inducing alveolar bone loss in mice (Sharma *et al.*, 2005).

1.4.2.3 Proteases of *T. forsythia*

Proteases are important enzymes that are also secreted by *T. forsythia,* which were shown to be important contributing factors to periodontal tissue destruction by so many mechanisms which includes; activating host degradative enzymes, direct tissue

degradation and modulation of host inflammatory responses (Potempa and Pike, 2009). Also, they are involved in exposing the host cryptotopes for bacterial colonisation by modifying the host cell proteins, degrading the host periodontal tissues and also cleaving components such as cytokines/chemokines and complement factors involved in innate immunity and immunoglobulins involved in adaptive immunity, thereby activating components needed for clotting or fibrinolysis (Bodet *et al.*, 2006 and Potempa and Pike, 2009).

Two proteolytic enzymes were reported to play some major roles especially in the breakdown of host proteins, needed for the provision of heme, peptides and essential amino acids for the growth of *T. forsythia* which include, karilysin and PrtH (same as forsythia detachment factor, FDF). The two proteases are distinct; karilysin termed as matrix metalloprotease-like enzyme (MMP) which was reported to be involved in immunomodulation by first, shielding *T. forsythia* from the antimicrobial effects of human serum, while PrtH facilitates the removal of adherent cells from the substratum thereby increasing the mitochondrial oxidative membrane potential in cells, which results in the secretion of IL-8 by detached cells (Tomi *et al.*, 2008 and Karim *et al.*, 2010).

1.4.2.4 Surface Lipoproteins of *T. forsythia*

Other research has shown that the surface lipoproteins of *T. forsythia* possessed the ability to activate host cells thereby releasing proinflammatory cytokines and inducing cellular apoptosis (Hasebe et al., 2004). Also, it was reported that fractions of *T. forsythia* lipoprotein contain ester-bound fatty acids which stimulate human gingival fibroblasts and monocytic cells to produce IL-6 and TNF-α. Lipoprotein-mediated cytokine expression by host cells was shown to be activated by the transcription factor nuclear factor-kappa B as a result of Toll-like receptor 2, not CD14- or Toll-like receptor 4-mediated signalling (Hasebe *et al.*, 2004). Also, the lipoprotein fraction from *T. forsythia* has been reported to be responsible for the apoptotic cell death of human gingival fibroblasts, HL-60 cells (a human myeloid leukaemia cell line), KB cells (an epithelial cell line) and THP-1 cells (a monocytic cell line), but not MOLT4 cells (a T-cell leukaemia cell line) (Hasebe *et al.*, 2004). For the lipoprotein to be able to induce cell death, it must involve the activation of caspase-8, an initiator of the caspase cascade in apoptosis. This therefore suggests that the lipoproteins of *T. forsythia* may play some

key roles in the pathogenesis of periodontal disease by the induction of cell activation and apoptosis (Hasebe *et al.*, 2004).

1.4.2.5 Glycosidic Activity of *T. forsythia*

Sialidase activity is a putative virulence factor of *T. forsythia,* an organism reported to encode glycosidic enzyme NanH that removes terminal sialic acid from the host glycoconjugates (Thompson *et al.*, 2009 and Stafford *et al.*, 2012). The NanH sialidase was shown to have a preference for α2-3 glycosidic linkages of the glycoconjugates, indicating the likeliness of its involvement in nutrient acquisition (Thompson *et al.*, 2009). Studies also revealed the important roles of NanH sialidase of *T. forsythia* in adherence to sialylated mucous-coated surfaces such as epithelial cells, colonisation, invasion of host tissues, involvement in biofilm formation and being up-regulated in dental plaque (Roy et al., 2011).

Furthermore, the genome of *T. forsythia* has been predicted to express several other putative glycosidases such as β-hexosaminidases shown to degrade β-linked glucosamine or galactosamine (Roy et al., 2012), α-D-glucosidase and *N*-acetyl-β-D-glucosaminidase (Hughes et al., 2003), β-glucanase of *T. forsythia* that was reported to enhance the hydrolysis of dietary β-glucans needed for the development of mixed biofilm between *T. forsythia* and *F. nucleatum* (Honma et al., 2018), and α-L-fucosidases that were reported to cleave fructose found on host glycoprotein chain (Megson et al., 2015). Interestingly, these glycosidases have been reported to hydrolyze terminal glycosidic bonds of the complex oligosaccharides and proteoglycans found in saliva, gingival crevicular fluid (GCF) and periodontal tissue (Roy *et al.*, 2011 and Stafford *et al.*, 2012).

1.4.3   Biofilm Formation by Periodontal Pathogens

Formation of biofilm by oral microorganisms creates an alternative way of life in which these pathogens use in facilitating and prolonging their survival in diverse environmental conditions (Bowen et al., 2018). Biofilms in the host protect microorganisms from innate immune defences thereby persisting and developing resistance to antimicrobials (Kostakioti *et al.,* 2013). The pathogens in biofilms produce and live in their own hydrated matrix referred to as extracellular polymeric substances

(EPS), which forms their immediate environment (Flemming et al., 2016). EPS are composed mainly of polysaccharides, nucleic acids, proteins and lipids which provide the mechanical stability needed by the biofilms, facilitates their attachment to surfaces and form a cohesive, three-dimensional polymer network that interconnects and transiently immobilises biofilm cells (Marsh & Zaura, 2017). Furthermore, the EPS serves as an external digestive system that keeps the extracellular enzymes close to the cells thereby enabling them to metabolise dissolved, colloidal and solid biopolymers (Flemming and Wingender, 2010).

In general, biofilm formation has been shown to involve multiple steps beginning with the newly adherent cells loosely attaching to biotic or abiotic surfaces, readily able to detach which is often referred to as reversible phase (Armbruster & Parsek, 2018). With time however, some of the cells enter an irreversible attachment phase making it difficult to be dislodged mechanically. After the irreversible attachment phase, cells divide and produce biofilm matrix components, forming small aggregates of bacteria referred to as microcolonies that is composed of aggregates of different species that adapt to their site in the biofilm (figure 1.6) (Armbruster and Parsek, 2018).
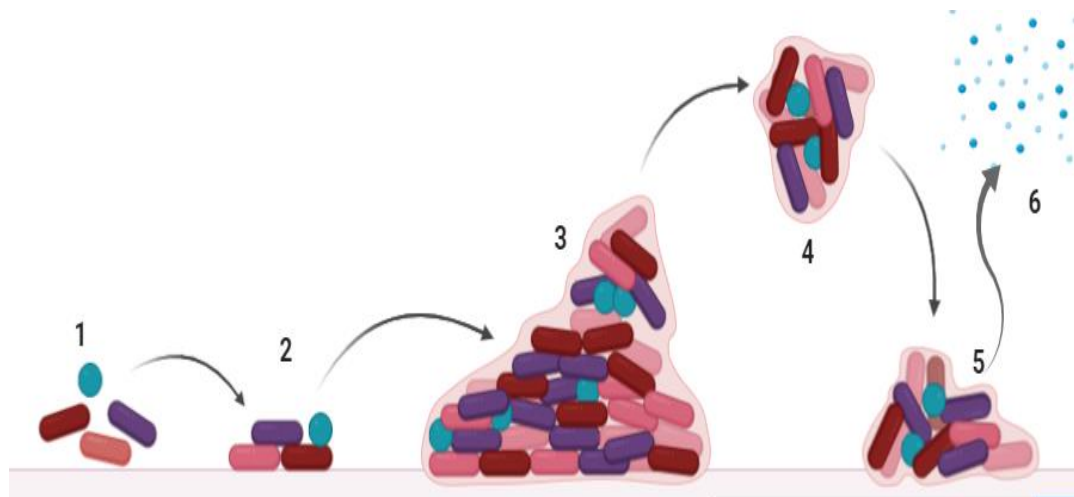
Figure 1.6: Schematic representation of stages involved in biofilm formation

Stage 1 & 2; Attachment of different planktonic bacterial cells to the surface, 3; Growth of bacterial cells into biofilm embedded in EPS, 4 & 5; Detachment from the parent biofilm and 6; Dispersal of cells into the surrounding

In the oral cavity, however, sialic acid and other sugars found in salivary mucins serve as recognition motifs and binding sites for some strains of pathogens thereby promoting biofilm formation (Cross & Ruhl, 2018). The first stage involves the formation of a thin layer of adsorbed salivary proteins and glycoproteins referred to as pellicle coating the tooth enamel surfaces and thus supporting the interactions between bacterial lectin-like adhesins with glycan motifs on glycoproteins leading to the initial bacterial colonisation and plaque formation (figure 1.7) (reviewed in Lendenmann et al., 2009). Secondly, bacterial adhesins adhere to glycans of other microbes however, this may be agglutinated by the salivary glycoprotein.

Both *P. gingivalis* and *T. forsythia* (red complex microorganisms) are found in supra- and subgingival plaque as part of the polymicrobial biofilm community involved in attachment, colonisation of oral surfaces and the subsequent pathogenesis of tooth decay (periodontitis) (Bowen *et al.*, 2018).
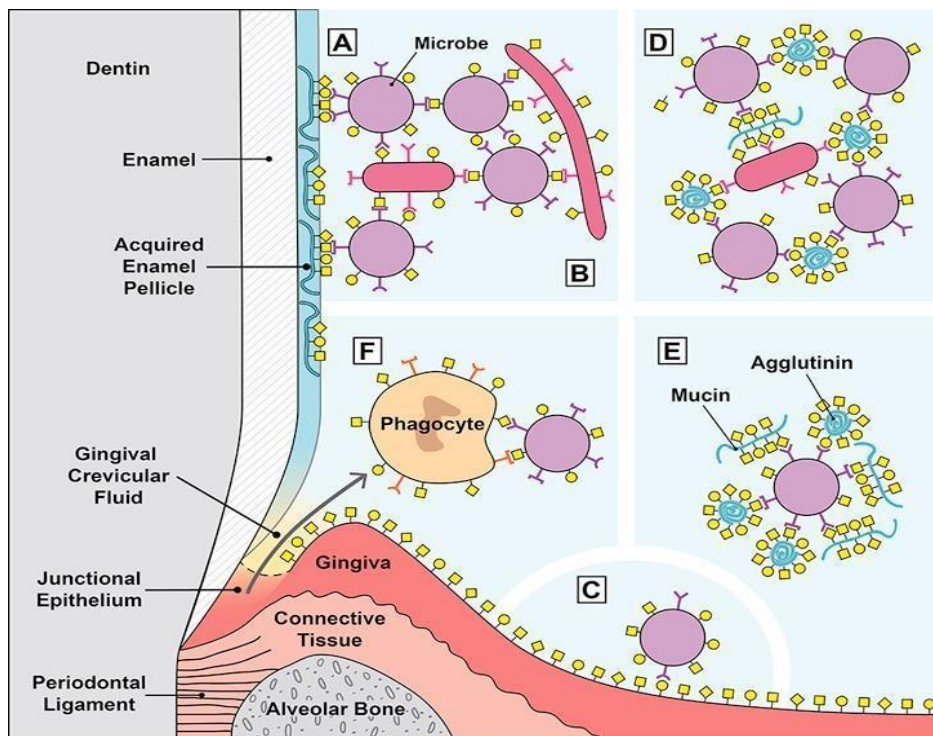
Figure 1.7: Glycan-mediated interactions in the oral cavity

[A]. Microbial attachment to the tooth surface. Microbial adhesins attach to mostly salivary glycoproteins adsorbed to the tooth surface as part of the acquired enamel pellicle. This is typically the first step in oral biofilm formation. **[B].** Microbial adhesins attach to glycans on other microbes. This example shows microbial *coadhesion*, the process of attaching to microbes that are part of a biofilm. If this microbe-microbe attachment occurs in suspension, i.e. in the planktonic phase, it is called microbial *coaggregation.* **[C].** Microbial adhesins attach to glycans on oral epithelia. This interaction normally does not result in long-term colonization because the oral epithelium is a shedding surface. **[D].** Salivary glycoproteins agglutinate microbes. Natural salivary flow causes these aggregates to be swallowed, resulting in the clearance of the microbes from the oral cavity. **[E].** Salivary glycoproteins can serve as molecular camouflage. A microbial cell is covered by multiple-bound salivary agglutinins and mucins. This might protect the microbe from immune surveillance by masking the underlying microbial cell surface. **[F].** Lectin-mediated phagocytosis. Phagocyte lectins bind to microbial glycans, and microbial adhesins bind to phagocyte glycans. These interactions can both potentially lead to phagocyte activation and phagocytosis of the bacteria. (Adapted from: https://doi.org/10.1016/j.cellimm.2018.08.008. This work is licensed under the Creative Commons Attribution-NonCommercial 3.0 Unported License.

1.4.3.1 *Porphyromonas gingivalis* **Biofilm**

P. gingivalis, a keystone red complex microorganism, is found in supra- and subgingival plaque as part of the polymicrobial biofilm community involved in attachment, colonisation of oral surfaces and the subsequent pathogenesis of periodontitis (Bowen et al., 2018). This Gram-negative facultative anaerobe expresses a range of other virulence factors that support its survival, regulate its communication with other species in the biofilm, or modulate the inflammatory responses of the colonised host tissue (Bao et al., 2014).

The gingipains of *P. gingivalis* have been reported to promote biofilm formation and may qualitatively and quantitatively affect composition of polymicrobial biofilms (Bao et al., 2014). Additionally, the sialidase of *P. gingivalis* with the assistance of NanS sialate-esterase from *T. forsythia* was shown to cleave diacetylated sialic acids needed for biofilm formation and bacterial growth in general (Frey et al., 2019).

Recent findings also attribute the pathogenesis of periodontitis to dysbiosis caused by oral microbes, with *P. gingivalis* acting as the key pathogen that disrupts the host immune homeostasis (Xu et al., 2020). Proteases, lipopolysaccharide (LPS), fimbriae (fimA), and many other virulence factors comprise the strategies deployed by *P. gingivalis* to support its colonisation thereby facilitating the outgrowth of the surrounding microbial community (Xu et al., 2020). These virulence factors support the coaggregation of *P. gingivalis* with other oral bacteria and subsequent formation of dental plaque. In addition, virulence factors are also shown to modulate a variety of host immune components and subvert the immune response in order to evade bacterial clearance or induce an inflammatory environment (Xu et al., 2020).

P. gingivalis enclosed in the biofilm structure in the form of dental plaque are reported to be resistant to attack by the host immune system and most antimicrobials, hence enabling persistent infection (Kariu et al., 2017). Thus, inhibition of biofilm formation by *P. gingivalis* may serve as a novel treatment of periodontitis and inflammation.

1.4.3.2 *Tannerella forsythia* **Biofilm**

T. forsythia is an anaerobic, fastidious, Gram-negative bacterium which together with *P. gingivalis* and *T. denticola*, constitute the red-complex and is shown to be associated with severe and chronic periodontitis (Sharma, 2010 and Shimotahira et al., 2013). This oral pathobiont *T. forsythia*, is known to be isolated from the gingival sulci and periodontal pockets of patients with periodontitis (Socransky et al., 1998 and Tanner & Izard, 2006).

Several virulence factors of *T. forsythia* were identified to include; the S-layer, BspA, glycosidases, metalloproteinase and lipoproteins (Sharma, 2010 and Roy et al., 2010). These virulence factors are reported to be involved in cell adhesion and surface recognition (Sharma, 2010), adhesion and invasion of host epithelial cell (Sakakibara et al., 2007), degradation of host periodontal tissues, modification of host cell proteins for bacterial colonisation, and cleaving components that are involved in innate and adaptive immunity (Sharma, 2010), as well as in biofilm formation (Roy et al., 2011).

Roy et al., reported *T. forsythia* to form biofilm by utilising sialic acid and that sialidase activity of this pathobiont is key to utilisation of these sialoconjugate sugars and is involved in host-pathogen interactions in vitro (Roy et al., 2011). Also, *T. forsythia* was shown to have synergy with *F. nucleatum* during biofilm formation by coaggregation-mediated mechanisms (Sharma et al., 2005), and in multispecies oral biofilms model which revealed the role of surface proteins in biofilm formation (Bloch et al., 2017).

Since sialidase activity enhance biofilm formation by periodontal bacteria (Roy et al., 2010), and which are regarded as vital in disease progression and pose difficulties in treatment (Sharma, 2010), it is therefore important to investigate the antibacterial and biofilm inhibitory properties of the sialidase inhibitors.

1.5   Sialic Acids

1.5.1   Sialic Acid Structure

Sialic acids have a core structure of a nine carbon α-keto acid (9-C). They are often found at the terminus of host glycoconjugates playing different biological roles in nature such as cell-to-cell attachment, immune signalling etc (Schauer, 1985). The amino acid group is found at position 5 while the carboxyl group is at position 1 which confers negative charge on the molecule under physiological conditions thereby making

sialic acid a strong organic acid (figure 1.8) (Traving and Schauer, 1998). Among the different types of sialic acids, *N*-acetylneuraminic acid (Neu5Ac) is the most abundant, and has an α(2,3)- or α(2,6)- bonding to galactose (Gal), *N*-acetylgalactosamine (GalNAc), and *N*-acetylglucosamine (GlcNAc) or an α(2,8)-linkage to another *N*-acetylneuraminic acid unit at the terminal position of *N*-glycans, *O*-glycans, and glycosphingolipids in animals, bacteria, viruses, protozoa and pathogenic fungi (Angata and Varki, 2002; Schnaar, Gerardy-Schahn and Hildebrandt, 2014). Meanwhile, replacing one of the hydrogen atoms in the methyl moiety of acetyl group with a hydroxyl group results in the formation of *N*-glycolylneuraminic acid (Neu5Gc) (Schauer et al., 1995). Modifications can also occur at the C-4, C-7, C-8, and C-9 hydroxyl groups, e.g., O-acetylesters (Traving and Schauer, 1998 and Angata and Varki, 2002).
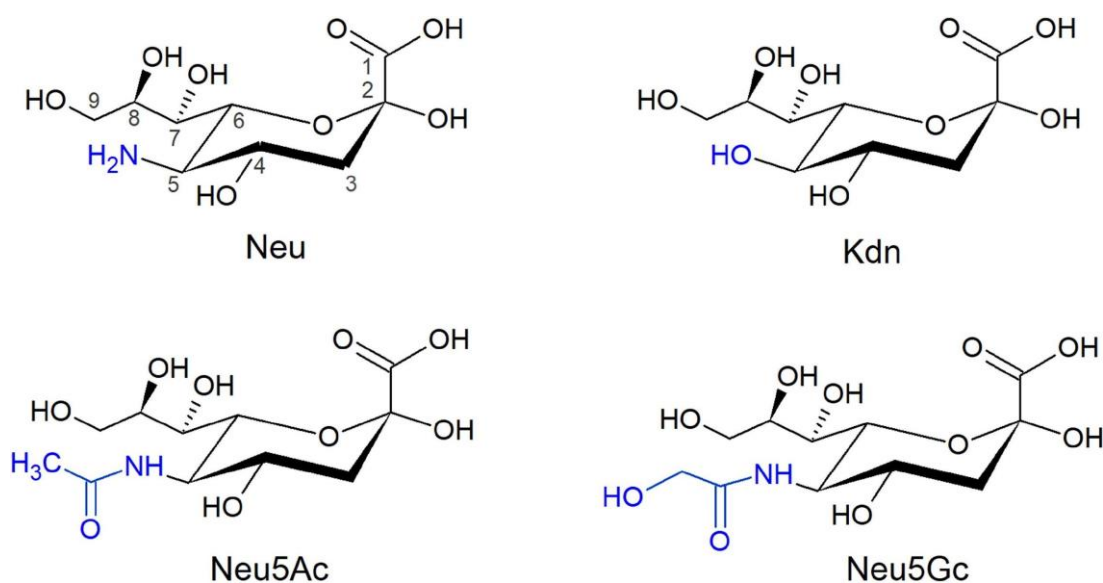
Figure 1.8: Main structures of commonly found sialic acids:

Neu; neuraminic acid, Kdn; 2-keto-deoxynonulosonic acid, Neu5Ac; *N*-acetylneuraminic acid, and Neu5Gc;*N*-glycolylneuraminic acid.

1.5.2 Occurrence

Worthy of note is the discovery of sialic acids (neuraminic acids) in the 1930s by two scientists, Klenk Ersnt and Gunnar Blix. While Blix isolated sialic acid from submaxillary mucin (sialos = saliva in Greek), Ersnt isolated neuraminic acid derivative from brain glycolipids (neuro- + amine + acid) (Angata and Varki, 2002).

Sialic acids have been found in Deuterostomes (vertebrates, ascidians, and echinoderms), commonly linked through the α2-3 linkage to Galactose, via an α2-6 linkage to Gal and GalNAc, or via an α2-8 linkage to another sialic acid (Corfield and Schauer, 1982). Protozoans like *Trypanosoma cruzi* (causative agent of Chagas' disease) has also been reported to possess sialic acids, however, they do not produce their own sialic acids but rather "scavenged" it from the glycoproteins of their host by the help of an enzyme called trans-sialidase (Bary, 1959; Schuaer et al., 1983 and Cross & Ruhl, 2018)

Additionally, sialic acids have been reported to be found on capsular polysaccharides (K-antigens) and lipopolysaccharides (O-antigens) of mostly pathogenic Gram-negative bacterial cells (Vimr *et al.*, 2004). These sialic acids often occur as internal residues, either in homopolymers (polysialic acids) bonded through α2-8 and/or α2-9 linkages or in repetitive units comprised of several sugar residues (Schauer and Kamerling, 1997 and Vimr *et al.*, 2004). The presence of sialic acids on the surfaces of these pathogens have been shown to contribute to host immune response evasion (Varki, 1992 and Angata & Varki, 2002).

1.5.3 Function

The negatively charged sialic acid binds and transport positively charged molecules (e.g Ca^{2+}), which are used in attraction or repulsion amongst cells and molecules (Traving and Schauer, 1998 and Iijima et al., 2004). Also, they hinder the degradative actions of proteases on the host glycoproteins thereby limiting bacterial colonisation by the neuraminic acid film covering the host cell surface. Nonetheless, pathogens such as viruses (influenza), toxins (cholera toxin), bacteria (*Escherichia coli*, *Helicobacter pylori*) and protozoa (*Trypanosoma cruzi*), also bind to the host cells through sialic acid-containing receptors (Schauer and Kamerling, 1997 and Traving and Schauer, 1998 and Buschiazzo et al., 2000).

Another interesting aspect of sialic acids is their recognition ability amongst cells and molecules (Paulson et al., 2012). This characteristic helps the immune system to differentiate between self and nonself structures according to the pattern of their sialic acid structure (Pillai et al., 2012). Additionally, sialic acids-recognizing molecules known as lectins which are oligomeric glycoproteins from plants, invertebrates and animals have also been reported to bind to specific sugar residues (Avril et al., 2006).

In contrast to recognition ability of sialic acids, is their masking of cells and molecules processes (Crocker et al., 2007). This mechanism of sialic acids prevents erythrocytes from being degraded, because they mask the subterminal galactose residues (Bratosin *et al.*, 1995).

Pathogenic bacteria have developed a mechanism of using this molecule to their benefit in two major ways: by coating themselves in sialic acid, which provides resistance to the host's innate immune response, as well as nutrient needed for their survival (Severi, Hood and Thomas, 2007). These bacteria can either scavenge sialic acids directly from the environment (host) or synthesise it de novo (Severi, Hood and Thomas, 2007; Roy *et al.*, 2011; Roy, Douglas and Stafford, 2010).

1.5.4 Metabolism

Although complex, the metabolism of sialic acids explains the link between the structure and function of a sialic acid derivative and the relationship between health and severe illness which may depend on the presence or absence of a given enzyme during the synthesis of sialic acids (Traving and Schauer, 1998 and Schauer & Kamerling, 2018). Additionally, the metabolic pathways for the commonest sialic acid (Neu5Ac), in nature differs in vertebrates and bacteria, furthermore, the localization sites of enzymes responsible for activation of sialic acid as well as transfer and degradation of sialyl glycoconjugate are different in eukaryotes and bacteria (Li and Chen, 2012 and Bowles & Gloster, 2021).

In vertebrates and higher invertebrates, sialic acid biosynthesis occurs in the cytosol where three enzymes are involved in a four-step process. The bifunctional hydrolysing UDP-GlcNAc 2-epimerase/ManNAc-6-kinase (GNE) catalyses the initial two steps having the enzymes hydrolysing UDP-GlcNAc 2-epimerase and ManNAc kinase activities (figure 1.8). The GNE conversion of UDPGlcNAc to ManNAc with removal

of the UDP moiety and epimerization of the GlcNAc is the key function of epimerase enzymes. While the phosphorylation of ManNAc to form ManNAc-6-P is done by kinase enzymes. In addition, condensation and dephosphorylation reactions catalysed by Neu5Ac 9-phosphate synthase (NanS) and Neu5Ac-9-phosphate phosphatase (NanP) results in the production of Neu5Ac (Varki and Schauer 2008). The sialic acid (Neu5Ac) produced in the cytosol is then transferred to the nucleus to be activated by cytosine 5′-monophosphate *N*-acetylneuraminic acid (CMPNeu5Ac) synthetase (EC 2.7.7.43) to form CMP-Neu5Ac which is then moved to the Golgi to be utilised by sialyl-transferases for the production of glycoproteins that are secreted or delivered to the cell surface subsequently (figure 1.9) (Kean, Münster-Kühnel and Gerardy-Schahn, 2004).
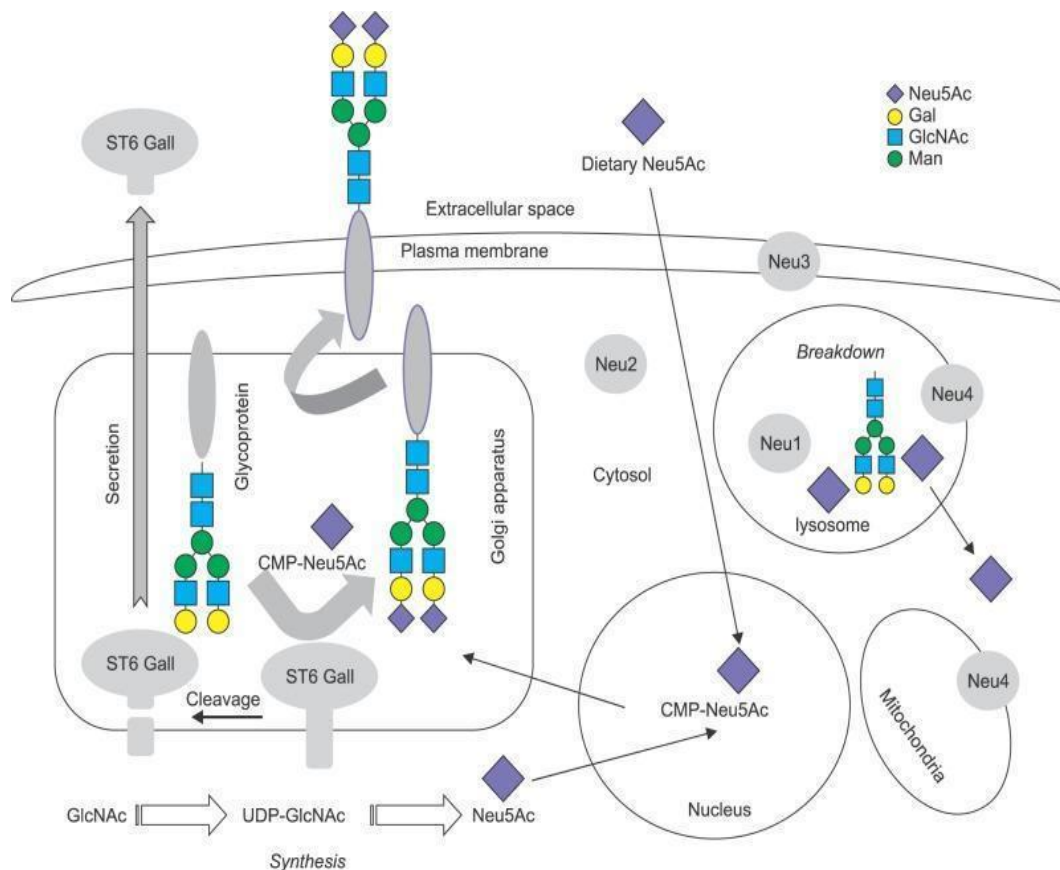
Figure 1.9: Sialic acid metabolism in Eukaryotic cells

Production, activation, conjugation, and catabolism of sialic acid in mammals (*N*-acetyl neuraminic acid, Neu5Ac) are as shown above. Sialic acid is obtained from diet or can be synthesised in the cytosol. It is then conveyed to the nucleus, where cytidine monophosphate (CMP)-sialic acid is synthesised. While in the Golgi apparatus, ST6 Gal I transfer the sialic acid from CMP-sialic acid to a glycoprotein. Cathepsin-like proteases cleaves ST6 Gal I, and then released from the cell. Sialidases can clear the sialylated conjugates in lysosomes, cytosol, plasma membrane, and mitochondria. Gal, galactose; GlcNAc, *N*-acetyl glucosamine; Man, mannose; Neu, neuraminidase.

(Adapted from: Jung-Jin Park and Minyoung Lee, 2013 (CC BY-NC 3.0). To view a copy of this licence, visit http://creativecommons.org/licenses/by-nc/3.0/

Although most bacteria have been shown not to synthesise their own sialic acids, a few pathogenic Gram-negative bacteria associated with humans are able to (Crocker and Varki, 2001 and Li and Chen, 2012). Furthermore, sialic acid which is part of a larger family of di-*N*-acetylated nonulosonic acid (Nulo) molecules, is shown to be composed of pseudaminic and legionaminic acids (Ricaldi et al., 2012). Research has also shown that pathogenic organisms such as *Legionella interrogans* (Ricaldi et al., 2012), *Campylobacter jejuni*, *Campylobacter coli* (Goon et al., 2003), *L.* strains, Vibrio strains, *T, forsythia* (Friedrich et al., 2017), and *H. pylori* (Schoenhofen et al., 2006), express these unique acids on their surfaces, which are needed for host-microbe interactions, colonisation of mucosal surfaces, immune subversion, motility, recognition and even in biofilm formation (Ricaldi et al., 2012).

Similar to the mechanism in mammals, the *de novo* means of making sialic acids by bacteria such as *E. coli* K1, *Neisseria meningitidis*, *C. jejuni*, and *Streptococcus agalactiae*, follow the same pattern with the conversion of UDP-GlcNAc to ManNAc by hydrolyzing UDP-GlcNAc 2-epimerase (NeuC) (figure 1.8). Different from mammals however, ManNAc which is secreted by bacteria is used straight in the presence of phosphoenolpyruvate (PEP) by an enzyme Neu5Ac synthase (NeuB) to form Neu5Ac and inorganic phosphate without involving kinase or a phosphatase (Angata and Varki, 2002 and Bravo *et al.*, 2004).

The scavenging pathway on the other hand, comprises of two channels: precursor scavenging as seen in *H. influenzae*, *Haemophilus ducreyi*, *Histophilus somni*, and *Pasteurella multocida* that belongs to the *Haemophilus–Actinobacillus– Pasteurella* or HAP group, here, free sialic acid however, is acquired directly from the host (Schilling *et al.*, 2001 and Steenbergen *et al.*, 2005), and donor scavenging (found in *Neisseria gonorrheae*) in which CMP-sialic acid is scavenged from the hosts (figure 1.10) (Parsons *et al.*, 1994).

Lastly, sialylation of bacterial lipopolysaccharides (LPS) and the polysialic acid capsule (CPS) as well as sialylation in eukaryotes is mainly catalysed by sialyltransferase (STs), while catabolism of sialic acid is done by sialidases and Neu5Ac lyase (or sialic acid aldolases, NanA in *E. coli* K1 and K12), which catalyses the breakdown of Neu5Ac to form ManNAc and pyruvate (Vimr *et al.*, 2004).
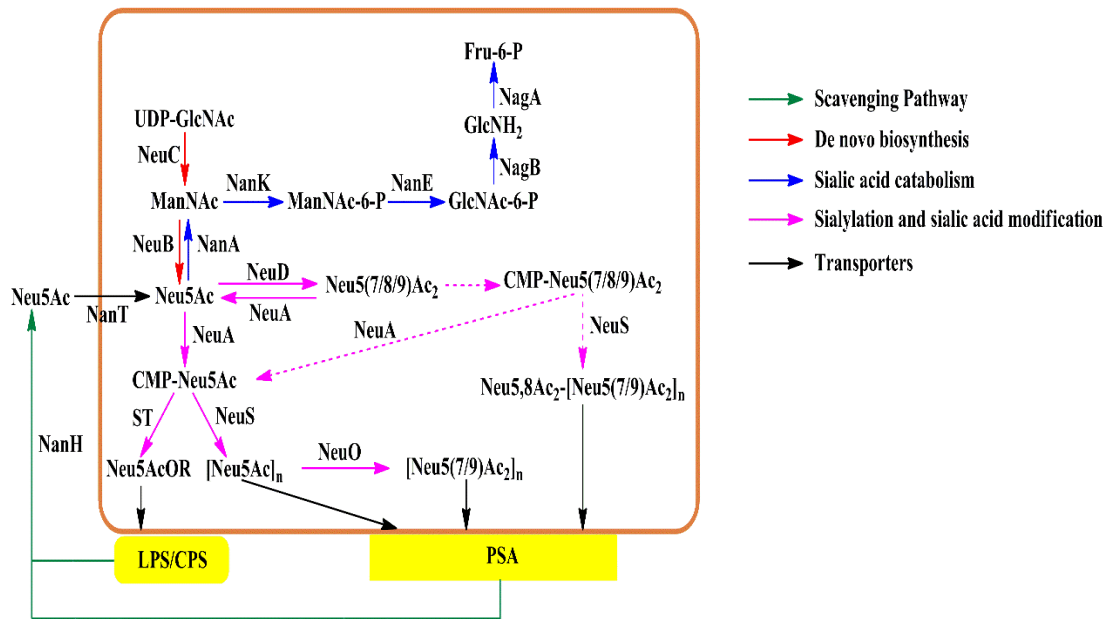
Figure 1.10: An overview of sialic acid metabolism pathways in *E. coli*

5′-diphosphate-*N*-acetylglucosamine=*UDP-GlcNAc* uridine, *N*-acetylneuraminic acid=*Neu5Ac, N*-acetylmannosamine=*ManNAc,* 5′-monophospho-*N*-acetylneuraminic acid=*CMP-Neu5Ac* cytidine, *N*-acetylglucosamine= *GlcNAc*, ` *LPS* lipopolysaccharide, *CPS* capsule, *Fru* fructose, Polysaccharide, *PSA* polysialic acid, *R* LPS or CPS. Enzymes: *NeuC* hydrolyzing UDP-GlcNAc 2-epimerase, *NeuB* sialic acid synthase, *NanA* sialic acid aldolase, *NeuA* CMP-sialic acid synthetase (NeuA in *E. coli* K1 and *S. agalactiae* also possesses *O*-acetylesterase activity), *NeuD* sialic acid *O*-acetyltransferase, *ST* sialyltransferase, *NeuS* polysialyltransferase, *NeuO* polysialic acid *O*-acetyltransferase, *NanK* ManNAc kinase, *NanE* ManNAc-6-phosphate epimerase, *NagB* GlcNAc-6-phosphate deacetylase, *NagA* glucosamine-6-phosphate deaminase, *NanH* sialidase, *NanT* Neu5Ac transporter.

Adapted from "Sialic acid metabolism and sialyltransferases: natural functions and applications: Applied Microbiology and Biotechnology" with permission from Springer Nature, Licence Number 4761370000923.

1.6   Immune Pathways and Inflammatory Responses in the Pathogenicity of Periodontitis

Periodontitis pathogenicity involves a complex succession of inflammatory host immune responses initiated because of plaque formation on the tooth surfaces. The ability of the host to respond by activating the immune pathways determines the susceptibility to periodontal diseases (Cekici *et al.*, 2014).

1.6.1   Innate Immunity and its Role in Periodontitis

Within the periodontium, the dysbiosis in oral microbial compositions in health and disease is shown to correlate with different innate immune responses and this influences inflammation of the gingiva (Silva et al., 2015). Gram-negative and Gram-positive bacteria have been involved in eliciting some specific inflammatory signals to the periodontal tissues however; the host has developed specific mechanisms of identifying and responding to the released signals (Dixon, Bainbridge and Darveau, 2004 and Silva et al., 2015).

Macrophages and neutrophils are believed to be the most valuable sources of pro-inflammatory chemokines in periodontitis thereby switching the host cell phenotypes to conditions closely related to the disease (Silva et al., 2015). In innate immunity, overactivation of the neutrophils leads to increased production of cytokines and subsequent migration into periodontium while for macrophages, most of the population differentiate to form "M1"-macrophages which are responsible for causing inflammation than "M2"-macrophages which are used for healing and regulating inflammatory responses (Parisi *et al.*, 2018).

1.6.1.1 Neutrophils

Neutrophils are the short-lived effector cells of the innate immune system that are primarily responsible for acute inflammatory responses and the clearing of extracellular pathogens in a host (Mantovani *et al.*, 2011). Also referred to as polymorphonuclear leukocytes (PMNs), neutrophils are the most widely spread white blood cells found in the periodontal pocket and gingival crevice, playing an important role in the host innate immune response against viral, bacterial, fungal, and protozoan infections, thereby

maintaining good homeostasis in periodontal structures (Faurschou and Borregaard, 2003).

Additionally, neutrophils have been shown to express inflammatory mediators such as cytokines and chemokines (Mantovani et al., 2011). Furthermore, they have been reported to contribute to the activation, regulation, and effector functions of innate and adaptive immunity. The role of neutrophils in the pathogenesis of a wide range of infectious diseases such as chronic inflammation, periodontitis, cancer, and infections caused by intracellular pathogens, therefore, becomes crucial (Mantovani *et al.*, 2011, Sochalska & Potempa, 2017).

1.6.1.2 Macrophages

Macrophages, which are differentiated peripheral monocytes, are the major constituents of innate immunity providing a first line of defence against pathogens, thereby modulating homeostasis as well as inflammatory responses. Macrophages are generally polarised into two main subtypes as either classically activated (M1) or alternatively activated (M2) (Nisha et al., 2018). Basically, M1 macrophages are considered pro-inflammatory "killer M1" involved in the secretion of cytokines such as interleukins 6 and 8 (IL-6 and IL-8), while M2 macrophages referred to as anti-inflammatory "builder M2" are thought to be involved in repairing (healing) process thereby secreting IL-10 and other factors (Parisi *et al.*, 2018 and Nisha et al., 2018).

1.6.1.3 Toll-Like Receptors (TLRs) and Innate Immunity

Toll-like receptors (TLRs) are thought to be evolutionarily conserved innate receptors produced in several immune and non-immune cells of the eukaryotic host. TLRs play a vital role in curtailing and protecting the mammalian host against infections caused by invading pathogens by secreting the inflammatory cytokines and type I interferons (Yuk & Jo, 2011). Also, TLRs contribute to shaping pathogen-specific humoral and cellular adaptive immune responses (Hawn and Underhill, 2005).

Toll-like receptors and other related pathogen sensors were reported to have leucine-rich repeat motifs that create docking sites for pathogen ligands or adaptors that bind

pathogen ligands, thereby activating the signal transduction pathways (McGettrick and O'Neill, 2004).

The mammalian TLRs play an important role in innate immune responses to a wide range of infections elicited by viruses, bacteria, parasites and fungi (Hayashi et al., 2001). Furthermore, differences in human susceptibility to microbial infections are associated with polymorphisms in TLRs and components of TLR signalling pathways (Hawn and Underhill, 2005). Microbial infection elicits the TLR responses, and this association between TLRs and pathogen-associated molecular patterns (PAMPs), may result in the introduction of an array of antimicrobial immune responses. Many other cytokines such as TNF-α, cytokines of the IL-1 family (IL-1β, IL-18), IFN-γ and IL-12, can be induced by the recognition of PAMPs by TLRs (Hawn and Underhill, 2005 and Yuk and Jo, 2011).

TLRs are reported to be the most characterised membrane-bound receptors in innate immune cells including macrophages and dendritic cells (Yuk and Jo, 2011). TLRs initiate intracellular signalling cascades involving different adaptor proteins and enzymes upon recognition of specific ligands elicited by self- or pathogen-derived molecules, thereby resulting in the creation of proinflammatory and antimicrobial responses via the activation of transcription factors such as nuclear factor-κB. TLR-dependent signalling pathways are reported to be tightly regulated during innate immune responses by various negative regulators (Yuk and Jo, 2011).

In addition, Toll-like receptors (TLRs) were shown to play critical roles in connecting the innate and adaptive immune responses. For example, the human TLR-3 functions in recognizing nonself double stranded RNA and endogenous necrotic cell RNA as ligands (Sun *et al.*, 2006), whereas TLR-7 and TLR-8 are involved in recognising viral-derived ssRNA (Medzhitov et al., 1997). Furthermore, TLR1 and TLR6 assist TLR2 in mediating responses to bacterial peptidoglycan and acylated (diacyl and triacyl) lipopeptides as well as recognising LPS preparation from pathogens such as *P. gingivalis* (Werts et al., 2001). TLR4 appears to mediate bacterial lipopolysaccharide and the expression of genes involved in inflammatory responses (Weber et al., 2004). Meanwhile, TLR5 is often expressed in the intestinal endothelial cells which recognizes bacterial flagellin that stimulates production of inflammatory cytokines (Hayashi et al., 2001). TLR9 however, is important in the recognition of bacterial unmethylated CpG

DNA as well as viral-derived CpG DNA that has immuno-stimulatory activity that elicits a strong T-helper-1-like inflammatory response by the host (Hemmi et al., 2000 and Lund et al., 2003).

Furthermore, polyinosinepolycytidylic acid (poly(I:C)), RNAs extracted from necrotic cells and other forms of glycosylation were found to influence the activation of human TLR3 (Bhuyan *et al.*, 2004 and Weber et al., 2004). Interestingly, all TLRs were reported to contain *N*-linked glycosylation consensus sites; therefore, sialylation of Toll-like receptor is likely to upregulate receptor surface representation, trafficking, as well as pattern recognition especially in TLR2 (Weber et al., 2004). In other separate findings, TLR3 ectodomain receptor was shown to be highly glycosylated with all the fifteen *N*-linked sites masked in carbohydrates nonetheless, one face was reported to be devoid of any form of glycosylation (Choe et al., 2005).

1.6.1.4 Oral Epithelial Responses

The oral cavity is covered by mucosal epithelium which prevents invasion by pathogens amongst other functions, thus immune system of the mucosal is responsible for the host innate and adaptive immune responses by responding to harmful invading bacteria during infection, also to antigens delivered during vaccination (Lamichhane et al., 2014). Epithelial cells, antimicrobial peptides such as defensins, secretory immunoglobulin A (SIgA) and TLRs protect the oral cavity from attachment and invasion by pathogens (Lamichhane et al., 2014).

1.6.2   The Role of Sialic acids in Innate Immunity

1.6.2.1 Sialic acids and Siglecs

Siglecs are sialic acid binding immunoglobulin (Ig) lectins, reported to be secreted mainly by cells of the hematopoietic system or white blood cells of the immune system which are shown to modulate the activity of cell signalling receptors through regulatory motifs in their cytoplasmic domains (figure 1.11) (Crocker and Varki, 2001 and Paulson et al., 2012).

Siglecs includes two subsets that have different functions, and these are; the first group are distantly interrelated (25–30% sequence identity) and comprise Siglec-1

(Sialoadhesin, Sn), -2 (CD22), -4 [myelin-associated glycoprotein (MAG)], and -15. The second group comprise the constantly changing CD33-related Siglecs, reported to showing high homology to CD33 in their extracellular domains (50–85% identity) as well as Siglec-3 (CD33), -5, -6, -7, -8, -9, -10, -11, and -14 (Crocker et al., 2007). However, an additional six human CD33-related Siglecs with inhibitory receptors features were reported and demonstrated to be expressed by the discrete subsets of leukocytes (figure 1.11) (Freeman *et al.*, 1995 and Crocker and Varki, 2001).

Siglecs are reported to play key roles in host–pathogen interactions, cell to cell communication, regulation of immune tolerance as well as maintaining immune homeostasis and in the regulation of inflammatory processes (Magesh et al., 2011 and MacAuley et al., 2014). Additionally, siglecs have been shown to take part in pathogen internalisation and immune evasion, attenuation of inflammation mediated by damage-associated molecular pattern (DAMP), also, in inhibiting natural killer (NK) cell function. Furthermore, siglecs in adaptive immunity function as modulators of T-cell activation and polarisation also as regulators of B cells and plasmacytoid DCs (Pillai et all., 2012).

The ability of Siglecs to recognize sialic acid containing polysaccharides (glycans) as ligands, helps the innate immune system to differentiate between self and nonself, thereby dampening the autoimmune responses (Paulson et al., 2012). For example, sialylation of group B Streptococcus capsule (CPS) was shown to engage Siglec-9 thereby suppressing the activation of neutrophils (Carlin et al., 2009). Furthermore, the binding of sialylated lipooligosaccharide (LOS) of *C. jejuni* with Siglec-7 was shown to influence dendritic cell-mediated T cell responses to T-helper 1 (Th1) or Th2 polarisation (Brunner et al., 2010)

Sialic acids found on the surfaces of pathogenic bacteria, which is vital in host mimicry, stoppage of complement activation, as well as attenuation of antibody production and nonspecific charge-repulsion effects, has been shown to interact with inhibitory CD33-related Siglecs (Crocker and Varki, 2001). Recently, a study reported that the lipooligosaccharides on the cell surface of Nontypeable *H. influenzae* (NTHi) displayed a complex glycan that mimic host structures, thereby allowing it to evade recognition by the host immune system as such, exploiting the normal functions of siglecs to down

regulate an immune response against them (Cao and Crocker, 2011; Paulson et al., 2012 and Jackson et al., 2019).

Nonetheless, lipooligosaccharides found on glycans are also potential targets of host adaptive and innate immune responses. To evade host's innate immune responses therefore, LOS structures exhibit interstrain heterogeneity, reported to be dependent on phase variation, the random on and off switching of gene expression, and generating intrastrain population diversity (Jackson et al., 2019).

B and T lymphocytes involves in the humoral and cell mediated aspect of the adaptive immune system, have also been reported in humans and mice to express two major siglecs, CD22 and Siglec-10/G (murine ortholog is Siglec-G), playing a key part in the regulation of B cell receptor signalling (Tedder et al., 2005; Varki, 2009 and Paulson et al., 2012). Nevertheless, in the innate immune system, several siglecs identified as inhibitory receptors were also reported (Crocker and Redelinghuys, 2008). Previous studies have shown crosslinking of Siglec-7 or Siglec-9 to activation receptors has resulted in inhibition of the cytolytic activity of natural killer (NK) cells against cancer cells and release of chemical mediators from mast cells (Avril *et al.*, 2005 and Paulson et al., 2012).
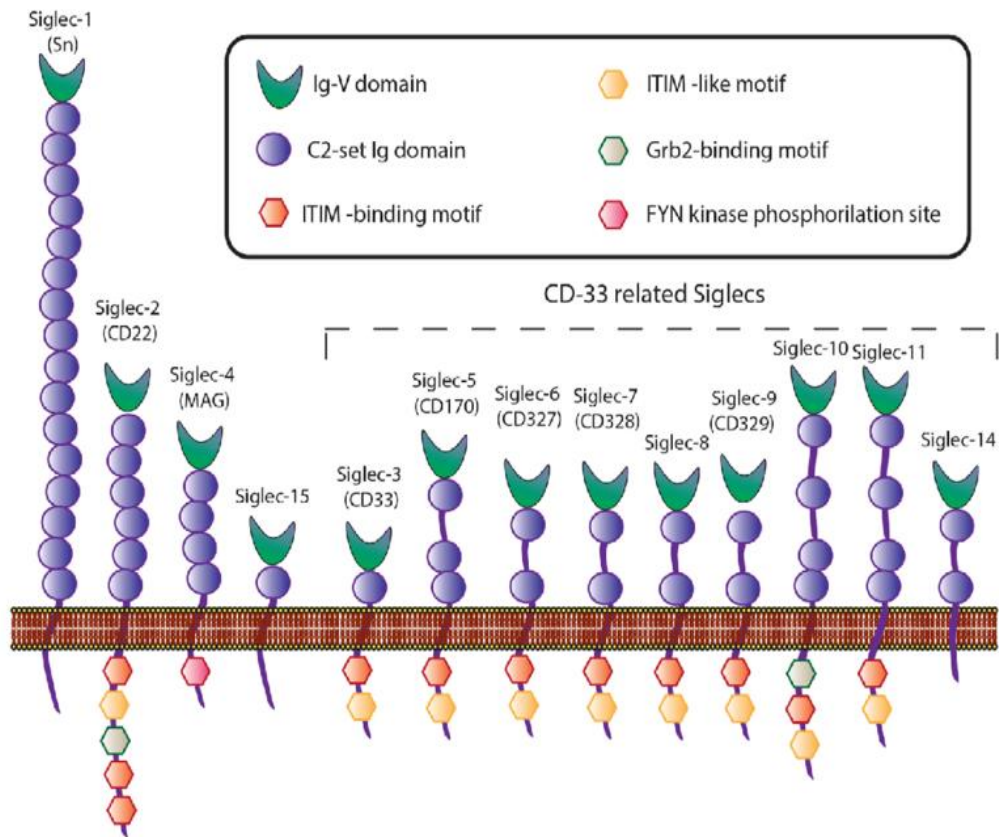
Figure 1.11: Representation of Siglecs subsets

The transmembrane type I receptors bearing 2 to 16 extracellular C2-set immunoglobulin domains, with an extracellular *N*-terminal V-set Ig (Ig-V) domain are responsible for the binding of sialoside ligands, a single transmembrane domain, and varying lengths of cytosolic tails. (Adapted from (Cagnoni et al., 2016): https://doi.org/10.3389/fonc.2016.00109 Licensed under the Creative Commons Attribution-NonCommercial 3.0 Unported License.

1.6.2.2 Sialic Acids and Toll-Like Receptors

As outlined above, Toll-like receptors (TLRs) are the major molecules of the innate immune system that function by recognizing pathogen-associated molecular patterns (PAMPs), and rapidly informing the host to the presence of potentially harmful microorganisms (Yuk & Jo, 2011). They contain a cytoplasmic signalling domain identified as Toll/interleukin-1 receptor (TIR). Both pathogen- and tissue damage-associated molecular patterns were shown to elicit inflammation via TLRs, whereas siglecs provide negative regulation (Chen et al., 2014) also, in cellular and molecular recognition (Akira et al., 2001).

Human Neu1 sialidase was shown to form complexes with the heavily glycosylated TLR-2 and TLR-4 found on dendritic cells and macrophages, which results in the pro-inflammatory responses and DCs maturation (Amith et al., 2010). Additionally, Neu1 also regulates the intracellular Toll-Like receptor 9 (TLR-9) (Amith et al., 2010 and Chen et al., 2014). Furthermore, human Neu1 sialidase was shown to be activated by the TLR ligand binding receptors, which may hydrolyse sialic acid residues thereby facilitating TLR dimerization (Amith et al., 2010).

In another study carried out by Chen et al., (2011), they demonstrated that interaction between the signal transducer CD24 with siglecG/10 was negatively affected due to desialylation of the cell adhesion molecule CD24 by bacterial sialidases (Chen et al., 2011). The CD24-SiglecG/10 interaction, which is dependent on sialylation of CD24, is needed to regulate inflammation in sepsis caused by danger-associated molecular patterns (DAMPs) or pathogen-associated molecular patterns (PAMPs). Additionally, disruption of this interaction was shown to increase inflammatory cytokine production, which also increases dendritic responses to DAMPs (Chen et al., 2011).

Furthermore, importance of glycosylation has been elucidated when cells treated with tunicamycin downregulate the TLR3-induced NF-κB activation, signifying the role of *N*-linked glycosylation in the signalling ability of this receptor (Sun et al., 2006). Therefore, the ability of sialic acid to recognize self from nonself structures impacts greatly on the host immune system (Cross & Ruhl, 2018).

1.6.2.3 Sialic Acids and Complement

One underlying property of the immune systems (adaptive and innate immunity), is its ability to recognize host cells, pathogens and damaged host cells (Blaum et al., 2015). Complement, however, is an important part of the innate immune system which is vital for defence against pathogens, as well as clearance of immune complexes and injured cells (Noris & Remuzzi, 2013). Despite the lack of specificity distinguishing the components of the acquired immunity, complement were reported to recognize pathogens and damaged host cells selectively, using the recognition molecules of the classic, lectin, and alternative pathways (Noris & Remuzzi, 2013).

Some pathogenic bacteria were shown to use sialic acids in coating themselves, thereby, shielding them from the actions of the host immune system by modulating complement interaction and downregulating the responses of adaptive and innate immune systems (Varki et. al., 2011). Additionally, sialylation has been shown to contribute to complement evasion of pathogens such as *Neisseria* via recruitment of factor H (Ram et al., 1998). Factor H (FH) helps the complement in recognising sialic acid as a Self-Associated Molecular Pattern (SAMP), that attaches to sialoglycans found on host cells thereby preventing complement deposition (Meri & Pangburn, 1990). The serum protein complement factor H (FH) guarantees downregulation of the complement alternative pathway, an integral part of innate immunity, upon interaction with specific glycans on host cell surfaces (Blaum et al., 2015).

1.6.2.4 Sialic Acids and Integrins

Integrins are transmembrane receptors which facilitate cell cytoskeleton-extracellular matrix (ECM) adhesion, for example, the mediation of adhesion of neutrophils to endothelial cells (Barczyk et al., 2010). These heterodimer glycoproteins are composed of 18 α- and 8 β-chain subunits with their binding ability depending on the extracellular divalent cations Ca^{2+} and Mg^{2+} (Barczyk et al., 2010). The bidirectional signalling ability of integrins is often referred to as "outside-in" and "inside-out" signalling (Arnaout et al., 2005), and their binding to extracellular ligands is highly specific.

Sialic acid on the other hand, is found at the oligosaccharidic segment of integrins, thereby supporting the receptor's interactions with extracellular matrix (ECM) components and growth factors which regulates cell adhesion, migration, and proliferation. Masking or removal of terminal sialic acid by neuraminidase will,

therefore, affect the endothelial cells (EC) adhesion as evidenced in the abrogation of interaction between Tat (cationic polypeptide released by HIV-1^{+} cells) and $\alpha_v\beta_3$ (Chiodelli et al., 2012). This means that integrin-dependent cell attachment, which depends on binding of integrins to specific peptide sequence of extracellular protein, is being modulated by glycosylation modification amongst other factors (Gu et al., 2009).

Furthermore, the activity of integrin α5β1-dependent cell adhesion to fibronectin was reported to be mediated by cell surface α2,6-linked sialic acid (Razani & Lisanti, 2001). Caveolin-1, which is involved in the transport of lipids, signal transduction and cancer progression in mouse, was reported to up-regulate α2,6-sialylation which in turn influenced integrin α5β1-dependent hepatocarcinoma cell adhesion (Yu et al., 2013).

Interestingly, cells found in the periodontal tissues were reported to secrete numerous integrins with overlapping ligand-binding capabilities, and integrin α11β1 has also been shown to possess some regulatory effect in the periodontal ligament of continuously erupting incisors in mice (Larjava et al., 2014). Additionally, animals deficient in integrin αvβ6 developed classical signs of periodontal diseases such as inflammation, apical migration of the junctional epithelium and bone loss (Larjava et al., 2014). Lastly, Yilmaz and colleagues reported that the major fimbriae (FimA) protein of *P. gingivalis* physically associates with β1 integrins. Also, adhesion and invasion of endothelial cells by *P. gingivalis* was inhibited by the β1 integrin antibodies signifying the function of integrins as the invasion-associated receptor for *P. gingivalis* fimbriae (Yilmaz et al., 2002).

1.7 Sialic Acid found in the Oral Cavity

Sialic acid is a protein-bound monosaccharide which is often found attached to other monosaccharides such as galactose, mannose, glucosamine and fucose. It is a major constituent of many proteins in saliva and is mainly present in salivary mucin, gingival crevicular fluids (GCF), serum and fetuin amongst other mucosal fluids (Lewis & Lewis, 2012).

Mucins are expressed by different human mucosal surfaces, and in oral cavity they are shown to be the most frequent protein found in saliva with a "bottle-brush" appearance of sialic acid linked to a large number of glycan chains that is usually attached to serine/threonine protein backbone (Lewis & Lewis, 2012). Salivary mucins like

MUC5B and MUC7 Gel-forming mucins, function by binding to lectins and adhesins, antibodies, growth factors, as well as cytokines and chemokines thereby preventing the wet epithelial layers of the host from infection by the vast majority of pathogenic microbes (Frenkel & Ribbeck, 2015). Nonetheless, aside from the normal human mucins, production of mucins was also shown to be induced as a response to microorganisms and pathogen-associated molecular patterns (PAMPS), several cytokines, and enzymes secreted by phagocytic cells, signifying the role of mucins in innate immunity (McGuckin et al., 2011). Interestingly, downregulation of mucin production in the oral cavity has been reported to be linked to increased incidences of oral candidiasis and dental caries in elderly individuals (reviewed in Turner and Ship, 2007).

Secondly, secreted immune proteins such as immunoglobulins (IgA and IgG) and lactoferrin are also important sialylated glycoproteins, with sialic acids attached to their termini, which are involved in interaction with macrophages, also contributing to protein stability by protecting the molecules from proteolysis (Lewis & Lewis, 2012). In addition, fetuin which is also a sialylated glycoprotein found in the oral cavity involved in dampening inflammatory responses, has been shown to be degraded by *T. forsythia* (Roy et al., 2011).

Due to the strategic positions and vital roles played by these sialoglycan-rich mucosal secretions, oral pathogens have developed several means that target host sialic acids for adherence, mimicry and/or degradation (Haines-menges et al., 2015). The ability of these pathogenic microorganisms to use sialic acid as their carbon source has therefore contributed to their virulence, especially, in the oral cavity which is shown to be a sialic acid-rich environment (Lewis & Lewis, 2012 and Haines-menges et al., 2015).

1.8   Sialidases

1.8.1   Function, Classes and Types of Sialidases

Sialidases (EC 3.2.1.18) also referred to as neuraminidases or receptor destroying enzymes (RDEs), since they were first described for viruses (Traving and Schauer, 1998), are the key exo-glycosidases, found in mammals and some types of

microorganisms, involved with the cleavage of α-glycosidically linked sialic acid residues found at the termini of carbohydrate groups of glycoconjugates and oligosaccharides (Traving and Schauer, 1998). Based upon similarities in protein sequences, all known exo-sialidases are classed into three major glycoside hydrolases families (GH33, GH34 and GH83) (table 1.1), as found in the Carbohydrate Active enZyme (CAZy) database (http://www.cazy.org) (Terrapon et al., 2017 and Keil et al., 2022).

In higher animals that possess the corresponding sialic acid-containing substrates as components of an autonomous sialic acid metabolism, sialidases are specifically expressed and distributed in cells and tissues or organs and reported to be involved in different cellular activities including lysosomal catabolism. Meanwhile, the roles of microbial sialidases is restricted to nutrition and pathogenesis (Traving and Schauer, 1998; Monti *et al.*, 2010; Miyagi and Yamaguchi, 2012 and Keil et al., 2022).

Table 1.1: Classification of Sialidases

| | Exosialidases | | | | | |
	Hydrolytic Sialidases	**Trans-sialidases**	**Anhydro-sialidases**	**Endo-sialidases**	**CAZy families**	**Sia-linkage specificity**
Human sialidase	x				GH33	α2,3-, α2,6-, α2,8-Sia
Bacterial sialidase	x	x	x	x	GH33 GH156	α2,3-, α2,6-, α2,8-Sia
Viral sialidase	x			x	GH34 GH58 GH83	α2,3-, α2,6-Sia
Protozoa sialidase	x	x			GH33	α2,3-Sia

Table showing the different types of sialidases and their CAZy families. Keil et al., (2022).

1.8.1.1 Function

Although most pathogenic microorganisms do not secrete sialic acids, the presence of sialidases in them implies its role in scavenging these sugar moieties for carbon and nutritional purposes (Iwaki et al., 2020). Sialidases have also been reported to act as virulence factors in some pathogenic microorganisms such as *Clostridium perfringens*, causative agent of gas gangrene (Li & McClane, 2014). These organisms, like many others, destroy the initial line of host defence by removing the terminal sialic acid residues thereby degrading a variety of host structures (Stafford et al., 2012). Another possible functions of sialidases are their involvement in spreading factors that facilitate the multiplication of bacterial cells and their ability in invading host cells (Frey et al., 2019). Additionally, neuraminidase from *V. cholerae* (NANase) has been reported to work in a synergistic manner with cholera toxin (CT), thereby increasing the severity of a secretory response by upregulating the binding and penetration of CT to enterocytes (Galen *et al.*, 1991 and Moustafa et al., 2004).

1.8.2   Bacterial Sialidases

Some host-associated bacteria like *Pseudomonas aeruginosa*, *V. cholerae*, *S. pneumoniae*, *Salmonella typhi*, *Arthrobacter nicotianae, Arthrobacter ureafaciens C. perfringens*, *P. gingivalis*, *T. forsythia*, *T. denticola* and other major groups of mammalian pathogens and commensals were reported to possess sialidases (Roy *et al.*, 2011; Kim *et al.*, 2011 and Frey *et al.*, 2019). These glycosyl hydrolase (GH) enzymes remove terminal *N*-acylneuraminate residues from the host glycoconjugates (glycoproteins, glycolipids, and polysaccharides), mainly for nutrition and peptidoglycan biosynthesis which contribute to colonisation, persistence and ultimately disease (Galen *et al.*, 1991; Vimr *et al.*, 2004 and Parker *et al.*, 2009).

In addition, bacterial sialidases have been shown to catalyse the transfer of sialic acids from sialoglycans to asialoglycoconjugates through the mechanism of transglycosylation reaction (Lourbakos *et al.*, 2001 and Kim *et al.*, 2011). Further, sialidases of pathogenic bacterial cells serve as potential virulence factors which contribute to the recognizing sialic acids that are exposed on the surface of the host cell (Vimr *et al.*, 2004 and Sudhakara et al., 2019).

Although different bacteria express sialidases, these bacterial enzymes differ in their biochemical properties such as substrate specificities and expression patterns. For

example, the cell-surface-anchored NanA neuraminidase of *S. pneumoniae* has been implicated in the colonisation of nasopharyngeal and subsequent exposure of the glycan receptors for attachment thereby causing respiratory tract infections (Tong *et al.*, 2000). Further, NanA was shown to provide free carbon needed for bacterial growth and survival (Blevins et al., 2017). In addition, the extracellular secretory isoenzyme, NanB of *S. pneumoniae* was reported to contribute to pneumococcal infection of the respiratory tract and sepsis (Manco *et al.*, 2006).

Periodontal pathogens such as *P. gingivalis*, *T. forsythia* and *T. denticola* associated with severe periodontitis were also reported to express sialidases thereby contributing to disease progression (Frey *et al.*, 2019). The *P. gingivalis* sialidase SiaPG (PG_0352) together with NanS sialate-esterase from *T. forsythia* were shown to harvest sialic acids from bovine salivary mucin (BSM), a heavily *O*-acetylated substrate through an interspecies mechanism (Kelly *et al.*, 2015 and Frey *et al.*, 2019). Additionally, strains of *P. gingivalis* deficient in SiaPG (ΔSiaPG) showed defects in capsule formation as well as reduced virulence when observed from a mouse abscess model as compared to the wild strain (Li *et al.*, 2012). Furthermore, the mutant strain of *P. gingivalis* (ΔSiaPG) exhibited reduced biofilm formation, cell attachment and invasion of oral epithelial cells (H357), in comparison to the parent strain (Frey *et al.*, 2019).

T. forsythia NanH sialidase was also reported to remove sialic acid from the glycoprotein fetuin and bovine submaxillary mucin (Stafford et al., 2012). Roy and colleagues also reported the significance of NanH sialidase in enhancing biofilm formation, cell attachment and invasion (Roy *et al.*, 2011). NanH enzyme was shown to be an active sialidase with a wide range of pH values having optimal activity at pH ~5.2–5.6, which enables the colonisation of sub- and supra-gingival plaque biofilms more effectively by *T. forsythia* (Frey *et al.*, 2018). Also, Gram-positive *C. perfringens* implicated in causing gas gangrene, bacteremia and food poisoning, was reported to express three sialidases, NanI, NanH and NanJ, which are used in harvesting sialic acids from different glycoconjugates playing important role in nutrition and pathogenesis (Shimizu et al., 2002).

Furthermore, biochemical studies have shown that different bacterial sialidases have their preferred glycosidic linkages which they can cleave. For example, SiaPG and NanH could cleave 3- and 6-linked sialic acid under physiological-mimicking

conditions, with the latter having a preference for the α2-3 epitope (Table 1.2). Additionally, it was shown that the catalytic efficiency of NanH for sialyl Lewis ligands was four times less than that for 3-SL, despite all three possessing α2-3-linked sialic acid (Pratten *et al.*, 2018).

More important however, is the possession of conserved catalytic modules by most glycosyl hydrolase enzymes. These features include the "FRIP" motifs (Phe-Arginine-Isoleucin-Proline), "Asp-boxes" or BNR (Bacterial Neuraminidase Residue) conserved sequences with the residues (Ser/Thr-X-Asp[X]-Gly-X-Thr-Trp/Phe) or [ST]xDx[GY]xx[WFY] occurring more often in enzymes that act on, or interact with, polysaccharides substrates that contain glycosyl hydrolases such as the sialidases, levanases, Avicelase III-like endoglucanases, sucrases, and fructanases (Russell, 1998). Also, they are shown to modulate the activities of some extracellular signalling proteins (Richard *et. al*., 2000).

Arginine of the FRIP motif found on sialidases of *Salmonella typhimurium* and *V. cholera* were reported to signify a catalytic triad of arginine which interacts with the carboxylate group of sialic acid, also, the Asp-boxes are remote from the active site, in topologically equivalent locations in the β-propeller fold (Gaskell *et al.,* 1995). In addition to "FRIP" motifs and BNR/Asp-boxes, are the disc-like shaped β-propellers (6-bladed) (figure 1.11), which are a common repeats of secondary protein structures (beta-sheets) with specific function according to the number of blades (propellers). These ranges from 4- and 5-, 6- and 7-, and 8- and 10-β-propellers and their functions range from ligand-binding proteins, hydrolases, transferases, lyases, oxidoreductases, signalling proteins, catalysis, sortilin and structural proteins (Chen *et. al.,* 2011).

Catalytic triads are a sets of three coordinated amino acids sequence (e.g Asp-His-Ser catalytic triad) that are reported to be found at the active site of some enzymes such as hydrolases and transferases. This acid-base-nucleophile is a common motif for generating a nucleophilic residue needed for covalent catalysis (Guy and Alexander, 1998). They are conserved structures found both in mammalian and bacterial sialidases, therefore, considered essential for catalytic activity (Guy and Alexander, 1998).

Additionally, many bacterial sialidases were reported to possess other domains neatly inserted in the β-propeller domain. For example, glycoside hydrolases of *Micromonospora viridifaciens* possesses a galactose-binding module C-terminal to the

catalytic domain which sits above the active site (Newstead et al., 2005). *V. cholerae* neuraminidase has a centrally placed β-propeller domain that is flanked by two lectin-like domains; of which, one binds to sialic acid (Moustafa et al., 2004). Also, while the intramolecular *trans*-sialidase from *Macrobdella decora* (Leech) has a lectin domain *N*-terminal and an irregular β-stranded domain (Luo et al., 1998), the *trans*-sialidase of *Trypanosome rangeli* has a lectin-like C-terminal domain flanking the catalytic domain respectively (Buschiazzo et al., 2000).

Interestingly, some bacterial sialidases including that of *T. forsythia* possess subunits of amino acid sequences within a carbohydrate-active enzyme having a discrete fold referred to as Carbohydrate Binding Module (CBM) (figure 1.12), which serves a non-catalytic function (Park et al. 2013 and Satur *et al*. 2022). The CBM functions by binding the enzyme to a given glycan (i.e ligand-enzymes interactions), while the active site is responsible for the catalytic activity (Park et al. 2013 and Satur *et al*. 2022). Nevertheless, the CBM found at the active site of bacterial sialidases is necessary for every enzyme as it promotes the enzyme-substrate reaction by prolonging the intimate association (higher binding activity and substrate specificity) between the two, thereby enhancing catalysis (Oded Shoseyov *et. al.,* 2006 and Satur *et al*. 2022).

The little so far on catalytic mechanisms of sialidases are considered vital in medicine and pharmaceutical industries for the development of sialidase inhibitors as potential drugs against diseases such as periodontitis.
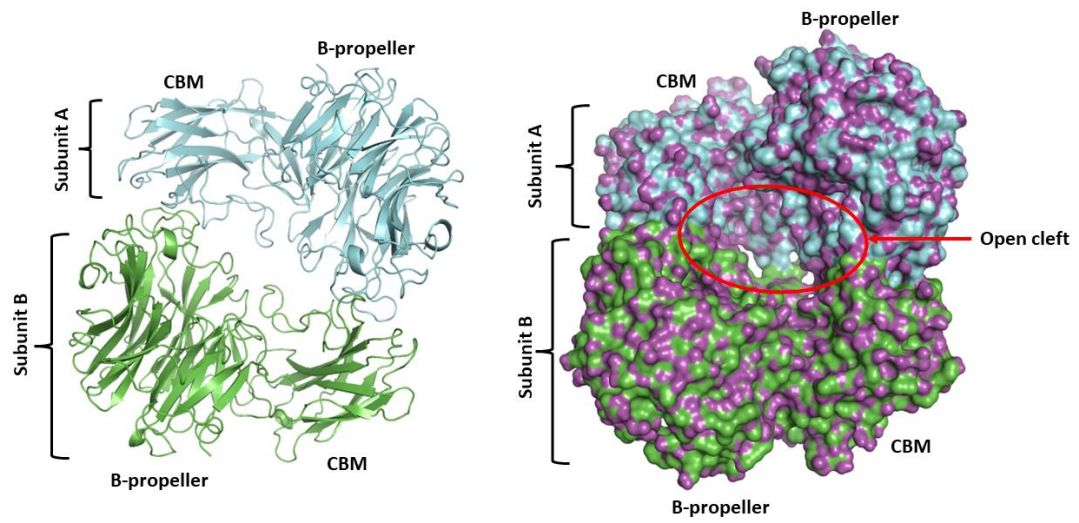
Figure 1.12: Crystal structure of *T. forsythia* NanH-apo

Each sub-unit (A in cyan and B in green) comprises a Beta-propeller (β-propeller) containing the Carbohydrate-Binding Module (CBM) and the active site. Visualised on PyMol to show the structure in cartoon and surface conformation with an open cleft found between the subunits.

Table 1.2: Sialic acid-linkage Preferences by Bacterial Sialidases from Different Mucosal sites

Site of infection	Organism	Sialidase	Linkages targeted	Linkage preference
Respiratory tract	*Streptococcus pneumoniae*	NanA NanB NanC	α2-3, α2-6 α2-3 α2-3	α2-6 α2-3 α2-3
	Pseudomonas aeruginosa	PA01 Neuraminidase	α2-3, α2-6	Unknown
	Pasturella multicocida	NanB NanH	(α2-3), α2-6 α2-3, (α2-6)	α2-6 α2-6
	Corynebacterium Diptheriae	NanH	α2-3, α2-6	α2-3
Oral cavity	*Porphyromonas gingivalis*	SiaPG	α2-3, α2-6	Unknown
	Tannerella forsythia	NanH	α2-3, α2-6	α2-3
	Treponema denticola	TDE0471	α2-3, α2-6	Unknown
	Streptococcus oralis	NanA	α2-3, α2-6	α2-3, α2-6
	Streptococcus mitis	NanA*	α2-3, α2-6	Unknown
Gastrointestinal tracks	*Clostridium perfringens*	NanH NanJ NanI	α2-3, α2-6 α2-3, α2-6 α2-3, α2-6	α2-3 α2-6 Unknown
	Salmonella typhimurium	NanH	α2-3, α2-6	α2-6
	Bacteroides thetaiotaomicron	VPI-5482	α2-3, α2-6	α2-6
	Ruminococcus gnavus	NanH	α2-3, α2-6	α2-3

1.8.3 Mammalian Sialidases

Unlike the bacterial sialidases that are mostly restricted to nutrition and pathogenesis, human sialidases have been implicated in the regulation of functional molecules which are needed for several biological processes like desialylation of surface molecules, hydrolyzation of glycoproteins, gangliosides, and oligosaccharides, in addition to the lysosomal catabolism effect (Table 1.3) (Monti *et al.*, 2002 and Miyagi, 2010).

At present, four mammalian sialidases have been identified and characterised and are thus named as; Neu1, Neu2, Neu3 and Neu4. These sialidases are encoded by different genes that differ in major subcellular and enzymatic characteristics such as substrate specificity while playing their unique role (Miyagi, 2010). Also, the sialidases were shown to be largely restricted to a particular cellular location such as Neu1 found in the lysosomes, Neu2 in cytosol, Neu3 in the plasma membrane and Neu4 which can either be found in lysosomes or mitochondrial membrane (Miyagi, 2010). Nonetheless, reaction to some stimuli, for example, exposure to PAMPS causing TLR activation may make the sialidases to assemble elsewhere (Miyagi and Yamaguchi, 2012). Also, human sialidases, i.e Neu1, Neu2, and the membrane-associated Neu3 and Neu4 were reported to be involved in the progression of diseases like cancer, type I and II sialidosis (Monti et al., 2004 and Caciotti et al., 2009).

Due to the abundant nature of sialic acids on the surfaces of mammalian cells, many bacterial pathogens express sialidases that they use in scavenging these sialic acids for nutrition and pathogenesis. Although there exists a vast phylogenetic difference between mammals and bacterial pathogens, some considerable similarities between the mammalian sialidases and bacterial sialidases such as conserved residual amino acid sequence topology have been reported (Miyagi & Yamaguchi 2012).

Additionally, the similarities between Neu2, Mammalian Neu and bacterial Nan sialidases shows the importance of these structural features in sialidase function (Eugenio Monti et al., 2010).

Table 1.3: Comparison of Mammalian Sialidases

	Neu1	Neu2	Neu3	Neu4
Major subcellular localization	Lysosome	Cytosol	Plasma membrane	Lysosome Mitochondria and ER
Good substrates	Oligosaccharide Glycopeptides	Oligosaccharides Glycopeptides Gangliosides	Gangliosides	Oligosaccharides Glycoproteins Gangliosides
Optimal pH	4.4-4.6	6.0-6.5	4.6-4.8	4.4-4.5
Total amino Acids (humans/mouse)	415/409	380/379	428/418	496(484)/497(413)
Chromosomal Location (human) (mouse)	6p21.3 17	2q37 1	11q13.5 7	2q37.3 10
Possible Function	Lysosomal degradation Immune function Elastic fibre assembly	Myoblast differentiation Neutral differentiation	Neutral differentiation Apoptosis Adhesion	Apoptosis

This table shows the localization sites, types of substrates each of the human sialidases binds to as well as their respective functions. Reproduced from "Mammalian sialidases: Physiological and pathological roles in cellular functions": Glycobiology by Miyagi, Taeko; Yamaguchi, Kazunori 2012, with Permission from Oxford University Press Licence Number: 4763240061150.

1.8.4   Sialidases, Lipopolysaccharides (LPS), and Gene Expression

Endogenous sialidase activity is shown to be upregulated in cells of the immune system during cell differentiation or activation (Stamatos et al., 2005 and Liang et al., 2006). The sialidase activities in these cells were shown to be involved in transendothelial migration, cytokine production, antigen uptake, retention of cells in bone marrow and supports the production of IFN-gamma (Nan et al., 2007). Lipopolysaccharides (LPS) endotoxin found on the outer membrane of Gram-negative organisms are bacterial products known to induce activation of cells of the host innate immune system, like the neutrophils and macrophages thereby, synthesising proinflammatory factors like TNF and IL-1β (Huang & Kraus, 2016).

Monocytes and dendritic cells (DCs) function in ligand-cell or cell-cell interactions, cell migration as well as expression of cytokines. Mature DCs therefore can recognize and process antigens as such present them to T lymphocytes (Stamatos et al., 2010). Although DCs are often activated by ligands or cytokines during inflammatory responses to infections, dendritic cells however, can produce proinflammatory cytokines as a response to several pathogenic substances such as bacterial LPS through TLR-4. Additionally, production of cytokines by mature DCs influences the actions of both adaptive and innate immune response (Stamatos et al., 2010).

In another study conducted by Stamatos et al., (2010), it was shown that bacterial lipopolysaccharides (LPS) induce cytokine secretion in human monocyte-derived dendritic cells (DCs). This response is enhanced by the cleavage of sialic acid from glycoconjugates on the surface of monocytes, leading to increased levels of cytokine; IL-12p40, TNF-α, and IL-6 production. These findings show that sialidase activity influences LPS-induced cytokine production, which is believed to be mediated by Neu3 and Neu1 human sialidases (Stamatos et al., 2010).

1.9   Sialidase Inhibition

Viruses, especially the highly pathogenic avian influenza H5N1 have been shown to express neuraminidase (sialidase), which has led to several human deaths (Itzstein and Thomson, 2009). Threats caused by viral strains such as this necessitated the need for therapeutic strategies in combating them. This has led to the development of influenza viral sialidase inhibitors such as Zanamivir (Relenza™), Oseltamivir (Tamiflu™),

Peramivir (Rapivab, BioCryst), and Laninamivir (figure 1.13) (von Itzstein, 2007; Itzstein and Thomson, 2009 and Keil et al., 2022).

As stated in section 1.8 above, the level of sialic acid found on cells and other mucosal surfaces is regulated by the activities of bacterial sialidases and the availability of sialyltransferases (Li & Chen, 2012). In addition, sialidases contribute to the pathogenesis of human pathogens such as *S. pneumoniae*, *C. perfringens*, *P. aeruginosa*, *P. gingivalis*, *T. forsythia*, *V. cholorae*, which cause a range of diseases including pneumonia, sepsis, gas gangrene, meningitis, periodontitis and cholera (Brear et al., 2012 and Li et al., 2019), respectively. Inhibition of sialidases encoded by human-associated pathogens therefore is an important area for development of uch needed new therapies.

With increased improvement in crystal structures of bacterial sialidases and an understanding of their mechanisms of action, the design of inhibitors with effective and selective activity on bacterial sialidases has been made possible (Slack et al., 2018; Li et al., 2019 and Bowles & Gloster, 2021). Sialidase inhibitors are mostly structural analogues of the transition state of sialic acid during catalysis (figure 1.13) (Itzstein & Thomson, 2009 and Bowles & Gloster, 2021), which act via competing with the endogenous ligands for the sialidase binding sites. Nonetheless, difluoro sialic acids analogues (Li et al., 2019), are the newly developed mechanism-based bacterial sialidase inhibitors, in addition to the well-known sialic acid transition-state analogue 2-deoxy-2,3-didehydro-*N*-acetylneuraminic acid (Neu5Ac2en or DANA) (Vavricka et al., 2017 and Slack et al., 2018). Most sialidase inhibitors in use now contain an anomeric carboxyl group that forms electrostatic bonds with amino acids in the active site of the enzyme (Vavricka *et al.*, 2017). Sialic acid anomeric sulfonic acid analogues have been suggested to be a better inhibitory compound because of their high acidity and electronegativity, which form strong bonds with the amino acids in the enzyme active sites (Vavricka *et al.*, 2017). Lastly, the selectivity property of most Neu5Ac2en-based sialidase inhibitors can be achieved through modification of the Neu5Ac2en at C-9 or both C-9 and C-5 (Khedri et al., 2012).

Bacterial sialidases of *S. pneumoniae* (NanA), an organism responsible for sepsis, *V. cholerae* causative agent of cholera, and *C. perfringens* (*Cp*-NanI) that causes gas gangrene, have been reported to be inhibited by curcumin derivatives, an active

compound from turmeric (Kim *et al.*, 2018). Also, Zanamivir has been reported to show a 30% reduction in whole-cell *Gardnerella vaginalis* sialidase; a causative agent of Bacterial vaginosis (Govinden *et al.*, 2018). Furthermore, Zanamivir was shown to have a 50% reduction in total association and invasion of HeLa cervical epithelial cells infected with *G. vaginalis* (Govinden *et al.*, 2018).

In another investigation conducted by Khedri et al., (2012), it was reported that Neu5Ac9N$_3$2en has an inhibitory activity against sialidases of α2–3-specific *S. typhimurium* and *S. pneumonia* just like Neu5Ac2en (Khedri et al., 2012). Nonetheless, Neu5Ac9N$_3$2en was less efficient against sialidases of *C. perfringens*, *V. cholorea,* and even on human Neu2 sialidase as compared to Neu5Ac2en (Khedri et al., 2012). This study reported the role of sialidase substrates in determining the selectivity and effectiveness of the sialidase inhibitors, which further stresses the preference for α-2,3 glycosidic-linkage (Khedri et al., 2012).

Additionally, the modification of sialic acid at C-2 with the addition of a fluorine atom which is highly electronegative, compound was reported to allow a covalent bond to be formed between sialic acid and the sialidase (Li et al., 2019). Furthermore, variation in the C-3 fluorine stereochemistry (axial or equatorial) and subsequent modification of the 2,3-difluorosialic acid-based sialidase inhibitor was shown to have inhibitory efficiency in nanomolar range with long effective duration on pathogenic bacterial sialidases of *S. pneumoniae* (SpNanA), *V. cholorea*, *C. perfringens* (CpNanI), and *Arthrobacter ureafaciens* (Li et al., 2019).

Zanamivir was also reported to have some inhibitory effect on sialidases of periodontal pathogens, also inhibiting sialic acid release from host glycoprotein and biofilm formation by *P. gingivalis* (Frey *et al.*, 2019). However, the viral neuraminidase inhibitor (Zanamivir) showed rather weaker activity on both *P. gingivalis* sialidase (SiaPg) and *T. forsythia* (NanH).

Inhibitors of this key virulence factor (sialidase), of these pathogenic bacteria, can serve as tools to gain a better understanding of their activities as well as form the basis for the development of novel therapy in the treatment of periodontitis and other inflammatory diseases.
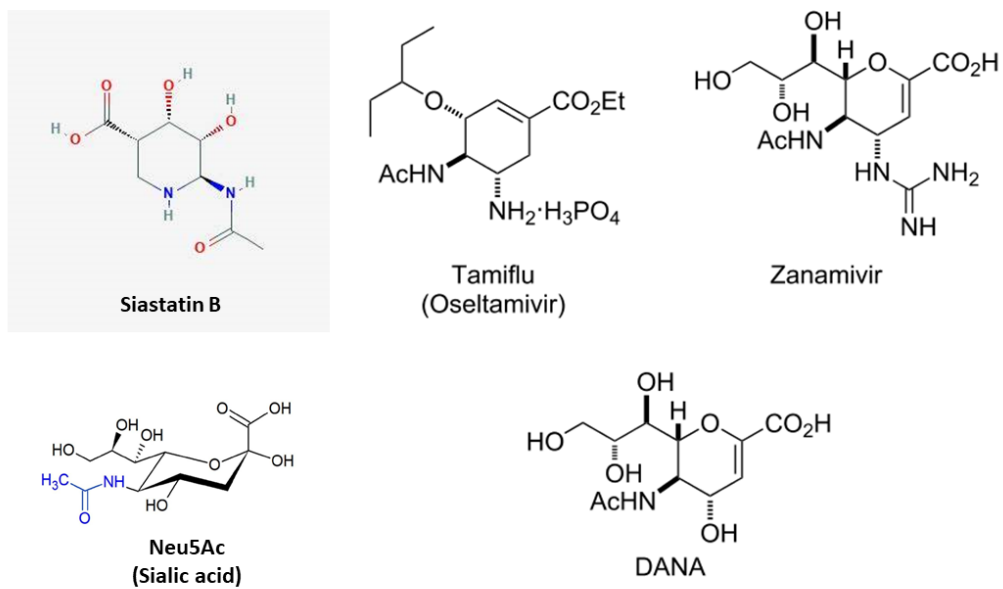
Figure 1.13: Structures of FDA-approved sialidase inhibitors

1.9.1   Drug Combination (synergistic effects) and Mechanism of Action

Drug combination also known as polytherapy is the use of more than one drug (inhibitor) to treat a single disease condition (Pritchard et al., 2013). Conditions such as cancer, HIV/AIDS, malaria, tuberculosis, leprosy and diarrhoea have been treated using drug combinations (Thakur et al., 2016). In many cases, this helps in overcoming drug resistance by microorganisms and increases the potency of the treatment, especially if the drugs target multiple proteins thereby reducing the duration of treatment (Cobo, 2014).

Although single-drug components are well researched, the mechanism by which drugs work together in clinical combination regimens needs to be researched more. The specific biochemical interaction by which a drug substance exerts its pharmacological effect is termed as mechanism of action (MOA) (Pritchard et al., 2013). This usually involves the specific molecular targets such as an enzyme or receptor to which the drug binds. In addition to problems related to efficacy or toxicity, drug mechanisms of action can also affect the approval of such drugs by the FDA (Lin et al., 2019).

Therefore, for the development of a target-based drug, a better understanding of drug mechanisms of action can give the required information about specificity and undesirable off-target activity which could lead to toxicity and a reduced therapeutic effect (Lin et al., 2019). As such, a detailed understanding of the enzymes kinetics, synergistic effects of drugs and their mechanism of action could signal a new therapeutic approach and help in developing novel inhibitors of periodontitis-associated sialidases. To achieve this therefore, the underlisted objectives (section 1.10), are outlined and researched upon.

1.10 Aim and Objectives

The aim of this study is to understand the role of glycans and glycosidases (sialidases) of *T. forsythia* and *P. gingivalis* in infection and biofilm formation as a route to the development of novel antimicrobials (drug development).

Specific objectives:

i. **To test a wide range of pharmaceutically approved and other plant-derived sialidase inhibitors**

Oral pathogens like *P. gingivalis* and *T. forsythia* are reported to express sialidases which they use to cleave sialic acids found at the terminal end of host glycoconjugates. Additionally, sialidases promote biofilm formation and enhance bacterial adhesion and invasion of host epithelial cells. Inhibiting these bacterial enzymes will prevent the pathogenesis and slow infections caused by these pathobionts. Wide range of pharmaceutically approved and plant-derived compounds were tested for their sialidase inhibitory ability which could serve as novel antimicrobials for the prevention of oral diseases such as periodontitis.

ii. **To investigate the antibacterial and antibiofilm activity of the sialidase inhibitors**

Oral pathogens are shown to bind to the pellicles thereby forming yellowish coloration on the tooth surfaces referred to as biofilm or dental plaque. The extracellular polymeric substances (EPS) secreted by these pathogens protect them from the actions of drugs as such, become resistant to most antimicrobials. The antibacterial and antibiofilm activity of the screened sialidase inhibitors was therefore investigated.

iii. **To examine the inhibition of host-pathogen interaction via adhesion and invasion of host oral epithelial cells (H357 OSCC).**

One of the mechanisms by which pathogenic microorganisms cause infections is via adhesion and subsequent invasion of the host tissues. This host-bacterial interaction is shown to be regulated by bacterial enzymes amongst other factors.

Therefore, the role of sialidase inhibitors in abrogating this host-pathogen relationship by inhibiting total bacterial association, adhesion, and invasion of the host oral epithelial cells (H357), using an antibiotic protection assay model was investigated.

iv. To investigate the role of sialylation and sialidases in innate immune modulation

During infection by harmful pathogens, the innate immune system through pathogen recognition receptors (PRRs) such as the toll-like receptors (TLRs), detects conserved bacterial components (Pathogen-Associated Molecular Patterns i.e. PAMPs), like the lipopolysaccharides (LPS), as such, respond by secreting proinflammatory cytokines like TNF, IL-6, IL-8, and IL-1β. Sialylation has been reported to regulate the host innate immune response, however, different cells respond to infections differently. The role of bacterial sialidases in modulation of host innate immune response using oral epithelial cells (H357), and the inhibition of this host-pathogen interaction was studied.

CHAPTER TWO
Materials and Methods

2.0   Bacterial Strains, Cloning, and Growth Conditions

The oral pathogens used in this study include the wild-type and mutant strains of *P. gingivalis* (Pg0381 and ΔPg0381) and *T. forsythia* (TF43037 and ΔTF035), respectively. Wild type *P. gingivalis* strain was grown on 10 % oxalated horse blood Fastidious anaerobic (FA) agar plates, while the mutant strain was maintained in 5 µg/ml erythromycin FA agar plates. The wild-type strain of *T. forsythia* (Tf43037) was grown on FA agar supplemented with 10 % oxalated horse blood containing 0.17 mM (w/v) *N*-acetylmuraminic acid (NAM), while 5 µg/ml erythromycin was added to the media in which the mutant strain (ΔTF035) were grown on. Both strains were incubated in an anaerobic chamber (Don Whitley Scientific, Shipley UK) at 37°C, 10 % CO_2, 10 % H_2 and 80 % N_2 and sub-cultured after 3-4 days.

2.1   Cloning of the NanH and SiaPg Sialidases

Cloning and transformation work was done by a previous PhD student from our lab Andrew Frey (Frey et al., 2018; Frey et al., 2019). In the course of this current project, therefore, the already cloned and transformed *Escherichia coli* (BL21 Origami) stored in a -80°C freezer were used for the expression and purification of recombinant proteins (NanH and SiaPg) as described below.

E. coli strains required for cloning and protein expression work (table 2.1) were cultured on Luria Bertani agar (LB agar) or Lysogeny broth (LB broth) (Thermo Fisher 70 Scientific). When attempting transformation, or culturing transformed strains, these were cultured on LB agar or LB broth supplemented with 50 µg/ml ampicillin, as the plasmids used confer ampicillin resistance. All cultures were incubated at 37°C, and broth cultures were shaken at 200-250 rpm. *E. coli* growth for protein expression studies is described below.

Table 2.1: *E. coli* strain used for the cloning

E. coli	Genotype	Reference
BL21 Origami B (DE3)	F$^-$ *ompT hsd*S$_B$(r$_B^-$ m$_B^-$) *gal dcm lacY1 ahpC* (DE3) *gor*522:: Tn*10 trxB* (Kan^R , Tet^R)	Novagen (MerckMIllipore)

Detail of the *E. coli* BL21 origami B strain is currently available at:
[Origami™ B(DE3) Competent Cells - Novagen | 70837 (merckmillipore.com)](#)

Plasmids for cloning and expression work (table 2.2) were either the pET plasmids pET21a, or pET20b, or the pJET plasmid which was commercially available with the blunt ended ligation kit that was used in the previous work.

Table 2.2: Plasmids for cloning and expression of recombinant proteins

Plasmid	Description	Phenotype	Source
pET21a	Suitable as a cloning vector, also for protein expression with *N*-terminal His$^+$ tag for affinity chromatography	Ampicillin Resistant	Novagen
pET20b	Suitable as a cloning vector, also for protein expression with C-terminal His$^+$ tag for affinity chromatography	Ampicillin Resistant	Novagen
pJET	Cloning vector only. Suitable for blunt ended ligation	Ampicillin Resistant	Novagen

2.1.1 Bacterial Transformation

E. coli strain used was the electrocompetent (BL21 Origami) from Sigma Aldrich.

2.1.1.0 Transformation of *E. coli* BL21 Origami

2.1.1.1 Preparation of Electrocompetent BL21 Origami

Preparation of electrocompetent *E. coli* largely involves removal of ionic components from the bacterial suspension in order to prevent arcing during electrotransformation. *E. coli* were cultured in 25 ml LB broth to an OD600 of 0.5-0.7 (mid log phase). Cultures were pelleted by centrifugation at 3500 g for 15 minutes, then resuspended gently in 25 ml icecold 10 % glycerol, and incubated on ice for 30 minutes. *E. coli* were pelleted, resuspended, and incubated in ice cold 10 % glycerol twice more; resuspended once in 12.5 ml glycerol, then in 1 ml glycerol. *E. coli* were aliquoted into 50 µl aliquots and stored at -80 °C until use in electrotransformation.

2.1.1.2 Electrotransformation

A Biorad Micropulser system was used according to manufacturer's instructions. Briefly, 10-100 ng of plasmid DNA was gently mixed with a 50 µl aliquot of electrocompetent *E. coli*. *E. coli*-plasmid mixtures were added to pre-chilled 0.1 cm electroporation cuvettes. The suspension was electroporated using a BioRad micropulser at the EC1 setting (1.8 kV potential difference, 200 Ω, time constants 1.0-4.0 milliseconds). After electroporation, cells in the cuvette were immediately mixed with 1 ml of room temperature LB, and incubated for 1 hour at 37 °C, with shaking at 200 rpm. 50 µl of recovered cell suspension 75 was plated onto LB agar supplemented with 50 µg/ml ampicillin, and incubated overnight at 37 °C. Colonies were patched by spreading over an area approximately 5 mm in diameter on a fresh LB agar plate (also supplemented with 50 µg/ml ampicillin and incubated overnight at 37 °C.

2.2 Protein Production and Purification by Affinity Chromatography

Expression strains could be induced to produce protein, then lysed, and lysates could undergo affinity chromatography to purify expressed protein. This relies on the production of a 6-Histidine tag (His+ tag) conjugated to the protein of interest in the cell lysate. In this project this was achieved using pET plasmid vectors. The His+ tagged protein can weakly bind to immobilised nickel (hence the term "affinity chromatography"), while the rest of the cell lysate flows through or is washed off. The His+ tagged protein is eluted from the nickel (Ni2+) using buffer containing imidazole, which interacts more strongly with nickel than the His+ tag. Affinity chromatography only works for purification of proteins in solution.

2.2.1   Protocol for Protein Expression

E. coli (Origami B) expressed strains from -80ºC were inoculated on freshly prepared LB (Luria Bertani) agar (Fisher Scientific, UK) supplemented with 50 µg/ml of Ampicillin (Amp.) (Sigma-Aldrich, Germany) and incubated at 37 °C for 24 hours. After the incubation period, a loopful of each bacterial strain was taken from the surfaces of respective LB agar plates using plastic disposable loops and was inoculated in a separate 1000 ml capacity beaker containing 500 ml 2XYT Broth (Fisher BioReagents, Belgium) (overhead space needed for aeration) and were incubated in an Innova 4300 Incubator Shaker (New Brunswick Scientific, UK) at 37 °C shaking at 200 rpm. The turbidity of the cultures was monitored using Jenway-7315

Spectrophotometer (Bibby Scientific Ltd, UK) until when the optical density (OD$_{600}$) of 0.6-0.7 nm was achieved (mid log phase). 1 ml of the liquid culture was taken and pelleted using LabBasics Microtubes Centrifuge (Scientific Laboratory Supplies), and the uninduced pellets were stored at -20 °C. The remaining large liquid culture was induced by the addition of 100 µl of 0.2 mM Isopropyl β-D-1-thiogalactopyranoside (IPTG) and left in the shaker incubator at 25°C overnight. 1 ml of the induced culture was also taken and pelleted, and the induced pellets stored at -20 °C. The remaining liquid cultures were transferred into falcon tubes and centrifuged at 10,000 rpm at 5 °C for 25 minutes using the high speed Beckman J2-21 Centrifuge (Beckman, USA), pellets were resuspended in 25 ml 50 mM sodium phosphate buffer and 500 mM sodium chloride (50 mM Na-Phosphate, 500 mM NaCl) at pH 7.4, and were frozen at -20 ˚C for storage until purification, or underwent protein purification immediately. The 1ml expressed uninduced and induced pellets were denatured using heat at 90ºC for 15 minutes and run on 12 % SDS-PAGE gels to determine the protein bands of interest.

2.2.2 Purification of Soluble Proteins

The *E.coli* that had been induced to express readily-soluble protein stored at -20 °C were thawed, if required, and resuspended in resuspension buffer (50 mM Sodium Phosphate buffer, 0.5 mM NaCl, 20 mM pH 7.4), and thoroughly mixed using pipette tips. 1 tablet of protease inhibitor (cOmplete cocktail EDTA free from Merck), was added to the 50ml resuspended pellets and were lysed by passing through a French Press machine (Thermo Electron Corporation) three times at 1000 psi. The lysate was first centrifuged at 5000 rpm and 4°C for 15 minutes and later at 10,000 rpm for 45 minutes using Beckman Coulter Avanti J26XP High-Speed Centrifuge (Beckman, USA). The supernatant was decanted into a new falcon tube and underwent affinity chromatography using a 1ml Ni^{2+} column (GEHealthcare, UK) set up on MasterFlex L/S Economy Drive (Cole-Parmer Instrument Company) at a flow rate of1 ml/min, which was washed using 10-20 ml of wash buffer (20 mM imidazole, 50 mM sodium phosphate buffer, 0.5 M NaCl, pH 7.4) at a flow rate set at 2 ml/min. Proteins were manually eluted from the column in 1 ml fractions using an elution buffer (300 mM imidazole, 50 mM sodium phosphate buffer, 0.5 M NaCl, pH 7.4). Cell lysates, flow-through, wash-through, and elutions 1 to 5 were tested for the presence of over-expressed protein and purity using 12 % SDS-PAGE. Fractions containing pure proteins were pooled and dialyzed in 2000 ml dialysis buffer (50 mM sodium

phosphate, 200 mM NaCl, pH 7.4) at 4 ˚C for 24 hours, after which, they were stored at 4 °C or can also be stored at -20˚C for longer-term.

2.3   Preparation of 12% Sodium Dodecyl Sulphate Polyacrylamide Gel Electrophoresis (SDS-PAGE)

12 % Sodium Dodecyl Sulphate Polyacrylamide Gel Electrophoresis (SDS-PAGE) was used in determining the different protein bands (molecular weight in kDa), of the expressed and purified proteins (NanH and SiaPg). Briefly, to prepare 1 gel of 12% SDS-Gel, resolving gel, 3ml of acrylamide, 2.5ml lower tris and 4.3ml of distil water were mixed in a 50ml falcon tube, followed by the addition of 5 µl of tetramethylethylenediamine (TEMED) and 350 µl of 10 % Ammonium persulphate (APS), and poured immediately into the Bio-Rad supplied glass compartment up to about three quarter (3/4) of the total height using Pasteur pipette and was allowed to polymerize (gel). The surface of the gel was overlaid with isopropanol to prevent air bubbles from disrupting proper gel formation and left to polymerise. The overlay was washed with water before pouring the stacking gel. Stacking gel is prepared by mixing 0.975 ml of acrylamide, 2.1 ml of upper tris and 4.725 ml of distil water in a falcon tube containing 17 µL of TEMED, 100 µL of 10 % APS and was added to fill up the remaining space in the Bio-Rad cassette. The sample well-comb was inserted immediately to form wells and the suspension was allowed to stand for 10-20 mins to polymerise.

After the gel has polymerised, it was placed in a Bio-Rad SDS-PAGE tank (mini–PROTEAN Tetra System) filled with a running buffer. The induced, uninduced, lysates, flow through, wash through and elution 1 to 5 of the protein samples were resuspended in 200 µl of SDS-PAGE lysis buffer and heated at 95 °C for 15 minutes on Jencons-PLS Dry bath (Jencons-PLS Bedfordshire) to denature the protein. 10 µl of each sample was loaded into respective wells of the SDS-PAGE gel, with the first well containing 3 µl of molecular weight marker (Protein Ladder, ThermoFisher Scientific).

Gels were run at 100 V for 15 minutes and later increased to 120 V for 80 minutes until the loading dye was seen at the bottom of the gels. The gels were removed from the glass cassette compartments using spatula and placed in a plastic container which was subsequently flooded with ~20 ml InstantBlue™ (Coomassie dye) to stain for at least

1 hour at room temperature with constant agitation after which the stained gels were washed using water.

Image of the stained gel showing the respective protein bands was captured using Syngene Ingenius 3 (GeneSys) UV machine and compared to the known bands of protein of interest on the protein ladder in kDa.

2.4   Bicinchoninic Acid Assay (BCA)

The BCA assay was used for colorimetric detection and quantification of total protein present in the purified samples. The principle of this method is that protein can reduce Cu^{+2} to Cu^{+1} in an alkaline solution thereby resulting in a purple colour formation by bicinchoninic acid. The Pierce BCA assay kit (Thermo-Fisher Scientific) reagent A and reagent B were routinely used according to the manufacturer's instructions. The protein samples and known concentrations of bovine serum albumin (BSA) standards used for standard curves were also diluted in the same resuspension buffer (50 mM Na-Phos, 200 mM NaCl at pH 7.4) used during protein purification. The BCA assay was conducted in a transparent 96-well plate and was incubated in a thermo-shaker (Grant Instruments Ltd, England) at 37°C for 30 minutes rotating at 500 rpm after which the absorbance was read using TECAN plate reader at OD_{562} nm and the result interpreted on Microsoft Excel to determine the protein concentrations.

2.5   Determination of Sialidase Activity

2.5.1 Reaction kinetics of sialidases (NanH and SiaPg) using 4-Methylumbelliferyl-*N*-acetyl-α-D-neuraminic acid sodium salt (MU-NANA)

4-Methylumbelliferyl-*N*-acetyl-α-D-neuraminic acid (MU-NANA) (Carbosynth) was used as the substrate to determine the reaction kinetics of purified NanH and SiaPg. Briefly, increasing concentrations of MU-NANA (10-400 µM) were exposed to 2.5nM of NanH or 5nM SiaPg in 50 mM sodium phosphate, 200 mM NaCl, pH 7.4. The reactions were incubated for up to 5 minutes at room temperature. After every1-minute interval, 50 µL of each reaction was taken and quenched by adding 75 µL of 100 mM sodium carbonate buffer, pH 10.5. Fluorescence of the 4-Methylumbelliferyl (4-MU) released at each time point was measured using a Tecan Infinite M200 microplate

reader (Tecan Australia GmbH) at excitation 355 nm and emission at 450 nm. Three (3) technical replicates were taken to calculate the reaction velocity for each substrate concentration (unless specified otherwise). The results were found to be similar to the previous experiments conducted in our laboratory. The 4-MU release rate was quantified by applying the fluorescence readings to the 4-MU standard curve. Rate of reaction was determined by first finding the initial rate of reaction, which occurred between 1 and 3 minutes for NanH and 3 to 5 minutes for SiaPg. The initial rate also referred to as velocity (V0, 4-MU release µmol/min/mg), was plotted against MU-NANA concentrations (µM), and the K_M and Vmax were determined in GraphPad PRISM 8.0 software by fitting the following nonlinear equation using the least-squares method:

$$Y = Vmax \; X \frac{X}{Km + X}$$

Where X stands for the substrate concentration, Y for the enzyme velocity, $Vmax$ is the maximum enzyme velocity and K_M (Michaelis constant) is the concentration at half maximal velocity when the enzyme becomes saturated. The $k$cat values were determined in GraphPad PRISM 8.0 software (or as stated under the analised figure), by fitting the following nonlinear equation using the least-squares method:

$$Y = Et \; x \; Kcat \; X \frac{X}{Km + X}$$

Where X refers to the substrate concentration, Y the enzyme velocity, Et is the concentration of enzyme active sites, $k$cat stands for the turnover number and K_M is the concentration at half maximal velocity when the enzyme becomes saturated.

2.5.2 Sialidase Activity of Purified Enzymes (NanH and SiaPG)

Sialidase activity of the purified enzymes was quantified by observing the cleavage of 4-methylumbelliferyl N-acetyl-α-D-neuraminic acid sodium salt (MUNANA; Carbosynth, UK), to yield Neu5Ac and the fluorochrome 4-Methylumbelliferone (4-MU). The reaction was conducted in triplicate in black non-transparent flat-bottomed 96-well polystyrene plates (Greiner, UK). Briefly, sodium phosphate buffer (50 mM sodium phosphate buffer, 200 mM sodium chloride) was adjusted to 0.1 N HCl to pH

7.4 with a pH meter (Thermo Fisher Scientific Inc.,Waltham, MA, USA). NanH (2.5nM) and SiaPg (5nM) were solubilized in sodium carbonate buffer and MUNANA substrate (0.2mM) was added and incubated at room temperature for 2 minutes (NanH) or 4 minutes (SiaPg). 75 µL of 100 mM sodium carbonate (Na_2CO_3) buffer pH 10.5 (which is a mixture of sodium carbonate and bicarbonate made according to Sigma-Aldrich buffer reference) was added to stop the reaction. Fluorescence was measured using a Tecan Infinite M200 microplate reader (Tecan Australia GmbH) at excitation 355 nm and emission at 450 nm.

2.5.3 Sialidase Activity of Whole Bacterial cells

Bacterial cells (*T. forsythia* or *P. gingivalis*) grown on FA agar plates were scraped and washed by resuspension in 1 ml PBS pH 7.4 (Sigma Aldrich), and centrifuged at 13,000 X g for 2-3 minutes. Supernatant was disposed of and cell pellets were resuspended in PBS and adjusted to optical density (OD_{600}) of 0.05. The reaction was conducted in triplicate in a black flat-bottomed 96 well polystyrene plates (Greiner, UK), and the reaction mixture include 80 µL PBS pH 7.4 (Sigma Aldrich), 10 µL 0.2 mM of 4-methylumbelliferyl *N*-acetyl-α-D-neuraminic acid sodium salt (MUNANA; Carbosynth, UK), and 10 µL 0.05 (OD_{600}) of bacterial suspension and incubated at 37 ˚C for 30 minutes (*T. forsythia*) or 1 hour (*P. gingivalis*). At respective time point, 50 µL of the reaction mixture was taken and stopped by adding 75 µL of 100 mM sodium carbonate buffer (Na_2CO_3), pH 10.5 and fluorescence was measured at excitation 355 nm, emission 430 nm using TECAN Infinite M200 plate reader. Sialidase activity was quantified by observing the cleavage of MU-NANA to yield Neu5Ac and the fluorochrome 4-Methylumbelliferone (4-MU).

2.6 Sialidase Inhibition Assay

2.6.1 Inhibition of purified NanH and SiaPg

A wide range of sialidase inhibitors (synthetic and plant-derived) listed in table 2.3, were used in this project to determine their effect on sialidase (NanH and SiaPg) inhibition. Stock concentrations of the inhibitors were prepared in their respective diluent (water, methanol, DMSO, acetone), and appropriate volume of each varying inhibitor's concentrations (0-10mM) diluted in the reaction mixtures was used. Briefly, 2.5 nM NanH or 5 nM SiaPg were solubilized in 50mM sodium phosphate, 200 mM

NaCl, pH 7.4, in the presence of increasing concentrations of an inhibitor and 0.2 mM MU-NANA was added and the reaction mixture incubated at room temperature for 2 minutes (NanH) or 4 minutes (SiaPg). 50 μL reactions were removed at 1 minute intervals and quenched by the addition of 75 μL 100 mM sodium carbonate, pH 10.5. Fluorescence of 4-MU release at each time point was measured using a Tecan Infinite M200 at excitation 355 nm and emission at 450 nm. Three experimental repeats were used in calculating the reaction velocity for each inhibitor concentration. Sialidase inhibition was expressed as the percentage change in fluorescence with a given concentration of inhibitor compared to fluorescence in the absence of inhibitor, as determined by the formula below.

Fluorescence at 0mM inhibitor $\qquad$ x 100 = Change in fluorescence (%)
Fluorescence at 0-10mM inhibitor

IC_{50} of the inhibitors was calculated by plotting the percentage sialidase activity relative to no inhibitor (%) against Log[inhibitor], and the variable slope model was applied to obtain the IC_{50} of each inhibitor on NanH and SiaPg using the formula below;

$$Y = \frac{100}{(1 + 10(LogIC50 - X) \ X \ Hillslope)}$$

Where; Y = Sialidase Activity relative to no inhibitor condition (%)

X = Log[Inhibitor]

Hillslope = Steepness of the curve.

Table 2.3: List of Inhibitors Tested in this Project

S/No.	Inhibitors	Supplier/Product code/CAS-No.	Diluent
01.	Zanamivir	CarboSynth/BZ164566/551942-41-7	dH$_2$O
02.	Siastatin B	CarboSynth/FS11418/54795-58-3	"
03.	DANA	CarboSynth/MA05288/25875-99-4	"
04.	Oseltamivir	CarboSynth/FO26594/197227-45-8	"
05.	Epicatechin gallate	CarboSynth/ABA61505/25615-05-8	DMSO
06.	Berberine chloride	CarboSynth/FB64955/2086-83-1	Methanol
07.	Palmatine	CarboSynth/FP65894/3486-67-7	PBS
08.	idoBR1 (Iminosugars from PhytoQuest)	CarboSynth/MI164687/108428-44-0	dH$_2$O
09.	BR1 (Iminosugars from PhytoQuest)	CarboSynth/FT181792/96861-04-0	"
10	DNJ (Iminosugars from PhytoQuest)	CarboSynth/ MD05255/19130-96-2	"
11	Neu5Ac2en	Prof. Xi Chen	"
12	Neu5Gc2en	"	"
13	Neu5Ac9N$_3$2en	"	"
14	Neu5Ac9NAc2en	"	"
15	Neu5Ac9cyclo2en	"	"
16	Pra-Neu5Ac2en	"	"
17	2e3eDFNeu5Ac	"	"
18	2e3aDFNeu5Ac	"	"
19	2e3eDFNeu5Ac9N$_3$	"	"
20	2e3aDFNeu5Ac9N$_3$	"	"

dH$_2$O = distilled water, DMSO = Dimethyl sulfoxide, PBS = Phosphate-Buffered Saline, Prof. Xi Chen, Department of Chemistry, University of California-Davis One Shields Avenue, Davis, CA 95616

2.7 Synergistic effects (Combination therapy) of inhibitors on NanH sialidase

The synergistic effects of Palmatine and Berberine chloride on NanH sialidase inhibition were measured according to the drug combination studies described by Chou (2008). Briefly, 10 µL of each varying concentration: Palmatine (0.225, 0.2, 0.15, 0.125, and 0.1 mM), Berberine chloride (0.55, 0.5, 0.45, 0.4, 0.35 mM) were added in a constant ratio (1:1) to the MUNANA substrate (0.2 mM), and the enzyme reaction was initiated by the addition of NanH sialidase (2.5 nM) a black flat-bottomed 96-well polystyrene plate and incubated at room temperature for 2 minutes. The reaction was stopped by the addition of 75 µL of sodium carbonate buffer (pH 10.5). The absorbances were obtained using a Tecan Infinite M200 microplate reader (Tecan Australia GmbH) at excitation 355 nm and emission at 450 nm. The IC_{50} values of each compound and IC_{50} value in combination were determined separately using the CompuSyn software (version 1.0) of Chou and Martin (2005) to assess synergistic, additive, or antagonistic effects of the compounds. Figure 2.1 below illustrates the combination format, while figure 2.2 illustrates the mechanism of action (MOA) of inhibitors.
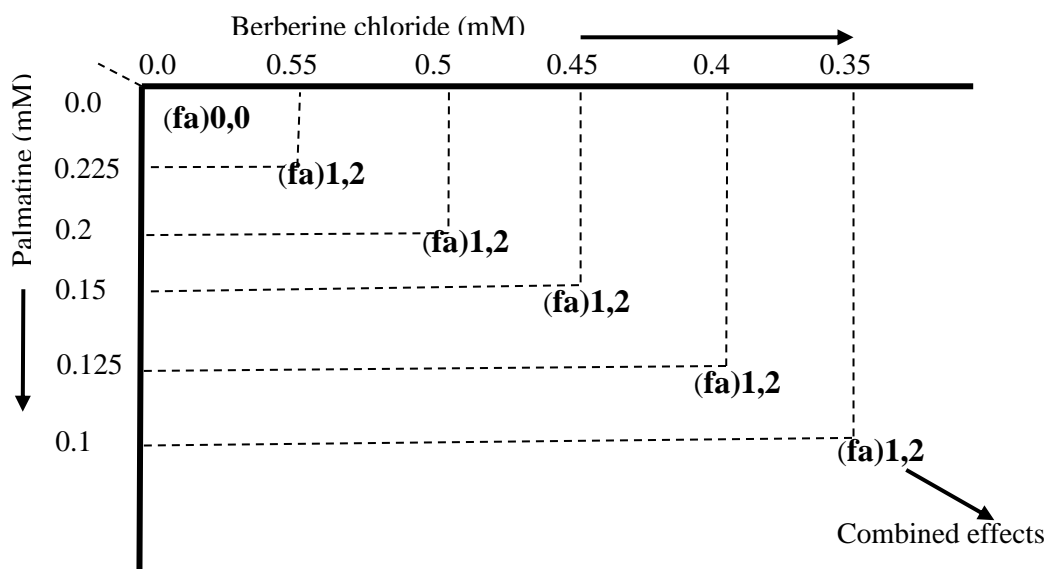
Figure 2.1: Drug Combination layout

10 µL of each varying concentration of Palmatine and Berberine chloride as indicated above were added in constant ratio (1:1) to the MUNANA substrate (0.2mM), and the enzyme reaction was initiated by the addition of NanH sialidase (2.5nM) in a black flat-bottomed 96-well polystyrene plates, and incubated at room temperature for 2 mins. Absorbance was read at 355 nm and at emission 450nm.

2.7.1 Determination of the combination index (CI)

The combination index (CI) values were determined by the method described by Chou (2006). This method provides the theoretical background for the CI-isobologram equation that allows for the determination of compound interactions. Therefore, CompuSyn (version 1.0) was used to simulate the synergism and antagonism of the compounds at any ratio. The CI equation for two compounds is.

$$CI = (D)1/(Dx)1 + (D)2/(Dx)2 = (D)1/(Dm)1[fa/(1 - fa)]^{1/m1} + (D)2/(Dm)2[fa/(1 - fa)]^{1/m2}$$

where (Dx)1 for (D)1 "alone" that inhibits a system x%, and (Dx)2 for (D)2 "alone" that inhibits a system x% whereas in the numerator, (D)1 + (D)2, "in combination" also inhibit x%. Note that the denominators of the last two terms are expressed as median effects. The CI value quantitatively defines synergism (CI < 1), an additive effect (CI = 1), and antagonism (CI > 1) (table 2.4).

In single drug dynamics, the equation is defined as $fa/fu = [D/Dm]^m$, where fa is the affected fraction of the system and fu is the unaffected fraction (fu = 1 - fa); D is the dose required to produce fa; Dm is the dose required to produce median effects, such as ED50 or IC50; and m is sigmoidicity (shape).

Table 2.4: Description and symbols of synergism or antagonism in drug combination studies analyzed with the CI method.

Range of combination index	Description	Graded symbols	Graphic symbols
<0.1	very strong synergism	+++++	■
0.1-0.3	strong synergism	++++	■
0.3-0.7	synergism	+++	▪
0.7-0.85	moderate synergism	++	▪
0.90-1.10	nearly additive	±	▪
1.10-1.20	slight antagonism	-	▪
1.20-1.45	moderate antagonism	- -	▪
1.45-3.3	antagonism	- - -	▪
3.3-10	strong antagonism	- - - -	■
>10	very strong antagonism	- - - - -	■

Explanation: The combination index (CI) method is based on those described by Chou and Talalay and the computer software of Chou and Martin (2005). The ranges of CI and the symbols are refined from those described earlier by Chou (1991). CI<1, =1 and >1 indicates synergism, additive effect and antagonism, respectively (Reproduced from Ting-Chao Chou, 2008).

2.8   Determination of Mechanisms of Action (MOA)

2.8.1   Lineweaver Burk plot model

Lineweaver Burk plot model as described by Cornish-Bowden (1999), and the non-linear fit were used in determining the mechanism of action (MOA) of the sialidase inhibitors on NanH. For Lineweaver-Burk Plot model, varying MUNANA substrate concentrations (0.5, 1, 2 and 4mM) were exposed to NanH sialidase (2.5nM) diluted in 50 mM sodium phosphate buffer, 200 mM NaCl at pH 7.4 and incubated at room temperature. 50µL of the reaction set up was taken and stopped by the addition of 75µL of 100mM Na_2CO_3 buffer pH10.5 at 1, 2, 3, and 4 minutes respectively. The fluorescence was measured using a TECAN M200 plate reader at excitation 355 nm and emission at 430 nm and the mode of enzyme inhibition was determined using the Lineweaver-Burk Plot model on Microsoft Excel version 2205.

2.8.2   Nonlinear fit model

For nonlinear fit model of determining the MOA of inhibitors, varying substrate (MUNANA) concentrations (0.05, 0.1, 0.15, 0.2 and 0.25mM) were exposed to NanH sialidase (2.5nM) in the presence and absence of the inhibitor (2e3aDFNeu5Ac9N3), and diluted in 50 mM sodium phosphate buffer, 200 mM NaCl at pH 7.4 and incubated at room temperature. 50µL of the reaction set up was taken and stopped by the addition of 75µL of 100mM Na_2CO_3 buffer pH10.5 at 1, 2, 3 and 4 minutes, respectively. The fluorescence was measured using TECAN M200 plate reader at excitation 355 nm and emission at 430 nm and the mode of enzyme inhibition was determined using Prism version 9.2.0.
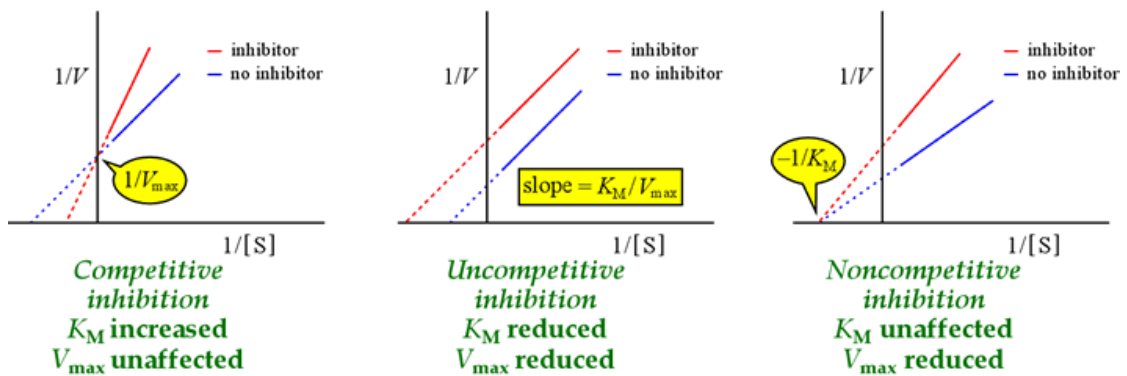
Figure 2.2: Illustration of Lineweaver-Burk plots for mechanisms of action

1. Competitive inhibitor (**Km**-pitive inhibitor): **Km increases**, Vmax doesn't change
2. Non-competitive inhibitor (**Non-Km**-pitivie inhibitor): **Km doesn't change**, Vmax decreases

2.9 Molecular docking and Protein-Ligand interactions

Molecular docking was done using AutoDock Vina (version 1.5.7) to study the binding efficiency of Oseltamivir, Siastatin B, DANA, and the di-fluoro sialic acid analogue 2e3aDFNeu5Ac9N3 into the active site of NanH-apo (PDB ID 7QYP) sialidase of *T. forsythia*. The protein-ligand interactions were visualised using PyMol (version 2.5.4). The protein (NanH-apo) and ligands (inhibitors) were prepared on AutoDock Vina, polar hydrogens were added to the protein and ligands, and Kollman and Gasteiger charges were added to the protein and ligands, respectively. Further, for docking score calculation, the grid box coordinates used were X = 60, Y = 44, Z = 52 and x = 21.959, y = -1.341, and z = 14.056, at an energy range of 3, and an exhaustiveness of 8.

2.10 The Role of Sialidase in Bacterial Growth and Biofilm Formation

2.10.1 *P. gingivalis* Growth, and Biofilm Enumeration using Crystal Violet Method

Wild-type and sialidase-deficient strains of *P. gingivalis* (PG0381 and ΔPG0381), were cultured on fastidious anaerobe (FA) plates supplemented with 10% oxalated horse blood (Oxoid), and incubated in an anaerobic chamber (Don Whitley Scientific, Shipley UK) at 37°C, 10% CO_2, 10% H_2, and 80% N_2 for 72 hours. Liquid cultures were grown

in Brain Heart Infusion Broth (Oxoid Ltd, UK) supplemented with 2% yeast extract (Oxoid Ltd, UK), 1mg/ml hemin, 250µg/ml cysteine, 1 mg/ml menadione (vitamin K), 5 µg/ml gentamicin and were equilibrated by incubating in an anaerobic chamber overnight at 37°C, 10% CO_2, 10% H_2, and 80% N_2.

The *P. gingivalis* (wild and mutant strains) liquid culture incubated overnight was diluted to OD_{600} 0.05 and 200 µL of the suspensions were seeded in the Bovine Submaxillary Mucin (BSM) coated flat-bottomed 96-well tissue culture polystyrene plate (Greiner, UK), while the remaining surrounding wells were filled with sterile supplemented BHI (negative control) and the plating container padded with a tissue soaked in distilled water (to avoid evaporation). The plate was incubated in an anaerobic chamber at 37°C, 10% CO_2, 10% H_2, and 80% N_2 for 72 hours after which, the total growth was determined by measuring the optical density at 600 nm using TECAN Infinite M200 plate reader. Suspensions were aspirated with a multi-channel pipette and washed three times with 200 µl PBS and blotted with absorbent paper to remove residual PBS then stained with 100 µl 0.1% crystal violet (CV) for 20 minutes at room temperature. The CV was discarded and washed with PBS thoroughly and then allowed to air dry. The stained biofilms were destained by adding 100 µl of ethanol: acetic acid (80:20) in each well and incubated at room temperature for 5 minutes before transferring to a new clear flat-bottomed 96-well polystyrene plate and read at 575 nm using TECAN plate reader. The biofilm formed was standardized against growth by dividing the OD_{575} absorbance values by the OD_{600} initial readings.

2.10.2 Autoaggregation and Sedimentation Assay

Autoaggregation of wild-type and mutant strains of *P. gingivalis* 0381 was performed as described by (Davey & Duncan, 2006). Briefly, the strains were grown on fastidious anaerobe (FA) agar plates as described in section (2.10.1), pelleted at 13000 xg for 5 minutes, and washed twice in phosphate-buffered saline (PBS) pH 7.4. The pellets were then resuspended in PBS and adjusted to an OD_{550} of 0.8 and incubated at 37°C in an anaerobic condition. The absorbance (OD_{550}) of the respective cell suspension (1 ml each) was taken gently after every 30 minutes and measured using a spectrophotometer (JENWAY 7315). A steady decrease in absorbance indicates autoaggregation and sedimentation.

2.10.3 *T. forsythia* Growth, and Biofilm Enumeration via Counting of Matured cells

T. forsythia (ATCC 43037) was routinely grown either in supplemented liquid culture [TSB: 10% trypticase soy broth (TSB; Oxoid) supplemented with 2% yeast extract (YE; Sigma), 1 mg haemin ml^{-1} and 1 mg menadione ml^{-1} (Sigma), 10 µg *N*-acetylmuraminic acid ml^{-1} (NAM; Sigma)], or on Fastidious Anaerobe agar plates (FA; Oxoid) supplemented with 5 % horse blood containing 10 µg NAM ml^{-1} and 50 µg gentamicin ml^{-1}. Broth cultures and FA-NAM plates were typically incubated at 37 °C in an anaerobic atmosphere (10 % CO_2, 10 % H_2, and 80 % N_2) for 5 days (or as stated). The sialidase mutant (ΔnanH) strain was grown in a similar manner but with 5 µg erythromycin ml^{-1} (Honma et al., 2011).

For biofilm growth, 5 days old bacterial cells growing on FA agar were harvested and washed twice in a fresh equilibrated TSB. The washed bacterial cells were diluted and adjusted to a final OD_{600} of 0.05 in the supplemented TSB and were used to inoculate the 96-well plate coated overnight with a commercially readily available bovine submaxillary gland (6 mM mucin) which serves as the source of glycoprotein. The glycoprotein-coated 96-well tissue culture plates were kept in the fridge at 4°C overnight before being washed gently with PBS (pH 7.4) to wash off excess protein. The inoculated coated plates were incubated at 37°C in an anaerobic atmosphere (10% CO_2, 10% H_2, and 80% N_2) for 5-6 days (Roy et al., 2010).

Matured biofilm cells were assessed as described previously. Briefly, after 5 days of growth and removal of the culture medium, sample wells were washed 2-3 times in sterile PBS, followed by vigorous resuspension of the biofilm cells in PBS using a pipette. 10 µL of the resuspended cells were placed on a glass slide and counted microscopically using a Helber counting chamber (Hawksley) under a phase-contrast lens (magnification x400) or the Olympus BX51 microscope. This method of counting the matured biofilm cells was used in place of crystal violet assay due to the light nature of the biofilms formed by *T. forsythia,* unlike *P. gingivalis* which forms a strong biofilm.

2.10.4 Investigating the Effect of Sialidase Inhibitors on Biofilm growth

The effect of the sialidase inhibitors against biofilms of *T. forsythia* or *P. gingivalis* was assessed by their inclusion at final respective concentrations in the medium. For *T. forsythia*, the matured biofilm cells were counted using the Olympus microscope, while

for *P. gingivalis*, the crystal violet method was used to ascertain the antibiofilm properties of the respective sialidase inhibitors. These concentrations (IC50 values of the inhibitors) were chosen because it was shown to inhibit whole-cell sialidase activities (Table 3.2) and suppressed planktonic growth of both *T. forsythia* and *P. gingivalis* ().

For the measurement of the antiadhesion properties of the compounds, the bacterial cells were incubated in the presence of the inhibitors for 3-4 hours to allow for preformed biofilms and matured cells were counted as described.

2.11 Determination of the Inhibitors' Effects on Bacterial Growth

2.11.1 Percentage *P. gingivalis* and *T. forsythia* Planktonic growth

To investigate the inhibitory effects of 2e3aDFNeu5Ac9N3 on bacterial planktonic growth, *P. gingivalis* or *T. forsythia* growing on supplemented FA plates were harvested and washed 2-3 times in BHI or TSB. Bacterial cells were adjusted to OD_{600} 0.05 to 0.1 in the supplemented liquid medium (BHI/TSB) and 200 µl were dispensed (in triplicate) into a 96-well polystyrene tissue culture plate (Greiner, UK) in the presence or absence of the compound and the plate was inserted into a Cerillo device and incubated anaerobically at 37°C for 3 days (*P. gingivalis*) or 5 days (*T. forsythia*). The Cerillo device was programmed to measure the absorbance (planktonic growth) after every 30 minutes, after which the data was collated and analysed on an Excel sheet and GraphPad Prism (version 9.5.1).

To assess the effect of Palmatine and Berberine chloride on the bacterial planktonic growth, a similar method was followed and the cells suspended in a supplemented liquid medium were dispensed (in triplicate) into a 96-well polystyrene tissue culture plate (Greiner, UK) in the presence or absence of the compounds Palmatine (1, 0.5, and 0.15mM); Berberine chloride (1, 0.5 and 0.45mM), respectively and incubated anaerobically at 37°C for 3 days (*P. gingivalis*) or 5 days (*T. forsythia*). Following the period of the incubation, OD_{600} absorbance of the plate was read using a TECAN M200 plate reader, followed by a Miles-Misra assay where the colony forming units (CFU) were determined and the percentage inhibition of planktonic growth was calculated.

2.11.2 Determination of Colony Forming Units (cfu)

The Miles-Misra technique was carried out to determine the colony-forming units after treating the bacterial cells with the inhibitors. 1 in 10 serial dilutions of the suspension was carried out, and 10 µl from each dilution factor containing varying concentrations of the plant-derived compounds were spotted in duplicate on fastidious agar plates and incubated anaerobically for 5 days. Following the incubation period, the colony-forming units (cfu) were assessed.

2.12 Sialic acid Utilization by *Tannerella forsythia* (ATCC 43037)

In order to assess if *T. forsythia* utilizes other forms of sialic acid such as 2-keto-3-deoxynononic acid (KDN) or *N*-acetylneuraminic acid (Neu5Ac) just as it requires *N*-acetylmuramic acid (NAM) for growth, bacterial cells were adjusted to OD_{600} 0.05 t0 0.1. After which, cells were suspended in a liquid medium supplemented with 6 mM of respective sialic acid, and 200 µL of each treatment in triplicates were dispensed in respective wells of a 96-well polystyrene tissue culture plate (Greiner, UK), and incubated at 37°C, 10% CO_2, 10% H_2, and 80% N_2 for 7 days. The bacterial planktonic growth was measured using a TECAN M200 plate reader. The gram-staining technique was used to study the morphological appearances and bacterial growth (utilization) data were analyzed using GraphPad Prism (version 9.5.1).

2.13 Passaging of H357 Oral Squamous Cell Carcinoma (OSCC)

The H357 oral squamous cell carcinoma (OSCC) were grown in T75 flask to a confluence level of 70-80% in Dulbecco's Modified Eagle's Medium (DMEM) low glucose supplemented with 5 ml L-glutamine, 5 ml Penicillin/Streptomycin and 50 ml foetal bovine serum (Sigma-Aldrich, Germany). The H357 cells were washed 2 to 3 times with sterile PBS then 2 ml of trypsin EDTA 1 x buffer was dispensed into the T75 flask and incubated at 37°C, 5% CO_2 for 10 minutes. The detached cells were viewed under x100 phase contrast microscope to ensure they are not over trypsinized after which 4 ml of the supplemented DMEM was added to neutralise the trypsin effect. The suspension was transferred to the centrifuge tube and centrifuged at 1000 rpm for 5 minutes after which the supernatant was discarded, and the cell pellets resuspended in 1 ml of DMEM and counted using Neubauer haemocytometer. Briefly; 10 µl of the suspension was dispensed in each well of the Neubaur improved haemocytometer,

covered with glass cover slip and counted under x100 magnification. 10 ml of fresh supplemented DMEM was dispensed in a new T75 flask and 200 µl of known concentrations of the resuspended pellets was added, rocked gently, and incubated at 37°C, 5% CO_2 for 3-4 days to get 70-80% confluence level.

2.14   Bacterial Invasion Assay

Bacterial attachment, total association and invasion assay was tested by infecting the H357 cells with both wild type and mutant strains of *T. forsythia* or *P. gingivalis*. Briefly, 1 ml of passaged H357 cells resuspended in supplemented DMEM was dispensed in each well of 24-well plates (including sacrificial wells) and incubated at 37°C, 5% CO_2 for 3-4 days to obtain 80-100% confluence level. At the end of the 3-4 days incubation period, the content of the sacrificial wells was discarded and washed 3 times with 1 ml sterile PBS after which, 500 µl of trypsin was added and incubated at 37°C, 5% CO_2 for 10 minutes to detach the cells. The cell pellets were treated and counted as described in section 2.13 above which was used in determining the multiplicity of infection (MoI) afterwards. The contents of the remaining wells (Total association and Invasion) were discarded and washed twice with sterile PBS followed by the addition of 500 µl of sterile filtered 2% Bovine serum albumin (BSA) and incubated at 37°C, 5% CO_2 for 1 hour. After the 1 hour incubation period, the BSA was discarded and washed three times with sterile PBS and 500 µl each of wild type and mutant strains of the pathogen (based on the MoI) were dispensed in both Total association (TA), Invasion (Inv) and Viability (Viab) wells (in triplicate) and incubated at 37°C, 5% CO_2 for 1.5 hours. The bacterial suspension in TA and Invasion wells were discarded leaving the one in viability wells (this does not contain H357 cells as such represents the total number of viable bacterial cells added in the assay), and the evacuated wells were washed three times with 1 ml sterile PBS. 500 µl of 200 µg/ml of metronidazole (Sigma-Aldrich) dissolved in DMEM with no supplement was added only to invasion wells (to inhibit any attached pathogen that did not invade the infected H357 cells), and was incubated at 37°C, 5% CO_2 for 1 hour after which it was washed three times with sterile PBS. 200 µl of sterile water was added only to TA and Invasion wells (to lyse the H357 cells) and was scraped with pipette tips for at least 45 seconds. Double fold serial dilutions were carried out in a clear flat-bottomed 96-well polystyrene plates (Greiner, UK), followed by Miles-Misra spotting (in triplicate) on either fastidious anaerobe agar with blood for *P. gingivalis* or fastidious anaerobe agar

(NeoGen Culture Media, UK) supplemented with oxalated horse blood (Oxoid) and NAM (*N*-acetylmuramic acid), for *T. forsythia*. The plates were incubated in an anaerobic chamber (Don Whitley Scientific, Shipley UK) at 37°C, 10% CO_2, 10% H_2 and 80% N_2 for 7 days for *P. gingivalis* and 9-10 days for *T. forsythia*. At the end of the incubation period, the colony forming units (CFU) were counted using the below formula and significant differences in total association, adhesion and invasion were determined by a series of paired t-tests or ANOVA in Prism GraphPad. This assay was considered appropriate since the main objective was to assess those bacteria that adhered or invaded the H357 OSCC independently of each other.

Viability = (CFU X 20) x Dilution factor x 2.5

>   Where: Viability = number of bacteria that survived

Invasion = (CFU x 20) x Dilution factor

>   Where: Invasion = number of bacteria that invaded the H357 cells

Total Association = (CFU x 20) x Dilution factor

>   Where: TA = total number of both bacteria that adhered and invaded the H357 cells

Percentage Invasion = Invasion/Viability X 100

Percentage TA = TA/Viability X 100

Since Total association = Adhesion + Invasion,

Adhesion (Attachment) = Total association – Invasion

Therefore, Percentage Adhesion = Adhesion/Viability x 100

2.15   Antibiotic Protection Assays (Anti-adhesion assay)

H357 cells were cultured as described in section 2.13, and resuspended at a density of $2x10^5$ cells ml^{-1} in DMEM supplemented with 10 % serum, 2 mM L-glutamine, and 1 ml of suspension per well was seeded into the wells of a 24-well tissue culture plate (Greiner, UK). Each of the experiments was divided into negative control (no sialidase inhibitors) and positive control to determine sialidase inhibition (media containing IC50

range of the inhibitors used), repeated in triplicate, and in duplicate on two separate plates: one plate for "total associated" bacteria, and one for "invaded" bacteria. The experimental set up were incubated at 37˚C, 5% CO_2 for 3-4 days to achieve at least 80% confluence level. After the 3 days incubation period, media from the "sacrificial well" was removed and the cells in the well were detached by trypsinization and counted by hemocytometer, to determine the number of cells per well.

The cell suspension (supernatants) in the remaining wells were discarded and washed gently 2-3 times with PBS pH 7.4 (Sigma Aldrich) and 500 µL of DMEM supplemented with 2% bovine serum albumin (BSA) was added to the wells and incubated at 37˚C, 5% CO_2 for 1 hour. Bacteria (*P. gingivalis* or *T. forsythia*) to be used in the assay were diluted in DMEM (un-supplemented) to a ratio of 1:100 host cells: bacteria in DMEM (un-supplemented). Bacterial suspension for the antibiotic protection assay was supplemented with IC50 range of the inhibitors used (to test for sialidase inhibition). Furthermore, bacterial suspension (conditions with and without inhibitors) was added to empty wells of the "invasion" plate. These bacteria form the bacterial "viability" control.

These suspensions were incubated with the host cells or in empty wells containing no host cells (bacterial viability) at 37 °C, 5 % CO_2 for 1hr30mins. After the 1hr30mins incubation period, the suspension in "invasion" wells were discarded and washed 2-3 times with filter-sterilised PBS, and DMEM which was supplemented with 200 µg/ml metronidazole was added only to wells of the designated "invasion" plate, then was further incubated at 37 °C, 5 % CO_2 for 1hr30mins. Suspensions from wells containing bacteria and host cells for "total associated" and "invaded" conditions were discarded, and wells were washed 2-3 times with filter-sterilised PBS before lysis using 200 µl of deionised water (sterile water), and scraping of the wells with a sterile pipette tip for one to two minutes. Bacterial suspension in the "viability" wells were resuspended by pipette mixing.

Bacterial suspension of the "viability" wells, cell lysates of the "total associated" and "invasion" wells then underwent four tenfold serial dilutions. The undiluted suspensions (in the first wells) and serially diluted suspensions were then plated onto the surfaces of fastidious anaerobe agar (appropriate for respective organisms) by Miles

and Misra method. Briefly: 10µl from each well of the serially diluted bacterial suspensions were spotted in triplicates (or as stated) onto FA agar appropriate for the organism, and incubated anaerobically at 37 °C, 5 % CO2 for 5 or 9 days.

After the required incubation period, individual colony formed (CFU) were counted, and the below formula was used to determine the number of bacteria/ml in each well of the "total associated" "invasion" or "viability" plates:

Total number of bacteria per ml = number of colonies formed x dilution factor x 20
After determining the mean number of viable bacteria per ml from the "viability" controls for no sialidase inhibitor and conditions with inhibitors (IC50 range), the percentage of viable bacteria that totally associated with and that which invaded the oral epithelial cells (H357), were calculated using the below formula. To obtain the number of attached bacteria (adhesion), the percentage of bacteria invaded (invasion) were subtracted from the percentage of total associated:

$$\frac{\text{Number of bacteria/ml}}{\text{Mean viable number of bacteria}} \times 100 = \% \text{Viable bacteria}$$

2.16   Cell Viability Assay

2.16.1 Trypan blue assay

Cytotoxicity is one of the most important indicators for biological evaluation in *in vitro* studies. To investigate cell death caused by a compound, various types of cytotoxicity or viability assays which depend largely on (i) dye exclusion assays; (ii) colorimetric assays; (iii) fluorometric assays; and (iv) luminometric assays are used.

Trypan blue assay, also known as dye exclusion method, helps in differentiating viable cells which exclude dyes, from dead cells that retain the dye. This assay is important in the determination of cell membrane integrity. Briefly, 200 µl H357 cells in DMEM were seeded at a density of 2×10^5 cells/ml into the wells of a 96-well tissue culture plate (Greiner), and incubated at 37°C, 5% CO_2 for 30 minutes and 1 hour in the presence or absence of 0.15 and 1mM Palmatine. After each time point, 50 µl of 0.4% trypan blue dye was taken and mixed with 50 µl of treated cells and allowed to stand for 3-4

minutes. The live and dead cells were counted under x100 phase contrast microscope using hemocytometer and the percentage viability calculated.

Cell counting

i.   The x10 objective was used. Both viable (unstained) and nonviable (stained) cell numbers were counted in each of the four corner quadrants (A, B, C, D), and the average of these four readings were taken and multiplied by 10^4 to obtain the total number of cells per mL in the cell sample that was placed on the hemocytometer.

ii. Multiply by two to take into account the 1:1 dilution of the sample in the trypan blue.

iii. Multiply by any dilutions in the original sample preparation of the cell suspension.

Number of cells (viable or nonviable)

$$= \frac{(A + B + C + D)}{4} \times 10^4 \times 2 \times \text{sample dilution}$$

iv. The percentage of unstained cells represents the percentage of viable cells in the suspension.

$$\% \text{ Viable cells} = \frac{\text{Number of viable cells}}{\text{Total number of cells}}$$

2.16.2 Lactate dehydrogenase (LDH) assay

The lactate dehydrogenase (LDH) assay depends on the detection of lactate dehydrogenase that has been released into culture supernatant from a damaged or lysed cell. During cytokine secretion experiments and cytotoxicity testing of different inhibitors, LDH from the supernatants of H357 oral squamous carcinoma cells was quantified using the Cytotox 96 LDH assay kit (Promega), according to the manufacturer's guides. Briefly, the assay detects the presence of lactate dehydrogenase in culture supernatant of H357 cells via the formation of a red formazan salt by components of a proprietary assay buffer and LDH. 50 µl of assay buffer was mixed with 50 µl of culture supernatant and incubated at 37 °C for 30 minutes after which, the reaction was stopped by the addition of 25 µl of a proprietary stop solution. The LDH was quantified by measuring the reaction optical density at OD_{490} using Tecan Infinite M200 plate reader. DMEM media alone was used as the negative control in all assays.

During cytokine secretion experiments using H357 cells, cells were seeded at a density 2×10^5 cells/ml with pathogens only or in the presence of inhibitors and incubated at 37°C, 5% CO_2 for 18-24 hours. The collected cell culture supernatants underwent an LDH assay immediately before storage at -20 °C to be used in cytokine assay.

2.16.3 PrestoBlue™ assay

The PrestoBlue is a ready-to-use cell permeable resazurin-based solution that functions as a cell viability indicator by using living cells' reducing power to quantitatively measure cell proliferation. When added to cells, the PrestoBlue® reagent is modified by the reducing environment of the viable cell and turns red in colour, becoming highly fluorescent. This colour change can be detected using fluorescence or absorbance measurements. The cell viability assay with PrestoBlue reagent was performed according to the manufacturer's protocol. Briefly, H357 cells in suspension were seeded at 2×10^5 cells per well in a 24-well tissue culture plate and incubated at 37 °C, 5% CO_2 for 24 hours to get 80% confluence. After 1hr 30 mins or 24 hours treatment of the cells with the sialidase inhibitors (1µM 2e3aDFNeu5Ac9N$_3$), the cells were washed and incubated with 10% PrestoBlue reagent and incubated at 37 °C, 5% CO_2 for 1 and 2 hours respectively. The cytotoxic effect of the sialidase inhibitor was detected by measuring the changes in cell viability using both fluorescence and absorbance spectroscopy. The absorbance was recorded at 570 nm after each time interval incubation with PrestoBlue reagent, whereas the fluorescence was read at excitation 570 nm and at emission 610 nm. The cell viability was expressed as a percentage relative to the cells untreated with sialidase inhibitors and analysed in Prism 9.2.0 (Graphpad, La Jolla, CA).

2.17 Immune-Signalling in oral epithelial cells

2.17.1 Cell treatments and harvesting of conditioned media

Oral squamous cell carcinoma (H357) was cultured as described above (section 2.13). Briefly, trypsinised H357 cells were resuspended at a density of 2×10^5 cells/ml in DMEM (10 % serum, 2 mM L-glutamine), and were seeded into the wells of a 12-well tissue culture plate (Greiner, UK), 2 ml of suspension per well. Cells were incubated for 18-24 hours (or as stated) at 37 °C, 5% CO_2, and exposed to a variety of different

conditions (Table 2.5). Each condition was performed in triplicate (or as stated otherwise) during each experiment. Prior to treatment, one sacrificial well underwent trypsinization and cells were counted using a haemocytometer to determine the number of cells per well at the beginning of the experiment. In an experimental setup containing live bacteria, cells were seeded at a given multiplicity of infection (MoI). Treated cells were incubated at 37 °C, 5 % CO_2 for 1hr:30 mins or 24 hours (same duration with antibiotic protection assay).

Supernatants were collected and were used for cytotoxicity assays before storage at -20 °C for Flow cytometry analysis.

5.17.2 Detection of cytokine expression using flow cytometry method

To assay the levels of secreted cytokines, H357 cells were treated as described in section 2.17.3 (Table 2.5) below, and the collected culture supernatants were used for the detection of multiple pro-inflammatory cytokines (Table 5.1) following the BD Cytometric Bead Array (CBA) protocol described in section 2.17.3, and as illustrated in figure 2.3 below.
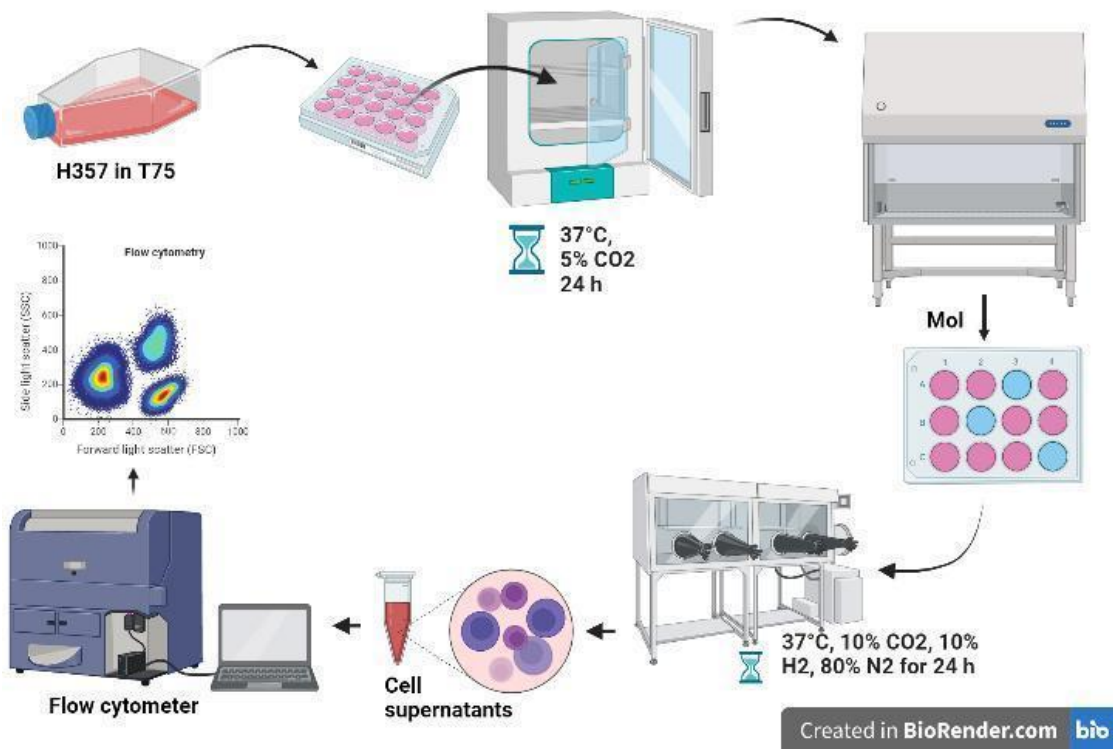
Figure 2.3: Diagrammatic representation of the immune signalling assay

Oral squamous cell carcinoma (H357) grown in supplemented DMEM were trypsonised and resuspended at a density of $2x10^5$ cells/ml and seeded into the wells of a 12-well tissue culture plate (Greiner, UK) in triplicate and incubated at 37 °C, 5% CO2 for 24 hours. The H357 cells were infected with live *T. forsythia* or *P. gingivalis* at MoI 1:100 in the presence or absence of the sialidase inhibitor (2e3aDFNeu5Ac9N3) and further incubated (anaerobically) for 24 hours. Culture supernatants produced after 24 hours period were collected and the concentrations of IL-1β, IL-6, IL-8, TNF-α, and MIP-1α were measured using the flow cytometry method according to the manufacturer's instructions.

2.17.3 Multiplex Cytokine Bead Array

Flow Cytometry employs the use of a Bead-based array purchased from BDbiosciences, the "BD Cytometric Bead Array (CBA)". Briefly, antibodies against the protein of interest are immobilized onto fluorescent beads, which are incubated with a given sample. A fluorescent antibody against the protein of interest is then applied, and the bead's fluorescence increases relative to the concentration of the protein of interest. Reactions containing known concentrations of the protein of interest are also performed, to produce a standard curve of known protein concentration. This is applied to quantify the protein of interest.

In this present research, proinflammatory cytokines (Table 5.1) that were suspected to be secreted by oral epithelial cells and might be influenced during infection with whole pathogens *P. gingivalis*, *T. forsythia*, as well as their purified SiaPg and NanH sialidases and treatment with 1µM (IC50 concentration) of sialidase inhibitor; 2e3aDFNeu5Ac9N3 was investigated. Cytokines quantified were Interleukin-6 (IL-6), IL-1β, IL-8, Monocyte Chemoattractant Protein (MCP-1), Macrophage Inflammatory Protein (MIP1α), and Tumour Necrosis Factor (TNFα).

Table 2.5: Conditions for treated H357 cells used for cytokine analysis.

Condition	Concentration or Seeding density	Serum	Commercial ELISA kit
Untreated	H357 only	10%	BD Biosciences & BioLegend
Inhibitor(s) only	IC50 range	10%	BD Biosciences & BioLegend
P. gingivalis	1:50 or 1:100	10%	BD Biosciences & BioLegend
T. forsythia	1:50 or 1:100	10%	BD Biosciences & BioLegend
P. gingivalis + Inhibitor	1:100 + IC50 range	10%	BD Biosciences & BioLegend
T. forsythia + Inhibitor	1:100 + IC50 range	10%	BD Biosciences & BioLegend

CHAPTER THREE

Sialidase Inhibitory Activities of a Selection of Synthetic and Plant-derived Compounds

3.1   Introduction

P. gingivalis and *T. forsythia* were shown to express sialidases which they use to cleave sialic acids found at the terminal end of host glycoconjugates (Stafford et al., 2012). The oral cavity where the periodontal pathogens live is endowed with glycoproteins and glycolipids (Frey et al., 2019). The major source of these glycoproteins in the supragingival plaque is from the surfaces of the oral epithelial cells or from salivary proteins such as the mucins (Douglas et al., 2014). In the subgingival plaque however, glycoproteins can be obtained from the gingival crevicular fluid (GCF), and immune cells such as neutrophils and macrophages that are often found in the periodontium (Douglas et al., 2014). Host glycoproteins and glycolipids have been reported to be rich in sialic acid which often occupies the terminal end of the sugar chain or cell surfaces of vertebrate cells, with diverse cellular functions such as in intercellular adhesion or cell signalling (Severi et al., 2007 and Li & Chen, 2012)

Bacteria have evolved a mechanism of harvesting these sialic acids with the help of the sialidase enzymes to be used as a carbon source for nutrition, or by coating themselves in the sialic acids to provide resistance to host innate immune response (Stafford et al., 2012 and Silva et al., 2015). The release of sialic acid by these pathogens can further expose the underlying sugars in the glycan chain to colonisation and utilisation by other bacterial enzymes. These activities have been suggested to favour disease progression (Xu et al., 2020).

Furthermore, sialidases have been shown to support biofilm formation and enhance bacterial attachment and invasion of host epithelial cells (Roy et al., 2011) (figure 3.1). Inhibiting these bacterial sialidase enzymes therefore may prevent the pathogenesis of these oral pathobionts. Pharmaceutically approved, plant-derived, and synthetic compounds were therefore tested for their sialidase inhibitory properties which may serve as novel therapy for the prevention of oral diseases such as periodontitis.
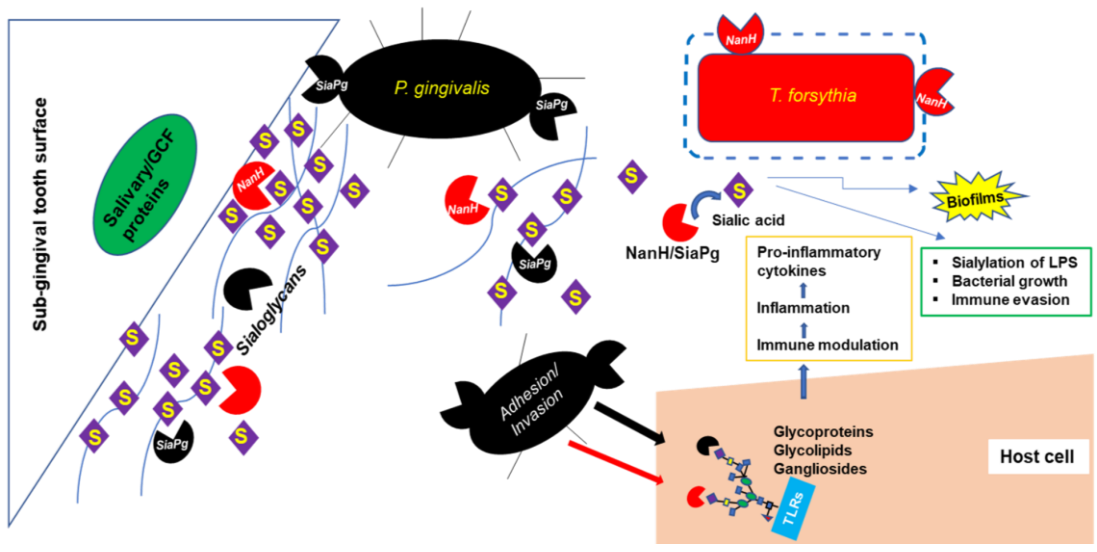
Figure 3.1: Sialidase (NanH/SiaPg) actions and host immune response

Schematic representation of the role of sialidases of *T. forsythia* and *P. gingivalis* in host-pathogen interactions such as promotion of bacterial growth, plaque (biofilm) formation, attachment, and invasion of host oral epithelial cells. These interactions could lead to immune modulation which may elicit host innate immune responses such as inflammation and expression of pro-inflammatory cytokines (IL-6, IL-1β, IL-8, TNF).

3.2 Results

3.2.1 Recombinant Protein Expression and Purification by Affinity Chromatography

To assess the sialidase inhibitory activities of the inhibitors, the proteins of interest, NanH and SiaPg of *T. forsythia* and *P. gingivalis* respectively, were expressed and purified as His-tagged proteins as described previously (sections 2.2.1 & 2.2.2). These were used for sialidase inhibition assay and other biochemical tests. This was aimed at determining the best inhibitor(s) for the oral pathogens' sialidases.

To test for the protein (NanH and SiaPg) expression, liquid cultures of transformed *Escherichia coli* (Origami B) were grown to an optical density (OD_{600}) of 0.6-0.7 and induced with 0.2 mM IPTG. 5-10 µl of the uninduced and induced bacterial pellets were resuspended in SDS-PAGE lysis buffer and underwent SDS-PAGE and the expected bands (~57.4 kDa for NanH and ~54.8 kDa for SiaPg) (Frey *et al*., 2019) of the protein of interest were as shown below (figure 3.2).
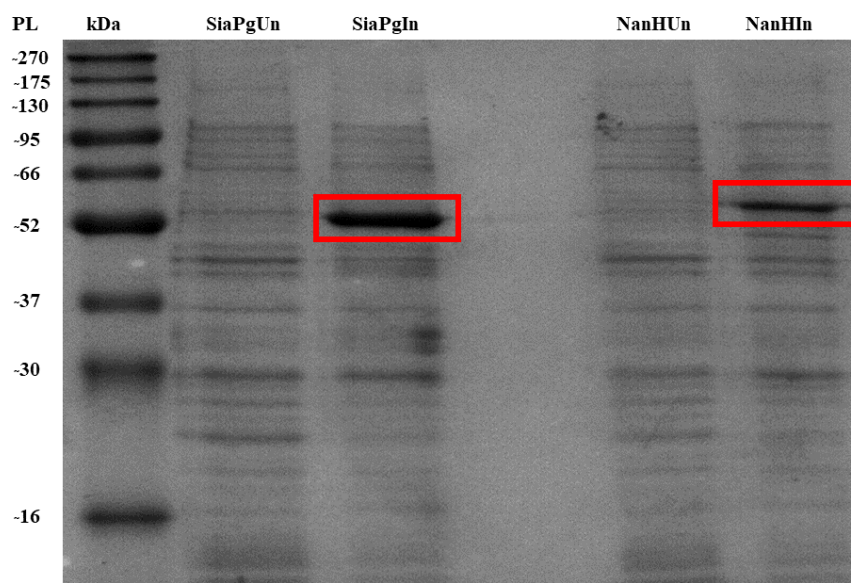
Figure 3.2: Protein (NanH and SiaPg) Expression:

Uninduced and induced cell pellets were separated by means of 12% SDS-PAGE gel and the InstantBlue Coomassie-stained gel showing protein expression of NanH and SiaPG. Protein bands suspected to represent proteins of interest are as indicated (SiaPg = 54.8 kDa, NanH = 57.4 kDa). PL = Protein ladder (size approximation based on manufacturer's guide), kDa = protein molecular weight, Un = uninduced pellets, In = induced pellets.

After the proteins of interest were expressed, a larger volume of the induced pellets was subjected to purification as described in chapter two (section 2.2.2). Previous work in our laboratory established that NanH and SiaPg are highly soluble proteins present in the soluble fractions of the cell lysates which were therefore incubated with Ni-NTA resin for purification. The eluted pure protein is shown in the elution fractions (figure 3.3 a & b). The concentrations of these proteins were then established using the bicinchoninic acid assay (BCA) described in chapter two (section 2.4). These purified proteins (NanH and SiaPg) were used in carrying out sialidase inhibition assay and other biochemical studies outlined below.
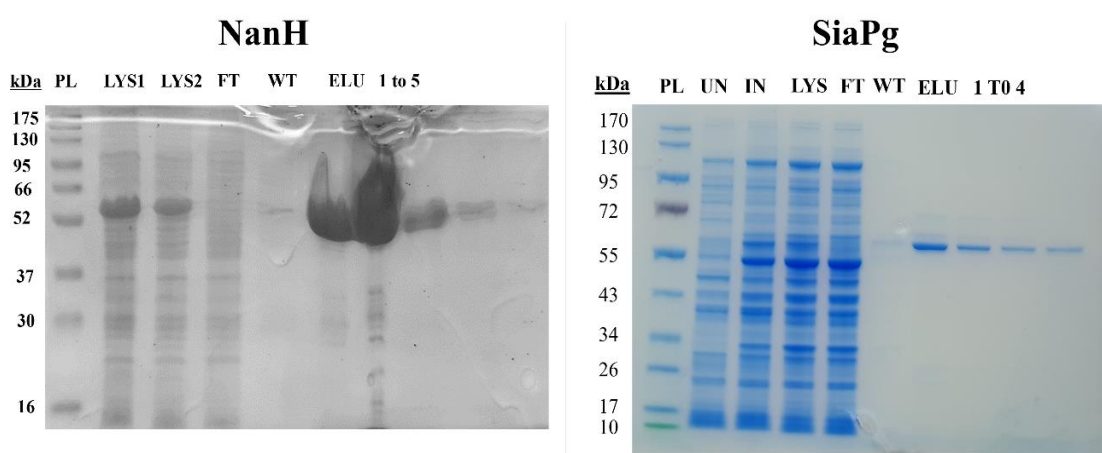
Figure 3.3 a & b: Protein (NanH and SiaPG) Purification

12% SDS-PAGE gel showing protein purification of NanH and SiaPg. LYS = Lysate, UN = Uninduced pellets, IN = Induced pellets, FT = Flow through, WT = Wash through, ELU = Elusions 1 to 5 represents purified NanH and SiaPg with a molecular weight of ~57.4 and ~55 kDa respectively. PL = Protein ladder (size approximation based on manufacturer's guide).

3.2.2 Determination of sialidase activity of purified periodontal pathogen sialidases

After the recombinant protein expression and purification, the sialidase activity of purified batches of proteins was investigated according to the protocol described (section 2.5.2). Nonetheless, a rapid determination of the sialidase activity using the UV light box (SynGene) to measure the MUNANA cleavage was often used (figure 3.4). Briefly, the reactivity of NanH or SiaPg in the presence of MUNANA was observed under the SynGene UV light to rapidly cleave MUNANA (increased fluorescence), with NanH getting to optimum reaction at about 2 mins while SiaPg lasted for about 4-5 mins (figure 3.4). This assay was routinely carried out to determine sialidase activity in each batch of the protein before use in further studies.
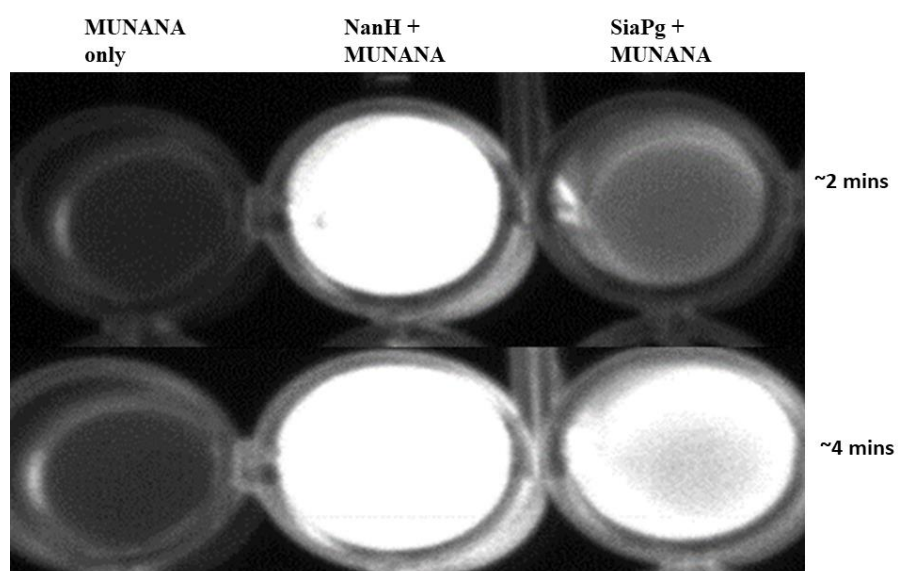
Figure 3.4: Rapid Determination of Sialidase Activity using UV light

MUNANA cleavage to rapidly confirm the sialidase activity of the purified proteins was carried out at different time intervals as shown above. In the first wells, MUNANA was exposed to no enzyme (MUNANA only), while in the second and third wells, MUNANA was exposed to either NanH or SiaPG as indicated. Rapid sialidase activity was confirmed by the release of 4-MU and the fluorescence under UV light was measured using SynGene3 (Ingenius 3, UK).

3.2.3　Determination of Sialidase Activity of whole bacterial cells

In the oral cavity, the sialidases do not exist in a pure form, rather, they are secreted or expressed on the outer membrane of oral pathogens (Honma et al., 2011). Even though the strains of *T. forsythia* (wtTf43037) and *P. gingivalis* (wtPg0381) used in this study were known sialidase producers (Roy et al., 2011 and Frey et al., 2019), it was important to reconfirm this in every experiment which is needed to ascertain the sialidase inhibitory properties of the compounds. Therefore, sialidase activities of the wild-type strains of *T. forsythia* and *P. gingivalis* were determined as described in (section 2.5.3), in comparison to their respective sialidase-deficient strains, and the results are as presented with significant differences in the sialidase activity between the wild-type and mutant strains of *T. forsythia* and *P. gingivalis* (figure 3.5 a & b). Although both the wild-type strains are sialidase positive, activity was observed to be two-fold higher in *T. forsythia* as compared to *P. gingivalis* (figure 3.5 a & b).
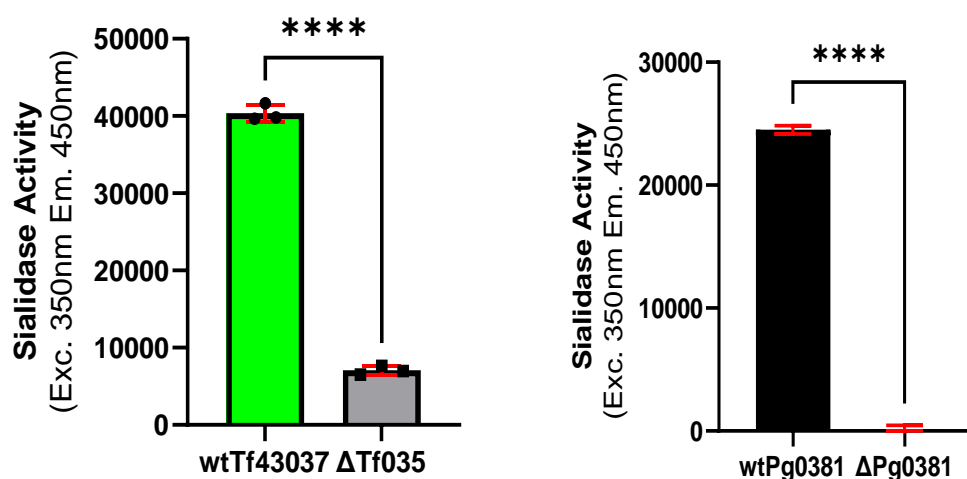
Figure 3.5 a & b: Determination of sialidase activity in wild type and mutant strains of *T. forsythia and P. gingivalis*

Sialidase activity of wild type (wtTf43037) and mutant (ΔTF035) strains of *T. forsythia* and that of *P. gingivalis* wtPg0381 versus sialidase-deficient strain (ΔPg0381), were carried out with the set up incubated at 37 ˚C and stopped by the addition of 150 μL of 100 mM Na_2CO_3 buffer pH10.5 after 30 minutes (*T. forsythia*) or 1 hour (*P. gingivalis*). The MUNANA cleavage (fluorescence) was measured using TECAN M200 plate reader at excitation 350 nm and emission at 450 nm to determine the sialidase activity. Error bars = SD (n = 3), Unpaired t test shows ****P value < 0.0001. Unpaired t-test was chosen because it compares the means of two samples (wild type and mutant) since each strain is independent of the other.

3.3   Chemical structures of the sialidase inhibitors tested

One of the major aims of this study is to ascertain the potential of the pharmaceutically approved, synthetic, and plant-derived compounds which will serve as novel inhibitors of periodontal pathogen sialidases.

The ability of Zanamivir and Oseltamivir, which are licensed neuraminidase (sialidase) inhibitors for the treatment of influenza, alongside other compounds with the potential to inhibit the purified pathogen sialidases were tested. Zanamivir, DANA, Siastatin B, and Oseltamivir (figure 3.6 a), which were earlier reported to significantly inhibit viral neuraminidases were used as positive controls. In addition, the inhibitory activities of a range of plant-derived compounds such as Epicatechin gallate, Berberine chloride, and Palmatine (figure 3.6 b), were screened and these compounds were also reported to have antibacterial activities. The sialidase inhibitory properties of the newly synthesized compounds 'USA inhibitors' by our collaborators in America (Li et al., 2019) (figure 3.6 c), were also screened. These sialic acid analogue compounds have the negatively charged carboxyl group at C-1 and the *N*-acetyl group at C-5 positions, also, various chemical modifications such as fluorine atoms at C-2 and C-3, and the azido group (N3) at C-9 position, are found on the di-fluoro sialic acid analogues (figure 3.6 c).
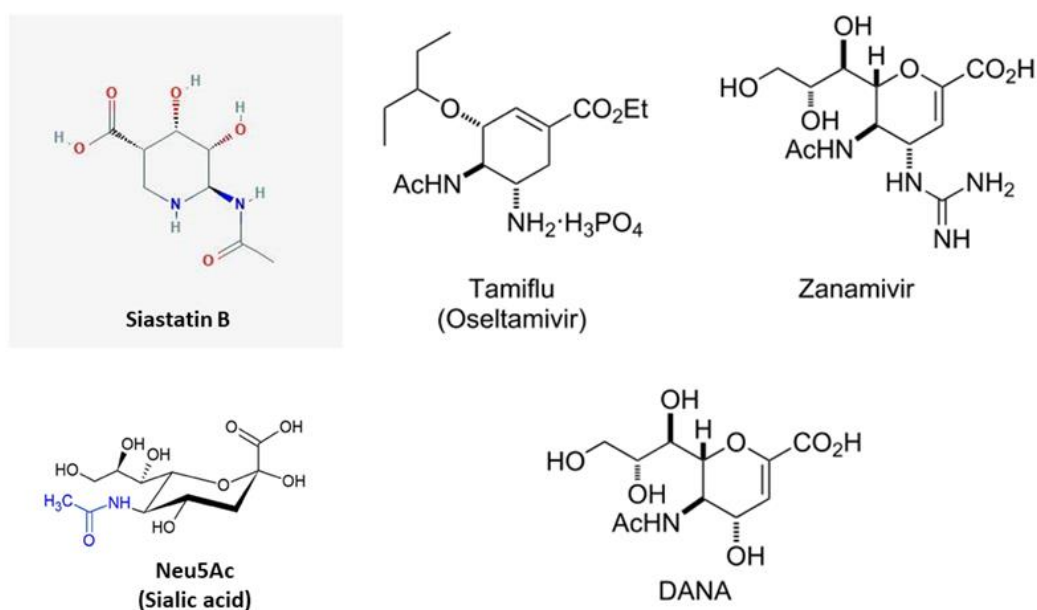
Figure 3.6 a: Chemical structures of Pharmaceutically approved sialidase inhibitors

Similar to the sialic acid (Neu5Ac), all the compounds have a carboxyl group at C-1.
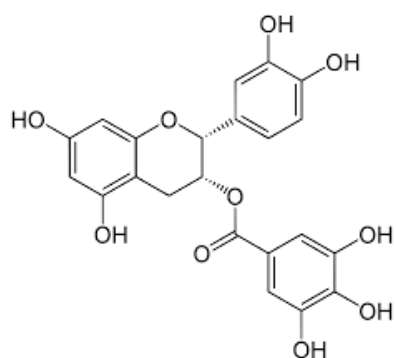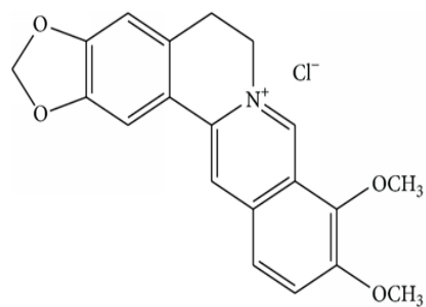
Epicatechin gallate   Berberine chloride
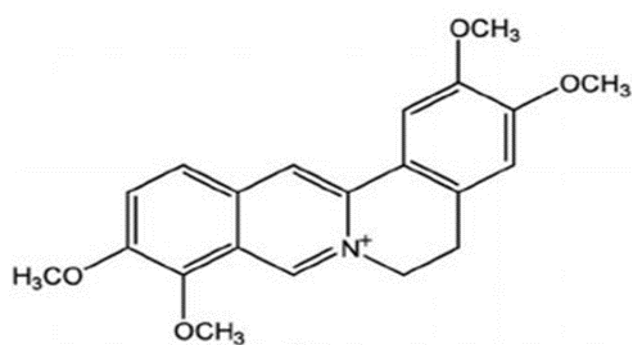
Palmatine

Figure 3.6 b: Chemical structures of plant-derived sialidase inhibitors

Neu5Ac2en (1)

Pra-Neu5Ac2en (6)

Neu5Gc2en (2)

2e3eDFNeu5Ac (7)

Neu5Ac9N₃2en (3)

2e3aDFNeu5Ac (8)

Neu5Ac9Ac2en (4)

2e3eDFNeu5Ac9N₃ (9)

Neu5Ac9cyclo2en (5)

2e3aDFNeu5Ac9N₃ (10)
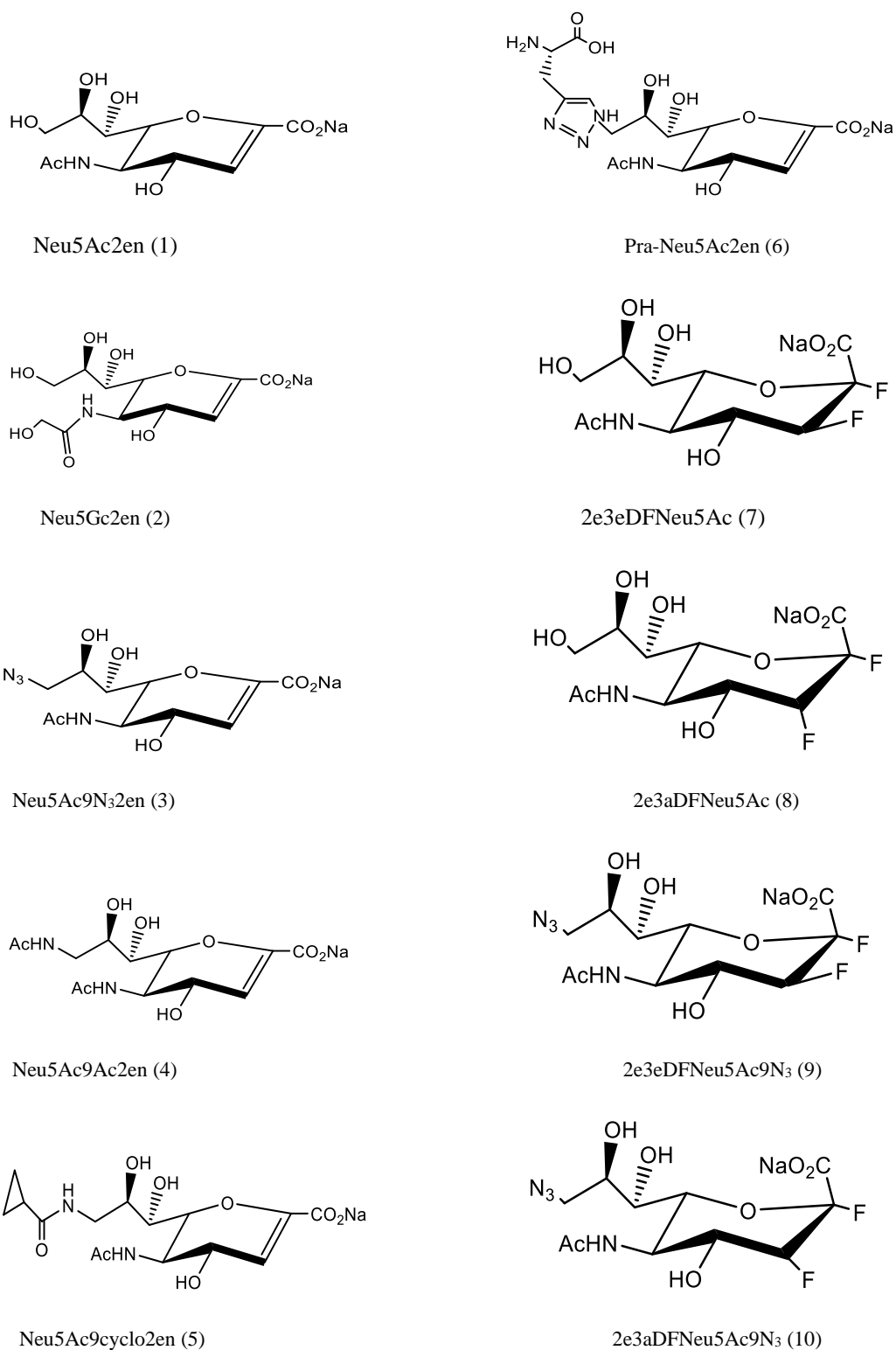
Figure 3.6 c: Newly synthesised "USA Sialidase Inhibitors"

Inhibitors 2-10 are derivatives of the common sialidase transition state analogue 2-deoxy-2,3-dehydro-*N*-acetylneuraminic acid (Neu5Ac2en or DANA) (Li et al., 2019).

3.4   Determination of the Sialidase Inhibitory Properties of the Compounds

3.4.1 IC50 of Plant-derived compounds on purified periodontal pathogen sialidases (NanH and SiaPg)

To investigate the sialidase inhibitory properties of the plant-derived compounds, the IC_{50} of these inhibitors was determined. The fluorescence (sialidase activity relative to no inhibitor) was measured and analysed on Prism GraphPad to determine the nonlinear regression curve. Epicatechin gallate appeared to be the most potent plant-derived inhibitor having IC50 values of 73.86 µM and 110.5 µM, Palmatine 166.2 µM and 531.7 µM, and Berberine chloride 445.1 µM and 106.2 µM, on purified NanH and SiaPg sialidases (figure 3.7 a & b), respectively.
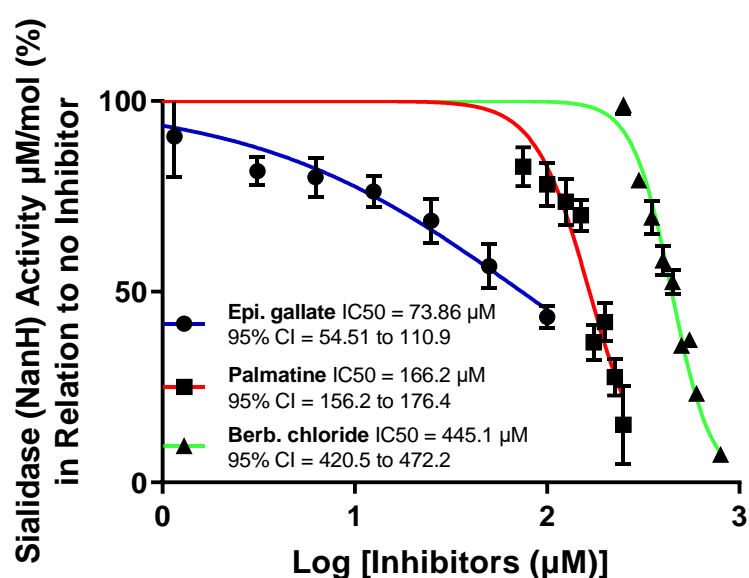
Figure 3.7 a: Log [Inhibitors] against Percentage of Sialidase (NanH) Activity

A plot of the Log [Inhibitors] against percentage of sialidase (NanH) activity relative to no inhibitor allows determination of the IC_{50} of Epicatechin gallate, Palmatine and Berberine chloride for inhibition of MUNANA cleavage by NanH sialidase. Data represent the mean of three experimental repeats (n=3), where each condition was conducted in triplicate.
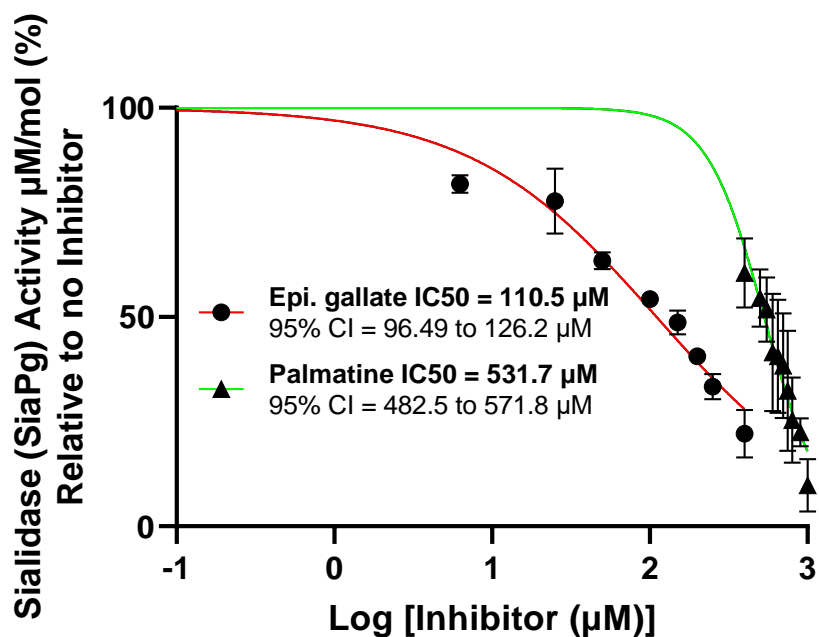
Figure 3.7 b: Log [Inhibitors] against Percentage of Sialidase (SiaPg) Activity

Plot of the Log [Inhibitors] against percentage of sialidase (SiaPg) activity relative to no inhibitor allows determination of the IC_{50} of Epicatechin gallate and Palmatine for inhibition of MUNANA cleavage by SiaPgh. Data represent the mean of three experimental repeats (n=3), where each condition was conducted in triplicate.

3.4.2 IC50 of Plant-derived compounds on whole periodontal pathogen sialidases

Inhibitory activities of the plant-derived compounds on the sialidases of wild-type *T. forsythia* (wtTf43037) and *P. gingivalis* (wtPg0381) were determined in the presence or absence of varying concentrations of the plant-derived inhibitors. Although both compounds showed inhibitory activities, Epicatechin gallate (ECG) appeared to be more potent (figure 3.8 a). Also, the whole-cell sialidase activity of *T. forsythia* appeared to be more susceptible to both the plant-derived compounds when compared to the sialidase activity of *P. gingivalis* (figure 3.8 a & b).
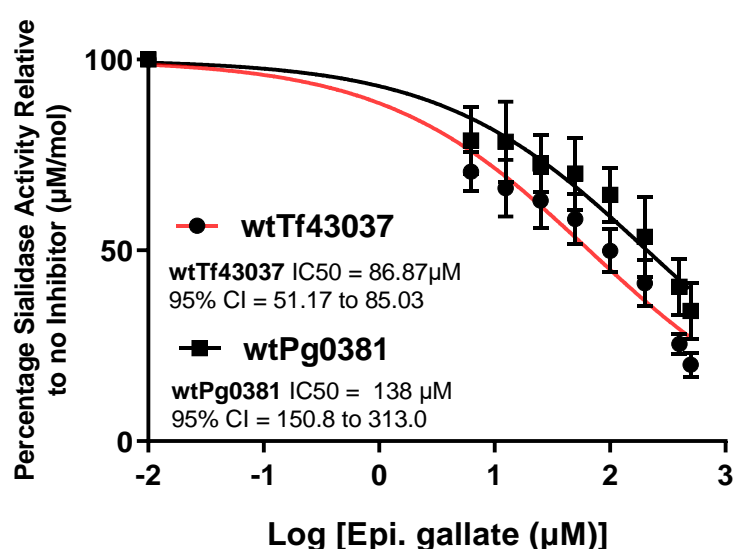
Figure 3.8 a: Log [Epicatechin gallate] against Percentage sialidase (wtTf43037 and wtPg0381) Activity

Plot of the Log [Inhibitors] against percentage of whole cell (wtTf43037 and wtPg0381) sialidase activity relative to no inhibitor allows determination of the IC_{50} of Epicatechin gallate for inhibition of MUNANA cleavage by these oral pathogens. The fluorescence was measured using a TECAN M200 plate reader at excitation 355 nm and emission at 430 nm and the IC50 was determined using Prism version 9.2.0. Data represent the mean of three experimental repeats (n=3), where each condition was conducted in triplicate. Error bars = SD
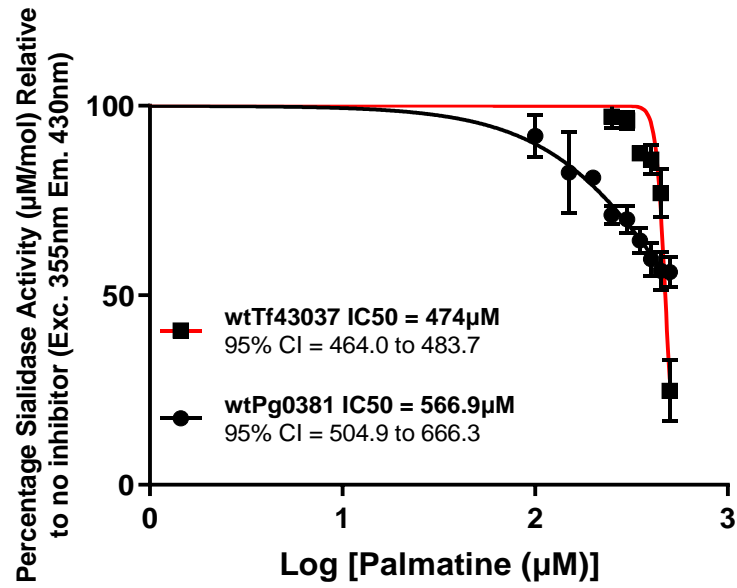
Figure 3.8 b: Log [Palmatine] against Percentage Sialidase (wtTf43037 and wtPg0381) Activity

A plot of the Log [Inhibitors] against percentage of a whole cell (wtTf43037 and wtPg0381) sialidase activity relative to no inhibitor allows determination of the IC_{50} of Palmatine for inhibition of MUNANA cleavage by these oral pathogens. Data represent the mean of two experimental repeats (n=2), where each condition was conducted in triplicate. Error bars = SD

3.4.3 IC50 of the synthesised 'USA Inhibitors' on purified sialidases (NanH and SiaPg)

The derivatives of the common sialidase transition state analogue of 2-deoxy-2,3-dehydro-*N*-acetylneuraminic acid (Neu5Ac2en or DANA) synthesised by our collaborators from the Department of Chemistry, University of California, One Shields Avenue, Davis, California, USA (Li et al., 2019) (figure 3.6 c), were also tested for their sialidase inhibitory activities. Some of the synthesized compounds were previously reported to be selective inhibitors against *V. cholerae* and human cytosolic NEU2 sialidases, respectively (Li et al., 2019). As such, we investigated their activity against the purified periodontal pathogen sialidases (NanH and SiaPg), and on whole bacterial cell sialidases.

Although most of the compounds tested in this study, showed promising inhibitory activities against purified NanH and SiaPg sialidases (table 3.1), the di-fluoro sialic acid compound with equatorial and axial fluorine molecules attached at the carbon 2 and 3 as well as the Azido group (N3) on carbon 9 (2e3aDFNeu5Ac9N$_3$), showed a superior and significant inhibition of both NanH and SiaPg with IC50 values of 0.1704 and 1.692 µM (figure 3.9), respectively. Interestingly, the 2e3a/2e3eDFNeu5Ac without the addition of the Azido group tends to inhibit SiaPg with better inhibitory activities as compared to NanH. However, while 2e3e/2e3aDFNeu5Ac showed selectivity to SiaPg, 2e3e/2e3aDFNeu5Ac9N3 were more potent against NanH sialidase (table 3.1). Overall, the effective binding and inhibitory activities of 2e3aDFNeu5Ac9N$_3$ on both NanH and SiaPg, may be due to the addition of azido group (N$_3$) at the C-9 position and the stereochemistry of the di-fluoro- side chains (Figure 3.6 c). A summary of the IC$_{50}$ values for the inhibition of periodontal sialidases (SiaPg and NanH) is as shown in table 3.1 below.
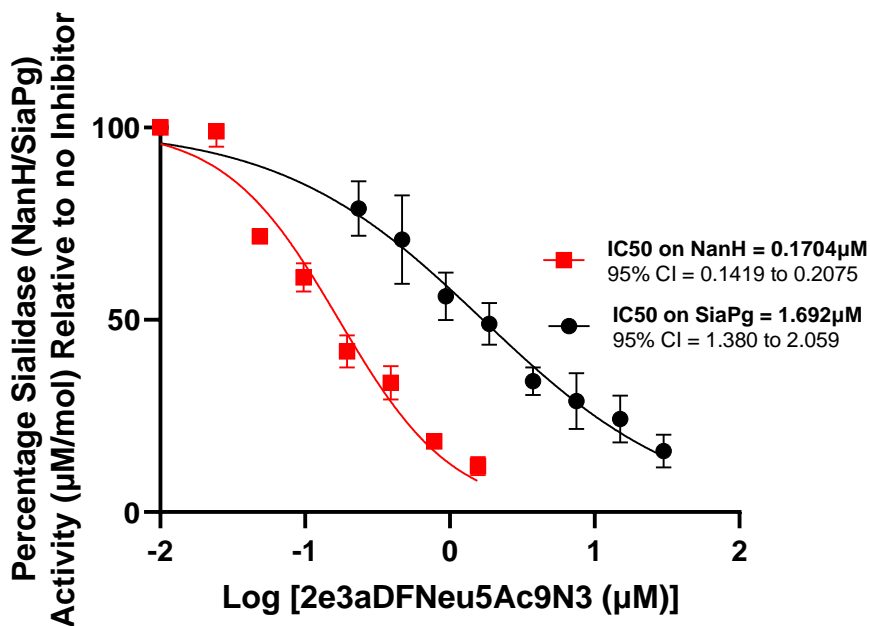
Figure 3.9: Non-linear fit of Log[2e3aDFNeu5Ac9N3] versus normalised

NanH/SiaPg Activity

Purified sialidase (NanH/SiaPg) activity were determined in the absence or presence of varying concentrations of 2e3aDFNeu5Ac9N$_3$ with the set up incubated at room temperature for 2 minutes (NanH) or 4 minutes (SiaPg) and stopped by the addition of 150 µL of 100 mM Na$_2$CO$_3$ buffer pH10.5. The fluorescence was measured using a TECAN M200 plate reader at excitation 355 nm and emission at 430 nm, and the IC50 at 95% CI was determined using Prism version 9.2.0. (non-linear fit vs normalised variable slope). Data represent the mean of three experimental repeats (n=3), where each condition was conducted in triplicate.

Note: The same assay was conducted under standard conditions to determine the IC50 values for all the remaining compounds shown in table 3.1 and 3.2 below. Refer to appendix 4-12 for individual figures.

Table 3.1: Summary of IC50 values for all the Inhibitors on Purified NanH/SiaPg Sialidases (μM)

Serial No.	Inhibitors	SiaPg	NanH
	FDA Approved		
01.	Zanamivir	292.1	6156
02.	Siastatin B	*	1081
03.	DANA	99.62	*
	Plant-derived		
04.	Epicatechin gallate	110.5	73.86
05.	Berberine chloride	106.2	445.1
06.	Palmatine	531.7	166.2
	USA Inhibitors		
07.	Neu5Ac2en	16.58	29.50
08.	Neu5Gc2en	63.35	247.8
09.	Neu5Ac9N$_3$2en	*	10.56
10	Neu5Ac9NAc2en	240.10	87.33
11	Neu5Ac9cyclo2en	205.30	60.73
12	Pra-Neu5Ac2en	*	38.51
13	2e3eDFNeu5Ac	4.681	9.913
14	2e3aDFNeu5Ac	3.358	19.71
15	2e3eDFNeu5Ac9N$_3$	119.2	8.048
16	2e3aDFNeu5Ac9N$_3$	1.692	0.1704

(*) = Not tested, μM = micromolar, nM = nanomolar, IC50 = Inhibitory concentration

Amongst the plant-derived compounds, Epicatechin gallate showed a better inhibition of the NanH and SiaPg sialidase in comparison to Palmatine and Berberine chloride. Of all the ten (10) synthesized "USA" inhibitors, 2e3aDFNeu5Ac9N3 is the most effective on both NanH and SiaPg. Also, it inhibits both purified and whole-cell sialidases better than the approved neuraminidase inhibitors; Zanamivir, DANA, and Siastatin B.

3.4.4 IC50 of the synthesized 'USA' inhibitors on whole periodontal pathogen Sialidases

The di-fluoro compound 2e3aDFNeu5Ac9N3; shows a promising inhibitory effect on the purified bacterial sialidases (NanH and SiaPg), at a lower concentration in relation to all the pharmaceutically approved inhibitors, and considering that it is the overall best compound amongst the "USA inhibitors", it was focused upon for subsequent assays. Furthermore, knowing that pathogens exist in the oral cavity as whole bacterial cells, it is therefore pertinent to investigate the effect of this particular compound on the sialidases of whole *T. forsythia* and *P. gingivalis*. Using the method described above, the inhibitory concentrations (IC50) of 2e3aDFNeu5Ac9N3 on whole-cell sialidases of *T. forsythia* (wtTf43037) and *P. gingivalis* (wtPg0381) were found to be 0.8394 and 3.651 µM, respectively (figure 3.10). Again, 2e3aDFNeu5Ac9N3 appears to inhibit whole-cell sialidase of *T. forsythia* more than it does to the sialidase of whole cells *P. gingivalis* (figure 3.10). Previously, the IC50 of Epicatechin gallate and Palmatine were determined (figure 3.8 a & b) and presented in Table 3.2 below.
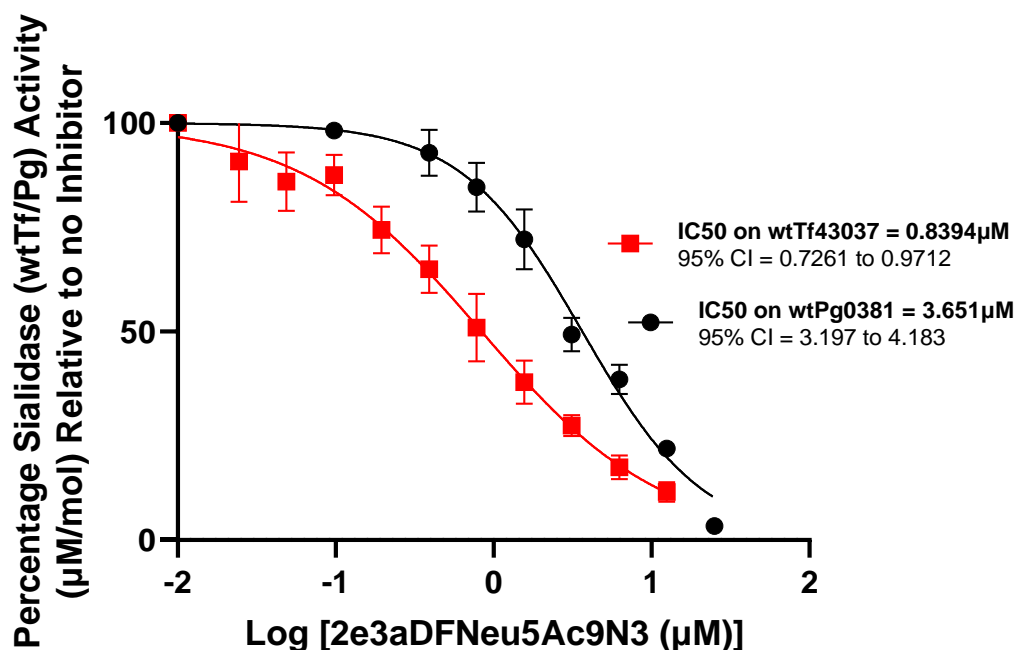
Figure 3.10: Log[Inhibitor] against Percentage of whole cell Sialidases of *T. forsythia* (wtTf43037) and *P. gingivalis* (wtPg0381) Activity

Sialidase activity of wild type *T. forsythia* (wtTf43037) and *P. gingivalis* (wtPg0381) were determined in the presence of varying concentrations of 2e3aDFNeu5Ac9N$_3$ with the set up incubated at 37 ˚C and stopped by the addition of 150µL of 100mM Na$_2$CO$_3$ buffer pH10.5 after 30 minutes respectively. The fluorescence was measured using TECAN M200 plate reader at excitation 355 nm and emission at 430 nm and the IC50 was determined using Prism version 9.2.0. Data represent the mean of three experimental repeats (n=3), where each condition was conducted in triplicate.

Table 3.2: Summary of IC50 values for Sialidase Inhibitors on whole cell *P. gingivalis* and *T. forsythia* (µM)

Serial No.	Inhibitors	wtPg0381	wtTf43037
01.	Epicatechin gallate	138	86.87
02.	Palmatine	566.9	474
03.	2e3aDFNeu5Ac9N3	3.651	0.8394

IC50 = Inhibitory concentration, µM = micromolar, wt = wild type

3.5 Determination of Synergistic Effects (Combination therapy)

3.5.1 Palmatine and Berberine chloride synergistically inhibit NanH sialidase of *T. forsythia*

Both Palmatine and Berberine chloride which are extracted from the same plant showed some promising sialidase inhibitory activity individually (figure 3.7). Their combined effect on NanH was therefore assessed to determine their synergistic effect. To do this, the inhibitory effects of Palmatine and Berberine chloride on NanH sialidase were determined individually to assess their dose-effect at varying concentrations (table 3.3). Individual Palmatine (Palma) and Berberine chloride (Berb) effects (inhibitory properties) on NanH sialidase are represented in blue circles and red rectangles (figure 3.11), respectively, followed by their combined effect (PalBer) on NanH; green rectangles (figure 3.11). Combination index (CI) values of the two compounds that indicate the level of synergism or antagonism were also assessed (table 3.4).

Drug/Combo	Dm (IC50)	m	r
Palma	0.14359	2.51870	0.90416
Berb	0.47443	4.22306	0.97424
PalBer	0.43290	10.1143	0.79833
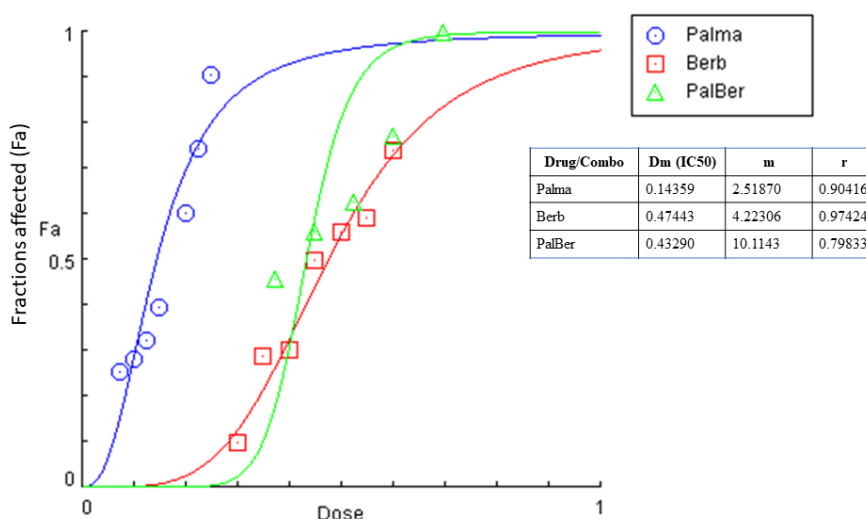
Figure 3.11: Dose-Effect curve of Palmatine and Berberine chloride on NanH sialidase

The effect of Palmatine (Palma) and Berberine chloride (Ber) individually and in combination (PalBer) on NanH sialidase inhibition was assessed. Varying doses of the compounds were added to NanH (2.5nM) solubilized in 50 mM sodium phosphate buffer, 200 mM NaCl at pH 7.4 and incubated at room temperature for 2 minutes after which the reaction was stopped with the addition of 100 mM Na_2CO_3 buffer pH10.5. Individual and combined fluorescence was measured and the dose-effect curve was plotted using CompuSyn software (version 1.0) to ascertain the IC50 (*Dm*), the shape (*m*), and the accuracy (*r*) of respective compounds as shown (embedded table). Each plot represents the results from three independent experiments (CompuSyn software does not display error bars).

Table 3.3: Individual Dose vs Effect of Palmatine and Berberine chloride on NanH Sialidase

Palmatine (mM)		Berberine chloride (mM)	
Dose	Effect	Dose	Effect
0.075	0.25285	0.3	0.09769
0.1	0.28157	0.35	0.28653
0.125	0.32281	0.4	0.30280
0.15	0.39648	0.45	0.49995
0.2	0.60332	0.5	0.55936
0.225	0.74437	0.55	0.58993
0.25	0.90633	0.6	0.73898

Varying concentrations (Dose) of Palmatine and Berberine chloride as indicated above were added in a constant ratio (1:1) to the MUNANA substrate (0.2 mM), and the enzyme reaction was initiated by the addition of NanH sialidase (2.5 nM) in a black non-transparent flat-bottomed 96-well polystyrene plates and incubated at room temperature for 2 minutes. Fluorescence was read at Absorbance 355 nm and at emission 450 nm and the individual effect (NanH affected), was determined using CompuSyn (version 1.0). Data represent the mean from three independent experiments conducted in triplicate.

mM = Millimolar, Dose = Concentrations used, Effect = NanH fractions that were reduced

3.5.2 Individual and combined effect of Palmatine and Berberine chloride on purified NanH sialidase

As stated above, the inhibitory properties of Palmatine and Berberine chloride on purified NanH sialidase were tested individually and in combination to ascertain the percentage inhibition. In comparison to the untreated condition, 0.2 mM of Palmatine causes a three-fold reduction while 0.5 mM of Berberine chloride causes a two-fold reduction (figure 3.12). Interestingly, the combination of Palmatine and Berberine chloride at (0.2 mM : 0.5 mM), showed a 99.9% reduction in NanH sialidase activity (figure 3.12), with a least combination index (CI value) of 0.26 (table 3.4). Chou (2008) states that a CI value of less than 1 (CI = < 1) signifies drug synergism (Chou, 2008). Therefore, at a combined concentration (0.7 mM), Palmatine acts synergistically with Berberine chloride (PalBer) to inhibit almost 100% NanH sialidase activity (figure 3.12 and Table 3.4).

Table 3.4: Combination Index (CI) values for actual experimental points

Total Dose (mM)	NanH fractions affected (Fa)	CI values
0.375	0.45683	1.81047
0.45	0.56162	1.86745
0.525	0.62622	1.97913
0.6	0.77106	1.76443
0.7	0.99929	0.26971

Table 3.4 shows the total dose (combined concentrations) of Palmatine:Berberine chloride (1:1) and the percentage of NanH sialidase affected (Fa). The combination index (CI) values signify either synergism, additive, or antagonistic effects of the compound. Total doses with CI value < 1 as Synergism; CI = 1 as Additive effect and CI > 1 as Antagonism (refer to table 2.2). Data represent the mean of three experimental repeats conducted in triplicate and generated using CompuSyn (version 1.0).
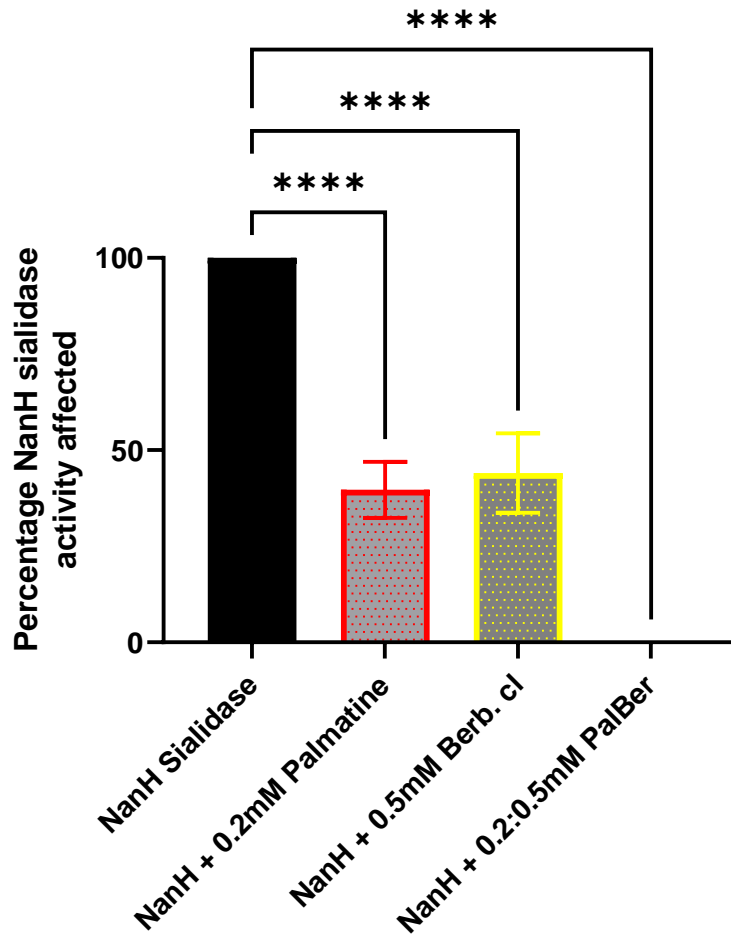
Figure 3.12: Percentage NanH sialidase affected by individual and combined doses (synergistic effect) of Palmatine and Berberine chloride

Varying concentrations (Doses) of Palmatine and Berberine chloride in a 1:1 ratio were assessed for their individual and combined effects on 2.5 nM NanH sialidase with a Total Dose of 0.7 mM (0.2:0.5 mM) Palmatine:Berberine chloride inhibiting almost 100% of NanH sialidase. Data represent the mean of three experimental repeats conducted in triplicate. *P* value < 0.0001 (Ordinary one-way ANOVA, n=3). One-way ANOVA is chosen because it analyses the differences between the means of the three treatments in comparison to the untreated (independent) condition.

Note: Figure 3.11 and Figure 3.12 represents the same data set with a different form of interpretation.

3.6 Determination of Mechanism of Action (MOA)

3.6.1 Mechanism of action (MOA) of plant-derived sialidase inhibitors

Having established the sialidase inhibitory activity of the plant-derived compounds previously, and knowing that Palmatine and Berberine chloride are alkaloids derived from the same plant *Rhizoma coptis* (Zhang et al., 2018), their mechanisms of action on the purified periodontal sialidase (NanH) was assessed using the Lineweaver Burk plot model (Figure 3.13). As described by Cornish-Bowden (1999), when a treated condition intersects with the untreated condition (No inhibitor) at X-axis (-1/Km), it signifies non-competitive inhibition (where Km is unaffected but Vmax is reduced), whereas, when it forms a parallel line with the untreated condition (No inhibitor) (slope = Km/Vmax), it indicates uncompetitive inhibition (where both Km and Vmax are reduced) (figure 2.2) (Cornish-Bowden, 1999). As seen in this study, therefore, Palmatine intersects with the untreated (No inhibitor) at X-axis, while Berberine chloride forms a parallel line with the untreated (No inhibitor) condition (figure 3.13). This shows that Palmatine is a non-competitive inhibitor while Berberine chloride is an uncompetitive inhibitor of NanH sialidase of *T. forsythia* (figure 3.13).

While non-competitive inhibitors bind equally well to the enzyme and enzyme–substrate complex, uncompetitive inhibitors on the other hand bind only to the enzyme–substrate complex. These different inhibitory mechanisms yield different relationships between the potency of the inhibitor and the concentration of the substrate (Cornish-Bowden, 1999; Pelley, 2012 and McPherson, 2022). In addition, non-competitive and uncompetitive inhibitors are structurally different from the substrate, unlike competitive inhibitors. This therefore may be why, non-competitive inhibitors can bind the enzyme at a distinct site different from the substrate binding site, as well as to the enzyme-substrate complex. Therefore, increasing the substrate concentration will not overcome non-competitive inhibition, hence, Vmax decreases while Km remains the same, and such inhibition may be reversible or irreversible. Uncompetitive inhibition on the hand occurs only when the substrate binds to the enzyme thereby creating a suitable binding site for the inhibitor. This form of inhibition leads to a decrease in both Vmax and Km and may also be reversible or irreversible (Cornish-Bowden, 1999; Pelley, 2012 and McPherson, 2022).
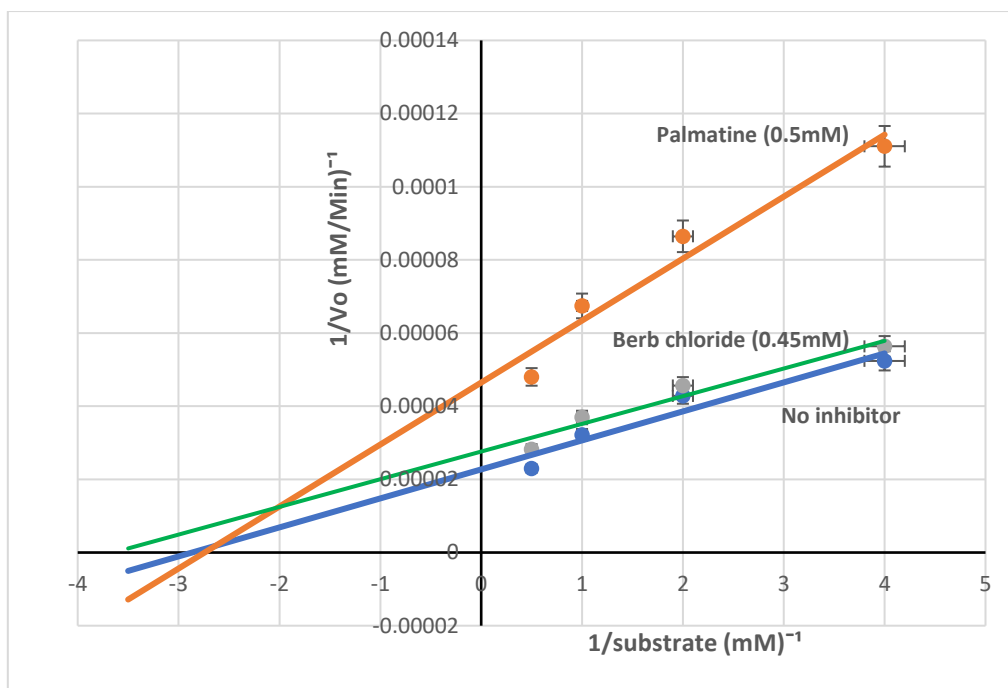
Figure 3.13: Lineweaver-Burk Plot showing the mechanism of action of Palmatine and Berberine chloride on NanH sialidase inhibition

Varying MUNANA substrate concentrations (0.5, 1, 2, and 4 mM), respectively were exposed to NanH sialidase (2.5 nM) diluted in 50 mM sodium phosphate buffer, 200 mM NaCl at pH 7.4 and incubated at room temperature. 50 µL of the reaction setup was taken and stopped by the addition of 75 µL of 100 mM Na_2CO_3 buffer pH10.5 at 1, 2, 3, and 4 minutes respectively. The fluorescence was measured using a TECAN M200 plate reader at excitation 355 nm and emission at 430 nm and the mode of enzyme inhibition was determined using the Lineweaver-Burk Plot model on Microsoft Excel version 2205. Data represent the combined mean of three experimental repeats (n=3), where each condition was conducted in triplicate. Fluorescence from the 2 minutes incubation period was used in plotting the graph. Error bars are in percentage.

3.6.2 Mechanism of action (MOA) of 2e3aDFNeu5Ac9N3 on NanH sialidase

Having established that 2e3aDFNeu5Ac9N3 is the best inhibitor of purified NanH and SiaPg, as well as sialidases of whole bacterial cells; *T. forsythia* and *P. gingivalis*, the mode of action (MOA) of the compound on the NanH sialidase was investigated.

Here, increased concentrations of 2e3aDFNeu5Ac9N3 led to a greater reduction in the NanH sialidase activity (figure 3.14). In addition, considering that the di-fluoro sialic acid compound 2e3aDFNeu5Ac9N3 is an analogue of the substrate (sialic acid), competition for binding to the active-site pocket of the enzyme may occur, thereby making 2e3aDFNeu5Ac9N3 a competitive inhibitor of NanH sialidase as seen in (figure 3.14).
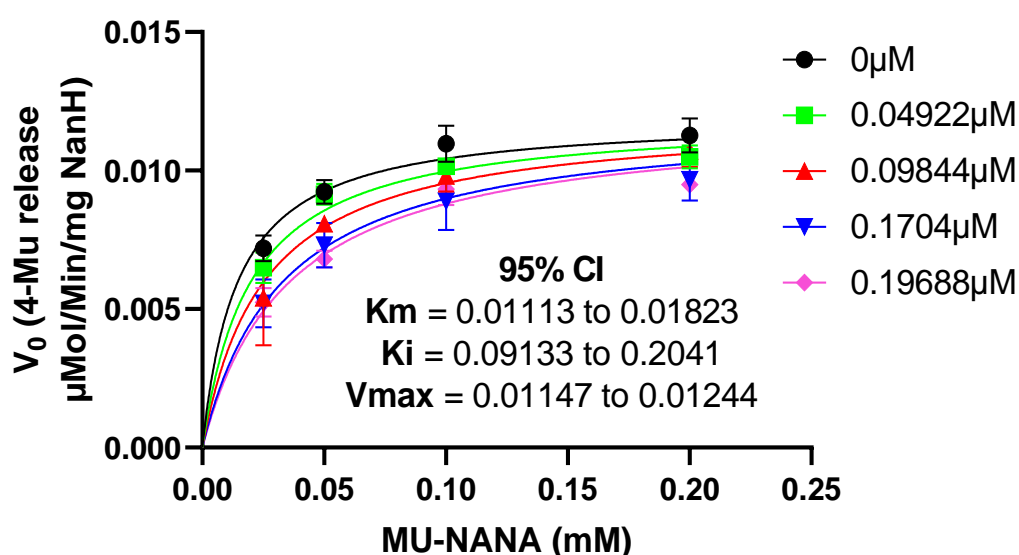
Figure 3.14: Competitive inhibition plot of 2e3aDFNeu5Ac9N3 on NanH Sialidase inhibition

Sialidase enzyme inhibition was determined in the absence or presence of varying concentrations of 2e3aDFNeu5Ac9N3 (µM) with the reaction set up containing varying substrate (MUNANA) concentrations (mM) that was exposed to NanH sialidase (2.5 nM) and diluted in 50 mM sodium phosphate buffer, 200 mM NaCl at pH 7.4 and incubated at room temperature. 50µL of the reaction set up was taken and stopped by the addition of 75 µL of 100 mM Na_2CO_3 buffer pH10.5 at 1, 2, 3 and 4 minutes respectively. The fluorescence was measured using TECAN M200 plate reader at excitation 355 nm and emission at 430 nm and the mode of enzyme inhibition was determined using Prism version 9.2.0. Data represent the mean of three experimental repeats (n=3), where each condition was conducted in triplicate.

3.7 Determination of Protein-Ligand Interactions for NanH

As outlined above in section 3.4 and Table 3.1, plant-derived and synthetic inhibitors are able to inhibit both purified (NanH and SiaPg), and whole-cell sialidase activities of *T. forsythia* and *P. gingivalis*. Further, the crystal structure of *T. forsythia* NanH-apo (PDB ID 7QYP), and that of *P. gingivalis* SiaPg-apo (PDB ID 8GN6), used in this study for molecular docking was recently established by Satur et al., (2022), and Wen-Bo et al., (2023), respectively. Therefore, given the information gained in this chapter, the theoretical nature of the interactions of these inhibitors with the NanH and SiaPg structural model was investigated. In this current project, molecular docking using AutoDock vina was used to interrogate the molecular nature of NanH-inhibitor or SiaPg-inhibitor (protein-ligand) interactions.

3.7.1 Structural basis for NanH and SiaPg sialidase docking

The NanH sialidase was reported to be a dimer with the crystal structure showing a two-fold symmetric and identical conformation with each of the catalytic domains facing the carbohydrate-binding modules (CBM) domain of the other subunit, and the active site of the enzyme located on the 6-bladed β-propeller (Satur et al., 2022) (figure 3.15).
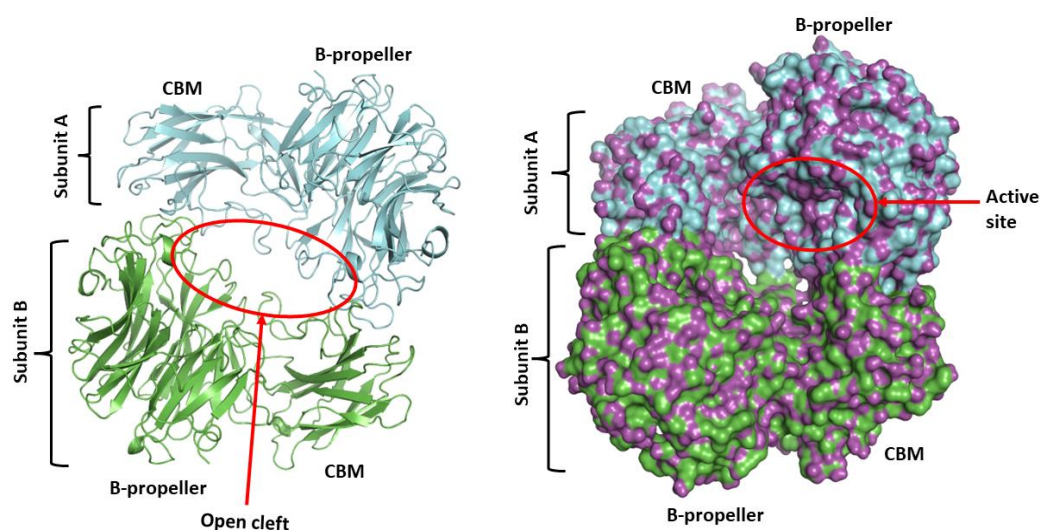
Figure 3.15: Crystal structure of *T. forsythia* NanH-apo

Each sub-unit (A in cyan and B in green) comprises a Beta-propeller (β-propeller) containing the Carbohydrate-Binding Module (CBM) and the active site. Visualized on PyMol to show the structure in cartoon and surface conformation with an open cleft found between the subunits.

SiaPg on the other hand was shown to be a monomer with each SiaPg molecule consisting of two canonical domains: a small carbohydrate-binding module (CBM; residues 31–175) with a β-barrel fold and a catalytic sialidase domain with a typical β-propeller fold (residues 176–526) (figure 3.16). The catalytic domain is shown to be composed of six sequential repeats, each of which consists of four antiparallel β-strands (Dong et al., 2023). The six repeats, which are well conserved in sialidases (Taylor, 1996), pack against each other and are arranged into a 6-bladed propeller forming a central cleft (figure 3.16a).
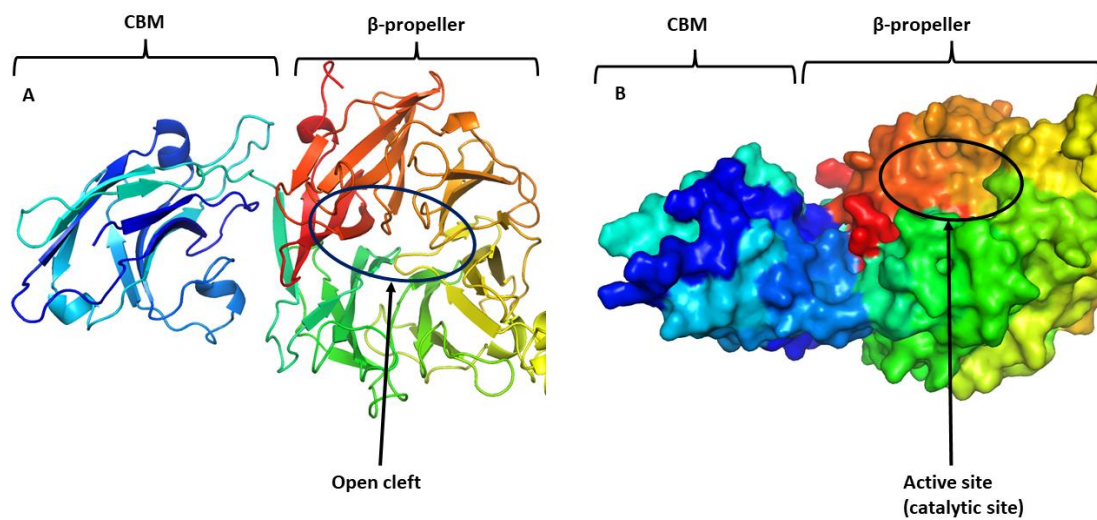
Figure 3.16: Crystal structure of *P. gingivalis* SiaPg-apo

The overall structure of SiaPG; the carbohydrate-binding module (CBM) and the catalytic domain (Active site) are colored in cyan/blue and red/green, respectively. Visualized on PyMol to show the structure in a cartoon [A] and surface [B] conformation with an open cleft found on the β-propeller (catalytic domain).

3.7.2 Investigation of Protein-Ligand Interactions

Previously, Satur and colleagues demonstrated that an inactive variant of NanH that has the ability to bind substrate but lacks catalytic activity was used to show how NanH sialidase might co-ordinate the native oligosaccharide binding substrates 3'-Sialyl-Lewis (3-SL) and 6'-Sialyl-Lewis (6-SL), (Satur et al., 2022) (figure 3.17). Further, NanH sialidase was shown to have a preference for α2-3 glycosidic linkages of the glycoconjugates, indicating the likeliness of its involvement in nutrient acquisition (Thompson *et al.*, 2009 and Frey et al., 2018). Here, both the 3-SL and 6-SL terminal sialic acids are shown to be seated at the active-site pocket of NanH with the carboxyl group at carbon position-1 (C-1) coordinating the arginine triad (Arg423, Arg487, and Arg212) via hydrogen bonds (figure 3.17). The conserved nucleophilic dyad Tyr518 and Glu407, which forms hydrogen bonds with the 3-SL, function as nucleophilic attack residues to stabilize the putative carbon positive ion in the transition state (Newstead et al., 2008). The hydroxyl group of Tyr518 directly points to the anomeric carbon at position C-2 of 3-SL, whereas Glu407, interacts with the hydroxyl group at C-8 of the 3-SL (figure 3.17). In addition, the C-4 hydroxyl of 3-SL forms a hydrogen bond to Arg231 and Asp219 to further stabilize the binding of 3-SL to the active-site pocket of NanH sialidase (figure 3.17). Asp219 also interacts with the 3-SL by making two hydrogen bonds to the hydroxyl group at C-4 and to the *N*-acetyl group at C-5 of 3-SL (figure 3.17). Interestingly, beyond these hydrophilic interactions, the sugar ring of 3-SL is mainly stabilized by the hydrophobic residues ILe213, Ala237, Leu238, Trp308, Phe352, Leu354, Gln373, Asn425, and ILe456 of NanH (figure 3.17), which form a generally hydrophobic pocket for 3-SL binding.
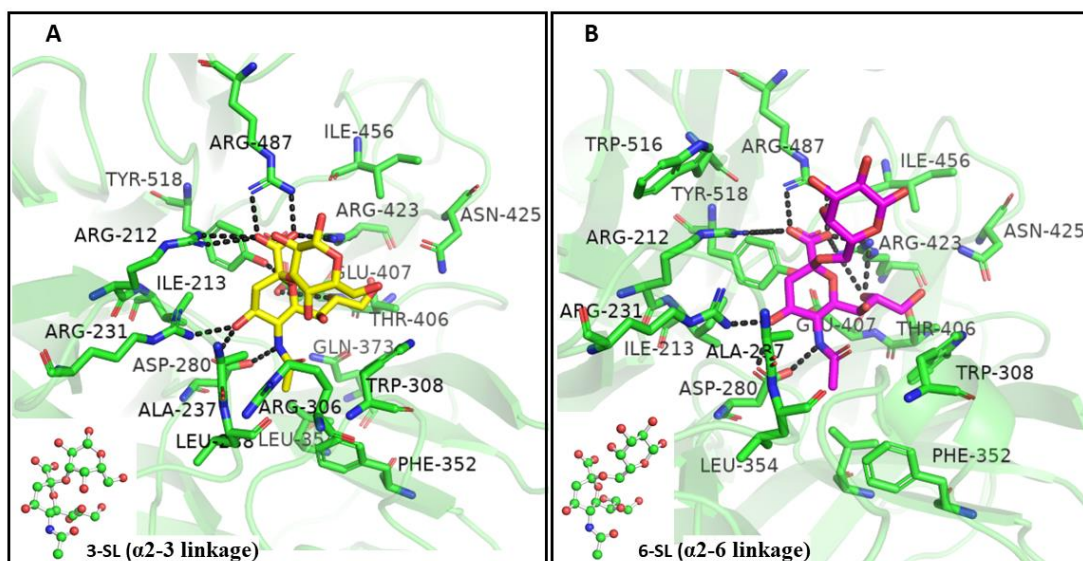
Figure 3.17: Molecular docking of 3'-Sialyl-Lewis (3-SL) and 6'-Sialyl-Lewis (6-SL) to the active-site pocket of NanH sialidase.

(**A**) 3-SL (yellow) and (**B**) 6-SL (magenta) showing interactions with catalytic residues (Arg triad R212, R423, R487) and other conserved catalytic residues. Hydrogen bonds are shown as grey dotted lines, with the polar and non-polar residues found at the active site interacting with the ligands. The inserts in a ball and stick conformation are the 3'-Sialyl-Lewis (3-SL) and 6'-Sialyl-Lewis (6-SL), respectively. These data were obtained from an *in silico* docking using AutoDock vina and visualized on PyMol.

Similarly, Dong et al., (2023) demonstrated using molecular docking to show the binding ability of a molecule of tartrate and sialic acid (also known as *N*-acetylneuraminic acid, Neu5Ac), the product of SiaPg into the active-site pocket of SiaPG (Dong et al., 2023). Here, the docking of Neu5Ac into the active-site pocket of SiaPG shows the carboxyl group at the C-1 position coordinating the arginine triad (R194, R460, and R398) (figure 3.18). Also, the hydroxyl group of the nucleophile Tyr488 forms a polar interaction with the carboxyl group at the C-1 position, whereas the carboxylate group of Glu382 interacted with the hydroxyl group at C-7 position of the sialic acid (figure 3.18). On the other hand, the acid/base residue Asp219 further stabilizes the sialic acid substrate in the active site pocket by forming a polar interaction with the *N*-acetyl group on the C-5 position of the Neu5Ac (figure 3.18). In addition to these catalytic residues, other hydrophobic residues involved in stabilizing the binding of Neu5Ac in the active-site pocket of SiaPg include Ile195, Leu220, Leu277, Trp278, Gln286, Phe327 (figure 3.18).
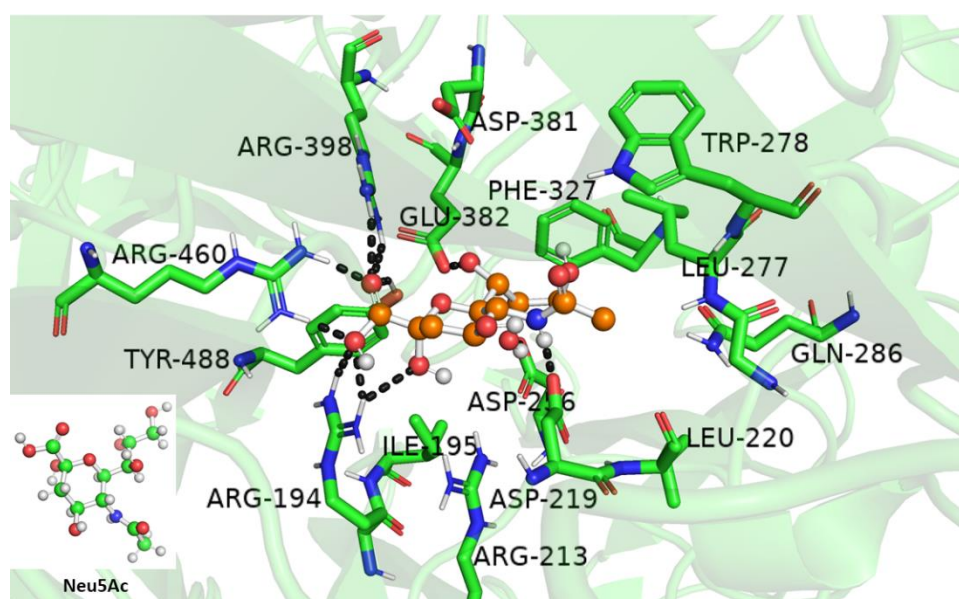
Figure 3.18: Molecular docking of Neu5Ac (sialic acid) to the active-site pocket of SiaPg.

The Neu5Ac is shown in a ball and stick conformation (orange) and the catalytic residues are shown as sticks. Hydrogen bonds are shown as grey dotted lines, with the polar and non-polar residues found at the active site interacting with the ligand. The insert in a ball and stick conformation (green) is a chemical structure of the Neu5Ac molecule. These data were obtained from an *in silico* docking using AutoDock vina and visualized on PyMol.

3.7.2.1 Determination of Inhibitors binding properties of NanH and SiaPg

As shown previously in this work, the sialic acid analogue inhibitors are able to inhibit the sialidase activity of both NanH and SiaPg (table 3.1). After establishing the IC50 of these inhibitors on purified NanH and SiaPg, and following the determination of the interactions of NanH and SiaPg with their respective native ligands (3-SL and Neu5Ac) (Figure 3.17 and Figure 3.18), molecular docking using AutoDock vina was carried out to study the protein-ligand interaction patterns of the sialidase inhibitors in the active-site pockets of NanH and SiaPg, respectively.

Similar to the interactions observed above with 3-SL and Neu5Ac (section 3.7.2), the negatively charged carboxyl group at the C-1 position of oseltamivir also coordinated the arginine triad (R423, R487, and R212) of NanH and (R194, R460, and R398) of SiaPg (figure 3.19 a & b). The nucleophilic dyads Tyr518/Tyr488 and Glu407/Glu382 also pointed directly to the anomeric carbon at C-2 position of the oseltamivir in the respective active-site pockets (figure 3.19 a & b). The amino group of oseltamivir (position C5, figure 3.19 a & b) interacts with the carboxylates of the acid/base Asp280 and Asp219 of NanH and SiaPg, respectively, while the *N*-acetyl tail sits in a hydrophobic pocket with a hydrogen bond forming between the amide of the *N*-acetyl and the carboxylate of Asp280 and Asp219 (figure 3.19 a & b). Other common residues found at the active-site pockets of the respective sialidases forming hydrophobic interactions with oseltamivir include ILe, Trp, Phe, Gln, Asn, Thr and Gly (figure 3.19 a & b).
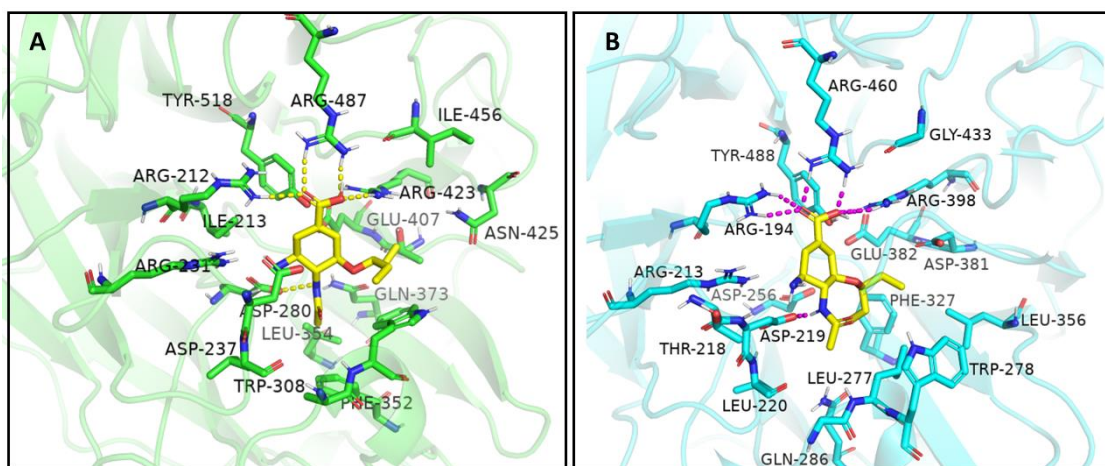
Figure 3.19 a&b: NanH and SiaPg active-site pockets bound in complex with Oseltamivir

(A) NanH (B) SiaPg in complex with oseltamivir (yellow sticks) interacting with the catalytic residues in the active-site pockets of NanH and SiaPg. Hydrogen bonds are shown as dotted lines, with the polar and non-polar residues found at the active site interacting with the ligand. These data were obtained from an *in silico* docking using AutoDock vina and PyMol.

Similarly, protein-ligand binding of other sialidase inhibitors including Siastatin B, and DANA into the active-site pockets of NanH and SiaPg, respectively, were also studied (figure 3.19 C to H). As observed with Oseltamivir (Figure 3.19 a & b), Siastatin B also lies in the hydrophobic pocket of NanH and SiaPg active-site pockets, respectively which is stabilized by extensive interactions (figure 3.19 C & D). Also, the negatively charged carboxyl group at the terminal C-1 position of Siastatin B forms hydrophilic bridges with the arginine triad (R423, R487, and R212) of NanH and (R194, R460, and R398) of SiaPg (figure 3.19 C & D). The conserved nucleophilic dyad Tyr518/Tyr488 and Glu407/Glu382 of NanH and SiaPg, respectively, also point directly to the anomeric carbon at C-2 of the inhibitor (figure 3.19 C & D). In addition to the hydrophobic residues that stabilizes the *N*-acetyl tail of the inhibitor in the active-site pockets, the carboxylates of the acid/base Asp280 and Asp219 of NanH and SiaPg, respectively, interacted with the amino group of Oseltamivir at C-5 (figure 3.21 C & D). While similar interaction pattern was observed with DANA in the active-site pocket of NanH (figure 3.19 E), a web of interactions was observed between the catalytic residues of SiaPg with the hydroxyl groups found on the surface of DANA (figure 3.19

F). Interestingly, these residues were also linked strongly to each other creating a web-like ring thereby stabilizing DANA in the active-site pocket of SiaPg ((figure 3.19 F).
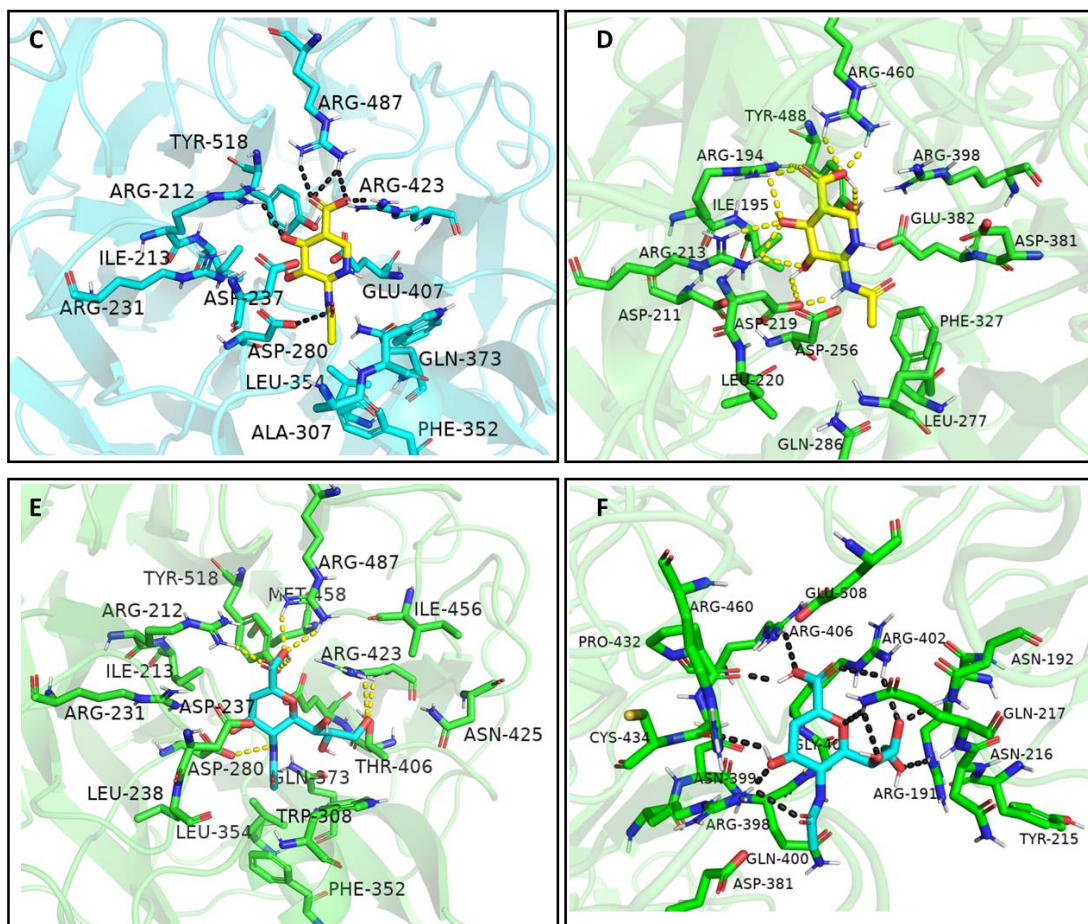
Figure 3.19 C-F: NanH and SiaPg active-site pockets bound in complex with Siastatin B and DANA

(C/E) NanH **(D/F)** SiaPg in complex with Siastatin B (C-D; yellow sticks) and DANA (E-F; cyan sticks) interacting with the catalytic residues in the active-site pockets of NanH and SiaPg. Hydrogen bonds are shown as dotted lines, with the polar and non-polar residues found at the active site interacting with respective ligands. These data were obtained from an *in silico* docking using AutoDock vina and PyMol.

Furthermore, docking of the di-fluoro sialic acid analogue; 2e3aDFNeu5Ac9N3 into the active-site pockets of NanH and SiaPg, respectively was also conducted to study the ligand interactions with the catalytic residues (figure 3.20). Similar with the transition state analogues (figure 3.19), the positively charged arginine triad also coordinates the negatively charged carboxyl group on C-1 position of 2e3aDFNeu5Ac9N3. In addition, the orientation of the di-fluoro sialic acid compound into the active-site pockets appeared to be tilted which may be due to the fluorine molecules attached at C-2 and C-3 positions on the compounds, thereby positioning the negatively charged carboxyl group at C-1 position to interact by forming hydrogen bonds with arginine triad (R212/R423/487 and R194/R460/R213) of NanH and SiaPg, respectively (figure 3.20 A & B). On the other hand, the conserved nucleophilic dyad Tyr518/Tyr488 and Glu407/Glu382 which function as nucleophilic attack residues appears to stabilize the compound by bringing it into close proximity with the fluorine molecule attached equatorially at C-2 (2e-), with the carboxylate group of the glutamate also in close contact with the hydroxyl group at C-7 of the di-fluoro sialic acid compounds (figure 3.20). Also, the carboxylates of the acid/base residue Asp237 and Asp219 of NanH and SiaPg, respectively, interacted with the *N*-acetyl group of 2e3aDFNeu5Ac9N3 at C-5 position (figure 3.20). Interestingly, the azido group (N3) on C-9 of 2e3aDFNeu5Ac9N3 forms a strong hydrogen bond with another acid/base residue Asp280 and Asp381, which is further stabilised by glycine (Gln355 and Gln400) in the active-site pockets of NanH and SiaPg, respectively (figure 3.20). Other conserved hydrophobic residues that stabilizes the azido tail in the respective active-site pockets include Trp308/Trp278, Leu354/Leu356, Gln373/Gln286 in addition to Pro357, Thr406 and Met458 found specifically in NanH active-site while, Phe327 specific to SiaPg active-site pocket (figure 3.20 C & D).
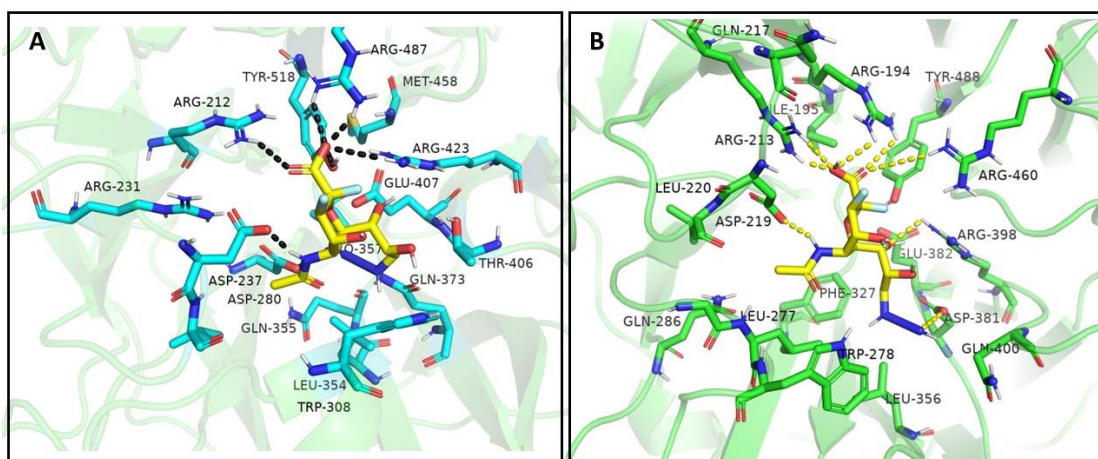
Figure 3.20: NanH and SiaPg active-site pockets bound in complex with 2e3aDFNeu5Ac and 2e3aDFNeu5Ac9N3

(A) NanH (B) SiaPg in complex with 2e3aDFNeu5Ac9N3 (yellow sticks) interacting with the catalytic residues in the active-site pockets of NanH and SiaPg. Hydrogen bonds are shown as dotted lines, with the polar and non-polar residues found at the active site interacting with respective ligands. These data were obtained from an *in silico* docking using AutoDock vina and PyMol.

3.8   Discussion

Expression and purification of recombinant proteins NanH and SiaPg were carried out using HisTag low-affinity chromatography. This is particularly important because it is key in answering the first objective of this research which is aimed at determining the sialidase inhibitory properties of a wide range of pharmaceutically approved, plant-derived, and synthetic compounds.

After purification of the sialidases, concentrations of the purified NanH and SiaPg were determined using bicinchoninic acid assay (BCA) followed by enzymes kinetics to determine the optimum reaction time and the sialidase inhibitory activities of the synthetic and plant-derived compounds was also investigated. In addition, drugs (compound) combination assay to determine synergistic effects, as well as the mechanism of action (MOA) of Palmatine, Berberine chloride, and 2e3aDFNeu5Ac9N3 on NanH, was also determined. Lastly, Protein-ligand interactions were also investigated to determine how the inhibitors bind in the active-site pockets of NanH and SiaPg, respectively.

3.8.1   Sialidase activity of *T. forsythia* and *P. gingivalis*

Sialidases are a large group of soluble enzymes that catalyzes the removal of sialic acids from complex host glycoproteins or glycolipids (Vimr et al., 2004 and Juge et al., 2016). Sialic acids are nine-carbon sugars mostly found at the terminal end of oligosaccharide chains on cell surfaces and are important for cell-to-cell attachment, immune signalling, and modulation, and are used by pathogenic microorganisms in coating themselves to evade host immune actions (Traving & Schauer, 1998 and Tanner, 2005).

Oral pathogens such as *T. forsythia* and *P. gingivalis* reported to be associated with periodontitis secretes sialidase enzymes (NanH and SiaPg), which promote their growth and survival in the oral cavity, biofilm formation, immune evasion, adherence, and colonisation of host surfaces (Stafford et al., 2012; Settem et al., 2013 and Frey et al., 2018). These Gram-negative anaerobes which possess sialic acid scavenging operons have been implicated in the causation of periodontal diseases such as periodontitis and other systemic diseases (Eke et al., 2012 and Mikuls et al., 2014). Sialidases are therefore believed to be key virulence factors of several pathogens including these oral pathobionts (Sudhakara et al., 2019) as such, they are a suitable target for novel inhibitors.

To determine the sialidase activity of the purified enzymes (NanH and SiaPg) and that of the whole bacterial cells therefore, the sialic acid-substrate 4-Methylumbelliferil-*N*-acetyl-α-D-neuraminic acid (MUNANA) assay aimed at the detection of 4-Methylumbelliferyl (4-MU) cleavage from MUNANA was used. Both the purified proteins were shown to be sialidase positive with NanH showing a rapid MUNANA cleavage (within 2 minutes) as compared to SiaPg which takes about 4-5 minutes. Additionally, the wild-type strains of the pathogens showed higher sialidase activities as compared to the mutant strains which show minimal or no sialidase activity. However, this is not a new finding, as it was previously reported in our Lab (Roy et al., 2010 and Frey et al., 2019). Nonetheless, reconfirmation of this claim was important as it served as the basis for testing for the novel inhibitors of this bacterial virulence factor.

3.8.2 Purified (NanH and SiaPg) and whole bacterial sialidases of *T. forsythia* and *P. gingivalis* were inhibited by synthetic and plant-derived inhibitors

Here, the inhibitory activities of the pharmaceutically approved sialidase inhibitors; Zanamivir, *N*-acetyl-2,3-dihydro-2-Deoxyneuraminic acid Methyl ester (DANA), Siastatin B (Synthetic), and plant-derived compounds Berberine chloride, Epicatechin gallate, Palmatine (Plant-derived) and the newly synthesized compounds "USA inhibitors" listed in (table 2.1), were investigated.

Amongst the approved neuraminidase (sialidase) inhibitors, DANA shows a better inhibitory activity on SiaPg with an IC_{50} value of 99.62 µM compares to Zanamivir that has 292.1 µM, while Siastatin B has 1081 µM on NanH as compared to 6156 µM of Zanamivir on NanH previously reported (Frey *et al.,* 2019).

Epicatechin gallate; a plant-derived polyphenol appears to be more effective against SiaPg and NanH when compared to Zanamivir; an FDA-approved neuraminidase inhibitor. The millimolar inhibition range of Zanamivir on SiaPg and NanH seen in this study was also reported in previous findings with 720 µM as the IC_{50} of Zanamivir on Pneumococcal sialidases and 6 mM on *T. forsythia sialidase* (Jasvinder *et al.,* 2012; Frey *et al.,* 2019). On the other hand, Epicatechin gallate used in this study, showed a better inhibitory activity on purified NanH sialidase of *T. forsythia*, as compared to its efficacy on *V. cholerae* neuraminidase reported to be 211 ± 19 µM (Stefania *et al.*, 2017). Furthermore, Palmatine and Berberine chloride were reported to have a strong inhibitory activity with IC_{50} values of 12.8 ± 1.5 and 13.5 ± 2.3 µM, respectively on *C. perfringens* neuraminidase (Kim et al 2014), was however seen in this present project

to possess moderate activity on both SiaPg and NanH sialidase (531.7 and 166.2 µM) and (IC$_{50}$ 106.2 and 445. 1 µM), for Palmatine and Berberine chloride, respectively. The observed variations in the inhibition of these enzymes by the same compound may be due to structural differences in active sites of the aforementioned enzymes, as well as the mechanisms of action of these compounds on respective enzymes.

The discrepancies of IC$_{50}$ of these sialidase inhibitors on purified NanH and SiaPg or whole bacterial sialidases may be due to the specific binding affinity of respective compounds to the active sites of the individual sialidases. For example, while Epicatechin gallate and Palmatine inhibit NanH better, Berberine chloride and Zanamivir were shown to possess better inhibitory efficacies on SiaPg (table 3.4). Also, the mechanisms of action of these compounds with respect to the binding sites of NanH and SiaPg could also be one of the reasons for their selectiveness on the bacterial sialidases. In addition, while these compounds showed a better efficacy on purified sialidases, their potency on sialidases of whole bacterial cells was observed to be reduced, which could be due to actions on other factors such as the bacterial capsules, S-layer, surface charge as well as penetration to the periplasm of the pathogens.

Furthermore, inhibition studies against the sialidases of *T. forsythia* (NanH) and *P. gingivalis* (SiaPg) using the synthetic compounds, indicated that the newly synthesised compounds by Xi Chen and colleagues (Li et al., 2019), were good inhibitors of these bacterial enzymes.

9-Azido-9-deoxy-2-(e)-3-(a)-difluoro-*N*-acetylneuraminic acid (2e3aDFNeu5Ac9N$_3$), was identified as the most effective compound against SiaPg and NanH with IC$_{50}$ values of 1.692 and 0.1704 µM, respectively (Table 3.4). Compounds with axial fluorine at C-3 were also reported to have better inhibitory properties against the sialidases of pathogenic bacteria such as *V. cholerae* and *C. perfringens* with IC$_{50}$ values of 0.18 and 0.024 µM, respectively (Li et al., 2019). Furthermore, 2e3eDFNeu5Ac9N$_3$ appears to be more effective on NanH as compared to SiaPg with IC$_{50}$ values of 8.048 and 119.2 µM, respectively (table 3.4). The differences in inhibitory activities observed between these similar compounds i.e., no.15 and no.16 (table 3.4), may be due to stereochemistry of the fluorine molecules with compound no.15 having 3F-equatorial and compound no.16 having 3F-axial positions, respectively (figure 3.8c) (Li et al., 2019). Lastly, the two azido-modified compounds showed selective activity with a preference for NanH sialidase of *T. forsythia*.

In contrast, however, di-fluoro compounds with no Azido group modification at C-9; 2e3eDFNeu5Ac, and 2e3aDFNeu5Ac, appear to have a better inhibitory effect on SiaPg than those observed with NanH (table 3.1). Nonetheless, they also showed some good inhibitory activities on both the sialidases. 2e3eDFNeu5Ac has IC_{50} values of 4.681 and 9.913 µM, while 2e3aDFNeu5Ac had IC_{50} values of 3.358 and 19.71 µM on SiaPg and NanH, respectively (table 3.4). Interestingly however, these compounds were reported to have poor inhibitory activities against the *S. pneumoniae* sialidases (SpNanB and SpNanC), with 2e3eDFNeu5Ac having IC_{50} values of $>1 \times 10^3$ µM on both SpNanB and SpNanC, respectively, while 2e3aDFNeu5Ac has $>1 \times 10^3$ µM on SpNanB and $(1-10) \times 10^2$ µM on SpNanC (Li et al., 2019).

Worthy of mention also, is the better inhibitory efficiencies of the modified compounds (di-fluoro compounds), in comparison to Neu5Ac2en (DANA), which has higher IC_{50} values (i.e., 16.58 and 29.5 µM), against the sialidases of *P. gingivalis* (SiaPg) and *T. forsythia* (NanH), respectively.

Although the compounds may have different inhibition mechanisms, comparing them therefore may not be ideal. Nonetheless, the IC_{50} values obtained at the same defined time frame for both compounds on SiaPg and NanH may provide a clear understanding of the effectiveness and selective properties of di-fluoro compounds. Furthermore, the strong binding and inhibitory properties of these inhibitors may be due to the di-fluoro atoms attached to the sialic acid analogue and the positions at which they are attached (figure 3.6 c). Interestingly, Li and colleagues reported that, while 2e3a/2e3eDFNeu5Ac9N3 enables the electronegative fluorine atom to form a covalent bond between the sialic acid and the *V. cholerae* sialidase, Neu5Ac2en forms non-covalent bond instead (Li et al., 2019).

Modification of Neu5Ac2en at C-9 also has made the new compound Neu5Ac9N$_3$2en a better sialidase inhibitor of NanH sialidase as compared to the former (table 3.4). Additionally, the differences in sialidase inhibitory activities between 2e3aDFNeu5Ac and 2e3aDFNeu5Ac9N$_3$ observed in this study may be due to the modification at C-9 (Li et al., 2019). This may suggest that the azido group (N3) on C-9 might have positioned the molecule more tightly in the enzyme active site thereby rotating the fluorine molecules to the glycosidic bonds, which Li et al., also shows that the stereochemistry of 3-fluorine of the difluoro-compounds influences how they interact with and influence its catalytic activity (Li et al., 2019).

Also, while 2e3aDFNeu5Ac9N$_3$ was shown to be an effective inhibitor with a long effective duration which was selective against pathogenic bacterial sialidases from *V. cholerae* and *C. perfringens* (CpNanI) (Li et al., 2019), it was observed also in this study to also have a good sialidase inhibitory activities on SiaPg and NanH at a shorter exposure time, making it a more promising compound amongst the rest.

Overall, most of the newly synthesized "USA inhibitors" were more effective against the purified and whole periodontal pathogen sialidases (SiaPg and NanH), when compared to the FDA-approved neuraminidase inhibitors i.e., Zanamivir, Oseltamivir, and Siastatin B or to the plant-derived compounds tested in this study. This, therefore, presents it as the best candidate for further sialidase inhibition, whole bacterial invasion inhibition, biofilm inhibition, and immune signalling works. In addition, the compounds can be explored for potential application as novel chemical glycobiological tools and/or strategies to combat infections caused by bacteria or in host immune regulation.

3.8.3 Palmatine in combination with Berberine chloride synergistically inhibits NanH sialidase activity of *T. forsythia*

Palmatine alongside Berberine chloride are two of the main four protoberberine alkaloids reported to be found at the bark, roots, and stem of several medicinal plants such as *Corydalis yanhusuo, Hydrastis canadensis, Coptidis rhizome,* and *Berberis aristate* (Ye et al., 2009). These phytochemicals were previously reported to possess anti-inflammatory, anti-tumor, and antibacterial properties (Kim et al., 2014 and Balkrishna et al., 2019). Also, combination therapy was shown to help in overcoming drug resistance by microorganisms as well as increase the potency of the combined drugs by targeting multiple proteins thereby reducing the duration of treatment (Cobo, 2014). Additionally, the synergistic effect of some certain drug combinations may be more efficacious as compared to a single drug, or, drug A may potentiate the mechanism of drug B or vice-versa (Pritchard et al., 2013).

As previously reported in this study, the individual inhibitory efficacies of Palmatine and Berberine chloride on NanH sialidase activity were both weak, however, knowing that these compounds can be gotten from the same plant, their combined synergistic effect (PalBer) on the purified NanH sialidase was therefore assessed. Furthermore, to confirm if the inhibition mode of the combination of Palmatine and Berberine chloride is synergistic, the combination index (CI) value of the experimental data was calculated

according to the method of Chou (2008). Here, combining Palmatine with Berberine chloride at a ratio of 0.2:0.5 (total dose 0.7 mM) synergistically inhibits almost 100% of the NanH sialidase activity of *T. forsythia*.

Investigation into the mechanisms of action (MOA), of these plant-derived compounds on NanH sialidase, shows Palmatine to be a non-competitive and Berberine chloride to be an un-competitive inhibitor of NanH sialidase, respectively. This may be the reason for the synergistic effect on NanH sialidase as observed in this current project. Interestingly, Balkrishna et al., (2019), also reported the mode of inhibition of Palmatine and Berberine on acetylcholinesterase (AChE), an enzyme mainly associated with Alzheimer's disease (AD), to be non-competitive. They also reported combinations of individual alkaloids Palmatine and Berberine resulting in a synergistic effect for AChE inhibition (Balkrishna et al., 2019). Further, Liu et al. (2013), also reported that a combination of inhibitors improves α-glucosidase inhibition, and the synergistic effects of the xanthone derivatives show 40% inhibition of α-glucosidase (Liu et al., 2013).

Lastly, the inhibition mode of the newly synthesized "USA inhibitor" 9-Azido-9-deoxy-2,3-difluorosialic Acid [2e3aDFNeu5Ac9N3] on the NanH sialidase of *T. forsythia* was revealed to be a competitive inhibitor with its increased concentration leading to an increased reduction in the activity of NanH sialidase of *T. forsythia*.

3.8.4 Determination of Ligand binding into the active-site pockets of NanH and SiaPg sialidase

Following the ability of the plant-derived and synthetic sialidase inhibitors to inhibit both purified (NanH and SiaPg) and whole-cell sialidase activities of *T. forsythia* and *P. gingivalis* reported earlier in this work, *in silico* docking with the crystal structure of *T. forsythia* NanH-apo (PDB ID 7QYP) and SiaPg-apo (PDB ID 8GN6), established recently (Satur et al., 2022; Dong et al., 2023), was used to study the protein-ligand interactions. Both the crystal structures of NanH and SiaPg are shown to have conserved carbohydrate binding modules (CBM) and catalytic domains that contain the six-bladed β-propeller fold (Figures 3.15 and 3.16), a characteristic reported to be commonly shared among sialidases from different organisms (Newstead et al., 2008; Telford et al., 2011).

Molecular docking of the native ligands (3'-Sialyl-Lewis (3-SL), 6'-Sialyl-Lewis (6-SL), and Neu5Ac) (Figures 3.17 and 3.18), as well as the inhibitors (section 3.7.2.1) into the active-site pockets of NanH and SiaPg, respectively were carried out using AutoDock Vina and PyMol to determine the conserved active-site residues, which include Arg423/194, Arg487/460, Arg212/398, Tyr518/Tyr488, Glu407/Glu382, Asp280 and Asp219 of NanH and SiaPg (Figures 3.19 and 3.20), respectively. The conserved arginine triad in both NanH and SiaPg bind to the negatively charged carboxyl group of the native ligands (3-SL, 6-SL, and Neu5Ac) as well as the inhibitors. Importantly, the arginine triad (Arg423/194, Arg487/460, Arg212/398), in addition to other conserved active-site residues (Tyr518/Tyr488, Glu407/Glu382, Asp280, and Asp219), were previously reported to be involved in catalysis (Newstead et al., 2008; Frey et al., 2018; Satur et al., 2022; Dong et al., 2023). While tyrosine and glutamate form a Tyr-Glu nucleophilic dyad, the aspartate Asp280/219 act as the acid/base catalyst needed in the catalytic processes of the sialidase enzyme (Newstead et al., 2008).

Beyond the conserved catalytic residues mentioned above, there are other non-polar residues in the active-site pockets of both NanH and SiaPg which provides a hydrophobic condition that helps in stabilizing inhibitor (s) in the active-site pockets which include ILe, Trp, Phe, Gln, Asn, Thr and Gly etc (Figures 3.19 and 3.20). In addition, while similar interactions was observed with Oseltamivir and Siatatin B in the respective active-site pockets, binding of DANA in the active-site pocket of SiaPg appears to be complicated, with both polar and non-polar residues strongly linked to each other thereby creating a web-like ring that stabilises DANA in the active-site pocket of SiaPg. Importantly, the mechanism of action of DANA on viral neuraminidase has been shown to bind to the conserved residues in the active site thereby outcompeting the sialic acids found at the terminal end of host glycoprotein chains, thus inhibiting the releases of virions from infected host (reviewed in Bowles & Gloster, 2021). Similarly, Neu5Ac2en (DANA) is reported to derive its potency from mimicking the oxocarbenium ion-like transition state (Bowles & Gloster, 2021). In addition, DANA was reported to synergistically inhibits the catalytic (domain) activity from sialidases of a respiratory tract infection pathogen; *S. pneumoniae* (NanA) and that of *Bacteroides thetaiotaomicron* (BtSA), a symbiotic commensal microbe of the intestinal tract (Assailly et al., 2021).

Of all the sialidase inhibitors screened, the di-fluoro sialic acid analogue; 2e3aDFNeu5Ac9N3 which is a mechanism-based inhibitor showed a superior inhibition of both NanH and SiaPg of *T. forsythia* and *P. gingivalis* respectively. Docking of the di-fluoro sialic acid analogue into the active-site pockets also showed the positively-charged arginine triad (Arg423/194, Arg487/460, Arg212/398), of NanH and SiaPg respectively coordinating the negatively-charged carboxylate group on C-2 position of 2e3aDFNeu5Ac9N3. Interestingly, the orientation of 2e3aDFNeu5Ac9N3 into the active-site pockets appears to be tilted slightly maybe due to the attached di-fluoro molecules on C-2 and C-3 positions of the compound thereby allowing an additional interaction between the azido group (N3) on C-9 with the acid/base aspartate (Asp280/Asp381) of NanH and SiaPg, respectively. Previous studies observed that C-3-fluorinated *N*-acetylneuraminic acid inhibit *C. perfringens* sialidase and viral neuraminidase such as that of Influenza virus competitively (Sun et al., 2000; Guo et al., 2002). Further, di-fluoro *N*-acetylneuraminic acid; 2e3aDFNeu5Ac was developed as a probe to confirm the two-step double-displacement mechanism of hydrolysis by GH33 (CAZy) sialidases where, tyrosine (Tyr) residue serve as the key catalytic nucleophile (Zechel & Withers, 2000), that form a unique covalent aryl-glycoside intermediate where it attenuates glycosylation (k1) and deglycosylation (k2) rates in the catalytic cycle of the sialidases (Keil et al., 2022). Specifically, the fluorine molecule attached to the C-3 position (3-F) is shown to inductively destabilizes the formation of a positive charge during the transition states, thereby reducing the rates of glycosylation (k_1) and deglycosylation (k_2) (Keil et al., 2022). Li et al., also reported the selectivity and superior *in vitro* activity of 2e3aDFNeu5Ac9N3 as a long effective inhibitor of *C. perfringens* (CpNanI), *V. cholorae* and cytosolic (hNeu1) sialidases, which was shown to be due to the axial fluorine molecule on C-3 and the azido group (N3) on the C-9 positions, respectively (Li et al., 2019).

Previously also, Li et al. demonstrated that modification of the compound by adding azido group (N3) at C-9, as well as the axial stereochemistry of 3-fluorine of 2e3aDFNeu5Ac9N3 influences how the compound interacts with and influences its catalytic activity (Li et al., 2019). Further, di-fluoro sialic acid compounds were shown to be mechanisms-based sialidase inhibitors which serve as useful tools to trap and probe reaction intermediates in enzymatic reactions and also the active sites of the enzymes (Keil et al., 2022). Therefore, with 2e3aDFNeu5Ac9N3 fitting into the enzyme's active site similar to Oseltamivir, Siastatin B and the native oligosaccharide

binding substrates 3-SL, 6-SL, and Neu5Ac, it further shows that 2e3aDFNeu5Ac9N3 is a competitive sialidase inhibitor as previously established (section 3.6.2). This might also contribute to the high inhibitory activity of 2e3aDFNeu5Ac9N3 over the other compounds observed in this study.

3.9   Chapter Summary

The sialidase inhibitory abilities, mechanisms of action of these compounds, as well as the NanH binding properties of 2e3aDFNeu5Ac9N3, provide useful insights which might be needed for subsequent inhibition assays towards the discovery of novel antimicrobials (drug development). Nevertheless, Covid-19 has impacted hugely my access to Lab., and other resources needed to conduct more experiments such as synergistic assays (drug combination assay) using different compounds and mechanisms of action of the compounds on both NanH and SiaPg. Going forward therefore, findings from this chapter shall serve as the basis for the continuation of the remaining part of the research, which is focused on the contributions of sialidases to bacterial growth, biofilm formation, and the determination of antibacterial, antibiofilm, and cytotoxic effects of these inhibitors. Lastly, the role of bacterial sialidases in host-pathogen interactions via adhesion and invasion, as well as in innate immune modulation was also investigated.

CHAPTER FOUR

Determination of the Effect of Sialidase Inhibitors on Bacterial Growth and Biofilm Formation

4.1 Introduction

One of the major virulence factors of bacterial cells is their ability to form biofilms. Bacterial cells embedded in biofilms' extracellular matrix (ECM) can withstand hostile environmental conditions such as desiccation and starvation which makes them capable of causing a wide range of chronic diseases. Furthermore, biofilm provides protection for the invading bacteria against the host immune system through impaired activation of phagocytes and the complements system (Cramton et al., 1999 and Götz, 2002). In addition, the multifactorial nature of biofilm development promotes drug tolerance which imposes great challenges in the use of the conventional antimicrobial regiments and this justifies the need for multitargeted or combinatorial therapies in managing biofilm-related infections (Koo et al., 2017).

4.1.1 Oral Biofilms

Bacterial biofilms have been shown to be the cause of many infectious diseases mainly due to their emergent properties such as the enhanced survival following exposure to antibiotics or antimicrobials (Flemming et al., 2016). Oral biofilms are a three-dimensional structured bacterial communities that are attached to solid surfaces like enamel of the teeth, the surface of the root or dental implants which are often embedded in an extracellular matrix (Saleem et al., 2016). Infectious diseases of the oral cavity such as periodontitis, dental caries and gingivitis are as a result of the interactions between the pathogenic microorganisms, their host and the host's diet, which promotes colonization of the oral surfaces like the teeth and subsequent formation of oral biofilms otherwise called dental plaque (Marsh & Zaura, 2017).

Composition of the microbiota found in different areas of the oral cavity is affected by many factors, such as when the teeth begins to erupt, thereby providing new, non-shedding surfaces for colonization by opportunistic pathogens and other commensals (Bowen et al., 2018). The age of the host, diet, systemic and immune conditions, oral hygiene, overexposure to dietary sugars, and the use of medications that promote hyposalivation can also affect the composition of the oral microbiome of the host (Bowen et al., 2018).

Polymicrobial interactions and the localized biofilm microenvironment embedded in the extracellular polymeric substances (EPS), play active roles in modulating health and disease conditions which promotes polymicrobial biofilm-associated infections such as periodontitis (Mira et al., 2017). Furthermore, oral pathogens such as *T. forsythia* (Roy et al., 2010), *P. gingivalis* and *T. denticola* (Bao et al., 2014), *F. nucleatum* (Honma et al., 2018), *S. aureus*, *S. mutans* and *Lactobacillus* sp. (Fayaz et al., 2014 and Krzyściak et al., 2014), were shown to form biofilms individually or in coaggregation as polymicrobial biofilms.

With this in mind and considering the role of dental plaque in periodontitis, the role of *T. forsythia* and *P. gingivalis* sialidases in biofilm formation, as well as the inhibitory effect of the sialidase inhibitors on bacterial growth and biofilm formation was investigated in this chapter.

4.2   Results

4.2.1   Sialidase Promotes the Growth of *P. gingivalis* and *T. forsythia*

To investigate (re-confirm) the role of sialidase in bacterial growth and biofilm formation as a prelude to determining the antibacterial and antibiofilm properties of the

sialidase inhibitors screened previously (Tables 3.1 and 3.2), experiment as outlined in (section 2.10) was conducted. For *P. gingivalis*, both the wild-type and sialidase-deficient strains were grown in supplemented BHI (erythromycin not included) for three days a significant difference in the growth rate of the wild type (wtPg0381) as compared to the sialidase-deficient strain (ΔPg0381), was observed (Figure 4.1). Similarly, *T. forsythia* was grown in supplemented TSB (erythromycin not included) for five days, and a similar trend was also observed in the growth of the wild-type *T. forsythia* (wtTf43037) in comparison to the sialidase-deficient strain (ΔTf035) (Figure 4.2). This information is important because it provides baseline exponential and optimum growth rates of these pathogens. The exponential growth of *P. gingivalis* (0381) was observed around 15-30 hours (Figure 4.1), while that of *T. forsythia* (ATCC43037) at about 36-60 hours (Figure 4.2). On the other hand, the exponential growth of the sialidase-deficient *T. forsythia* was delayed to about 50-72 hours (Figure 4.2), respectively. Although both strains showed similar growth patterns, the wild-type *P. gingivalis* and *T. forsythia* grow better than their respective mutant strains, indicating the important role of the sialidase gene in bacterial growth rate.
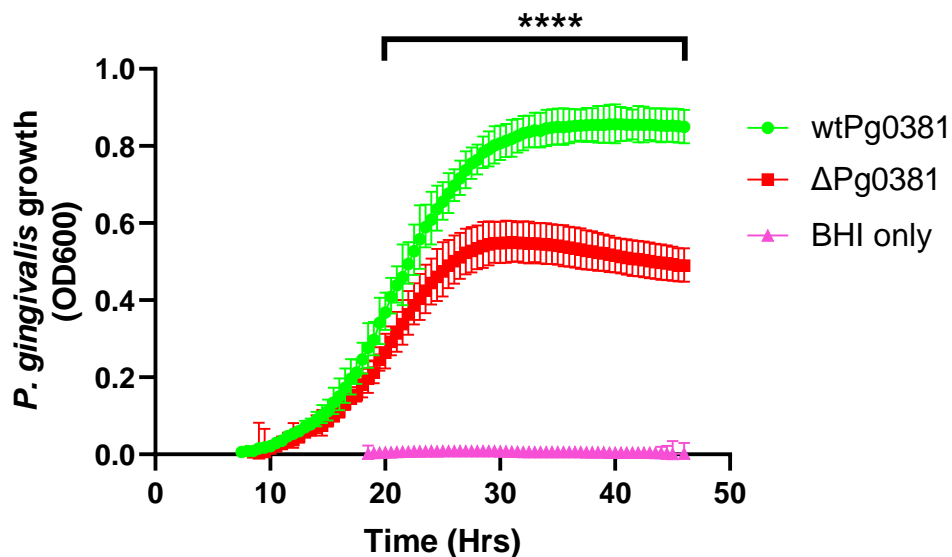
Figure 4.1: Bacterial growth curve of wild-type and sialidase-deficient strains of *P. gingivalis* (wtPg0381 and ΔPg0381).

Overnight broth culture of *P. gingivalis* grown in BHI was pelleted and adjusted to 0.1 in supplemented BHI (erythromycin not included). 200 µL of each strain were

dispensed in a flat bottom 96-well plate (in triplicate), and the plate was inserted in a Cerillo stratus plate reader and was incubated in an anaerobic chamber at 37°C, 10% CO_2, 10% H_2, and 80% N_2 for 3 days. Bacterial growth was measured after every 30 minutes, and the bacterial growth curve was plotted using GraphPad Prism (version 9.2.0). Data represent the mean of four experimental repeats (n=4), where each condition was conducted in triplicate. Ordinary one-way ANOVA with Dunnett's multiple comparison test was used to analyse the differences in the multiple means gotten from readings of the bacterial growth. Error bars = Geometric mean with error (95% CI). $P = <0.0001$.
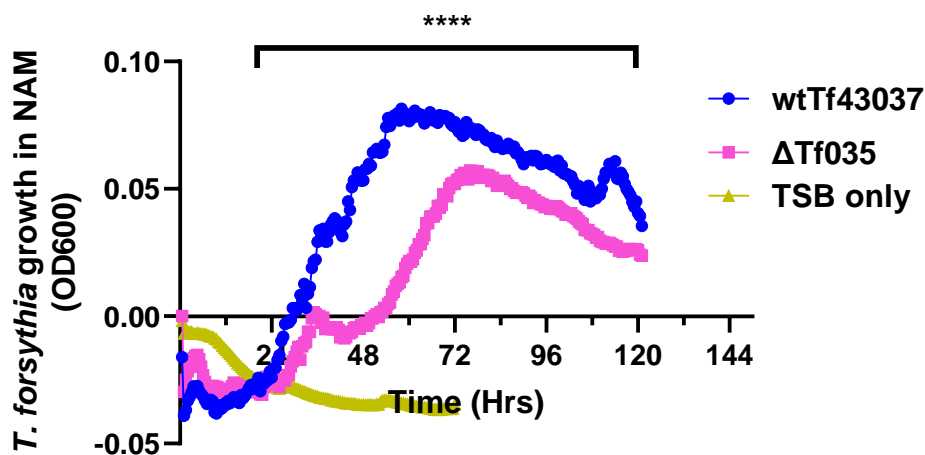
Figure 4.2: Bacterial growth curve of wild-type and sialidase-deficient strains of *T. forsythia* (wtTf43037 and ΔTf035)

Overnight broth culture of *T. forsythia* grown in TSB were pelleted and adjusted to 0.05 in supplemented TSB (erythromycin not included). 200 µL of each strain were dispensed in a flat bottom 96-well plate (in triplicate), and the plate was inserted in a Cerillo stratus plate reader and was incubated in an anaerobic chamber at 37°C, 10% CO_2, 10% H_2, and 80% N_2 for 5 days. Bacterial growth was measured after every 30 minutes, and the bacterial growth curve was plotted using GraphPad Prism (version 9.2.0). Data represent the mean of three experimental repeats (n=3), where each condition was conducted in triplicate. Ordinary one-way ANOVA with Dunnett's

multiple comparison test was used to analyse the differences in the multiple means gotten from readings of the bacterial growth. Error bars = SD. P = <0.0001.

4.2.2   Investigation of the Effect of Sialidase Inhibitors on Biofilm Formation and Bacterial viability

4.2.2.1 Determining the role of sialidase in biofilm formation by *P. gingivalis* and antibiofilm activity of 2e3aDFNeu5Ac9N3

After demonstrating that sialidase promoted the growth of wild-type *P. gingivalis* significantly in comparison to the sialidase-deficient strain (section 4.2.1), investigating the role of sialidase in biofilm formation by *P. gingivalis* becomes very important. Here, biofilm formation on a polystyrene 96-well plate was conducted as previously described in (section 2.10.1). The sialidase-deficient strain was found to form a strong biofilm with a significant difference when compared to the wild-type *P. gingivalis* (Figure 4.3). Interestingly, even at the highest concentration (4µM) of the sialidase inhibitor 2e3aDFNeu5Ac9N3 tested, it was unable to inhibit the biofilms formed by both wild-type or mutant strains of *P. gingivalis* (Figure 4.4).
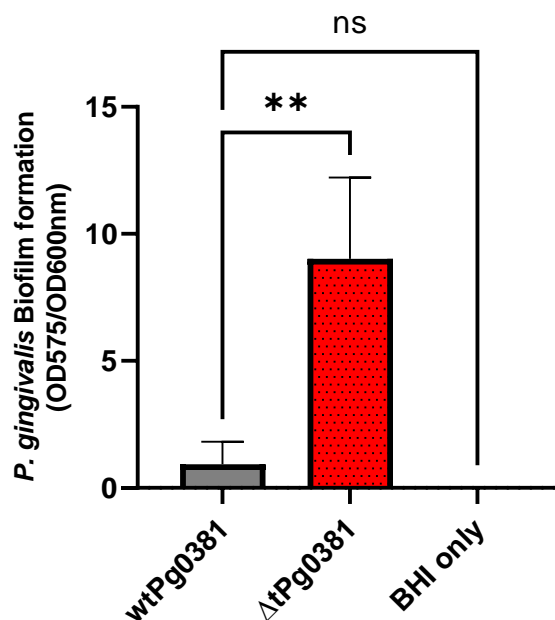
Figure 4.3: Biofilm formation by wild-type and sialidase-deficient *P. gingivalis*

Overnight broth culture of wild type (wtPg0381) and sialidase-deficient strain (ΔPg0381) of *P. gingivalis* grown in supplemented BHI (erythromycin not included), were adjusted to OD_{600} 0.1. 200 µL of each strain were dispensed in a flat bottom 96-well plate (in triplicate), and incubated anaerobically at 37°C for 3 days in a Cerillo device. The OD_{600} of the total planktonic growth was measured using an M200 TECAN plate reader. To quantify biofilm formation, wells were washed with PBS, stained with 0.1% crystal violet, and destained with ethanol: acetic acid (80:20), and OD_{575} of respective wells were measured and divided by OD_{600}. The data shown represent the mean of three independent experiments conducted in triplicates. Error bars = SD, Significance determined by Ordinary One-Way ANOVA with Dunnett's multiple comparison tests showing **p = 0.0038. Ordinary one-way ANOVA with Dunnett's multiple comparison test was used to analyse the differences in the multiple means gotten from readings of the biofilm growth.
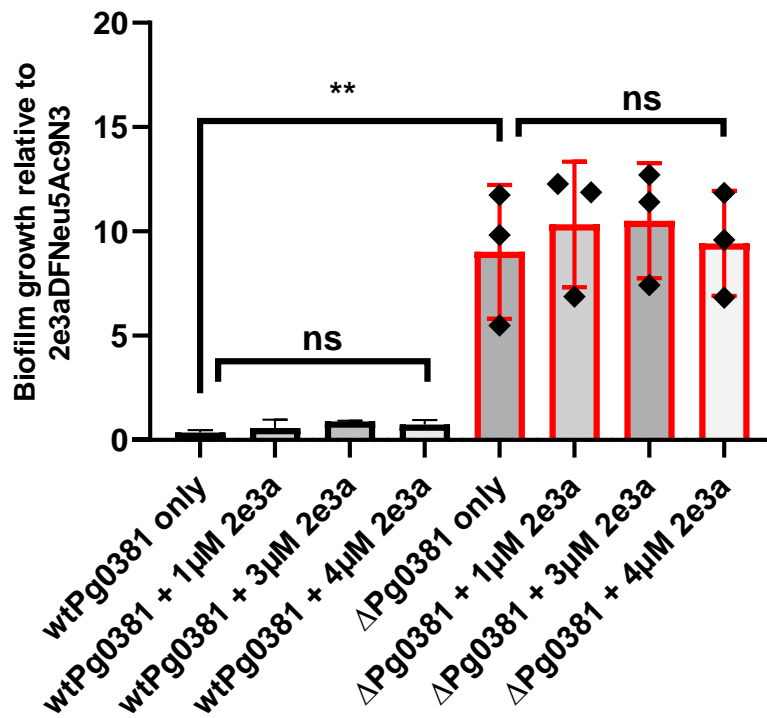
Figure 4.4: The effect of 2e3aDFNeu5Ac9N3 on *P. gingivalis* biofilm

P. gingivalis strains were resuspended in enriched BHI to final OD_{600} 0.1, and 200 µL of each in the presence or absence of varying concentrations of 2e3aDFNeu5Ac9N3 were dispensed in 96-well plate (in triplicate) and incubated at 37°C anaerobically in a Cerillo device for 3 days. Wells were washed with PBS, stained with 0.1% crystal violet and destained with ethanol:acetic acid (80:20). To determine the effect of 2e3aDFNeu5Ac9N3 on the biofilm, OD_{575} of treated destained wells were measured using TECAN M200 plate reader and mean values were divided by OD_{600} of planktonic growth. Data shown represents the mean of three independent experiments with each condition repeated in triplicate. Error bars = SD, significance determined by Ordinary One-Way ANOVA with Dunnett's multiple comparison test was used to analyse the differences in the multiple means gotten from the treated conditions.

4.2.2.2 Determination of Autoaggregation (Sedimentation) by *P. gingivalis* cells

For bacterial cells to be able to form biofilm, they must aggregate (sediment) in order to adhere to animate or inanimate surfaces (O'Toole, 2010). Therefore, to ascertain why despite the reduced planktonic growth (Figure 4.1), the sialidase-deficient strain (ΔPg0381) showed increased biofilm formation compared to that of the wild-type strain (wtPg0381) (figure 4.3). Cell surface characteristics of these strains were assessed using an autoaggregation and sedimentation assay, and interestingly, the sialidase-deficient strain exhibited some level of autoaggregation (sedimentation) better than the wild type (figure 4.5).
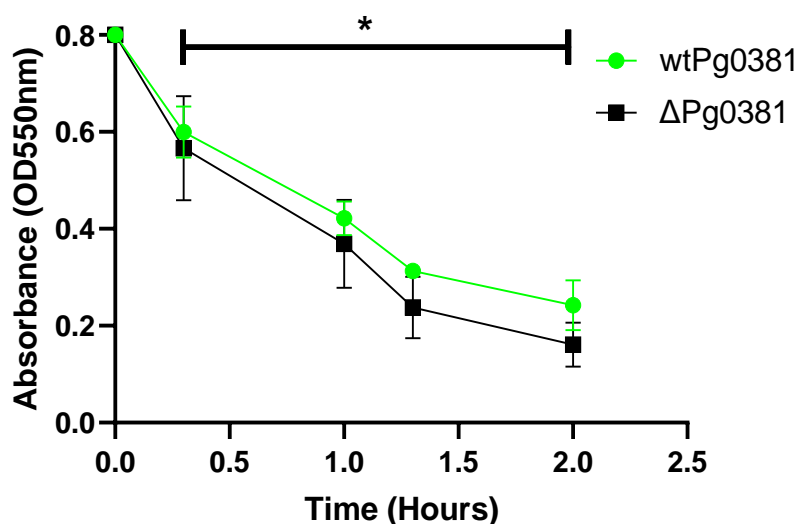
Figure 4.5: Autoaggregation by wild-type *P. gingivalis* (wtPg0381) and the corresponding sialidase-deficient strain (ΔPg0381).

Wild type and sialidase-deficient strains of *P. gingivalis* 0381 growing on FA plates were pelleted and washed twice with PBS. The pellets were then resuspended in PBS to a final OD_{550} of 0.8 (0 mins) and allowed to stand (anaerobically at 37°C). 1mL of the cell suspension was taken and measured after every 30 mins for a period of two (2) hours. A gradual but steady decrease in the absorbance indicated aggregation and sedimentation of cells. Each plot represents the results (absorbance readings) from two independent experiments. Differences between mean values in this experiment were evaluated by Paired t-test with $p < 0.05$ taken as the level of significance. Paired t-test was used because it compares the measurement of the optical density before and after sedimentation.

4.2.2.3 Determination of Antiadhesion and Antibiofilm Properties of Palmatine and Berberine chloride on *T. forsythia* (ATCC 43037) Biofilm growth

The initial stage in biofilm formation is the adhesion (attachment) of bacterial cells to animate or inanimate surfaces, and these pathogenic microorganisms uses multiple factors required for the initiation of biofilm formation such as pili, flagella, fimbriae, adhesins, enzymes involved in cyclic-di-GMP binding and in metabolism (O'Toole, 2010). Inhibiting this initial stage, therefore, will be valuable in combating dental plaque.

Having established the inhibitory effect of Palmatine and Berberine chloride on the growth of *T. forsythia* (figure 4.6), the antiadhesion ability of the plant-derived compounds in the early stage of biofilm formation by *T. forsythia* was investigated. Both Palmatine and Berberine chloride at the concentrations tested showed no significant inhibition (antiadhesion) on *T. forsythia* adhesion to the bottom of the plates (Figure 4.6). Additionally, there was no significant reduction (antibiofilm) in biofilms formed in conditions treated with plant-derived compounds in comparison to the untreated conditions (Figure 4.7). Nonetheless, Palmatine (green symbols) was observed to show more antiadhesive and antibiofilm tendencies on sessile growth of *T. forsythia* (Tf43037), when compared to Berberine chloride (blue symbols) (Figures 4.6 and 4.7), respectively.
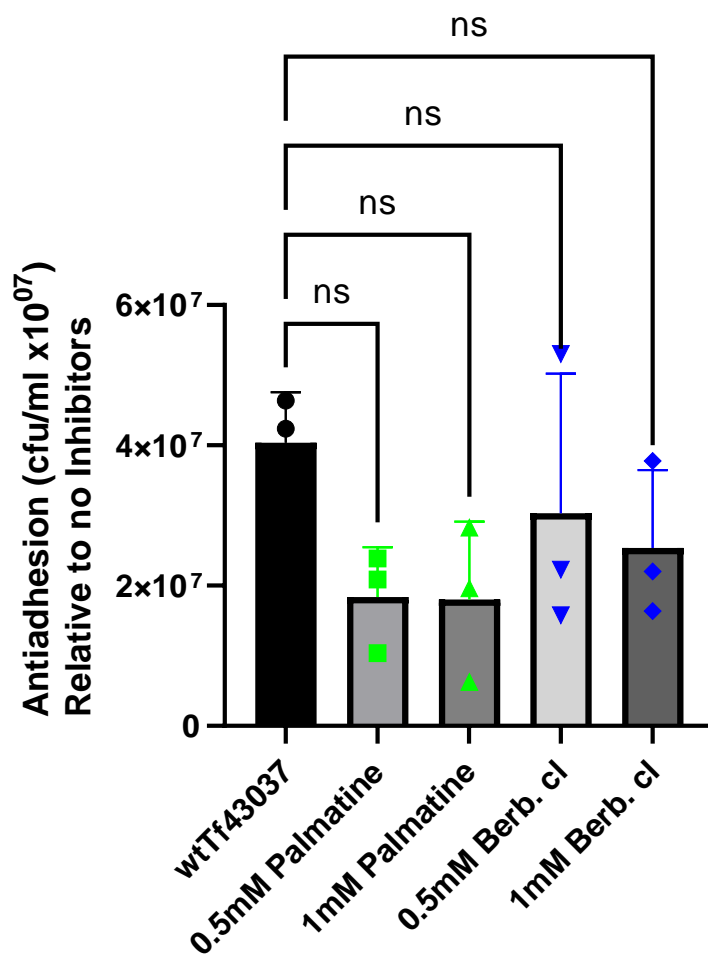
Figure 4.6: Antiadhesion of Palmatine and Berberine chloride on *T. forsythia* biofilm growth

Overnight *T. forsythia* (43037) growing in supplemented TSB (erythromycin not included) were adjusted to OD600 0.05, and 200µL was dispensed in mucin-coated (6mM) wells (in duplicate) in the presence or absence of Palmatine or Berberine chloride. The plate was incubated anaerobically for 4 hours and the bacterial cells were counted using a light microscope to assess the antiadhesive properties of the compounds. Each plot represents the results from three independent experiments conducted in duplicate. Differences between mean values in this experiment were evaluated by ordinary one-way ANOVA, with $P < 0.05$ being taken as the level of significance. One-way ANOVA is chosen because it analyses the differences between the means of the respective treatments in comparison to the untreated (wt43037) condition.
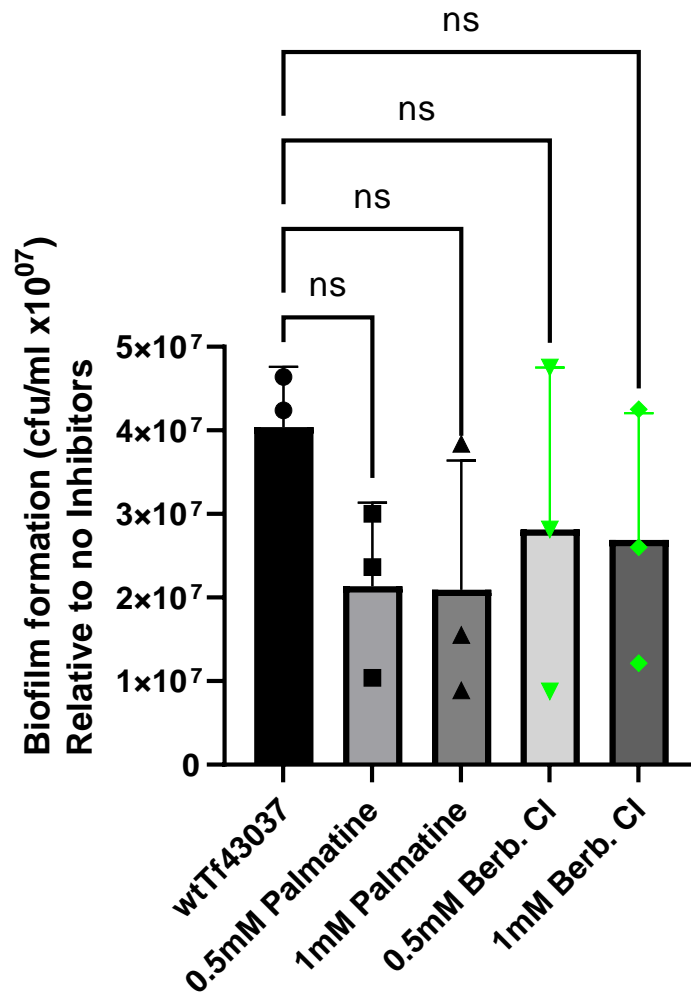
Figure 4.7: Effect of Palmatine and Berberine chloride on *T. forsythia* biofilm growth

Overnight *T. forsythia* (43037) growing in supplemented TSB (erythromycin not included) were adjusted to OD600 0.05, and 200µL was dispensed in mucin-coated (6mM) wells (in duplicate) in the presence or absence of Palmatine or Berberine chloride. For antibiofilm activity, cell suspensions were treated with respective concentrations of the compounds and further incubated anaerobically for 5 days after which, the matured biofilm cells were enumerated as above. Each plot represents the results from three independent experiments conducted in duplicate. Differences between mean values in this experiment were evaluated by ordinary one-way ANOVA, with $P < 0.05$ being taken as the level of significance. One-way ANOVA is chosen because it analyses the differences between the means of the respective treatments in comparison to the untreated (wt43037) condition.

4.3   Determination of the Effect of Sialidase Inhibitors on the Growth of *P. gingivalis* and *T. forsythia*

4.3.1   Effect of 2e3aDFNeu5Ac9N3 on *P. gingivalis* and *T. forsythia* growth

The inhibitory properties of 2e3aDFNeu5Ac9N3 on the growth of wild-type strains of *P. gingivalis* (wtPg0381) and *T. forsythia* (wtTf43037), were assessed in the absence and presence of varying concentrations of the compound (1, 3 and 4 µM) (Figures 4.8 and 4.9). These concentrations were chosen because they are within the range of inhibitory concentrations (IC50) of the compound on the sialidase activities of either *T. forsythia* (IC50 = 1 µM) or *P. gingivalis* (IC50 = 3 µM), of whole bacterial cells.

These outcomes are important because the main aim is to assess if at the concentrations tested, the compound will inhibit only the bacterial sialidases *in vitro* not necessarily the growth of whole bacterial cells. Importantly, 1 µM which is within the IC50 value of 2e3aDFNeu5Ac9N3 on sialidase of *T. forsythia* (Table 3.2), was found not to have a significant effect against the whole *T. forsythia* (figure 4.8). Further, 3 µM (IC50 value on SiaPg; Table 3.2) of 2e3aDFNeu5Ac9N3 was also found not to have a significant effect on the whole *P. gingivalis* (figure 4.9). Nonetheless, while 3 and 4 µM, respectively of 2e3aDFNeu5Ac9N3 were found to have minimal effect on whole *T. forsythia* (Figure 4.)8, only 4 µM have an inhibitory effect against *P. gingivalis* (Figure 4.9), which was reduced from 0.7325 to 0.6038, respectively.
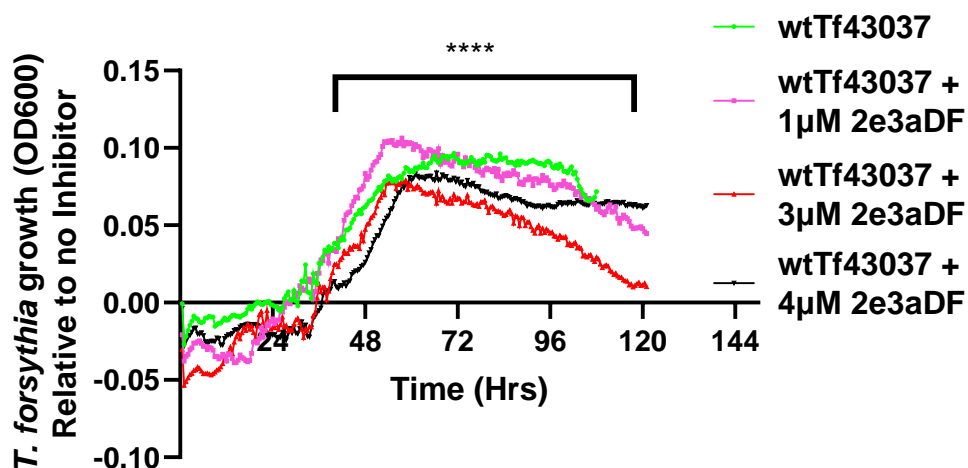
Figure 4.8: Effect of 2e3aDFNeu5Ac9N3 on wild type *T. forsythia* growth

Bacteria growing on FA + NAM were scraped and washed in TSB twice (erythromycin not included) and adjusted to OD_{600} 0.01, and 200 µL (with or without 2e3aDFNeu5Ac9N3) were dispensed in a 96-well plate and incubated anaerobically in a Cerillo device at 37°C for 5 days. OD_{600} of respective wells were measured and the antibacterial activity of the compound was enumerated. Data represent the mean of three experimental repeats (n=3), where each condition was conducted in triplicate. Error bars = SD. Ordinary One-way ANOVA with Dunnett's multiple comparison tests shows 3 and 4 µM as **** p = <0.0001. Dunnett's multiple comparison test was used to analyse the differences in the multiple means gotten from readings of the bacterial growth in the presence or absence of the inhibitor.
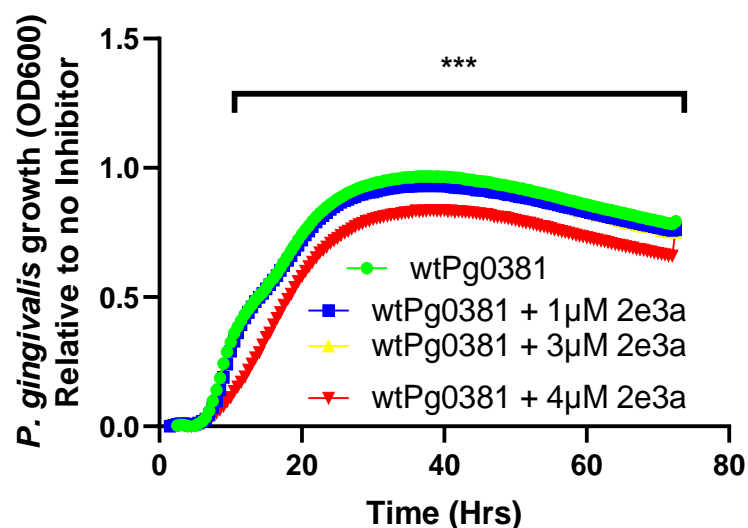
Figure 4.9: Effect of 2e3aDFNeu5Ac9N3 on *P. gingivalis* (wtPg0381) growth

Isolates growing in supplemented BHI broth (erythromycin not included) were adjusted to OD_{600} 0.1 and 200 µL (with or without 2e3aDFNeu5Ac9N3) were dispensed in a 96-well plate and incubated anaerobically in a Cerillo device at 37°C for 72hrs. OD_{600} of respective wells were measured and the antibacterial activity of the compound was enumerated. Data represent the mean of three experimental repeats (n=3), where each condition was conducted in triplicate. Error bars = SD. Ordinary One-way ANOVA with Dunnett's multiple comparison tests shows 4 µM as *** $p = 0.0006$. Dunnett's multiple comparison test was used to analyse the differences in the multiple means gotten from readings of the bacterial growth in the presence or absence of the inhibitor.

4.3.2 Palmatine and Berberine chloride significantly inhibit *T. forsythia* planktonic growth

Plant-derived Palmatine and Berberine chloride showed some promising inhibitory activities against the sialidases of *T. forsythia* and *P. gingivalis* (Tables 3.1 and 3.2). The inhibitory concentrations (IC50 range) of Palmatine and Berberine chloride on the total planktonic growth of *T. forsythia* were therefore assessed. Interestingly both Palmatine and Berberine chloride showed a double-fold reduction in the planktonic growth of *T. forsythia*, at the concentrations tested (Figure 4.10).
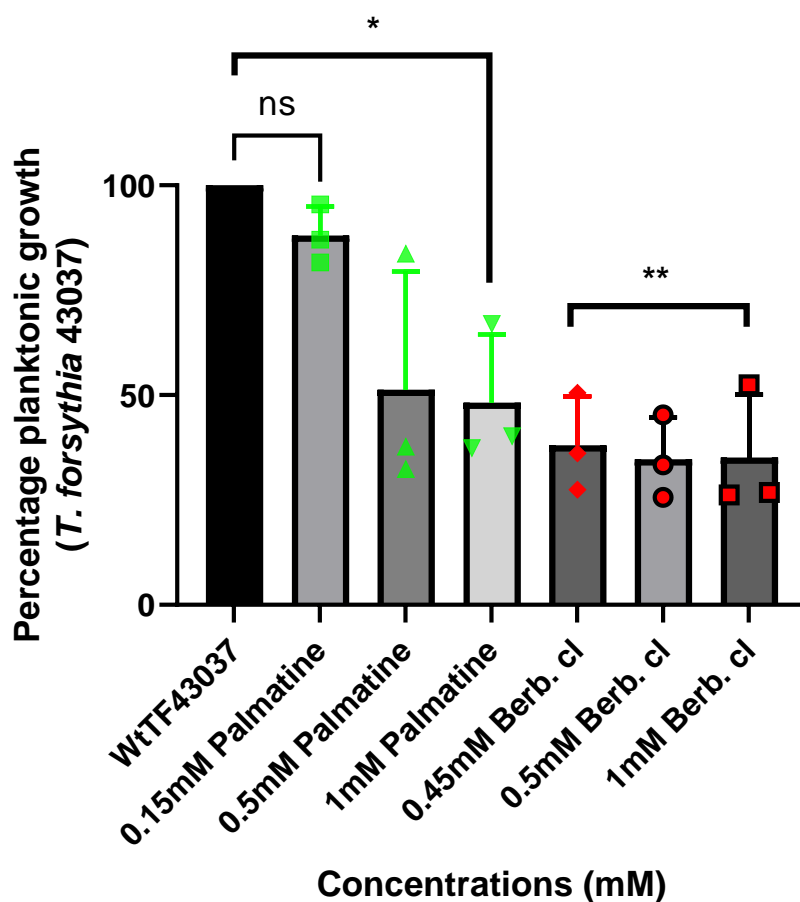
Figure 4.10: Effect of Palmatine and Berberine chloride on the planktonic growth of *T. forsythia* 43047

Bacterial cells growing on FA + NAM plate were harvested and resuspended in supplemented TSB (erythromycin not included) to an OD_{600} 0.05. 200 µL (with or without inhibitor) were dispensed in a mucin-coated flat bottom 96-well plate (in triplicate) and was incubated in an anaerobic chamber at 37°C, 10% CO_2, 10% H_2, and 80% N_2 for 5-7 days. Following incubation, the OD_{600} absorbance was measured using a TECAN M200 plate reader, and the percentage inhibition of the planktonic growth of wild-type *T. forsythia* (ATCC 43037) was enumerated and data plotted using GraphPad Prism (version 9.2.0). Each plot represents the results from three independent

experiments conducted in triplicate. Ordinary One-way ANOVA was conducted with Bartlett's test showing *P < 0.05, **P = 0.001

4.3.3   Determination of the Effect of Epicatechin gallate on *P. gingivalis* growth and the Role of SiaPg in Utilization of Glycoprotein

Previously, the role of NanH sialidase in the utilization of glycoproteins such as mucin and in biofilm formation was reported (Roy et al., 2011). Here, the role of *P. gingivalis* sialidase (SiaPg) in the utilization of mucin for growth, as well as the inhibitory properties of Epicatechin gallate (ECG) on planktonic growth of the keystone pathogen was assessed.

In comparison to the mucin-coated wells, wild-type *P. gingivalis* tend to grow better in uncoated wells (figure 4.11). However, there was no significant difference in the growth rates of *P. gingivalis* grown in mucin-coated wells from that grown in uncoated wells (figure 4.11). On the other hand, 0.2 mM which is within the IC50 range of Epicatechin gallate on whole-cell sialidase activity of *P. gingivalis* (Table 3.2), showed a double-fold reduction in the growth of wild-type *P. gingivalis* grown in the mucin-coated wells (figure 4.11). Nonetheless, ECG showed no significant reduction in the growth of the sialidase-deficient *P. gingivalis* (ΔPg0381) in coated and uncoated wells (Figure 4.11).
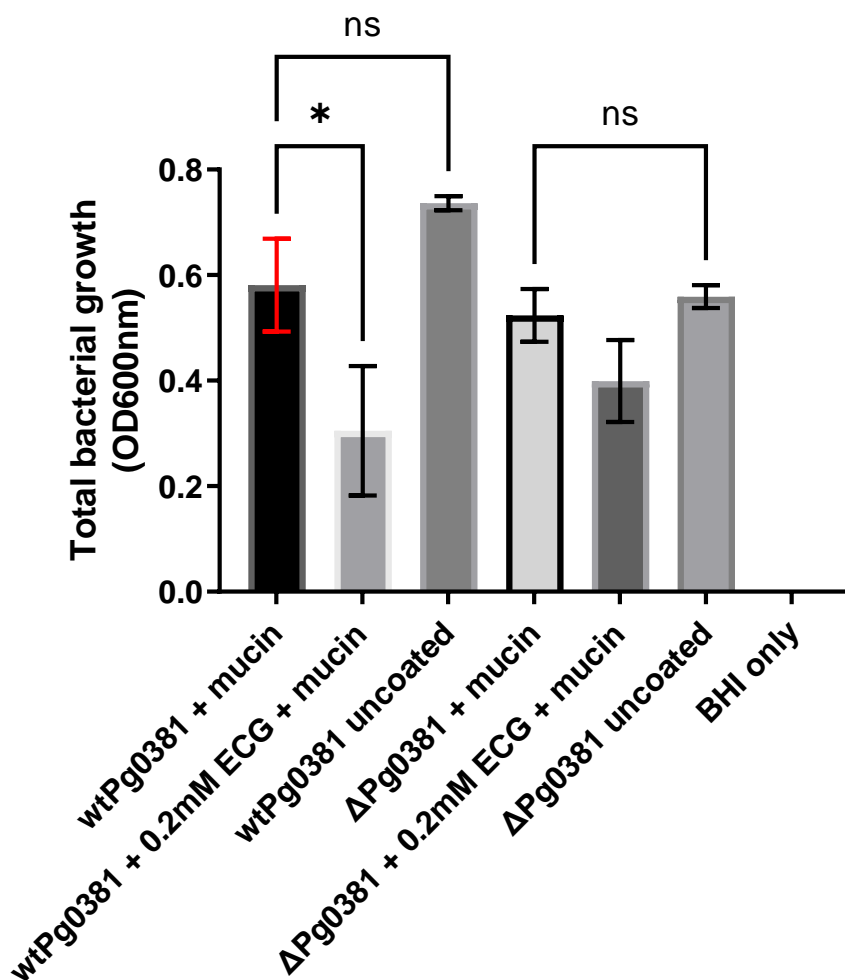
Figure 4.11: Effect of Epicatechin gallate on planktonic growth and utilization of mucin by *P. gingivalis*.

P. gingivalis growing on FA plates were scrapped and resuspended in supplemented BHI (erythromycin not included). Bacterial cells were adjusted to OD_{600} 0.1 and 200μL of respective strains were dispensed in mucin-coated or uncoated wells (in duplicate) in the presence or absence of 0.2 mM Epicatechin gallate, followed by incubating the plate in an anaerobic condition at 37°C for 3 days. Following incubation, the OD_{600} absorbance was measured using a TECAN M200 plate reader, and the inhibition of the planktonic growth was calculated and presented. Each plot represents the results from three independent experiments conducted in duplicate. Ordinary One-way ANOVA was conducted with Tukey's multiple comparison tests showing *P < 0.05. Tukey's multiple comparison was chosen because it compares the difference between the mucin coated and uncoated wells containing wild type or mutant strains.

4.3.4 The Role of NanH Sialidase in Utilization of Glycoprotein and the Effect of Epicatechin gallate on *T. forsythia* Biofilm formation

Previously, NanH sialidase was reported to promote biofilm formation in *T. forsythia* (Roy et al., 2010). Here, the role of NanH sialidase in the utilization of mucin was reassessed, and the effect of ECG on the biofilm form by *T. forsythia* was investigated.

Interestingly, wild-type *T. forsythia* showed a significant biofilm formation in the mucin-coated wells in comparison to its biofilms formed in the uncoated wells (figure 4.12). Nonetheless, there was no significant difference between biofilms formed in mucin-coated and uncoated wells by the sialidase-deficient strain (figure 4.12).

Lastly, 0.2 mM Epicatechin gallate significantly reduced the wild-type *T. forsythia* biofilms formed in mucin-coated wells by over two-fold (Figure 4.12).
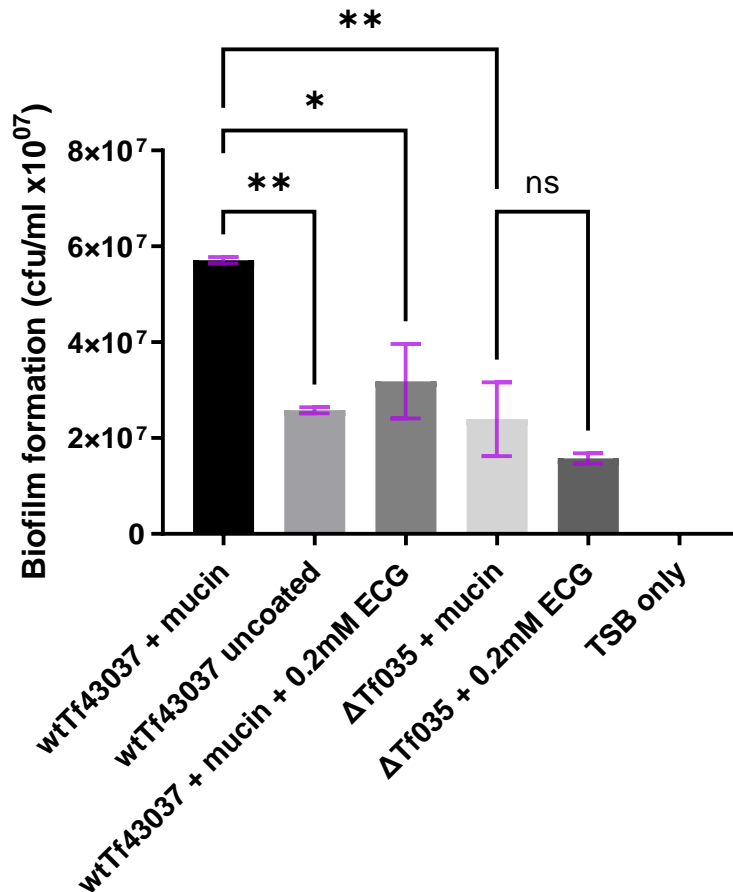
Figure 4.12: Role of NanH sialidase in mucin utilization and antibiofilm effect of Epicatechin gallate on *T. forsythia* biofilm growth

Overnight wild-type *T. forsythia* (43037) and sialidase-deficient strain (ΔTf035; ΔnanH) growing in supplemented TSB (erythromycin not included) were adjusted to OD_{600} 0.05, and 200 µL of respective strains were dispensed in wells coated with 6 mM mucin (in triplicate), in the presence or absence of 0.2 mM Epicatechin gallate (ECG) and incubated anaerobically at 37ºC for 5 days. Cells were resuspended in PBS and matured biofilm cells were counted using the Olympus Microscope. Each plot represents the results from two independent experiments conducted in triplicate. Differences between mean values in this experiment were evaluated by ordinary one-way ANOVA, with *P = 0.01 and **P = 0.001 being taken as the level of significance. One-way ANOVA is chosen because it analyses the differences between the means of the different conditions in comparison to the untreated (wt43037) condition.

4.4 Utilization of 3-keto-3-deoxy-D-glycero-D-galactonononic acid (KDN) by *Tannerella forsythia* (ATCC 43037)

T. forsythia which is a fastidious anaerobic organism requires sialic acid for its growth. Utilization of sialic acids such as *N*-acetylneuraminic acid (Neu5Ac), *N*-glycolylneuraminic acid (Neu5Gc), bovine submaxillary mucin (BSM) and sialyllactose by *T. forsythia* has been reported (Roy et al., 2011).

2-Keto-3-deoxy-D-glycero-D-galactonononic acid (KDN), is another form of sialic acid that was reported to be utilized as a carbon source by pathogens such as *Sphingobacterium multivorum* (Terada et al., 1997), *Aspergillus fumigatus* (Telford et al., 2011) and *E. coli* (Hopkins et al., 2013). In addition, *A. fumigatus* and *S. multivorum* were reported to secrete a special type of sialidase called the KDNase (Telford et al., 2011 and Terada et al., 1997). Furthermore, *S. multivorum* belongs to the phylum Bacteroidetes (Abro et al., 2016), the same as *T. forsythia* (Tanner et al., 2009). In addition, a putative KDNase gene; BFO_0701 from the *T. forsythia* genome has been reported to play a catalytic role. It was decided to see if *T. forsythia* can utilize KDN for growth.

Here, the ability of *T. forsythia* to grow and utilize KDN as a source of carbon was investigated. Wild-type *T. forsythia* (wtTf43037) was grown in TSB supplemented with 6 mM of either *N*-acetyl muramic acid (NAM), KDN, or Neu5Ac for 5 days and the total planktonic growth was measured. Significant growth of *T. forsythia* on *N*-acetylmuraminic acid (NAM) was observed (figure 4.13), however, there was no significant difference in its growth on KDN (wtTf43037 + KDN) and in Neu5Ac (wtTf43037 + Neu5Ac) in comparison to the untreated condition (wtTf43037 + TSB only) (figure 4.13). Interestingly, wild-type *T. forsythia* grew on FA plates supplemented with KDN up to two passages, however, its morphological appearance observed under the light microscope (Gram staining) shows the organism to be slightly elongated as compared to its original morphology when grown on FA + NAM plate (fig. 4.14).
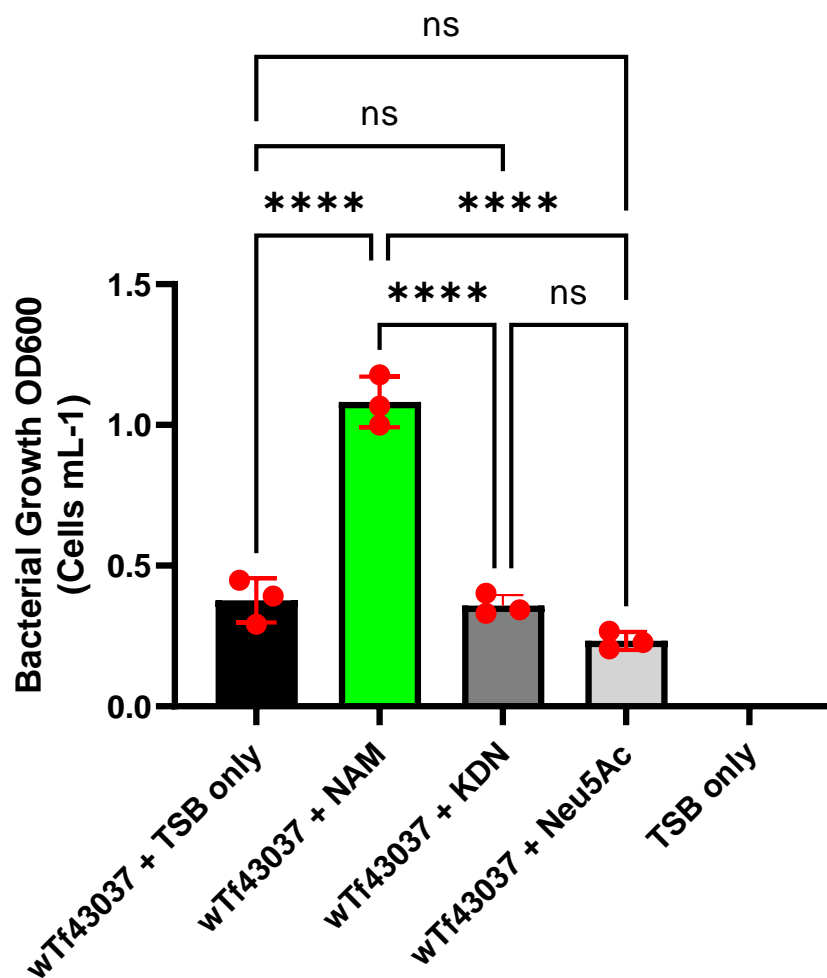
Figure 4.13: Utilization of NAM, KDN and Neu5Ac by *Tannerella forsythia* 43037.

Wild type strain of *T. forsythia* 43037 were harvested from the FA agar plate, washed in PBS (pH 7.4), and resuspended in fresh TSB supplemented with either 6 mM *N*-acetylmuramic acid (NAM), *N*-acetylneuraminic acid (Neu5AC) and 6 mM 3-keto-3-deoxy-D-glycero-D-galactonononic acid (KDN). The 96-well plate was incubated anaerobically in a Cerillo device at 37°C for 7 days. Each plot represents the results from three independent experiments conducted in triplicate. Differences between mean values in this experiment were evaluated by ordinary one-way ANOVA, with *$P > 0.05$ being taken as the level of significance. Tukey's multiple comparison was chosen because it compares the difference between the different types of sialic acids.

A — wtTf43037 + NAM

B — wtTf43037 + KDN

C — wtTf43037 + Neu5Ac
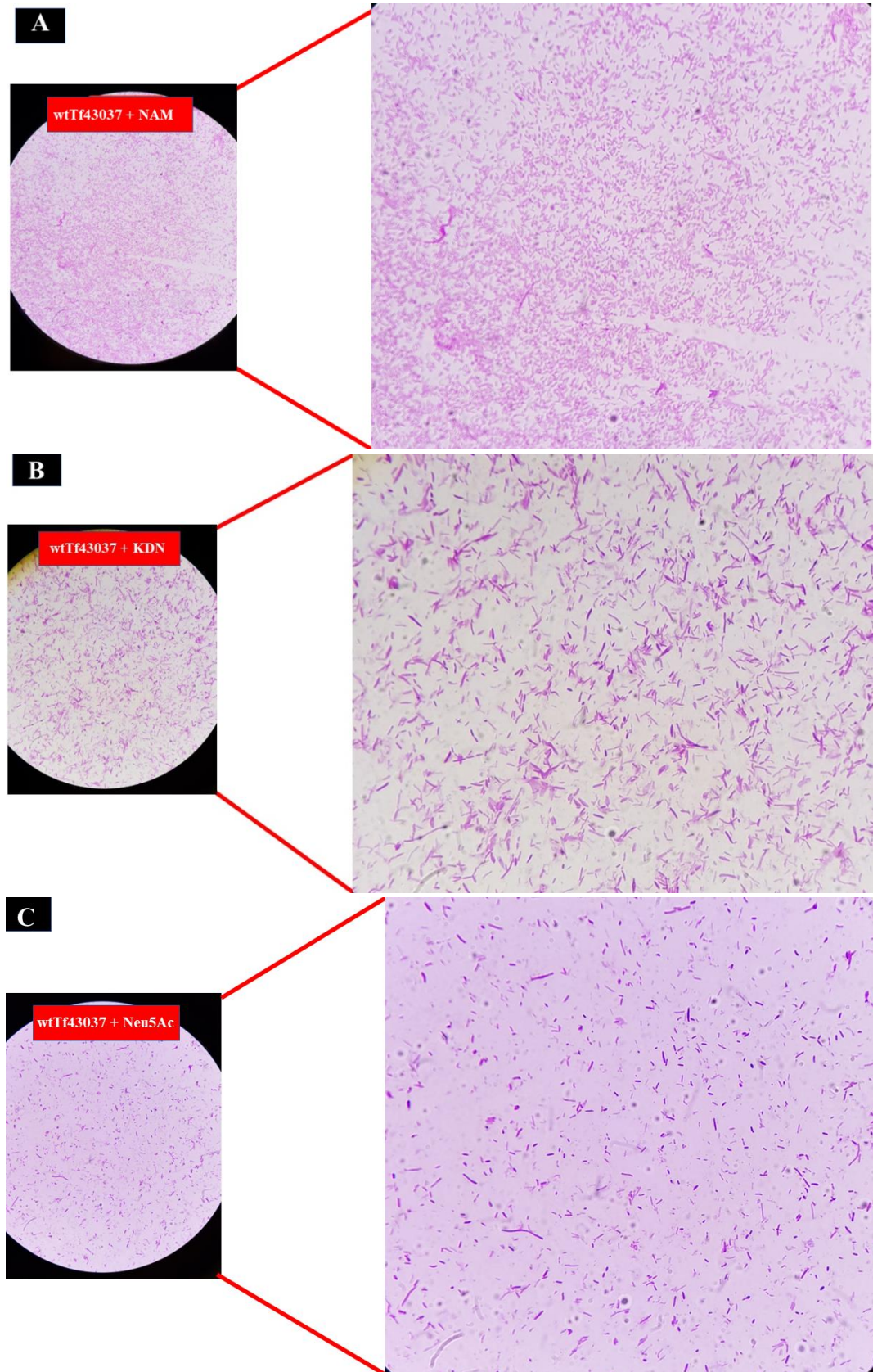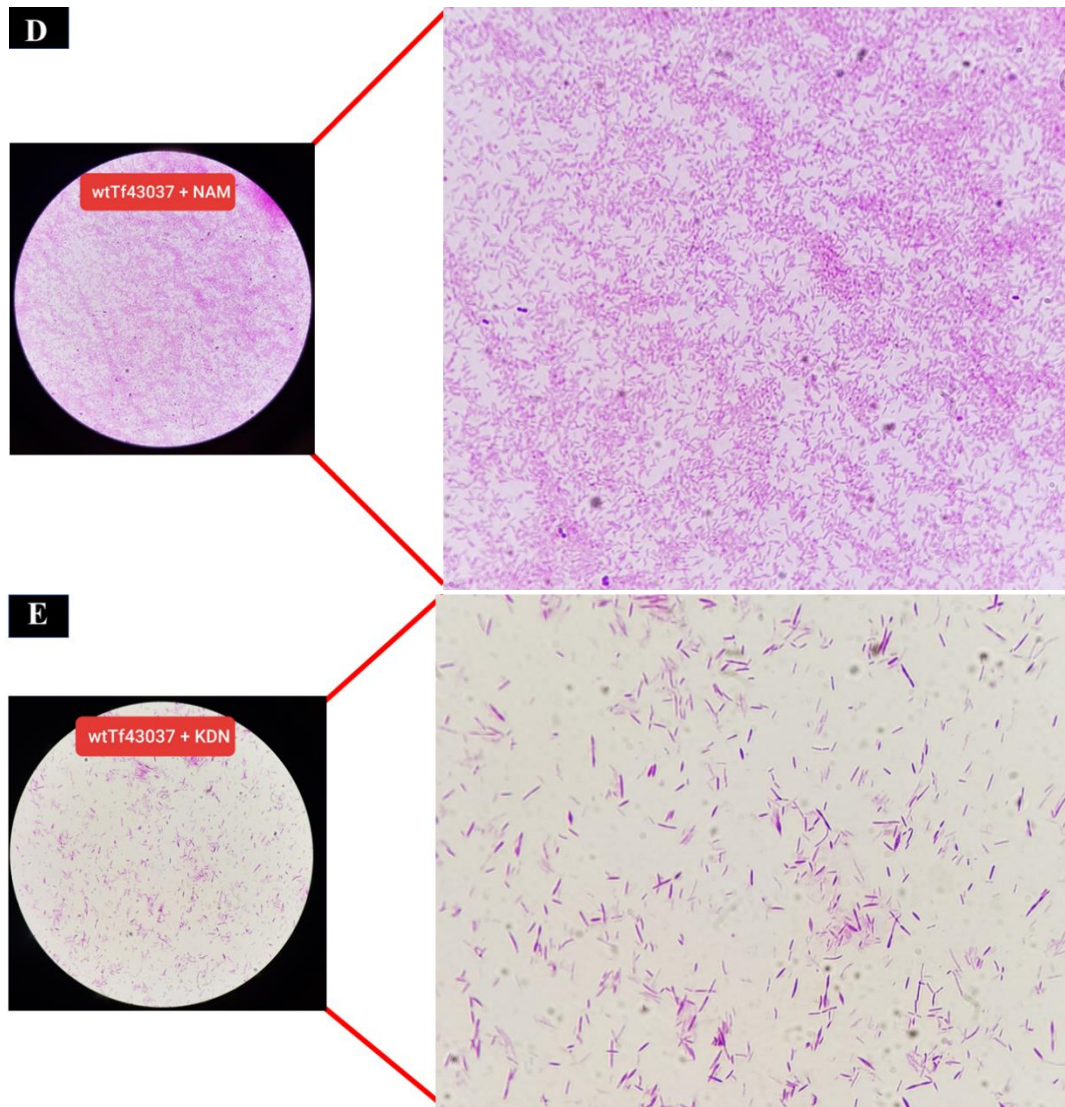
Figure 4.14: Morphological appearance (Gram staining) of *Tannerella forsythia* grown on FA agar plates supplemented with either NAM, KDN or Neu5Ac

Wild-type strain of *T. forsythia* (ATCC43037) grown on fastidious anaerobe agar plates supplemented with either 6 mM *N*-acetylmuramic acid (NAM), 3-keto-3-deoxy-D-glycero-D-galactononononic acid (KDN), or *N*-acetylneuraminic acid (Neu5AC), Gram-stained and viewed under X100 objective lens. **A-C = first passage, D-E = 2ⁿᵈ passage**

4.5 Discussion

Determination of the effect of sialidase inhibitors on bacterial growth, their effect on biofilm formation, and the synergistic effects of the sialidase inhibitors were carried out using various microbiological and pharmacological approaches as described above. The role of sialidases in promoting bacterial growth, biofilm formation, and the utilization of different sialic acids was also investigated.

Following the determination of individual inhibitory concentrations (IC50) of both plant-derived and synthetic compounds in Chapter Three, the work in this Chapter aimed at investigating their inhibitory activities against whole bacterial cells, and biofilms as well as the role of sialidases in the utilization of mucin, *N*-acetylmuramic acid (NAM), *N*-acetylneuraminic acid (Neu5AC), and 3-keto-3-deoxy-D-glycero-D-galactononnonic acid (KDN).

4.5.1 Bacterial Sialidases Promote *P. gingivalis* and *T. forsythia* growth

Sialidases are reported to be widely distributed in nature and have been shown to play an important role in the pathogenesis of many diseases (Crennell et al., 1993). A range of pathogens such as *N. gonorrhoea* (Ketterer et al., 2016), *V. cholerae* (Slack et al., 2018), *C. perfringens* (Newstead et al., 2008), *H. pylori* (Tsai et al., 2006), *S. pneumoniae* (Blevins et al., 2017), *G. vaginalis* (Govinden et al., 2018) and even parasitic *T. cruzi* (Buschiazzo et al., 2000), were reported to express sialidases which contribute to their growth and survival and in key aspects of host: pathogen or host: parasite interactions (Buschiazzo et al., 2000 and Blevins et al., 2017).

Previously, oral pathogens including *Streptococcus sanguis*, *Streptococcus orallis*, *Capnocytophaga carimorsus* (reviewed in Lewis & Lewis, 2012), *P. gingivalis* (Frey et al., 2019) and *T. forsythia* (Roy et al., 2010 and Roy et al., 2011), were also shown to express sialidases that promote their growth, biofilm formation and in utilization of glycoproteins. Although not a new finding, the data above further support previous claims that the sialidase gene is used by pathogens to scavenge sialic acids as a nutrient from various sialylated substrates and support bacterial growth which in turn promotes the pathogenic role of these oral pathogens. Nonetheless, findings in this chapter show

that the sialidase of *P. gingivalis* is not necessarily required for the utilization of glycoproteins such as mucin.

4.5.2 The Role of Bacterial Sialidases in Biofilm Formation by *P. gingivalis* and *T. forsythia*

4.5.2.1 Sialidase-deficient *Porphyromonas gingivalis* mutant shows an enhanced Biofilm formation

P. gingivalis, is the keystone red complex pathogen reported to be associated with periodontitis which is characterized by plaque (biofilm) formation on the tooth surfaces (Frey et al., 2019 and Sudhakara et al., 2019). Several virulence factors ranging from fimbriae, hemagglutinin, proteinases, gingipains-adhesins, outer membrane vesicles, and lipopolysaccharide (LPS), of *P. gingivalis* are previously shown to be involved in biofilm formation (Yamaguchi et al., 2010).

However, findings in this study show that the sialidase-deficient strain (ΔPG0381), produced an increased biofilm with some level of auto-aggregation (sedimentation) rate when compared to the wild-type strain. Although not entirely the same, previous research reported the coordinated role of fimbriae and gingipains in regulating biofilm formation in *P. gingivalis* (Kuboniwa et al., 2009). Also, Yamaguchi et al., (2010) reported strong autoaggregation and increased biofilm formation by *P. gingivalis* mutant (*gtfB*) that is defective in the biosynthesis of LPSs containing O side chain polysaccharide (O-LPS) and anionic polysaccharide (A-LPS) (Yamaguchi et al., 2010), and that defect in the bacterial LPS could be the reason for tight adherence of the cells to each other (Yamaguchi et al., 2010).

Although data in this project shows that *P. gingivalis* does not necessarily require sialidase to utilize glycoproteins, the aforementioned findings may suggest that altering some bacterial cell surface structures could impact the expression of other genes that could enhance autoaggregation, bacterial attachment to surfaces, and subsequent increase in biofilm formation (Davey & Duncan, 2006; Inaba et al., 2008 and Yamaguchi et al., 2010).

In contrast to the above, wild-type *T. forsythia* (ATCC43037) grown in mucin-coated wells showed an increased biofilm formation as compared to the sialidase-deficient strain (ΔTf035). Thus, this suggests the important role of NanH sialidase in the

utilization of glycoproteins which is needed for bacterial growth and biofilm formation as earlier reported (Roy et al., 2011).

4.5.3 Plant-derived and Synthetic Sialidase Inhibitors Impacted Bacterial Growth and Biofilm Formation by *P. gingivalis* and *T. forsythia*

The oral cavity is a suitable niche for bacterial growth, survival, and propagation (Stafford et al., 2012). Pathogens residing in the mouth readily stimulate the formation of oral biofilms, which accumulates on both soft and hard tissues as dental calculus (Lee et al., 2017). *P. gingivalis* and *T. forsythia* are among the prevalent anaerobic gram-negative pathogens found in the subgingival region and are critical in the onset and subsequent development of periodontitis (Stafford et al., 2012). Dental plaque formed by these bacteria can trigger the immune system imbalance thereby leading to inflammatory responses (Fomby & Cherlin, 2011). Resistance to antimicrobials by these oral pathogens, and difficulties in treating oral plaque (biofilms) therefore, if left unchecked, periodontitis can lead to the destruction of the gingival tissues and subsequent destruction of periodontal ligaments (Lee et al., 2017).

Here, both the synthetic sialidase inhibitor 2e3aDFNeu5Ac9N$_3$, and the plant-derived Epicatechin gallate, Palmatine, and Berberine chloride impacted the growth of *P. gingivalis* and on *T, forsythia* significantly. Nonetheless, at the concentrations tested, the sialidase inhibitors with the exception of Epicatechin gallate were unable to inhibit biofilm formation. This is the first time the effect of these compounds is screened against bacterial growth and biofilm formation by *P. gingivalis* and *T. forsythia,* respectively.

Palmatine and Berberine chloride which are isoquinoline-type alkaloids isolated from different types of medicinal plants have also been reported to have efficacy against a broad spectrum of microorganisms ranging from antibacterial, antidiabetic, wound healing, anticancer, immuno-stimulating and anti-inflammatory properties (reviewed in Wojtyczka et al., 2014). Additionally, Berberine chloride in combination with other antibacterial compounds was shown to inhibit the growth of oral Streptococci including *Streptococcus mutans*, *S. sanguinis,* and *S. oralis* (Dziedzic et al., 2015). Furthermore, the bactericidal mechanism of Palmatine was reported to include inhibition of DNA synthesis, inhibition of cell-cell proliferation, inhibition of protein biosynthesis and induction of bacterial apoptosis (Thakur et al., 2016). In addition, Palmatine was

reported to inhibit the sialidase (neuraminidase) of *C. perfringens* by binding to the neuraminidase through π–π stacking with HIS346 (Kim et al., 2014), as well as having a strong antifungal activity against the biofilms of *Candida albicans* (Wang et al., 2018), Methicillin Resistant *Staphylococcus aureus* (MRSA) and *H. pylori*, respectively (reviewed in Long et al., 2019).

Furthermore, Epicatechin gallate (ECG) which is a polyphenol often isolated from green tea has also been shown to possess antibacterial, anticarcinogenic, antioxidant, and anti-inflammatory effects in addition to its use in oral health where its daily intake was shown to promote healthy teeth and gums (Jigisha et al., 2012). Also, it inhibits *S. mutans* attachment to oral surfaces (Reygaert, 2014), *Lactobacillus acidophilus*, *C. albicans,* and even neuraminidase of the influenza virus (Jigisha et al., 2012). Lastly, Epicatechin gallate is reported to be effective in reducing acid production in dental plaque by inhibiting the lactate dehydrogenase of *S. mutans* (Hirasawa et al., 2004).

Lastly, the inability of most of the compounds to inhibit biofilms formed by *P. gingivalis* and *T. forsythia* further confirms the complexity of biofilm architecture with cells embedded in the extracellular matrix, involvement in many subacute and chronic bacterial infections such as periodontitis thereby making it notoriously difficult to eradicate with conventional antimicrobial agents (Del Pozo & Patel, 2007 and Dziedzic et al., 2015).

4.5.4 Utilization of 3-keto-3-deoxy-D-glycero-D-galactonononic acid (KDN) by *Tannerella forsythia*

T. forsythia is one of the dominant organisms in periodontitis which are shown to transport and utilize several sialic acids and glycoproteins including *N*-acetylneuraminic acid (Neu5Ac), *N*-glycolylneuraminic acid (Neu5Gc), bovine submaxillary mucin and sialyllactose as a sole source of carbon and nitrogen (Roy et al., 2010; Roy et al., 2011 and Stafford et al., 2012). Other important pathogens such as *E. coli* and *P. aeruginosa* were also reported to utilize these sialic acids for their growth and in biofilm formation (Fux et al., 2005 and Hopkins et al., 2013).

Also, previous findings revealed that the sialic acid utilization and uptake system in *T. forsythia* is orchestrated mainly by the sialic acid utilization locus which encodes a

putative inner membrane sialic acid permease (NanT) (Roy et al., 2010). Interestingly, findings in this current study show that *T. forsythia* (ATCC43037) was able to utilize KDN for its growth however, the growth rate was poor when compared to its growth on *N*-acetylmuramic acid (NAM). Worthy of mention, is the morphological appearance of *T. forsythia* grown on a fastidious anaerobe (FA) agar plate supplemented with KDN. It appeared to be elongated under the light microscope when compared to its original form that grows on an FA plate supplemented with *N*-acetylmuramic acid (NAM).

There is a paucity of research showing bacterial growth on KDN, but with growing knowledge of its occurrence in biological systems, it is perhaps not surprising that KDN utilization has evolved (Hopkins et al., 2013). The bacterium *S. multivorum* was also reported to express KDNase enzyme that allows this bacteria to grow on KDN-containing oligosaccharide (Terada et al., 1997 and Iwaki et al., 2020). More recently, Telford and colleagues demonstrated that KDN is the sole carbon source that supports the growth of *A. fumigatus*; a filamentous fungus involved in causing respiratory diseases in immunocompromised individuals, which also secrets a specific type of sialidase referred to as KDNase (Telford et al., 2011).

Although this is preliminary data, more investigation on the utilization and uptake of KDN by *T. forsythia* is needed to be looked upon, considering that *S. multivorum* belongs to the same phyla Bacteroidetes (Abro et al., 2016) as *T. forsythia* (Tanner et al., 2009), and maybe NanH sialidase of *T. forsythia* could also be a KDNase.

4.6   Chapter Summary

This chapter focuses on testing for the effect of sialidase inhibitors on bacterial growth and biofilm formation by *P. gingivalis* and *T. forsythia*. Also, sialic acid (KDN) utilization and update by the periodontal pathogen *T. forsythia* and biofilm formation were evaluated.
Of all the plant-derived compounds tested, Epicatechin gallate (ECG) appears to be the most effective inhibitor followed by Palmatine then Berberine chloride. While both compounds reduced the planktonic growth of the oral pathogens significantly, only Epicatechin gallate was able to inhibit biofilm formation by *T. forsythia*. Also, the inability of most of the compounds to inhibit these oral biofilms further confirms how

difficult it is to treat chronic infections such as periodontitis and other biofilm-associated infections.

Furthermore, while the sialidase gene supports planktonic growth of the wild-type strains of *P. gingivalis* and *T. forsythia*, the sialidase-deficient strain of *P. gingivalis* on the other hand appears to show an enhanced autoaggregation and an increased biofilm formation. This may be due to alterations in the bacterial cell surface structures.

Lastly, this preliminary data shows that *T. forsythia* was able to utilize 2-keto-3-deoxynononic acid (KDN) for growth however, its morphological appearance (Gram stained) appears to be slightly elongated under the light microscope when compared to its original form that grows on FA plate supplemented with other forms of sialic acids such as *N*-acetylneuraminic acid (Neu5Ac) or *N*-acetylmuramic acid (NAM). This may suggest that *T. forsythia* encodes the KDNase gene in its genome. Also, more experiments to confirm this claim such as the determination of sialidase activity using 4MU-KDN, substrate specificity, molecular modelling to ascertain KDN transport genes, and determination of optimal temperature and pH need to be conducted.

CHAPTER FIVE

The Role of Sialidases in Host-Pathogen Interactions, Immune Signalling, and Cytotoxic Effects of the Sialidase Inhibitors

5.1   Introduction

One of the mechanisms by which pathogenic microorganisms cause infection is via adhesion and subsequent invasion of the host tissues. This host-bacterial interaction is shown to be regulated by bacterial enzymes amongst other factors. The aim of this chapter is to examine the ability of our inhibitors to abrogate this relationship by inhibiting total bacterial association, adhesion, and invasion of the host oral epithelial cells (H357) using antibiotic protection assay, and also, to investigate the action of bacterial sialidase enzymes from *T. forsythia* and *P. gingivalis* on host immune modulation leading to cytokine expression.

Periodontitis pathogenicity involves a complex succession of inflammatory host immune responses initiated because of plaque formation on the tooth surfaces. The ability of the host to respond by activating the immune pathways determines the susceptibility of periodontal diseases (Cekici et al., 2014). *P. gingivalis* and *T. forsythia* are predominant periodontal pathogens, which expresses a number of potential virulence factors that are involved in the pathogenesis of periodontitis (Amano, 2003 and Stafford et al., 2012). Among them, S-layer, fimbriae, gingipains, BspA and sialidases are critical factors shown to mediate the bacterial interactions with host tissues, which promote the adhesion of bacterial cells to and subsequent invasion of the host tissues (Jotwani & Cutler, 2004; Guo et al., 2010; Mishima & Sharma, 2011; Aruni et al., 2011 and Bloch et al., 2017).

5.1.1   Bacterial sialidases, adhesion and invasion of host tissues

NanH sialidase of *T. forsythia* is reported to be both surface localized and secreted, hence, promote bacterial colonization by exposing sialic acid hidden epitopes on epithelial cells (Honma et al., 2011). Roy et al., demonstrated that the sialidase activity of *T. forsythia* promotes bacterial adhesion and invasion of oral epithelial cells (Roy et al., 2010), while the sialidase-deficient strain shows reduced epithelial cell binding and invasive abilities (Honma et al., 2011).

Sialidases of *P. gingivalis*, *V. cholerae* and *S. pneumoniae* also known as neuraminidase (especially in viruses) are used by these and other gut and nasopharyngeal pathogens as virulence factors which contribute to adherence, colonization, invasion and persistence thereby causing disease to the host (Parker et al., 2009 and Frey et al., 2019). Furthermore, sialidase deficient strain of *P. gingivalis* (ΔsiaPG) has shown decreased association with host cells as compared to the parent strain where the wild-type *P. gingivalis* (W83) led to increased formation of abscesses and lethal infection in mouse (Li et al., 2012).

This further affirms the important roles of bacterial sialidases in virulence, therefore, indicates that their inhibition with chemotherapeutics could be a promising strategy for the development of novel therapy for periodontitis.

5.1.2   Oral pathogens and host immune modulation

Pathobionts residing in the oral cavity such as *P. gingivalis*, *T. forsythia*, *T. denticola* and *A. actinomycetecomitans* are reported to be involved in triggering the innate, inflammatory and adaptive immune responses of the host (Silva et al., 2015). Activities of these oral pathogens result in the destruction of tissues that surround and support the teeth which eventually lead to tissue, bone and tooth loss (Silva et al., 2015). Innate immunity is the first line of defence characterized by recognizing the invading bacteria as non-self, thereby triggering immune response to eliminate them (figure 5.1). Additionally, adaptive immune cells and cytokines have been described as key players in the periodontal disease pathogenesis (Silva et al., 2015).

In innate immunity, the primary response to pathogens is first triggered by Pattern Recognition Receptors (PRRs), and these receptors are involved in recognizing conserved molecular patterns otherwise known as Pathogen-Associated Molecular Patterns (PAMPs), which are commonly shared by the majority of microorganisms. These receptors include toll-like receptors (TLRs), nucleotide-binding oligomerization (NOD) proteins, cluster of differentiation 14 (CD14), complement receptor-3, lectins and scavenger receptors (Akira et al., 2001). For example, in the presence of bacterial lipopolysaccharide (LPS) or any pathogen-associated molecular patterns (PAMPs) in the host cell, pattern recognition receptors (PRRs) binds to it thereby activating toll-like receptors (TLRs) such as TLR-2, TLR-3 and TLR-4. These receptors triggers the

myeloid differentiation primary response 88 (MyD88) that couples TIR-domain thereby activating mitogen-activated protein kinases (MAPK) signalling pathway that leads to nuclear factor kabba B (NF-κB) nuclear trans-location and subsequent regulation of the pro-inflammatory cytokine (IL-1β, IL-6, IL-8 and TNF-α) (figure 5.1) as well as expression and deployment of several cytokines (table 5.1) to the site of infection.

The oral cavity is an exclusive niche for pathogens such as *P. gingivalis* which was shown to hijack leukocytes in the oral cavity altering their migration and defence mechanism, thereby eliciting inflammation to obtain nutrients from the tissue breakdown (Maekawa et al., 2014). It also subverts the host immunity to remodel a normally symbiotic microbiota into a dysbiotic, disease-provoking state (Maekawa et al., 2014). They do this with neutrophil which creates a wall-like defence in the healthy oral tissues (Ryder, 2010), by disarming the host protective TLR2-MyD88 pathway through proteasomal degradation of MyD88, thereby activating an alternate TLR2-Mal-PI3K pathway. This TLR2-Mal-PI3K pathway further prevent phagocytosis, provides interim protection to formally susceptible bacteria, and subsequently promotes dysbiotic inflammation *in vivo* (Maekawa et al., 2014 and Zenobia & Hajishengallis, 2015).

In addition, surface proteins found on periodontal pathobionts such as *T. forsythia* was reported to orchestrate dendritic cell cytokine responses to drive T cell immunity in a fashion that promote bacterial persistence in the host and induce periodontal inflammation (reviewed in Settem et al., 2013). Furthermore, glycosylation of bacterial surfaces such as the S-layer of *T. forsythia* helps protect bacteria from serum complement attack or in subverting host immune detection by coating themselves in the surface glycans (reviewed in Settem et al., 2013). In addition, the S-layer is reported to help bacteria in blocking the early release of inflammatory cytokines by immune cells thereby directly modulating host immunity to impact its *in vivo* life-cycle (reviewed in Settem et al., 2013).

Sialidases of oral pathogens have also been shown to provide pathogenic benefits to bacteria by counteracting the host's adaptive and innate immune responses (Corfield, 1992), also, bacterial neuraminidase from *C. perfringens* was reported to upregulate

interleukin-8 (IL-8) cytokine release as well as nuclear factor-kappa-B (NF-κβ) from lung carcinoma epithelial cells (Kuroiwa et al., 2009).

Disruption of this host-pathogen interactions by assessing the effect of sialidase inhibitors on pro-inflammatory signalling by oral epithelial cells infected with live *T. forsythia* and *P. gingivalis* is therefore important.
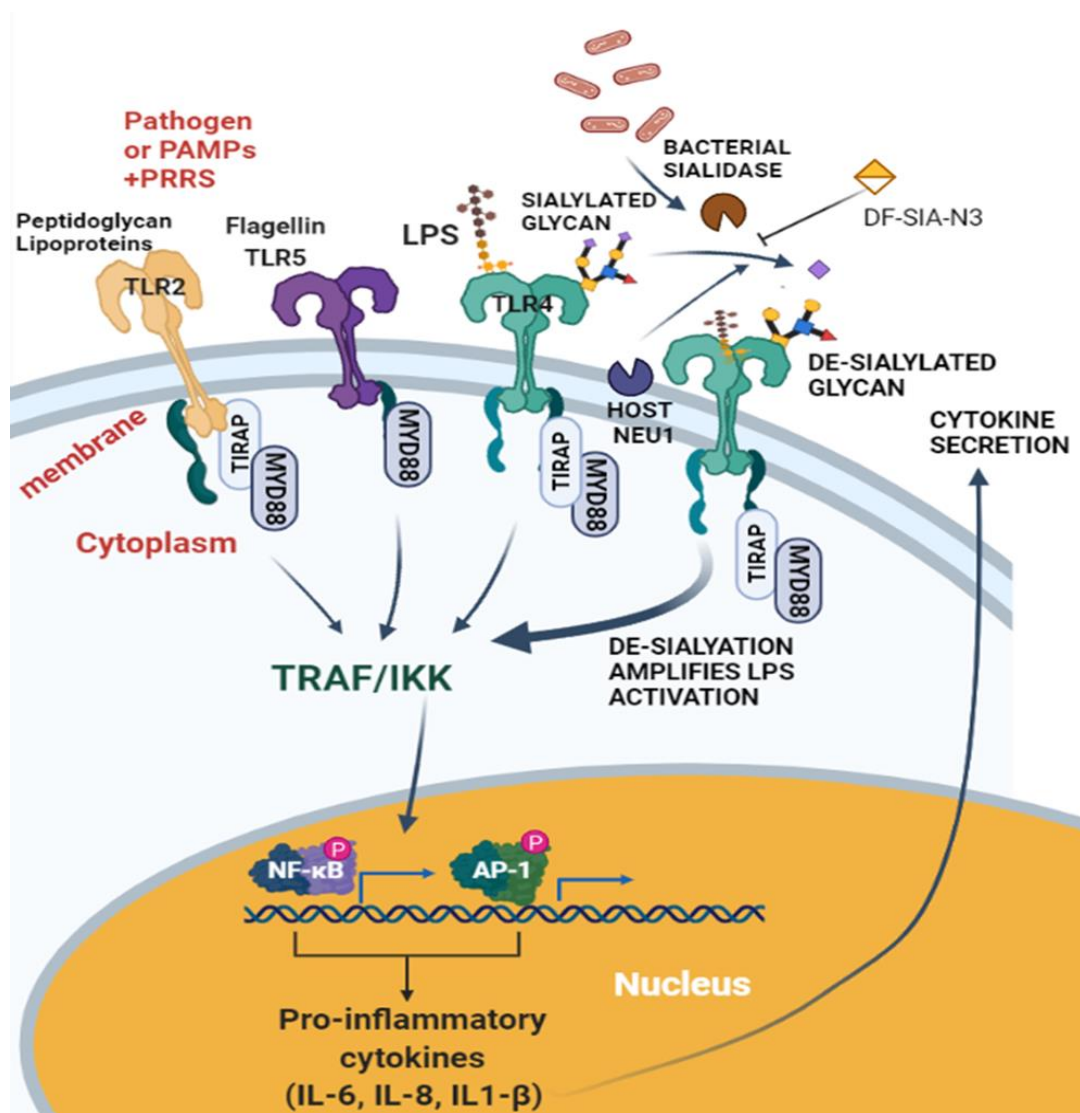
Figure 5.1: An hypothetical overview of Toll-Like Receptors (TLRs) and Innate immune Signalling Pathway

In the presence of bacterial lipopolysaccharide (LPS) or any pathogen-associated molecular patterns (PAMPs) in the host cell, pattern recognition receptors (PRRs) binds to it thereby activating toll-like receptors (TLRs) such as TLR-2, TLR-3 and TLR-4. These receptors triggers the myeloid differentiation primary response 88 (MyD88) that couples TIR-domain thereby activating mitogen-activated protein kinases (MAPK) signalling pathway that leads to nuclear factor kabba B (NF-κB) nuclear trans-location and subsequent regulation of the pro-inflammatory cytokine (IL-1β, IL-6, IL-8 and TNF-α) expression.

Table 5.1: Summary of screened Pro-inflammatory cytokines and their functions.

Cytokine	Classification	Main Sources	Receptor	Target Cell	Major Function
IL-1	Pro-inflammatory	Macrophages, B cells, DCs	CD121a	B cells, NK cells, T-cells	Pyrogenic, pro-inflammatory, proliferation and differentiation, BM cell proliferation
IL-6	Pro-inflammatory	Th Cells, macrophages, fibroblasts	CD126, 130	B-cells, plasma cells	B-cell differentiation
IL-8	Pro-inflammatory	Macrophages	IL-8R	Neutrophils	Chemotaxis for neutrophils and T cells
IFN-α	Pro-inflammatory	Macrophages, neutrophils, and some somatic cells	CD118 (IFNAR1, IFNAR2)	Various	Anti-viral
TNF-α	Pro-inflammatory	Macrophages	CD120a,b	Macrophages	Phagocyte cell activation, endotoxic shock

Abbreviations: IL; interleukin, TNF; tumor necrosis factor, IFN; interferon, CD; cluster of differentiation; CDw; cluster of differentiation designated by only one monoclonal antibody, DC; dendritic cells. *Source*: Pro-Inflammatory Cytokines Overview | Thermo Fisher Scientific - UK

5.1.3 Cell viability and cytotoxicity effects of sialidase inhibitors

Some chemical compounds used for therapy can affect the health and metabolism of host cells. These agents may cause toxicity in cells through the destruction of cell membranes, prevention of protein synthesis, irreversible binding to receptors, inhibition of polydeoxynucleotide elongation, and enzymatic reaction (Ishiyama et al., 1996). In addition, some chemical compounds may have cytotoxic effects on the biological activities of cells by altering their morphology, rate of cell growth, cell death, and cell disintegration (Boncler et al., 2014). Therefore, cell viability and cytotoxicity assay should be routinely performed for every compound of potential interest in drug discovery and experimental pharmacology.

5.2 Results

5.2.1 Investigation of Host-Pathogen Interactions via Adhesion and Invasion of Oral Epithelial Cells (H357 OSCC)

5.2.1.1 NanH Sialidase Promotes Host-Pathogen Interaction and was Abrogated by DANA and 2e3aDFNeu5Ac9N3

To investigate the role of the sialidase gene in host-pathogen interaction as a prelude to cytokine production assessment, the total bacterial association, attachment, and invasion assay (Antibiotics Protection Assay) as described in (section 2.15) was conducted. Previously, findings by other researchers suggested the important roles of sialidases of *T. forsythia* and *P. gingivalis* in the colonization and invasion of oral epithelial cells (Honma et al., 2011 and Aruni et al., 2011). It is important therefore to re-confirm these findings before continuing with the antibiotic protection assay aimed at investigating the ability of the new sialidase inhibitors in abrogating host-pathogen interactions.

The H357 OSCC were grown as a monolayer, and infected with either wild-type or sialidase-deficient strains of *T. forsythia* or *P. gingivalis*. As seen below (Figure 5.2), the wild-type *T. forsythia* (ATCC 43037) adheres and invades the oral epithelial cells better than the sialidase-deficient strain (ΔnanH). In addition, an increased total bacterial association (colonization) of the oral epithelial cells was observed with the wild-type *T. forsythia* (Figure 5.2). However, the sialidase inhibitor 2,3-dehydro-2-deoxy-*N*-acetylneuraminic acid (DANA) was able to significantly abrogate the host-pathogen interaction by reducing both the total association (colonization), adhesion, and invasion of oral epithelial cells by 50 % (Figure 5.3). Interestingly, inhibition of *T. forsythia* wild-type attachment and invasion to epithelial cells (KB or OBA-9) by Neu5Ac2en (DANA) was also reported (Honma et al., 2011). Nonetheless, at the concentration tested (1 µM), 2e3aDFNeu5Ac9N3 showed no significant reduction in the adhesion and invasion of oral epithelial cells (Figure 5.4), however, an increased concentration of 2e3aDFNeu5Ac9N3 may result in significant reduction in the host-pathogen interactions.
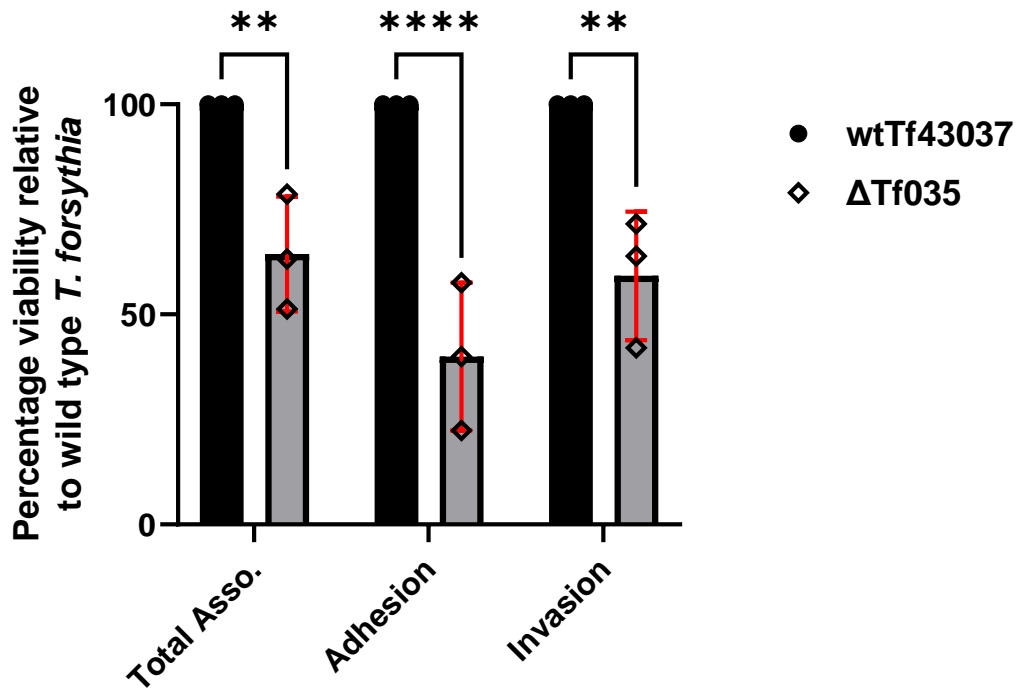
Figure 5.2: Total Association, Adhesion, and Invasion of H357 OSCC infected with wild-type and sialidase-deficient strains of *Tannerella forsythia*

Antibiotic protection assay was performed with wild-type (ATCC 43037) and sialidase-deficient (ΔTF035) strains of *T. forsythia*. Bacterial total association, adhesion (attachment), and invasion of the H357 OSCC cells were normalized to the number of bacteria that were used to infect each condition that had survived the duration of the assay (the percentage of viable bacteria). Data represent the mean from three independent experiments with each condition repeated in triplicate. Error bars=SD, Significance determined using Two-way ANOVA. *P* = < 0.05. Two-way ANOVA allows the quantitative measurement of the effect of NanH sialidase in total association, adhesion and invasion of oral epithelial cells by *T. forsythia* (ATCC43037).
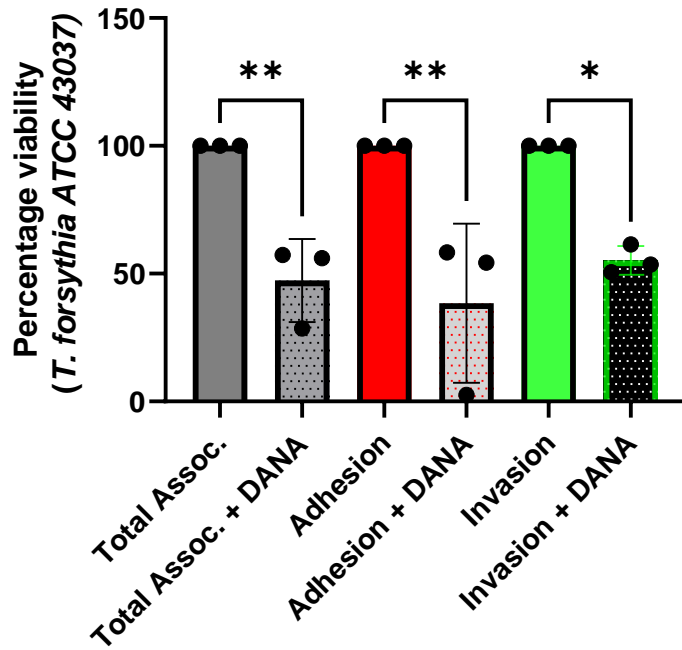
Figure 5.3: The effect of DANA on total association, attachment and invasion of H357 cells during mono-specie infection.

Antibiotic protection assays on H357 cell lines were performed in the presence or absence of 0.4mM DANA with *T. forsythia* (wtTf43037 & ΔTf035). Bacterial attachment, invasion and total association with host cells was normalized to the number of bacteria that were used to infect each condition that had survived the duration of the assay (the percentage of viable bacteria). Data represent the mean from three independent experimental repeats, and each condition was repeated in duplicate during each experiment. Error bars=SD, Significance determined using Ordinary one-way ANOVA. One-way ANOVA allows analyses of the differences in the means of the treated conditions in comparison to the untreated (independent) conditions.
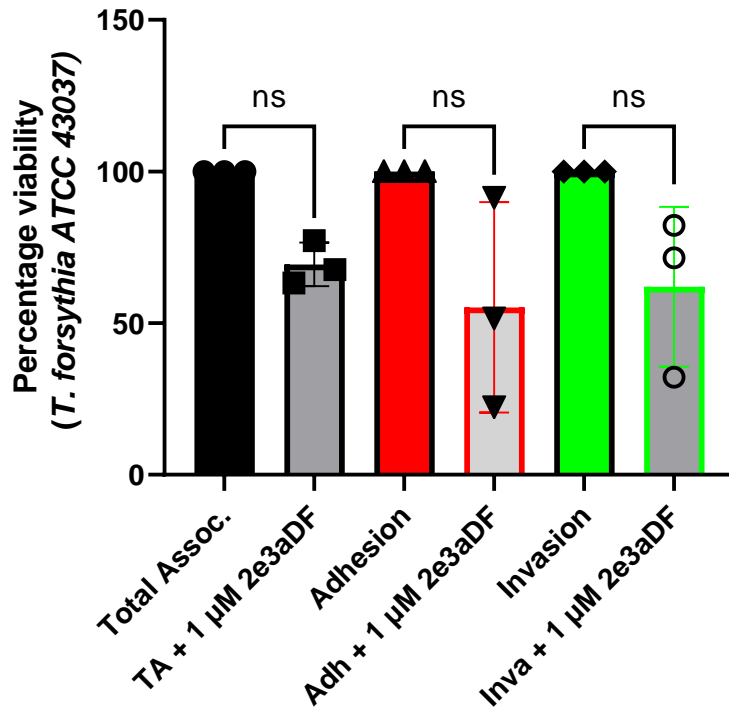
Figure 5.4: The effect of 2e3aDFNeu5Ac9N3 on the total association, adhesion, and invasion of oral epithelial cells (H357) during mono-specie infection

Antibiotic protection assays were performed in the presence or absence of 1 μM 2e3aDFNeu5Ac9N3 with the H357 cells infected with wild-type *T. forsythia* (wtTf43037) and sialidase-deficient strain (ΔTf035) at an MoI 1:100. Bacterial attachment, invasion and total association with host cells was normalized to the number of bacteria that were used to infect each condition that had survived the duration of the assay (the percentage of viable bacteria). Data represent the mean from three independent experiments with each condition repeated in triplicate. Error bars=SD, Significance determined using Ordinary One-way ANOVA. One-way ANOVA allows analyses of the differences in the means of the treated conditions in comparison to the untreated (independent) conditions.

5.3 Cell Viability and Determination of Cytotoxic Effects of Sialidase Inhibitors

5.3.1: Cytotoxic effects of Palmatine on H357 cells using Trypan blue assay

Here, the oral epithelial cells (H357) were incubated in the presence or absence of 0.15 mM (IC50 on NanH) and 1 mM (IC50 on SiaPg) of Palmatine, for 30 minutes and 1 hour, respectively to examine the dose and time cytotoxic effect on the oral epithelial cells. Trypan blue assay revealed the cell membrane integrity to be intact at 30 minutes, while at 1 hour, significant cytotoxicity was observed in the set-up treated with 1 mM of Palmatine (figure 5.3.1).
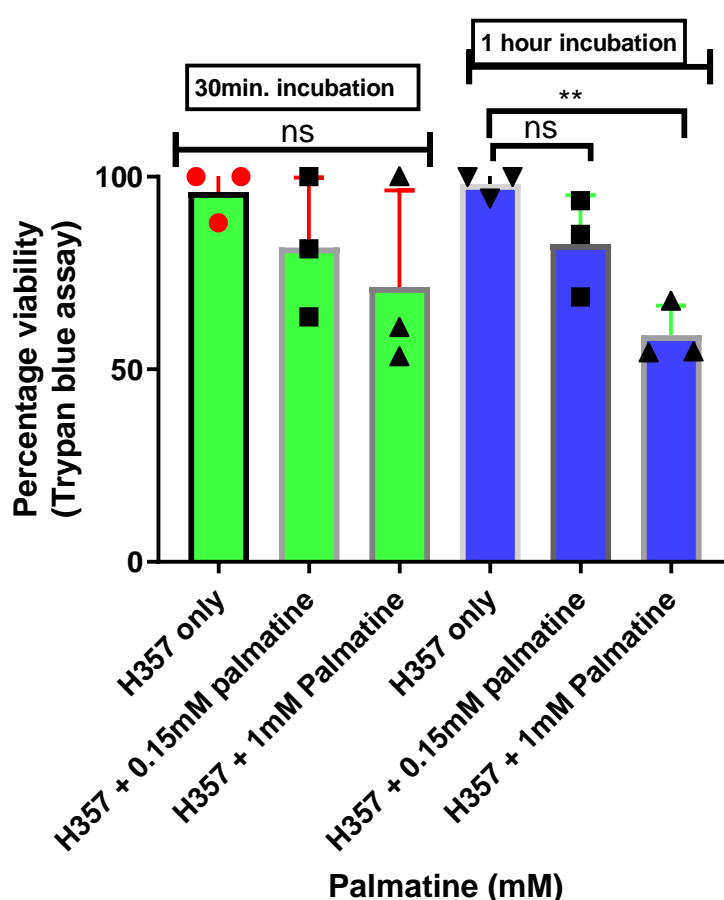
Figure 5.5: Dose/Time-Dependent cytotoxic effects of Palmatine on H357 cells

H357 cells were grown in a 12-well tissue culture plate in the presence or absence of varying concentrations of palmatine for 30 minutes and 1 hour respectively at 37ºC, 5% CO_2. 50µL of the cell suspension was stained with 50µL 0.4% trypan blue and the cell viability was determined by counting the viable and dead cells using hemocytometer and the percentage viability was plotted on Prism GrapPad (version 8.4.2). Each plot represents the results from three independent experiments. Ordinary One-way ANOVA was used and Tukey's multiple comparison test shows a *P* value < 0.05

5.3.2 Cytotoxic effects of Epicatechin gallate on H357 cells using Lactate dehydrogenase (LDH) and PrestoBlue assay

Lactate dehydrogenase (LDH) enzymes released into the H357 cell culture medium treated with varying concentrations of ECG were measured as described in section (2.16.2), and the percentage cytotoxicity was determined (Figure 5.6a). As a control, H357 cells treated with un-supplemented Dulbecco's Modified Eagle Medium (DMEM only), and with 10X LDH lysis buffer respectively, were used to ascertain the level of LDH that was released in the culture medium with complete lysis and all other treatments compared to this and the H357 alone. While the cells treated with DMEM only showed no LDH release into the medium, those treated with the 10X lysis buffer show 100% cell damage with a significant release of LDH in the medium (Figure 5.6a). Lastly, although there was a significant LDH release at higher concentrations of ECG (0.4, 0.35, 0.3, and 0.25 mM) respectfully, only 30-35 % of cell damage was observed, while at lower concentrations (0.2 – 0.025 mM), there was a minimal or no cytotoxic effect observed (Figure 5.6a).
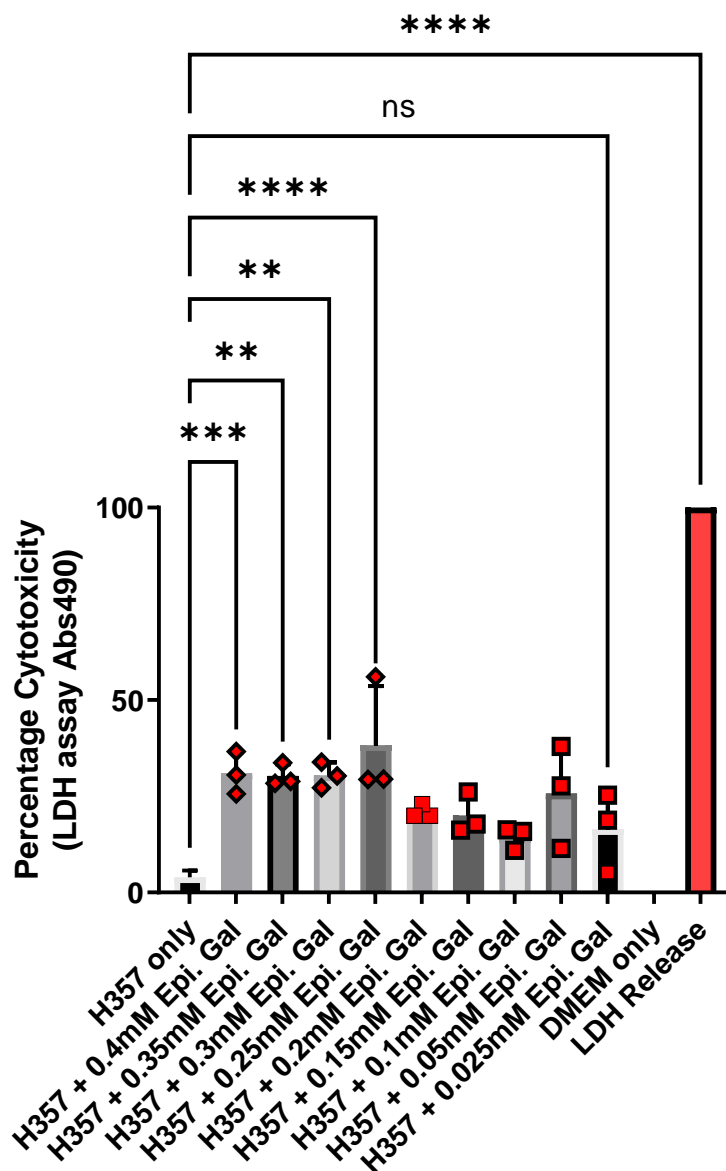
Figure 5.6a: Percentage Cytotoxicity (LDH assay) of Epicatechin gallate on H357 cells

H357 cells were grown in a 96-wells plate in the presence or absence of varying concentrations of Epicatechin gallate and 10X lysis buffer at 37ºC, 5% CO_2 for 1hr:30 Minutes. 50µL of respective supernatants were transferred to a new 96-well plate and 50µL of the CytoTox96® reagent was added to each well, wrapped in foil, and incubated in the dark for 30 minutes followed by the addition of CytoTox96® stop solution. The absorbance signal was measured at 490nm using a TECAN M200 plate reader. Percentage cytotoxicity was plotted using Prism GraphPad (version 9.2.0). Ordinary one-way ANOVA was conducted and each plot represents the results from three independent experiments with Dunnett's multiple comparison test at *P* <0.05. One-way ANOVA allows analyses of the differences in the means of the treated conditions in comparison to the untreated (H357 only) conditions.

Although ECG shows a minimal or no significant effect on H357 cells at 0.2 mM (IC50 value on whole sialidase activity), PrestoBlue assay which quantitatively measures cell viability, shows that ECG has a significant cytotoxic effect on H357 even at a micromolar range of 90 µM (Figure 5.6b).
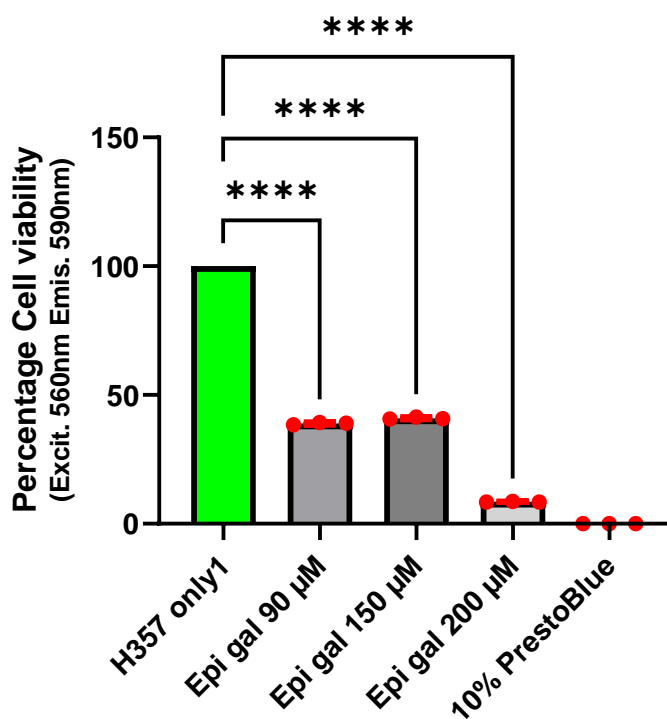
Figure 5.6b: PrestoBlue assay to determine the cytotoxic effect of Epicatechin gallate on H357 cells

H357 cells were seeded at $2x10^5$ /mL in a 12-well tissue culture plate and incubated at 37 ºC, 5% CO_2 for 24 hours. Culture supernatants were discarded and wells washed with PBS, varying concentrations of Epicatechin gallate were added and incubated for 24 hours. The wells were washed and 1 mL of 10 % PrestoBlue™ reagent prepared in un-supplemented DMEM was added to each well and incubated at 37ºC, 5% CO_2 for 1hr after which, 100 µL from each well were transferred to a flat bottom transparent 96-well plate and the reaction fluorescence was read at excitation 560 nm and emission at 590nm using TECAN M200 plate reader. Data represent a single experiment with each condition repeated in triplicate. Ordinary one-way ANOVA with Dunnett's Multiple Comparisons tests was conducted using Prism GraphPad (version 9.2.0). *P* value <0.05. Ordinary one-way ANOVA with Dunnett's multiple comparison test was used to analyse the differences in the multiple means gotten from the respective treatments.

5.3.3 Determination of the cytotoxic effects of 2e3aDFNeu5Ac9N3 on host oral squamous epithelial cells using Trypan blue and PrestoBlue™ assay

Cytotoxic effect of the difluoro-sialic acid compound 2e3aDFNeu5Ac9N3 earlier reported to be the most effective amongst all the sialidase inhibitors tested in this study (Table 3.1), on oral epithelial cells H357 was also investigated using trypan blue and PrestoBlue assays.

While trypan blue assay reveals that 4 µM has some level of cytotoxic effect on the H357 cells after 1hr:45Minutes incubation period (Figure 5.7), 3 and 4 µM respectively of 2e3aDFNeu5Ac9N3 were also found by PrestoBlue assay to have some minimal effect on the oral squamous carcinoma cells after 24 hours (Figure 5.8). Interestingly, both assays show that 1 µM (IC50 value of 2e3aDFNeu5Ac9N3 on purified NanH and wild-type *T. forsythia*), has no cytotoxic effect on the oral epithelial cells even after 24 hours of treatment (Figure 5.8).
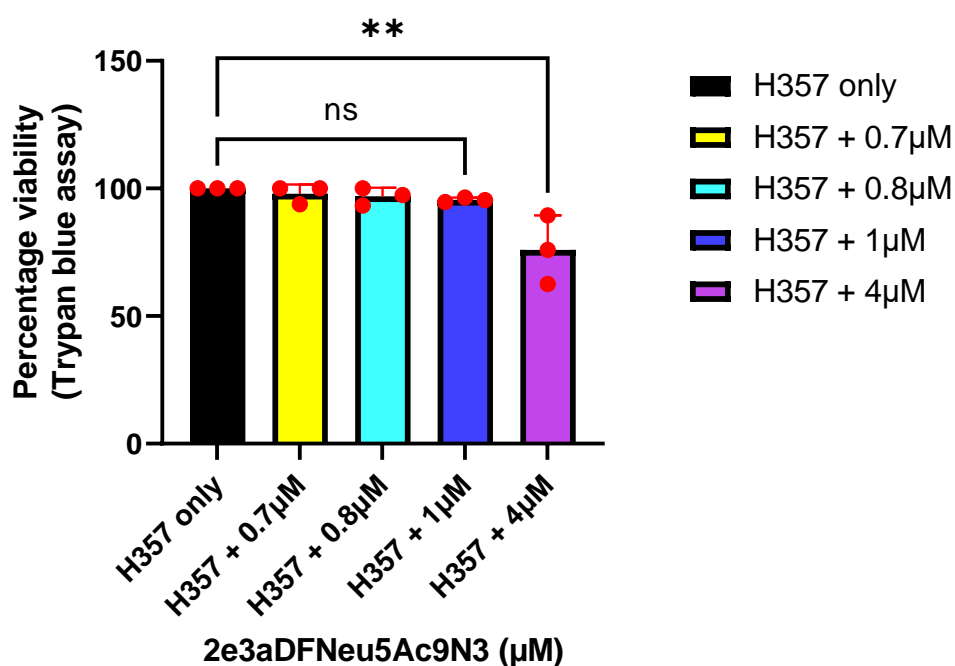
Figure 5.7: Dose-Dependent Cytotoxic effects of 2e3aDFNeu5Ac9N$_3$ on H357 cells (Trypan blue assay)

H357 cells were grown in a 12-well plate in the presence or absence of varying concentrations of 2e3aDFNeu5Ac9N$_3$ for 1hr:45Minutes at 37ºC, 5% CO_2. 50µL of the cell suspension was stained with 50 µL 0.4% trypan blue, and incubated for 2 minutes the cell viability was determined by counting the viable and dead cells using a hemocytometer and the percentage viability was plotted on Prism GraphPad (version 9.2.0). Each plot represents the results from three independent experiments. Data were analysed using Ordinary one-way ANOVA with Dunnett's Multiple Comparisons tests.

P value < 0.05. One-way ANOVA allows analyses of the differences in the means of the treated conditions in comparison to the untreated (H357 only) conditions.
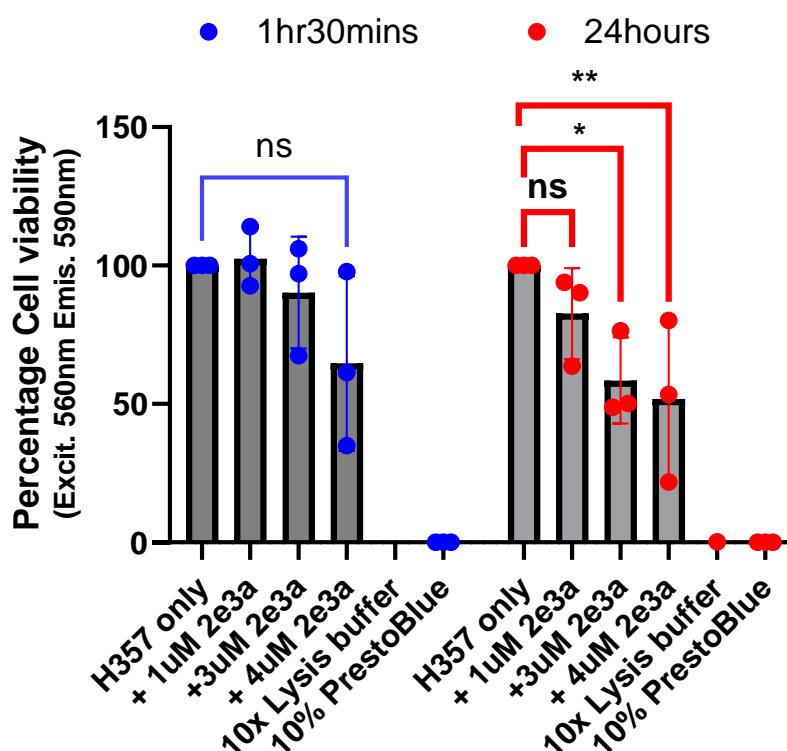

Figure 5.8: PrestoBlue assay to determine cytotoxic effect of 2e3aDFNeu5Ac9N$_3$ on H357 cells (1hr:30mins vs 24hrs treatment)

H357 cells were seeded at 2×10^5 /mL in a 24-well tissue culture plate and incubated at 37°C, 5% CO_2 for 24 hours. Culture supernatants were discarded and wells washed with PBS, varying concentrations of 2e3aDFNeu5Ac9N$_3$ prepared in DMEM were added and incubated for either 1hr30mins or 24hours. 50µL from respective treated wells were transferred to a new flat bottom transparent 96-well plate and 50µL of 10% PrestoBlue™ reagent was added to each well and incubated at 37°C, 5% CO_2 for 1hr or 2hrs. The reaction fluorescence was read at excitation 560nm and emission at 590nm using a TECAN M200 plate reader. Two-way ANOVA with Tukey's Multiple Comparisons tests was conducted using Prism GraphPad (version 9.2.0). *P* value <0.05. Tukey's multiple comparison test allows the comparison of the difference between the means of respective treatments across the two-time points.

5.4 The Role of Periodontal Pathogen Sialidases in Host-Pathogen Interactions and Secretion of Pro-inflammatory Cytokines (Immune Signalling)

Surfaces of immune, cancer, and epithelial cells have been shown to be sialylated (Crocker and Varki, 2001; Cao and Crocker, 2011 and Vajaria et al., 2016). In addition, OFk6, TR146, and H357 oral epithelial cells were shown to express TLR2-APC (unpublished data/personal discussion with Prof. Craig Murdoch). Desialylation of these surfaces by bacterial sialidases therefore may modulate the host's innate immune system, which may play an important role in inflammation and disease progression (Stamatos et al., 2004 and Lewis and Lewis, 2012).

To investigate the role of bacterial sialidases from *T. forsythia* and *P. gingivalis* on host innate immune modulation therefore, the oral epithelial cells (H357) were challenged with both wild-type and sialidase-deficient strains of *T. forsythia* and *P. gingivalis* at MoI of 1:100 respectfully, followed by quantification of the pro-inflammatory cytokines using flow cytometry method (section 5.17.2). Abrogation of the host-pathogen interaction leading to secretion of proinflammatory cytokines by the sialidase inhibitor; 2e3aDFNeu5Ac9N3, was also investigated. Importantly, 2e3aDFNeu5Ac9N3 was chosen because it was the most potent sialidase inhibitor (Table 3.1), and at the concentration (1 µM; which is the IC50 range of the compound on NanH sialidase) tested, there was no significant cytotoxic effect on the host oral epithelial cells (Figure 5.8).

5.4.1 NanH sialidase of *Tannerella forsythia* Upregulate Pro-inflammatory Cytokines in Oral Epithelial Cells (H357), and this was Abrogated by 2e3aDFNeu5Ac9N3

In this current study, the role of periodontal pathogen sialidases in modulating host innate immune response leading to the production of pro-inflammatory cytokines was investigated by exposing the oral epithelial cells (H357) to wild-type (wtTf43037) and sialidase-deficient (ΔnanH) strains of *T. forsythia* and wild type *P. gingivalis* (wtPg0381) and sialidase-deficient strain (ΔSiaPg), in the presence or absence of 1 µM 2e3aDFNeu5Ac9N3.

Conditions treated with the wild-type strain of *T. forsythia* (H357 + wtTf43037) appeared to significantly upregulate the production of the pro-inflammatory cytokines; interleukin-6 (IL-6), IL-8, and IL1-β in comparison to the untreated condition (H357

only). Interestingly, a five-fold upregulation of IL-6 was observed from 100% (347.5 pg/ml) in the untreated condition (H357 only) to about 500% (1623 pg/ml) in conditions that were challenged with wild-type *T. forsythia* (H357 + wtTf43037) (*p*= <0.0001) (Figure 5.9). Additionally, when the OSCC were challenged with the sialidase-deficient *T. forsythia* (H357 + ΔTf035), a twofold increase in IL-6 secretion was also observed from 100% (347.5 pg/ml) to about 300% (730.2 pg/ml) as compared to the untreated condition (*p*= 0.008) (Figure 5.9). Although both the wild-type and sialidase-deficient strains caused an increase in IL-6 secretion, the wild-type *T. forsythia* strain (wtTf43037) elicited a significant IL-6 secretion in comparison to the mutant strain (ΔnanH) (Figure 5.9). Importantly also, there was no significant difference in IL-6 expression in the untreated condition (H357 only) in comparison to the condition treated with the sialidase inhibitor (H357 + 2e3aDF) (figure 5.9). This could therefore mean that in addition to other cell surface structures, NanH sialidase also played a role in the amplification of the immune responses.

Furthermore, similar trends were also observed in IL-8 (Figure 5.10) and IL1-β (Figure 5.11) secretion with significant upregulation in pro-inflammatory cytokines in conditions treated with wild-type (H357 + wtTf43037) in contrast with the conditions treated with sialidase-deficient *T. forsythia* strain (H357 + ΔnanH) (*p* = 0.05) (Figure 5.10). Accordingly, the sialidase-deficient strain (H357 + ΔnanH) was unable to cause an increase in IL-8 when compared to the unchallenged condition (H357 only) with p = 0.4788 (Figure 5.10), unlike its ability to elicit IL-6 secretion observed earlier. Worthy of mention here is that the concentrations of IL-6 and IL1-β (pg/ml) secreted in all the conditions were quite similar but higher than that of IL-8 (Figure 5.12).

Similarly, Tumor necrosis factor (TNF-α) and Macrophage Inflammatory Proteins (MIP-1α) which are pro-inflammatory cytokine and chemokine respectively, were previously reported to be upregulated in conditions challenged with periodontal pathogens (Latorre Uriza et al., 2018 and Nisha et al., 2018), were also screened, but found to be below the detection level in all the conditions tested in this present study (data not shown here but see appendix). This may be due to variations in the cell lines used in the respective studies.

On the other hand, the ability of the sialidase inhibitor 2e3aDFNeu5Ac9N3; to inhibit cytokine production by the oral epithelial cells challenged with live *T. forsythia* was

also investigated. As stated above, upregulation of IL-6, IL-8, and IL1-β was observed in the presence of wild-type *T. forsythia* (ATC43037) in all the conditions tested, and this was significantly reduced by 1μM 2e3aDFNeu5Ac9N3. In the case of IL-6 (figure 5.6.1), the secretion was significantly downregulated from 1623.02 to 991.07 (61%), IL-8 from 394.07 to 338.36 (85%), and IL1-β from 1727.35 to 1040.25 (60%) pg/ml, respectively (figure 5.6.4). Importantly, in comparison to the untreated control (H357 only), epithelial cells exposed to 2e3aDFNeu5Ac9N3 alone (H357 + 2e3aDF) showed almost the same amount of cytokine production with no significant differences (figure 5.6.1; 5.6.2 and 5.6.3).
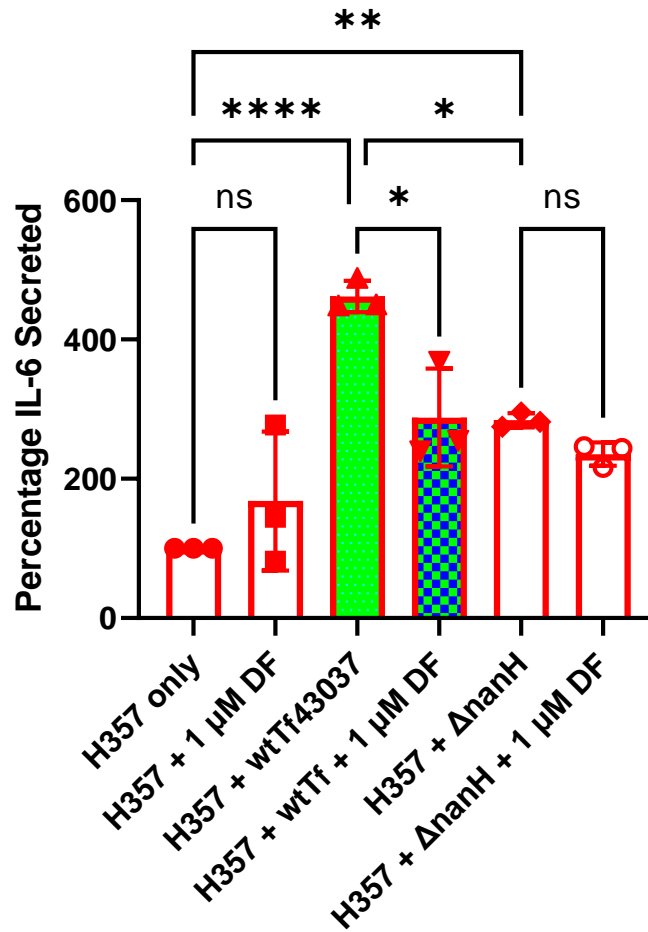
Figure 5.9: Percentage IL-6 secretion by oral epithelial cells (H357) exposed to *T. forsythia* and 1µM 2e3aDFNeu5Ac9N₃

H357 grown in supplemented DMEM were trypsinised, resuspended, and seeded at a density of $2x10^5$ cells/ml in a 12-well tissue culture plate (Greiner, UK) in triplicate and incubated at 37 °C, 5% CO2 for 24 hours. After which, the cells were exposed to wild-type (ATCC43037) and sialidase-deficient (ΔTFM0035) strains of *T. forsythia* at (MoI 1:100) host cell to bacterial cells, 1µM 2e3aDFNeu5Ac9N₃, or *T. forsythia* + 1µM 2e3aDFNeu5Ac9N₃. The experimental setup was incubated anaerobically at 37ºC, 5% CO_2 for 24 hours, and culture supernatant was harvested to determine IL-6 production (pg/ml) using flow cytometry assay. The data shown represent the mean of three experimental repeats, where each condition was repeated in triplicate. Ordinary one-way ANOVA with Tukey's Multiple Comparisons tests was conducted using Prism GraphPad (version 9.2.0) where Error bars = Mean with SD. *$p=$ <0.05, ***p=<0.0005 and ****p=<0.0001. One-way ANOVA with Tukey's multiple comparison was chosen because it compares the differences between the means of the treated conditions in relation to the independent (wtTf43037/ΔnanH), conditions. Same statistical method was used to analysed figures 5.9 to 5.14.
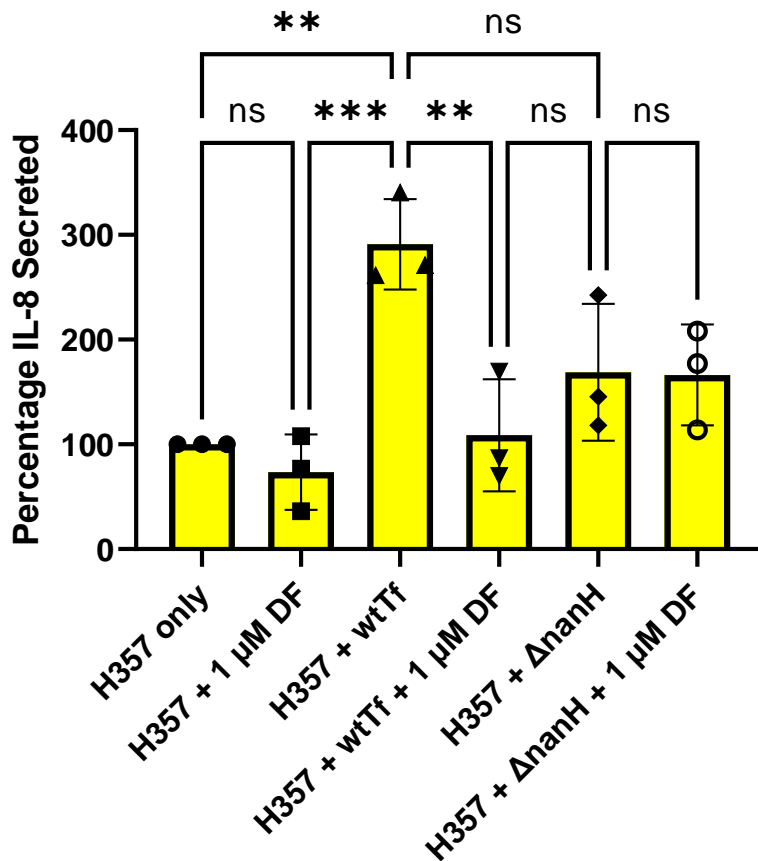
Figure 5.10: IL-8 secretion of oral epithelial cells exposed to *T. forsythia* and 1μM 2e3aDFNeu5Ac9N₃

H357 grown in supplemented DMEM were trypsinized, resuspended, and seeded at a density of 2×10^5 cells/ml in a 12-well tissue culture plate (Greiner, UK) in triplicate and incubated at 37 °C, 5% CO2 for 24 hours. After which, the cells were exposed to wild-type (ATCC43037) and sialidase-deficient (ΔTFM0035) strains of *T. forsythia* at (MoI 1:100) host cell to bacterial cells, 1μM 2e3aDFNeu5Ac9N₃, or *T. forsythia* + 1μM 2e3aDFNeu5Ac9N₃. The experimental setup was incubated anaerobically at 37ºC, 5% CO_2 for 24 hours, and culture supernatant was harvested to determine IL-8 production (pg/ml) using flow cytometry assay. The data shown represent the mean of three experimental repeats, where each condition was repeated in triplicate. Ordinary one-way ANOVA with Tukey's Multiple Comparisons tests was conducted using Prism GraphPad (version 9.2.0) where Error bars = Mean with SD. **p=<0.002 and ***p=<0.0009

Figure 5.11: IL1-β secretion of oral epithelial cells exposed to *T. forsythia* and 1μM 2e3aDFNeu5Ac9N₃

H357 grown in supplemented DMEM were trypsinized, resuspended, and seeded at a density of 2×10^5 cells/ml in a 12-well tissue culture plate (Greiner, UK) in triplicate and incubated at 37 °C, 5% CO2 for 24 hours. After which, the cells were exposed to wild-type (ATCC43037) and sialidase-deficient (ΔTFM0035) strains of *T. forsythia* at (MoI 1:100) host cell to bacterial cells, 1μM 2e3aDFNeu5Ac9N₃, or *T. forsythia* + 1μM 2e3aDFNeu5Ac9N₃. The experimental setup was incubated anaerobically at 37ºC, 5% CO₂ for 24 hours, and culture supernatant was harvested to determine IL1-β production (pg/ml) using flow cytometry assay. The data shown represent the mean of three experimental repeats, where each condition was repeated in triplicate. Ordinary one-way ANOVA with Tukey's Multiple Comparisons tests was conducted using Prism GraphPad (version 9.2.0) where Error bars = Mean with SD. **$p=0.0019$, ***$p=0.0002$ and ****$p=<0.0001$

Note: 2e3aDF = 2e3aDFNeu5Ac9N₃
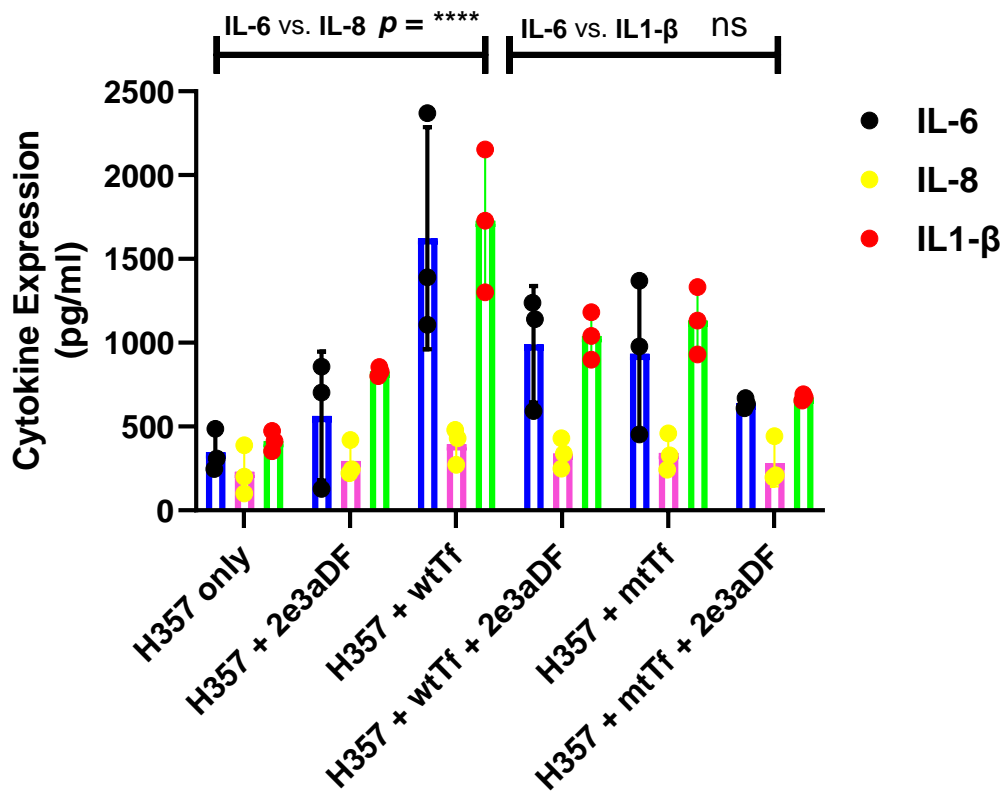
Figure 5.12: Comparing the amount of IL-6, IL-8 and IL1-β (pg/ml) expression by oral epithelial cells exposed to *T. forsythia* and 1μM 2e3aDFNeu5Ac9N₃

IL-6, IL-8 and IL1-β production (pg/ml) determined using flow cytometry assay as described above were compared to determine the most expressed proinflammatory cytokine. Data shown here represent the mean of respective cytokines, where each condition was repeated in triplicate. Two-way ANOVA and Dunnett's multiple comparisons test was conducted using Prism GraphPad (version 9.2.0) to determine the significance. ****p=<0.0001 and ns = 0.3083. Two-way ANOVA with Dunnett's multiple comparison test was used to analyse the differences in the multiple means gotten from the analysis of respective cytokines (IL-1β, IL-6 and IL-8).

Note: 2e3aDF = 2e3aDFNeu5Ac9N₃

5.4.2 *Porphyromonas gingivalis* (ATCC 0381) downregulates the expression of proinflammatory cytokines in oral epithelial cells (H357)

In the present study, oral squamous cell carcinoma (H357) was challenged with wild-type *P. gingivalis* (ATCC 0381) and sialidase-deficient strain (ΔSiaPg) at MoI 1:100 for 24 hours, and the proinflammatory cytokines were measured using flow cytometry as discussed in (section 5.17.2 and 5.17.3). Unsurprisingly, a complete downregulation of the pro-inflammatory cytokines was observed (Figures 5.13 and 5.14). In comparison to the untreated cells (H357 only), conditions challenged with both wild-type strain (H357 + wtPg0381) and sialidase-deficient strain (H357 + ΔSiaPg), show a significant downregulation in IL-6 and IL-8 (Figures 5.13 and 5.14).

Interestingly, there was no significant difference when the sialidase inhibitor was added to the conditions (H357 + wtPg0381 + 1μM 2e3aDF) and (H357 + ΔSiaPg + 1μM 2e3aDF) (Figures 5.13 and 5.14). This further shows that the sialidase inhibitor alone does not elicit cytokine production and the downregulation observed may be due to gingipains or proteases from *P. gingivalis*.

Note: 2e3aDF = 2e3aDFNeu5Ac9N$_3$
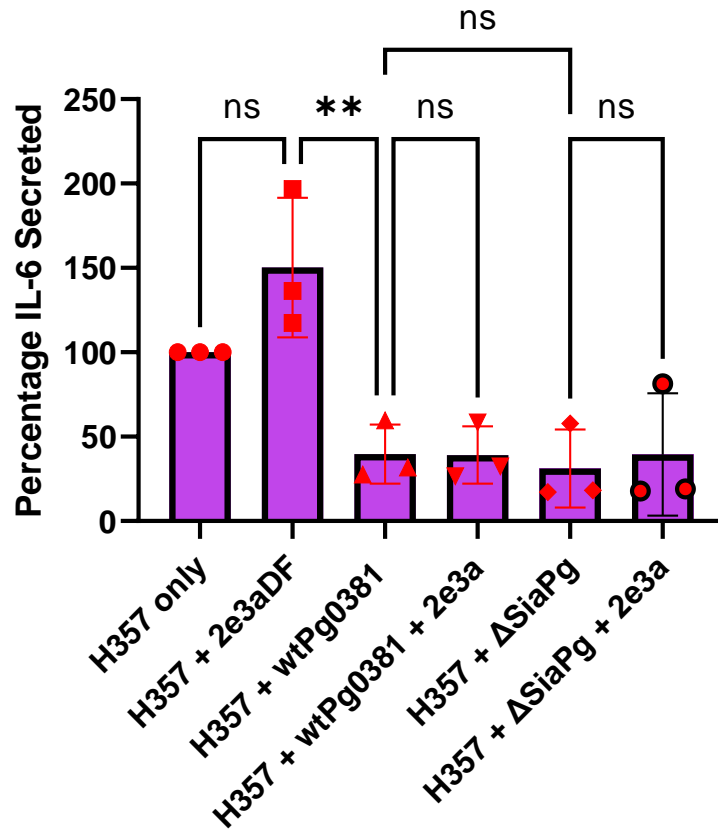
Figure 5.13: IL-6 secretion of oral epithelial cells exposed to *P. gingivalis* and 1μM 2e3aDFNeu5Ac9N$_3$

H357 grown in supplemented DMEM were trypsinized, resuspended, and seeded at a density of 2x10^5 cells/ml into the wells of a 12-well tissue culture plate (Greiner, UK) in triplicate and incubated at 37 °C, 5% CO2 for 24 hours. After which, the cells were exposed to wild-type and sialidase-deficient strains of *P. gingivalis* at (MoI 1:100) host cell to bacterial cells, 1μM 2e3aDFNeu5Ac9N$_3$, or *P. gingivalis* + 1μM 2e3aDFNeu5Ac9N$_3$. The experimental setup was incubated anaerobically at 37ºC, 5% CO$_2$ for 24 hours, and culture supernatant was harvested to determine IL-6 production (pg/ml) using flow cytometry assay. The data shown represent the mean of three experimental repeats, where each condition was repeated in triplicate. Ordinary one-way ANOVA with Tukey's Multiple Comparisons tests was conducted using Prism GraphPad (version 9.2.0) where Error bars = Mean with SD. **P =0.0026

Note: 2e3aDF = 2e3aDFNeu5Ac9N$_3$
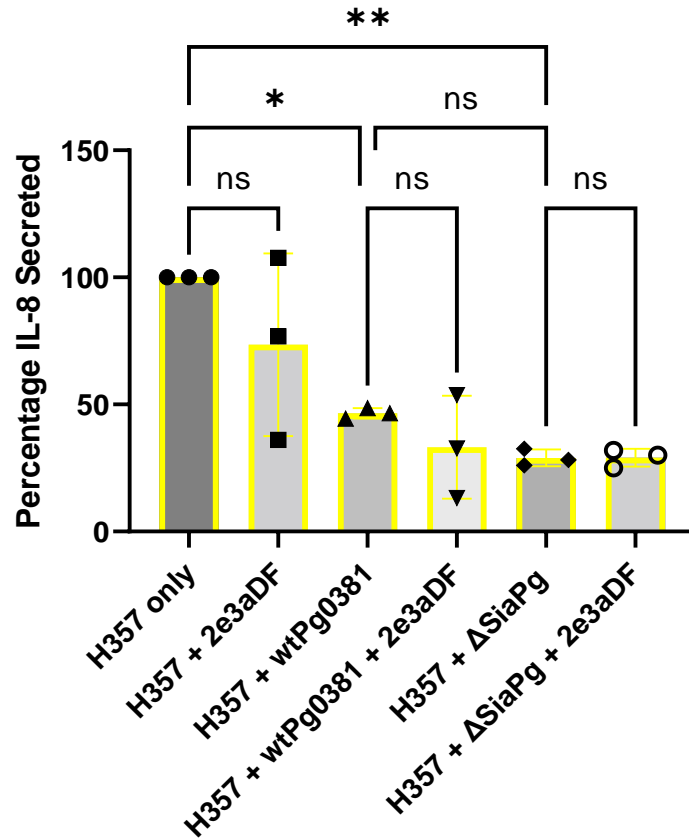
**Figure 5.14: IL-8 secretion of oral epithelial cells exposed to *P. gingivalis* and 1μM 2e3aDFNeu5Ac9N₃**

H357 grown in supplemented DMEM were trypsinized, resuspended, and seeded at a density of 2×10^5 cells/ml into the wells of a 12-well tissue culture plate (Greiner, UK) in triplicate and incubated at 37 °C, 5% CO2 for 24 hours. After which, the cells were exposed to wild-type and sialidase-deficient strains of *P. gingivalis* at (MoI 1:100) host cell to bacterial cells, 1μM 2e3aDFNeu5Ac9N₃, or *P. gingivalis* + 1μM 2e3aDFNeu5Ac9N₃. The experimental setup was incubated anaerobically at 37ºC, 5% CO_2 for 24 hours, and culture supernatant was harvested to determine IL-8 production (pg/ml) using flow cytometry assay. The data shown represent the mean of three experimental repeats, where each condition was repeated in triplicate. Ordinary one-way ANOVA with Tukey's Multiple Comparisons tests was conducted using Prism GraphPad (version 9.2.0) where Error bars = Mean with SD. **P** value <0.05

Note: 2e3aDF = 2e3aDFNeu5Ac9N₃

5.5 Discussion

In this chapter, the cytotoxic effects of the plant-derived and synthetic sialidase inhibitors on host oral squamous cell carcinoma (H357), the role of sialidase gene in host-bacterial interaction and their inhibition, as well as the role of sialidases in immune signalling pathways leading to expression of proinflammatory cytokines and abrogation of this pathway, were investigated.

Having established the IC_{50} values of these sialidase inhibitors (Chapter 3) and their effect on bacterial growth (Chapter 4), it is pertinent that we investigate the cytotoxic effect of these compounds on the host cells and the role of bacterial sialidases in immunological pathways.

5.5.1 Cytotoxic effects of Palmatine, Epicatechin gallate and 2e3aDFNeu5Ac9N3 on human oral squamous cell carcinoma (H357)

Palmatine; an isoquinoline alkaloid reported to have anticancer, antibacterial, antiviral, anti-inflammatory and many other pharmacological effects has been widely studied and used in pharmaceutical fields (Long et al., 2019). Previous research has also shown that palmatine had significant inhibitory effects on the growth of seven human cancer cell lines: SMMC7721, CEM, CEM/ VCR, 7701QGY, HepG2, K III and Lewis (Zhang et al., 2012). In addition, palmatine was shown to induced apoptosis in human epithelial skin carcinoma cells (A431) in a concentration- and time-dependent manner by damaging the DNA (Ali & Ali, 2014). Furthermore, Zhang et al., also reported the cytotoxic effect of palmatin on cardiomyocytes in time- and concentration-dependent manner resulting to arrhythmia and subsequent cardiac arrest (Zhang et al., 2018). In this present research, palmatine is also shown to be cytotoxic on human oral squamous cell carcinoma (H357) in a concentration- and time-dependent manner by inducing apoptosis. These pharmacological effects of palmatine might be valuable source for new potent anticancer drug candidates.

Epicatechin gallate (ECG); a polyphenol often extracted from green tea has also been reported to possess numerous pharmacological properties ranging from antimutagenic, antioxidative and anticancer effects amongst other (reviewed in Tu et al., 2010). Also, early findings had reported the strong apoptotic causing ability of ECG on human bladder cancer cells, human prostate cancer DU145 cells and on blastocysts stage of mouse embryos (Philips et al., 2009; Chung et al., 2001 and Tu et al., 2010).

In the present study, the cytotoxic effect of ECG on human oral squamous cell carcinoma (H357) following 1:30 or 24 hours treatment was also witnessed with an increased cell deaths and a significant reduction in cell proliferation. Although the underlying mechanisms of action of ECG is not clear, some researchers believes that the induction of apoptosis may be due to its effect on the reactive oxygen species (ROS) formation and mitochondrial depolarization (Chung et al., 2001). Additionally, the gallate moiety on the chemical structure of ECG has been shown to increase its biological effectiveness in inducing apoptosis and suppression of cell growth (Chung et al., 2001).

Furthermore, the inhibitory activities of polyphenolic components of green tea such as ECG has been attributed to their ability to interfere with receptor binding sites, blockage of nuclear factor κB, inhibition of protein kinase, induction of apoptosis among other mechanisms (Yang et al., 2002). These attributes may be due to its high partition coefficient (Hashimoto et al., 1999) and the pK_a value (Kumamoto et al., 2001) of Epicatechin gallate which enables their cellular absorption and diffusion via the phospholipid bilayer of plasma membrane (Hong et al., 2002). In addition, the antioxidant, antimicrobial, chemopreventive activities of ECG and it roles in oral health has been reported (reviewed by Venkateswara et al., 2011).

Lastly, the cytotoxic effect of the di-fluoro sialic acid compound; 2e3aDFNeu5Ac9N3 on human oral squamous cell carcinoma (H357), was also investigated. At the concentrations there was a minimal to no significant cytotoxic effect on the H357 cells even after 24 hours.

5.5.2 Sialidases of *T. forsythia* and *P. gingivalis* Promote Attachment and Invasion of Oral Epithelial cells (H357 OSCC)

Periodontal pathogens such as *P. gingivalis* and *T. forsythia* have been reported to possess a range of virulence factors amongst which is their ability to attach and invade epithelial cells (Aruni et al., 2011 and Honma et al., 2011). Previous investigations from our Lab also reported the ability of the wild type strains of *T. forsythia* (Frey et al., 2018) and *P. gingivalis* (Frey et al., 2019) to also attach and invade oral epithelial cells H357 better than their sialidase-knockout strains ((Frey et al., 2018 and Frey et al., 2019) Ability to adhere and invade epithelial cells by these oral pathogens is therefore

important for pathogenicity. Thus, revalidating these findings was important, thus, serves as the basis for studying the role of sialidase in host-pathogen interactions and immune modulation.

Importantly, the initial stage in infection is for the pathogen to colonize the host cells (Boyle, 2008), thus, these red complex periodontal pathogens: *P. gingivalis* and *T. forsythia* possess the ability to adhere and invade the oral epithelial cells which is key to onset and progression of periodontitis (Frey et al., 2019). This is facilitated by the secretion of sialidase enzymes which contribute to disease progression via different mechanisms (Roy et al., 2011 and Stafford et al., 2012). Similarly, in this study, the wild type strain of *T. forsythia* (ATCC43037) has shown an increased total association, attachment and invasion of the oral epithelial cells as compared to the sialidase-deficient strain.

Interestingly, this host-pathogen interaction were significantly abrogated by the sialidase inhibitor; 2,3-dehydro-2-deoxy-*N*-acetylneuraminic acid (DANA) with both the bacterial total association, adhesion and invasion of the oral epithelial cells having a two-fold reduction from 100% to 50%, 47% and 55% respectively. However, at the concentration tested, 2e3aDFNeu5Ac9N3 show a minimal reduction but with a higher concentration, a significant reduction in bacterial adhesion and invasion to host oral epithelial cells (H357), may be observed.

In this present study, DANA was able to reduce both total association, adhesion and invasion of the oral epithelial cells (H357) by the red complex oral pathogen *T. forsythia* (ATCC43037), and this may support its use as a novel therapy for periodontitis. As stated earlier, bacterial adhesion is important for the colonisation of host tissues and subsequently, invasion of the host cells may provide a niche for the pathogen to evade host immune response thereby subverting antimicrobial actions. Furthermore, sialidase activity has been shown to support attachment and invasion of host epithelial cells which will in turn activate the host immune system. Consequently, 2,3-dehydro-2-deoxy-*N*-acetylneuraminic acid (DANA), which is a viral neuraminidase inhibitor can be employed as a novel inhibitor of bacterial sialidases (NanH and SiaPg) which may serve as therapeutic agent against periodontitis and other inflammatory diseases.

5.5.3 The role of NanH sialidase of *T. forsythia* in immune signalling and secretion of pro-inflammatory cytokines and its abrogation by 2e3aDFNeu5Ac9N₃

Periodontitis is a chronic inflammatory disease that is linked to red complex oral pathogens such as *P. gingivalis* and *T. forsythia* (Stafford et al., 2012 and Takahashi, 2015). The presence of bacterial LPS or pathogen-associated molecular patterns (PAMPS) in the oral cavity could trigger the host innate and adaptive immune responses thereby leading to inflammation of the gingiva thus resulting in periodontitis and other inflammatory diseases (Silva et al., 2015). These processes, therefore, result in the destruction of the tissues surrounding and supporting the teeth and subsequently resulting in tissue, bone, and tooth loss (Silva et al., 2015). In addition, pathogens have developed a mechanism of using their sialoglycosidases in targeting host sialoglycans for immune dysregulation via pathogen-toll-like receptor (TLR) interactions which are mediated through sialic acid receptor ligand mechanisms (Sudhakara et al., 2019).

Bacterial sialidases are considered virulence factors and are shown to be involved in peroxide scavenging during oxidative stress (Iijima et al., 2004), infection and tissue destruction (Wang et al., 2010), as well as impairment of the host innate immune system (Sudhakara et al., 2019). Pattern-recognition receptors (PRRs) such as the toll-like receptors (TLRs) in mammals, play an important role in recognising microbial components as well as endogenous ligands induced during inflammatory responses (Akira et al., 2001). The presence of pathogens or their products triggers the secretion of cytokines such as interleukin-12 (IL-12) and IL-18 by the TLRs in the antigen-presenting cells (APC), produced in the early stages of infection to provide immunity against the invading pathogens (Akira et al., 2001). Sialidases from periodontal pathogens could also mediate the activation of these in a number of ways, possibly through direct desialylation of host cell surface structures such as the TLRs resulting in cell death, or by indirectly influencing the bacterial adhesion and invasion of host cells as seen in this study.

TLRs expression is observed in several cells including vascular endothelial cells, cardiac myocytes, adipocytes, and epithelial cells (Akira et al., 2001). In addition to neutrophils and macrophages, oral epithelial cells are also capable of secreting pro-inflammatory cytokines (Stathopoulou et al., 2010). Furthermore, TLR4 recognises

bacterial lipopolysaccharide (LPS); an integral component of the outer membrane of Gram-negative bacteria, and TLR2 recognises lipoproteins and glycolipids, while TLR5 and TLR9 recognises bacterial flagellin and bacterial (CpG) DNA respectively (Akira et al., 2001). These TLRs are considered to be important in the up-regulation of inflammatory cytokines during periodontitis and are also shown to be regulated by human cytosolic neuraminidase (hNeu1) (Amith et al., 2010).

Furthermore, The first host cells to have direct contact with oral pathogens and their by-products are the epithelial cells of the gingival epithelium. Once in contact with pathogens (PAMPs), inflammatory responses by the oral epithelial cells are induced leading to the secretion and deployment of pro-inflammatory cytokines and chemokines to the site of infection for defence (Stathopoulou et al., 2010). Previous findings have also revealed the presence of pro-inflammatory cytokines and chemokines in gingival crevicular fluid (GCF), both in health and disease and are upregulated in sites showing signs of inflammation (Zhong et al., 2007).

Furthermore, lipopolysaccharide from clinical isolates of *T. forsythia* was reported to differentially induce proinflammatory cytokine expression of interferon-gamma protein IP-10 (CXCL10) in macrophages (Chinthamani et al., 2022), and its role in inducing pro-inflammatory cytokines such as IL-1β and IL-6 by CD4 + T helper cells and TNF-α was also investigated (Malinowski et al., 2019). Additionally, lipopolysaccharide of Gram-negative bacteria has been shown to activate TLR-4 (Holt et al., 1999 and Yuk & Jo, 2011). With the increased cytokine expression observed in this current study, the combined effect of NanH sialidase of *T. forsythia* (ATCC43037) may be responsible, or at least in part, for amplifying immune signaling pathway and subsequent upregulation of the pro-inflammatory cytokines by oral squamous epithelial cells (H357). Interestingly, Stamatos et al., (2010) also reported the role of Neu3 sialidase in LPS-induced proinflammatory cytokine secretion in human dendritic cells. They demonstrated that inhibiting Neu3 sialidase activity with Zanamivir during differentiation to dendritic cells (DCs), resulted in stabilizing the amount of sialic acid found on the surface makers of matured DCs (Stamatos et al., 2010). Additionally, differentiation of human monocytes to dendritic cells in the presence of Zanamivir caused a reduced LPS-induced secretion of IL-12p40, IL-6, and TNF-α by mature DCs, signifying the important role of Neu3 sialidase in regulating proinflammatory cytokine production (Stamatos et al., 2010). This further proves the role of sialidases in

desialylating sialic acid content on cell surfaces, thereby leading to mediating host immune responses.

Lastly, in addition to the recognition of PAMPs by TLRs, they are also crucial in the pathophysiology of inflammatory, infectious and autoimmune diseases (Amith et al., 2010). Importantly, the mechanism by which TLRs are been activated has been shown to be tightly regulated by Neu1 sialidase activation, since Neu1 sialidase is reported to be in complex with TLR-2, TLR-3 and TLR-4 receptors, and is induced upon ligand binding to either of the receptors (Amith et al., 2010).

On the other hand, the ability of 2e3aDFNeu5Ac9N3 to significantly reduce the secretion of the pro-inflammatory cytokines in response to wild-type *T. forsythia* in this present study may be attributed to the stereochemistry of this compound (Li et al., 2019), which was reported to be a covalent sialidase inhibitor (Li et al., 2019 and Bowles & Gloster, 2021). Li and colleagues also reported that the addition of fluorine molecules at C2 and C3 as well as the azido group at C9 of the sialic acid ring enables covalent bonding and specific selectivity of 2e3aDFNeu5Ac9N3 to sialidases of *C. perfringens* and *V. cholerae* (Li et al., 2019). In this study, however, such a claim with NanH sialidase from *T. forsythia* hasn't been established. Nonetheless, in addition to the low micromolar (IC_{50} values) inhibitory properties of this compound on the sialidases of *T. forsythia* and *P. gingivalis*, protein-ligand interaction studies, enzyme kinetics and mechanism of inhibition assays revealed that 2e3aDFNeu5Ac9N3 is a competitive inhibitor of NanH sialidase.

Interestingly, Zanamivir (Govinden et al., 2018), Oseltamivir (Roy et al., 2011), and plant-derived compounds (Miyaichi et al., 1990), were also shown to inhibit other bacterial and viral sialidases respectively. More importantly, however, 2e3aDFNeu5Ac9N3 was observed in this study to have superior sialidase inhibitory activity against the sialidases of oral pathogens at a micromolar concentration. This important finding in addition to its minimal cytotoxicity on oral epithelial cells, provides support for the need to consider 2e3aDFNeu5Ac9N3 or similar compounds as a novel periodontitis therapy since upregulation of inflammation is an important phenomenon in disease progression.

5.5.4 The Role of *Porphyromonas gingivalis* Sialidase (SiaPg) in Modulation of host innate immune response

As seen above with *P. gingivalis*, this demonstrates the role of periodontal pathogens in inducing different cytokine responses as well as in modulating host innate immunity using oral squamous cell carcinoma (H357). In this present study, oral squamous cell carcinoma (H357) challenged with wild-type *P. gingivalis* (ATCC 0381) and sialidase-deficient strains of *P. gingivalis* at MoI 1:100 for 24 hours showed a complete downregulation of the pro-inflammatory cytokines (IL-6 and IL-8).

The downregulation of these cytokines could suggest that the pathogen has developed mechanisms to reduce inflammatory responses by the oral epithelial cells (H357). Previously, Stathopoulou et al., (2010), also reported a downregulation in the secretion of secondary cytokines (IL-6 and IL-8) by human gingival epithelial cells (HGECs) challenged with live *P. gingivalis* (ATCC 33277) at MoI 1:100 for 24 hours (Stathopoulou et al., 2010). They state that the lack of these secondary cytokines may suggest that *P. gingivalis* has developed a mechanism to reduce the inflammatory responses of the host (Stathopoulou et al., 2010). In addition, gingipains and proteases secreted by *P. gingivalis* were also shown to be involved in subverting protective host pro-inflammatory responses, thereby degrading these secondary cytokines (IL-6, IL-8) at a higher rate than the primary cytokines (IL1-β), and that the cytokines reduced production does not occur at the transcriptional level (Stathopoulou et al., 2009).

As stated above, TNF-α and MIP-1α were below the detection threshold in all conditions tested and for both *T. forsythia* or *P. gingivalis* (data not shown). This could mean that oral squamous epithelial cells (H357) either do not secrete TNF-α and MIP-1α or the concentrations and duration to which the H357 cells were exposed to the bacteria were not adequate to elicit an inflammatory response. Interestingly however, Emingil and colleagues (2005), also reported a low level of MIP-1α in gingival crevicular fluid (GCF) which they said, does not have any discriminatory role in periodontitis, and may be due to a lack of macrophages as well as lymphocytes with specific receptors for MIP-1α (Emingil et al., 2005). Also, an in vivo murine model of wound healing revealed a low level of MIP-1α production in mice deficient in TLR-4 or incapable of TLR-4 activation (Brancato et al., 2013).

In conclusion, these findings suggest that the red complex pathogens associated with periodontitis; *T. forsythia* and *P. gingivalis* elicit different inflammatory responses in oral squamous cell carcinoma (H357), and this may reflect their virulence. While *T. forsythia* induces proinflammatory cytokines (IL-6, IL-8, and IL1-β), *P. gingivalis* on the other hand subverted the host innate immune responses by downregulating the cytokine profiles. Although an *in vitro* model is used in this study, the findings suggest that the NanH sialidase of *T. forsythia* (ATCC 43037), is capable of triggering or amplifying pro-inflammatory cytokines (IL-6, IL-8, and IL1-β) release and deployment of these immune and inflammatory cells to the infection sites. Most importantly however, the sialidase inhibitor 2e3aDFNeu5Ac9N3; at a micromolar range was able to significantly abrogate this host-pathogen interaction, indicating its potential as a virulence inhibitor as well as an immunomodulatory agent.

Going further, polymicrobial infections which are more representative of the diseased conditions such as that reported by Frey et al., (2019), should be looked upon in the presence of 2e3aDFNeu5Ac9N3. In their work, they found out that NanS sialate-esterase from *T. forsythia* enhances the ability of *P. gingivalis* sialidase (SiaPG) in utilizing sialic acids found on host sialoglycoproteins like the heavily O-acetylated substrates such as bovine salivary mucin (BSM), suggesting the need for interspecies cooperation (Frey et al., 2019). In addition, zanamivir was shown to abrogate adhesion and invasion of oral epithelial cells by periodontal pathogens both in mono- and multispecies infection models (Frey et al., 2019). With the superior inhibitory properties of 2e3aDFNeu5Ac9N3 on both the sialidases of *P. gingivalis* and *T. forsythia* in comparison to zanamivir, as well as its minimal cytotoxic effect on oral epithelial cells (H357), its inclusion in periodontitis and other inflammatory diseases therapy could be a game changer.

Furthermore, sialidases of the human oral microbiome have been reported to degrade host sialoglycoconjugates, resulting in exposed terminal sialic acid (Sudhakara et al., 2019). Activities of these periodontal pathogens therefore could lead to pathogen-toll-like receptor (TLR) interactions which are mediated via sialic acid receptor ligand mechanisms. Investigating the interactions between sialidases of *T. forsythia* and *P. gingivalis* with host' TLRs in the presence of 2e3aDFNeu5Ac9N3 could create a way to design target-specific drugs.

5.6   Chapter Summary

Having established the anti-sialidase, antibacterial, and antibiofilm properties of the plant-derived and synthetic compounds tested in this study earlier, investigating the cytotoxic effect of these compounds on the host oral epithelial cells and the role of bacterial sialidases in pathogenesis as well as in immunological pathways is therefore important.

Palmatine; an isoquinoline alkaloid, and Epicatechin gallate (ECG); a polyphenol often extracted from green tea, are plant-derived compounds that were previously reported to possess numerous pharmacological properties ranging from anticancer, antibacterial, antiviral, anti-inflammatory, antimutagenic and antioxidative effects amongst other. In this present study, these compounds were also found to have sialidase inhibitory properties even though cytotoxic to oral epithelial (H357) cells. The synthetic difluoro-sialic compound; 2e3aDFNeu5Ac9N3 was also found to inhibit the sialidases of *T. forsythia* and *P. gingivalis* at a low micromolar concentration. Furthermore, although Epicatechin gallate was found to be significantly cytotoxic, Palmatine and 2e3aDFNeu5Ac9N3 were seen to have minimal or no cytotoxic effects on the oral epithelial cells (H357), hence may serve as novel therapeutic agents for periodontitis.

Secondly, the host-pathogen interaction reveals that the sialidases of periodontopathogens; *T. forsythia* and *P. gingivalis* are essential for the bacterial adhesion and invasion of host oral epithelial cells, and this was abrogated using the sialidase inhibitor DANA (Neu5Ac2en). Additionally, the NanH sialidase of *T. forsythia* has elicited an upregulation of pro-inflammatory cytokines including IL-6, IL-8, and IL1-β which were downregulated by 2e3aDFNeu5Ac9N3. On the other hand, *P. gingivalis* shows a downregulation in the secretion of pro-inflammatory cytokines, which may be attributed to its ability to degrade these secondary cytokines (IL-6, IL-8) using its gingipains and proteases. Also, with TNF-α and MIP-1α production below detection level, and differences in cytokine expression in response to these periodontopathogens, it can be attributed to the specificity conferred to the innate immune system by a wide range of pattern-recognition receptors (PRRs) such as Toll-like receptors (TLRs) that are important in recognising highly conserved microbe-associated molecular patterns (MAPs),

Lastly, the present study further provides evidence that supports previous findings on the role of bacterial sialidases in the adhesion and invasion of oral epithelial cells, and that NanH sialidase of *T. forsythia* is partly responsible for the induction of different pro-inflammatory cytokines including; IL-6, IL-8 and IL1-β expression in oral epithelial cells (H357), which may reflect their virulence in periodontitis. Most importantly however, this host-pathogen interaction was inhibited by the covalent sialidase inhibitor; 2e3aDFNeu5Ac9N3 at a low micromolar concentration.

CHAPTER SIX

6.1 Discussion

The overall aim of this research was to test a wide range of synthetic and plant-derived inhibitors of periodontal pathogen sialidases (NanH and SiaPg) of *T. forsythia* and *P. gingivalis*, respectively. In addition, the role of these bacterial sialidases in host-pathogen interactions such as bacterial growth, biofilm formation, adhesion and invasion, of host oral epithelial cells, as well as in immune modulation, with a view to abrogate the expressed pro-inflammatory cytokines using the most promising inhibitor, were also investigated. Together with the protein-ligand interactions aimed at studying how the inhibitors fit into the active-site pockets of both NanH and SiaPg, this current project is geared towards the development of novel inhibitors of periodontitis and other inflammatory diseases in the future.

The sialidase inhibitory properties of over 20 compounds against hi-purified NanH and SiaPg were tested. These included pharmaceutically approved neuraminidase inhibitors like Zanamivir, Oseltamivir, Siastatin B and DANA, plant-derived; like Epicatechin gallate, Palmatine and Berberine chloride and several newly synthesized compounds by our collaborators from the UC-Davis. Of these, the di-fluoro sialic acid analogue 2e3aDFNeu5Ac9N3; was found to be the most potent inhibitor of both NanH and SiaPg. Accordingly, Li et al., (2019), also reported the inhibitory properties of 2e3aDFNeu5Ac9N3 against several pathogenic bacterial sialidases including *C. perfringens* (CpNanI), *V. cholerae* and a recombinant human cytosolic (hNeu2) sialidase (Li et al., 2019).

Further, the drug combination assays and the mechanism of action (MOA) of some of the compounds investigated including Palmatine, Berberine chloride and 2e3aDFNeu5Ac9N3 has shown that the compounds are noncompetitive, uncompetitive and competitive inhibitors of NanH sialidase, respectively. This experiment together with the protein-ligand interaction studies, gives an understanding of how inhibitors binds and coordinate the catalytic residues in the enzyme's active-site pocket in order to inhibit the enzymes activity as well as the possibility of combination therapies in the treatment of periodontitis or other inflammatory diseases. Interestingly, Satur and colleagues recently reported the binding ability of Oseltamivir into the active-site pocket of NanH-apo (Satur et al., 2022), just as Wen-bo et al., demonstrated the ability

194

of SiaPg to coordinate the carboxyl group of sialic acid (Neu5Ac) together with other conswerved catalytic residues like the neucleophilic dyad tyrosine and glutamate (Dong et al., 2023). In addition, synergistic effect and mechanism of action of other plant-derived inhibitors on bacterial enzymes was also reported (Thakur et al., 2016 and Hyeong-U et al., 2019).

Interestingly as reported earlier (Roy et al., 2011, Frey et al., 2019), sialidase gene promote the growth of wild-type *P. gingivalis*, *T. forsythia,* as well as biofilm formation by *T. forsythia*. On the other hand, however, the sialidase-deficient strain of *P. gingivalis* showed an increased biofilm formation in comparison to the wild-type strain. This may suggest that deletion of some bacterial cell surface structures could impact on the overall behaviour of the pathogen as observed by Yamaguchi et al., (Yamaguchi et al., 2010). Also, while sialidase appears not to be necessary in the utilization of glycoproteins (mucin) by *P. gingivalis*, *T. forsythia* requires it to utilize mucin for growth and in biofilm formation. In addition, *T. forsythia* was seen to utilize 2-Keto-3-deoxy-D-glycero-D-galactononononic acid (KDN), for growth via an unknown mechanism, which may implies that NanH could also be a KDNase (Telford et al., 2011). Importantly, the sialidase inhibitors tested in this current research were able to inhibit the planktonic growth of both *P. gingivalis* and *T. forsythia*, with the plant-derived Epicatechin gallate (ECG) inhibiting biofilm formation by *T. forsythia*.

Lastly, the role of NanH sialidase of *T. forsythia* in upregulating the expression of pro-inflammatory cytokines including IL1-β, IL-6, and IL-8, could suggest the important role of NanH sialidase in amplifying the immune signalling cascade thus, leading to inflammation which is key in periodontitis (Sharma, 2010,Chen et al., 2014, Cardoso et al., 2018). Interestingly, the overexpressed pro-inflammatory cytokines were downregulated by the di-fluoro compound 2e3aDFNeu5Ac9N3 at a millimolar concentration. With its superior sialidase inhibitory properties, minimal cytotoxic effect on oral epithelial cells, and its ability to abrogate pro-inflammatory cytokine expression elicited by the NanH sialidase, 2e3aDFNeu5Ac9N3 can further be developed as a novel therapy of periodontitis or as an immunomodulatory agent.

6.2   Conclusions

The outcome of this study so far has expanded knowledge of the molecular basis and pathogenicity of the periodontal pathogens most commonly associated with periodontitis i.e *P. gingivalis* and *T. forsythia*. Most importantly, however, is the promising results recorded from the wide range of sialidase inhibitors tested, and the role of NanH sialidase of *T. forsythia* in host innate immune modulation.

Furthermore, with the promising inhibitory properties of 2e3aDFNeu5Ac9N3 on the periodontal pathogen sialidases, and its ability to downregulate the pro-inflammatory cytokines secreted by the oral epithelial cells, it advocates its potential as an anti-virulence therapeutic for the treatment of periodontal and other inflammatory diseases.

However, due to the impact of Covid-19 and limited access to the lab., I was unable to carry out some of the experiments initially planned for. These include more work on synergistic assays involving plant-derived and synthetic compounds, mechanisms of action of the compound on both NanH and SiaPg, in vivo infection assays using Zebrafish or Mice as well as investigating the expression of TLRs by H357 cells, which would have given this research a wholistic view.

6.3   Recommendations and Future Work:

1. The role of sialic acid-mediated mechanisms in enhancing subversion of host innate immune responses in relation to Siglec interactions with sialidases of *T. forsythia* and *P. gingivalis* needs to be investigated.

   Sialic acids are known to be found on the surfaces of the terminal residue of cell surface glycans. On the other hand, Sialic acid-binding immunoglobulins (Ig) like-lectins (Siglecs), are shown to be expressed on surfaces of various immune cells such as macrophages and neutrophils and are involved in a variety of cellular functions including inhibitory, cell signaling and cell-cell interactions (ITIMs), etc. Furthermore, some human pathogens are shown to express sialic acids which are recognized by several Siglecs (Crocker et al., 2007). Siglec-dependent recognition of these pathogens may promote association with the immune cells thereby playing an important role in subverting the host's innate immune responses (Khatua et al., 2013). Investigating the role of NanH and SiaPg in promoting the subversion of the host's immunity by *T. forsythia* and *P. gingivalis* is therefore recommended to be looked at.

2. The mechanism of interactions between sialidases of *T. forsythia* and *P. gingivalis* with host TLRs (pathogen-TLR binding) leading to modulation of host immune responses in the presence of 2e3aDFNeu5Ac9N3 should be investigated.

   Sialic acids are found scattered on the surfaces of host innate immune cells like the macrophages, dendritic cells (DCs), and epithelial cells (Lewis & Lewis, 2012). The host's innate immune system detects the presence of invading microbes through the pathogen recognition receptors (PRRs) such as the Toll-like receptors (TLRs) (Kawai & Akira, 2010). These TLRs are reported to be expressed on cell surfaces, lysosomes, endosomes, or cytoplasm and are involved in inducing inflammatory responses as well as activating some specific signaling pathways that can lead to the expression of genes that inform immune responses to microbes or any other pathogen-associated molecular patterns (PAMPs) (Kawai & Akira, 2010 and Yuk & Jo, 2011). Investigating the role of the sialidases of *T. forsythia* and *P. gingivalis* in activating Toll-like receptors (TLRs)-dependent pathways in the presence or absence of the sialidase inhibitor 2e3aDFNeu5Ac9N3 to see if it can act as an inhibitor of TLRs is also recommended.

3. Polymicrobial infection and *in vivo* determination of cytotoxicity of the sialidase inhibitors using the Zebrafish model for *in vivo* discovery of novel antimicrobials (drug discovery).

   The Zebrafish model for research in biomedical sciences developed by Streisinger and colleagues has numerous advantages over other animal models like laboratory mice, pigs, dogs, etc. used in modelling human diseases (Streisinger et al., 1981 and Choi et al., 2021). A recent review also reported the use of Zebrafish as an *in vivo* model for screening novel drug compounds and testing for drug toxicity (Cassar et al., 2020), furthermore, the use of Zebrafish as a model to investigate single species and polymicrobial infection has been established (Farrugia et al., 2022). With the promising *in vitro* activity of the sialidase inhibitor, 2e3aDFNeu5Ac9N3 observed in this study on the sialidases of *T. forsythia and P. gingivalis* and its role in abrogating pro-inflammatory cytokines, an *in vivo* assay are needed to investigate polymicrobial infection (periodontitis) in the presence or absence of the compound as well as, to determine its toxicity using an animal model.

However, due to time constraint caused by Covid-19 pandemic, inhibition of attachment and invasion (Antibiotic protection assay) of the oral epithelial cells (H357) by 2e3aDFNeu5Ac9N3 at a higher concentration and the recommended assays were not achieved. It will be great to look at this in the future.

6.4   Doctoral Development Programme (DDP)

At the course of my PhD research, I undertook some trainings and courses geared at developing me into a better researcher and these includes;

Trainings:
i.   Attended training on Data Protection and Confidentiality held on 25th February 2019 at the Hicks Building, Room K14
ii.   Attended training on How to write a successful Grant Application on 22nd March 2019 at Barber House Board Room: This interactive session gave me an opportunity to experience the difficulties faced by Grant Committee Members and also how one can present his grant application to influence its chance of success via real life examples with a mock panel discussion session.
iii.   Trained on how to become an Effective Secretary organized by the Student Union Government on 1st May 2019 at Gallery Room 2, SU Building.
iv.   Attended a training on Maya Software Session 14th June 2019 at Seminar Room 3, SoCD
v.   Attended training on RStudio Software Session on 5th July 2019
vi.   Attended ChemDraw Software Session organized by DSRS
vii.   Attended Training on How to be an International and EU Student Ambassador on 28th November 2019 at John Carr Design Suite, Portobello Centre.
viii.   Attended a Training on How to use Turnitin on 26th November 2019 at LT3 Medical School.
ix.   Sheffield Teaching Assistant Workshops on;
 - Research Ethics and Integrity
 - Assessment and Feedback
 - Lecturing
 - Laboratory Demonstration
 - Introduction to being a Graduate Teaching Assistant (GTA)
 - Teaching Design and Delivery
 - Research Supervision
 - Seminar Facilitation
 - Setting Boundaries

Teaching, Research and GTA roles: I have been involved in teaching, administration, and research across undergraduate and postgraduate programmes.

 - **Module Facilitator**: Research, Ethics and Integrity Module for Doctoral Development Program (2021/2022): Faculty of Medicine, Dentistry and Health, The University of Sheffield, United Kingdom.

Responsibilities:
i.   Facilitated discussions with a group of 15-20 students on Research Ethics and Integrity (via Blackboard collaborate, Current Communities and Google meet).
ii.   Assessed and gave feedback to participants (via Turnitin or Email).

 - **GTA roles**:

Responsibilities:

    iii.   Assisted undergraduate students on placement and Masters' students with experimental procedures and data analysis

    iv.   Involved in Laboratory demonstration together with my Supervisors for Bachelor of Dental Sciences (BDS)

    v.   Assessed and gave feedback to students.

    vi.   Engaged with prospective students during PhD Open Day

Seminars, Webinars and Conferences Attended:

i.   Early Career Microbiologists (ECM) Forum Summer Conference 2022: Organizing, Oral Presentation and Chairing sessions 12th to 13th July, 2022

ii.   Oral Microbiology and Immunology Group (OMiG) ECR/PGR Symposium 30th June- 1st July, 2022 at Birmingham: Oral Presentation

iii.   Microbiology Society Annual Conference 4th to 7th April, 2022 at Belfast International Conference Centre: Poster Presentation

iv.   Forsyth Institute Scientific Symposium: Oral Microbiome Beyond Bacteria 28th October, 2021: Poster Presentation

v.   European Oral Microbiology Workshop (EOMW2021) 27th to 28th May, 2021: Poster Presentation

vi.   Microbiology Society Annual Conference 26th to 30th April, 2021: Poster Presentation

vii.   Oral Microbiology and Immunology Group (OMiG) PGR Symposium 26th March, 2021: Poster Presentation

viii.   School of Clinical Dentistry Annual Research Meeting 18th to 19th March, 2021: Poster Presentation

ix.   Early Career Microbiologists (ECM) Online Forum 2021: Presenting and Networking Online 16th March, 2021

x.   Multidisciplinary Approach to Antimicrobial Resistance (AMR): Bench to Bedside and beyond 30th Nov., to 4th December, 2020

xi.   Forsyth Science Symposium 28th October, 2020

xii.   Sheffield Microbiomics Symposium 17th September, 2020

xiii.   Microbiology Society Early Career Microbiologists (ECM) Forum 16th-17th July 2020: Poster on Testing for Novel Inhibitors of Periodontitis-Associated Sialidases.

xiv.   Biofilms in Health and Diseases Webinar: Cardiff University (CITER) 24th June 2020

xv.   1st year Talk on Investigating Novel Sialidase Inhibitors: School of Clinical Dentistry Annual Postgraduate Symposium 17th June 2020

xvi.   Social Biofilm Network (SBN) Online Conference: University of Washington USA 1-5th June 2020

xvii.   BioRender Webinar: Top Tips for a Winning Graphical Abstract 28th May 2020.

xviii.   School of Clinical Dentistry Annual Postgraduate Research 28-29th March 2019.

xix.   The Oral Microbiology and Immunology Group (OMiG) PGR Prize Symposium: 21st February 2019 at The Newcastle University, United Kingdom.

Scholarships, Grants, Awards and Honours

❖ Access Microbiology "Most Promising Science Poster Prize" Winner 2022.

- ❖ Letter of Appreciation from the Grants and Professional Development, Microbiology Society, UK, for my Role as ECM co-Chair of Public Health Microbiology Session at the Annual Conference 2021.
- ❖ Microbiology Society United Kingdom Grant (GA002048) 2020

Leadership Roles

- ❖ Early Career Microbiologist (ECM) Forum Representative in the Scientific Conferences Panel, Microbiology Society, United Kingdom 2021/2022.
- ❖ Councillor Representing School of Clinical Dentistry, University of Sheffield Students Union Government 2020/2021.
- ❖ Elections Committee Member Sheffield Students Union 2020/2021.
- ❖ International Student Ambassador for Africa and Middle East, University of Sheffield, United Kingdom 2019/2020 and 2020/2021.
- ❖ Secretary, Nigeria Society, University of Sheffield, United Kingdom 2019/2020.
- ❖ Social Media Secretary, Dental Society Research Students (DSRS) University of Sheffield, United Kingdom 2019/2020.

Service to Public and Academic Communities

- ❖ Organizing Committee Member for Early Career Microbiologists Summer Conference 12th-13th July, 2022 at University of Sheffield, United Kingdom.
- ❖ Editorial Board Member for Microbiology Today Magazine: Microbiology Society January 2022 to December 2024.
- ❖ Early Career Microbiologist Forum Scientific Conferences Executive Committee Member: Microbiology Society September 2021 till date.
- ❖ **Co-Chair** for Public Health Microbiology Session at Microbiology Society Annual Conference 26th-30th April, 2021.
- ❖ **Panelist:** 2020 Microbiology Essay Competition: How can Microbiology improve lives and livelihood in Nigeria? Essay Competition - R-BRIDGE

Volunteering and Responsibilities:
i. Peer reviewer: Journal of Access Microbiology   July 2022
ii. I became Students Representative (General Secretary Nigerian Society and Social Media and Communication Secretary DSRS)
iii. Assisted my Supervisor Prof. Graham in conducting practical for undergraduates Dental Students on 26th June 2019.
iv. Participated at the International Cultural Evening (ICE) held on 23rd March 2019 at the Sheffield City Hall
v. Helped in speaking to people during the World Food Festival Day held on 4th May 2019 at the SU Building
vi. I chaired the iBio Journal Club session of 4th November 2019.

Membership of Professional bodies
i. Member Microbiology Society (UK)
ii. Member American Society of Microbiology
iii. Member British Oral Microbiology and Immunology Group (OMiG).

iv.   Member Nigerian Society of Microbiology
v.   Associate Fellow of Higher Education Academy (AFHEA)

6.5 Publications/Blog Post Arising due to Work Performed As Part of This Project

i.   Palmatine and Berberine chloride synergistically Inhibit NanH sialidase of *Tannerella forsythia.* **P. R. Galleh**[1,2], D. W. Lambert[1], G. P. Stafford[1] *Access Microbiology Journal https://doi.org/10.1099/acmi.ac2021.po0337* (Published Abstract) 27 May 2022.

ii.   Testing for Novel Inhibitors of Periodontitis-Associated Sialidases
Galleh, P.R[*1'2], Chen, X[3], Lambert, D.W[1] and Stafford G.P[1]
Access Microbiology Journal https://doi.org/10.1099/acmi.ac2020.po0070 (Published Poster) 10 July 2020.

iii.   Sialidase of *Tannerella forsythia* Upregulates Pro-inflammatory cytokines and is inhibited by- di-fluoro sialic acid 2e3aDFNeu5Ac9N[3] **Galleh, P.R.*[1]**, Chen, X[2], Santra, A[2], Lambert, D.W[1] and Stafford G.P[1] *Microbiology Society News:* Most Promising Science Poster Prize 2022: Access Microbiology | Microbiology Society

iv.   Periodontitis: The Irreversible Gum Disease: **Galleh Peter Raphael**. Microbiology Society (Blog Post) 24th/9/2020 Periodontitis: the irreversible gum disease | Microbiology Society

Bibliography

Akira, S., Takeda, K., & Kaisho, T. (2001). Toll-like receptors: critical proteins linking innate and acquired immunity. *Nature Publishing Group*. http://immunol.nature.com

Ali, D., & Ali, H. (2014). Assessment of DNA damage and cytotoxicity of palmatine on human skin epithelial carcinoma cells. *Toxicological and Environmental Chemistry*, *96*(6), 941–950. https://doi.org/10.1080/02772248.2014.987510

Amano, A. (2003). Molecular Interaction of *Porphyromonas gingivalis* with Host Cells: Implication for the Microbial Pathogenesis of Periodontal Disease . *Journal of Periodontology*, *74*(1), 90–96. https://doi.org/10.1902/jop.2003.74.1.90

Amith, S. R., Jayanth, P., Franchuk, S., Finlay, T., Seyrantepe, V., Beyaert, R., Pshezhetsky, A. V., & Szewczuk, M. R. (2010). Neu1 desialylation of sialyl α-2,3-linked β-galactosyl residues of TOLL-like receptor 4 is essential for receptor activation and cellular signaling. *Cellular Signalling*. https://doi.org/10.1016/j.cellsig.2009.09.038

Amith, Schammim R., Jayanth, P., Finlay, T., Franchuk, S., Gilmour, A., Abdulkhalek, S., & Szewczuk, M. R. (2010). Detection of Neu1 sialidase activity in regulating TOLL-like receptor activation. *Journal of Visualized Experiments*. https://doi.org/10.3791/2142

Amith, Schammim Ray, Jayanth, P., Franchuk, S., Siddiqui, S., Seyrantepe, V., Gee, K., Basta, S., Beyaert, R., Pshezhetsky, A. V., & Szewczuk, M. R. (2009). Dependence of pathogen molecule-induced Toll-like receptor activation and cell function on Neu1 sialidase. *Glycoconjugate Journal*. https://doi.org/10.1007/s10719-009-9239-8

Angata, T., & Varki, A. (2002). Chemical diversity in the sialic acids and related α-keto acids: An evolutionary perspective. *Chemical Reviews*. https://doi.org/10.1021/cr000407m

Armbruster, C. R., & Parsek, M. R. (2018). New insight into the early stages of biofilm formation. *Proceedings of the National Academy of Sciences*. https://doi.org/10.1073/pnas.1804084115

Arnaout, M. A., Mahalingam, B., & Xiong, J.-P. (2005). INTEGRIN STRUCTURE, ALLOSTERY, AND BIDIRECTIONAL SIGNALING. *Annual Review of Cell and Developmental Biology*. https://doi.org/10.1146/annurev.cellbio.21.090704.151217

Aruni, W., Vanterpool, E., Osbourne, D., Roy, F., Muthiah, A., Dou, Y., & Fletcher, H. M. (2011). Sialidase and sialoglycoproteases can modulate virulence in *Porphyromonas gingivalis*. *Infection and Immunity*. https://doi.org/10.1128/IAI.00106-11

Assailly, C., Bridot, C., Saumonneau, A., Lottin, P., Roubinet, B., Krammer, E. M., François, F., Vena, F., Landemarre, L., Alvarez Dorta, D., Deniaud, D., Grandjean, C., Tellier, C., Pascual, S., Montembault, V., Fontaine, L., Daligault, F., Bouckaert, J., & Gouin, S. G. (2021). Polyvalent Transition-State Analogues of Sialyl Substrates Strongly Inhibit Bacterial Sialidases**. *Chemistry - A European Journal*, *27*(9), 3142–3150. https://doi.org/10.1002/chem.202004672.

Avril, T., Wagner, E. R., Willison, H. J., & Crocker, P. R. (2006). Sialic acid-binding immunoglobulin-like lectin 7 mediates selective recognition of sialylated glycans expressed on

Campylobacter jejuni lipooligosaccharides. *Infection and Immunity*. https://doi.org/10.1128/IAI.02094-05

Babich H, Krupka ME, Nissim HA, Zuckerbraun HL. Differential in vitro cytotoxicity of (-)-epicatechin gallate (ECG) to cancer and normal cells from the human oral cavity. Toxicol In Vitro. 2005 Mar;19(2):231-42. doi: 10.1016/j.tiv.2004.09.001. PMID: 15649637.

Balkrishna, A., Pokhrel, S., Tomer, M., Verma, S., Kumar, A., Nain, P., Gupta, A., & Varshney, A. (2019). Anti-acetylcholinesterase activities of mono-herbal extracts and exhibited synergistic effects of the phytoconstituents: A biochemical and computational study. *Molecules*. https://doi.org/10.3390/molecules24224175

Barczyk, M., Carracedo, S., & Gullberg, D. (2010). Integrins. In *Cell and Tissue Research*. https://doi.org/10.1007/s00441-009-0834-6

Blaum, B. S., Hannan, J. P., Herbert, A. P., Kavanagh, D., Uhrín, D., & Stehle, T. (2015). Structural basis for sialic acid-mediated self-recognition by complement factor H. *Nature Chemical Biology*. https://doi.org/10.1038/nchembio.1696

Blevins, L. K., Wren, J. T., Oliver, M. B., Alexander-Miller, M. A., Wozniak, J. E., Pang, B., Basu Roy, A., Reimche, J. L., & Swords, W. E. (2017). Pneumococcal Neuraminidase A (NanA) Promotes Biofilm Formation and Synergizes with Influenza A Virus in Nasal Colonization and Middle Ear Infection. *Infection and Immunity*, *85*(4), 1–10. https://doi.org/10.1128/iai.01044-16

Bloch, S., Thurnheer, T., Murakami, Y., Belibasakis, G. N., & Schäffer, C. (2017). Behavior of two *Tannerella forsythia* strains and their cell surface mutants in multispecies oral biofilms. *Molecular Oral Microbiology*, *32*(5). https://doi.org/10.1111/omi.12182

Boncler, M., Rózalski, M., Krajewska, U., Podswdek, A., & Watala, C. (2014). Comparison of PrestoBlue and MTT assays of cellular viability in the assessment of anti-proliferative effects of plant extracts on human endothelial cells. *Journal of Pharmacological and Toxicological Methods*, *69*(1), 9–16. https://doi.org/10.1016/j.vascn.2013.09.003

Bostanci, N., & Belibasakis, G. N. (2012). *Porphyromonas gingivalis*: An invasive and evasive opportunistic oral pathogen. In *FEMS Microbiology Letters*. https://doi.org/10.1111/j.1574-6968.2012.02579.x

Bourgeois, D., Inquimbert, C., Ottolenghi, L., & Carrouel, F. (2019). Periodontal pathogens as risk factors of cardiovascular diseases, diabetes, rheumatoid arthritis, cancer, and chronic obstructive pulmonary disease—is there cause for consideration? In *Microorganisms* (Vol. 7, Issue 10). https://doi.org/10.3390/microorganisms7100424

Bowen, W. H., Burne, R. A., Wu, H., & Koo, H. (2018). Oral Biofilms: Pathogens, Matrix, and Polymicrobial Interactions in Microenvironments. In *Trends in Microbiology*. https://doi.org/10.1016/j.tim.2017.09.008

Bowles, W. H. D., & Gloster, T. M. (2021). Sialidase and Sialyltransferase Inhibitors: Targeting Pathogenicity and Disease. *Frontiers in Molecular Biosciences*, *8*(July), 1–10. https://doi.org/10.3389/fmolb.2021.705133

Boyle, J. (2008). Molecular biology of the cell, 5th edition by B. Alberts, A. Johnson, J. Lewis, M. Raff, K. Roberts, and P. Walter. *Biochemistry and Molecular Biology Education*, *36*(4), 317–318. https://doi.org/10.1002/bmb.20192.

Brear, P., Telford, J., Taylor, G. L., & Westwood, N. J. (2012). Synthesis and Structural Characterisation of Selective Non-Carbohydrate-Based Inhibitors of Bacterial Sialidases. *ChemBioChem*. https://doi.org/10.1002/cbic.201200433

Brunner, J., Scheres, N., El Idrissi, N. B., Deng, D. M., Laine, M. L., Van Winkelhoff, A. J., & Crielaard, W. (2010). The capsule of *Porphyromonas gingivalis* reduces the immune response of human gingival fibroblasts. *BMC Microbiology*. https://doi.org/10.1186/1471-2180-10-5

Buschiazzo, A., Amaya, M. F., & Alzari, P. (2000). Structural basis of sialyl-transferase activity in trypanosomal sialidases. *Acta Crystallographica Section A Foundations of Crystallography*. https://doi.org/10.1107/s0108767300025149

Caciotti, A., Di Rocco, M., Filocamo, M., Grossi, S., Traverso, F., D'Azzo, A., Cavicchi, C., Messeri, A., Guerrini, R., Zammarchi, E., Donati, M. A., & Morrone, A. (2009). Type II sialidosis: Review of the clinical spectrum and identification of a new splicing defect with chitotriosidase assessment in two patients. *Journal of Neurology*. https://doi.org/10.1007/s00415-009-5213-4

Cagnoni, A. J., Pérez Sáez, J. M., Rabinovich, G. A., & Mariño, K. V. (2016). Turning-off signaling by siglecs, selectins, and galectins: Chemical inhibition of glycan-dependent interactions in cancer. In *Frontiers in Oncology*. https://doi.org/10.3389/fonc.2016.00109

Cao, H., & Crocker, P. R. (2011). Evolution of CD33-related siglecs: Regulating host immune functions and escaping pathogen exploitation? *Immunology*. https://doi.org/10.1111/j.1365-2567.2010.03368.x

Carlin, A. F., Uchiyama, S., Chang, Y. C., Lewis, A. L., Nizet, V., & Varki, A. (2009). Molecular mimicry of host sialylated glycans allows a bacterial pathogen to engage neutrophil Siglec-9 and dampen the innate immune response. *Blood*. https://doi.org/10.1182/blood-2008-11-187302

Cassar, S., Adatto, I., Freeman, J. L., Gamse, J. T., Iturria, I., Lawrence, C., Muriana, A., Peterson, R. T., Van Cruchten, S., & Zon, L. I. (2020). Use of Zebrafish in Drug Discovery Toxicology. *Chemical Research in Toxicology*, *33*(1), 95–118. https://doi.org/10.1021/acs.chemrestox.9b00335

Cekici, A., Kantarci, A., Hasturk, H., & Van Dyke, T. E. (2014). Inflammatory and immune pathways in the pathogenesis of periodontal disease. *Periodontology 2000*. https://doi.org/10.1111/prd.12002

Chen, G. Y., Chen, X., King, S., Cavassani, K. A., Cheng, J., Zheng, X., Cao, H., Yu, H., Qu, J., Fang, D., Wu, W., Bai, X. F., Liu, J. Q., Woodiga, S. A., Chen, C., Sun, L., Hogaboam, C. M., Kunkel, S. L., Zheng, P., & Liu, Y. (2011). Amelioration of sepsis by inhibiting sialidase-mediated disruption of the CD24-SiglecG interaction. *Nature Biotechnology*. https://doi.org/10.1038/nbt.1846

Chen, G. Y., Tang, J., Zheng, P., & Liu, Y. (2009). CD24 and siglec-10 selectively repress tissue damage - Induced immune responses. *Science*. https://doi.org/10.1126/science.1168988

Chen, G.-Y., Brown, N. K., Wu, W., Khedri, Z., Yu, H., Chen, X., van de Vlekkert, D., D'Azzo, A., Zheng, P., & Liu, Y. (2014). Broad and direct interaction between TLR and Siglec families of pattern recognition receptors and its regulation by Neu1. *ELife*. https://doi.org/10.7554/elife.04066

Chinthamani, S., Settem, R. P., Honma, K., Kay, J. G., & Sharma, A. (2017). Macrophage inducible C-type lectin (Mincle) recognizes glycosylated surface (S)-layer of the periodontal pathogen Tannerella forsythia. *PLoS ONE*. https://doi.org/10.1371/journal.pone.0173394

Chiodelli, P., Urbinati, C., Mitola, S., Tanghetti, E., & Rusnati, M. (2012). Sialic acid associated with αvβ3 integrin mediates HIV-1 Tat protein interaction and endothelial cell proangiogenic activation. *Journal of Biological Chemistry*. https://doi.org/10.1074/jbc.M111.337139

Choe, J., Kelker, M. S., & Wilson, I. A. (2005). Structural biology: Crystal structure of human toll-like receptor 3 (TLR3) ectodomain. *Science*. https://doi.org/10.1126/science.1115253

Choi, T. Y., Choi, T. I., Lee, Y. R., Choe, S. K., & Kim, C. H. (2021). Zebrafish as an animal model for biomedical research. *Experimental and Molecular Medicine*, *53*(3), 310–317. https://doi.org/10.1038/s12276-021-00571-5

Chou, T. C. (2008). Preclinical versus clinical drug combination studies. *Leukemia and Lymphoma*, *49*(11), 2059–2080. https://doi.org/10.1080/10428190802353591

Chung, L. Y., Cheung, T. C., Kong, S. K., Fung, K. P., Choy, Y. M., Chan, Z. Y., & Kwok, T. T. (2001). Induction of apoptosis by green tea catechins in human prostate cancer DU145 cells. *Life Sciences*, *68*(10), 1207–1214. https://doi.org/10.1016/S0024-3205(00)01020-1

Corfield, T. (1992). Bacterial sialidases - roles in pathogenicity and nutrition. In *Glycobiology*. https://doi.org/10.1093/glycob/2.6.509

Cornish-Bowden, A. (1999). Fundamentals of Enzyme Kinetics. *Portland Press*

Crocker, P. R., & Varki, A. (2001). Siglecs, sialic acids and innate immunity. *Trends in Immunology*. https://doi.org/10.1016/S1471-4906(01)01930-5.

Crocker, P. R., Paulson, J. C., & Varki, A. (2007). Siglecs and their roles in the immune system. In *Nature Reviews Immunology*. https://doi.org/10.1038/nri2056

Cross, B. W., & Ruhl, S. (2018). Glycan recognition at the saliva – oral microbiome interface. In *Cellular Immunology*. https://doi.org/10.1016/j.cellimm.2018.08.008

Dong, C., Davis, R. J., & Flavell, R. A. (2002). MAP kinases in the immune response. *Annual Review of Immunology*, *20*, 55–72. https://doi.org/10.1146/annurev.immunol.20.091301.131133

Dong, W., Jiang, Y., Zhu, Z., Zhu, J., Li, Y., Xia, R., & Zhou, K. (2023). Structural and enzymatic characterization of the sialidase SiaPG from *Porphyromonas gingivalis* research communications. 1–8. https://doi.org/10.1107/S2053230X23001735

Douglas, C. W. I., Naylor, K., Phansopa, C., Frey, A. M., Farmilo, T., & Stafford, G. P. (2014). Advances in Bacterial Pathogen Biology. In *Advances in Microbial Physiology* (Vol. 65). https://doi.org/10.1016/bs.ampbs.2014.08.005

Drent, M., Cobben, N. A. M., Henderson, R. F., Wouters, E. F. M., & Van Dieijen-Visser, M. (1996). Usefulness of lactate dehydrogenase and its isoenzymes as indicators of lung damage or inflammation. *European Respiratory Journal*, *9*(8), 1736–1742. https://doi.org/10.1183/09031936.96.09081736

Eke, P. I., Dye, B. A., Wei, L., Thornton-Evans, G. O., & Genco, R. J. (2012). Prevalence of periodontitis in adults in the united states: 2009 and 2010. *Journal of Dental Research*. https://doi.org/10.1177/0022034512457373

Ellamurugan, N. (2013). Periodontitis and Rheumatoid arthritis – A Review. *IOSR Journal of Dental and Medical Sciences*. https://doi.org/10.9790/0853-104102105

Emingil, G., Atilla, G., Başkesen, A., & Berdeli, A. (2005). Gingival crevicular fluid EMAP-II, MIP-1α and MIP-1β levels of patients with periodontal disease. *Journal of Clinical Periodontology*, *32*(8), 880–885. https://doi.org/10.1111/j.1600-051X.2005.00780.x

Enersen, M., Nakano, K., & Amano, A. (2013). *Porphyromonas gingivalis* fimbriae. *Journal of Oral Microbiology*. https://doi.org/10.3402/jom.v5i0.20265

etTadashi Gomi, M. T. (2002). NII-Electronic Library Service. *Chemical Pharmaceutical Bulletin*, *43*, 2091. http://www.mendeley.com/research/geology-volcanic-history-eruptive-style-yakedake-volcano-group-central-japan/

Farrugia, C., Stafford, G. P., Gains, A. F., Cutts, A. R., & Murdoch, C. (2022). Fusobacterium nucleatum mediates endothelial damage and increased permeability following single species and polymicrobial infection. *Journal of Periodontology*, *93*(9), 1421–1433. https://doi.org/10.1002/JPER.21-0671

Flemming, H. C., Wingender, J., Szewzyk, U., Steinberg, P., Rice, S. A., & Kjelleberg, S. (2016). Biofilms: An emergent form of bacterial life. *Nature Reviews Microbiology*, *14*(9), 563–575. https://doi.org/10.1038/nrmicro.2016.94

Frenkel, E. S., & Ribbeck, K. (2015). Salivary mucins in host defense and disease prevention. *Journal of Oral Microbiology*. https://doi.org/10.3402/jom.v7.29759

Frey, A. M., Satur, M. J., Phansopa, C., Honma, K., Urbanowicz, P. A., Spencer, D. I. R., Pratten, J., Bradshaw, D., Sharma, A., & Stafford, G. (2019). Characterization of *Porphyromonas gingivalis* sialidase and disruption of its role in host–pathogen interactions. *Microbiology*. https://doi.org/10.1099/mic.0.000851

Frey, A. M., Satur, M. J., Phansopa, C., Parker, J. L., Bradshaw, D., Pratten, J., & Stafford, G. P. (2018). Evidence for a carbohydrate-binding module (CBM) of *Tannerella forsythia* NanH sialidase, key to interactions at the host–pathogen interface. *Biochemical Journal*. https://doi.org/10.1042/BCJ20170592

Friedrich, V., Janesch, B., Windwarder, M., Maresch, D., Braun, M. L., Megson, Z. A., Vinogradov, E., Goneau, M. F., Sharma, A., Altmann, F., Messner, P., Schoenhofen, I. C., & Schäffer, C.

(2017). *Tannerella forsythia* strains display different cell-surface nonulosonic acids: Biosynthetic pathway characterization and first insight into biological implications. *Glycobiology*. https://doi.org/10.1093/glycob/cww129

Goon, S., Kelly, J. F., Logan, S. M., Ewing, C. P., & Guerry, P. (2003). Pseudaminic acid, the major modification on *Campylobacter flagellin*, is synthesized via the Cj1293 gene. *Molecular Microbiology*. https://doi.org/10.1046/j.1365-2958.2003.03725.x

Govinden, G., Parker, J. L., Naylor, K. L., Frey, A. M., Anumba, D. O. C., & Stafford, G. P. (2018). Inhibition of sialidase activity and cellular invasion by the bacterial vaginosis pathogen *Gardnerella vaginalis*. *Archives of Microbiology*. https://doi.org/10.1007/s00203-018-1520-4

Gu, J., Isaji, T., Sato, Y., Kariya, Y., & Fukuda, T. (2009). Importance of N-glycosylation on α5β1 integrin for its biological functions. *Biological and Pharmaceutical Bulletin*. https://doi.org/10.1248/bpb.32.780

Guerrero, A., Griffiths, G. S., Nibali, L., Suvan, J., Moles, D. R., Laurell, L., & Tonetti, M. S. (2005). Adjunctive benefits of systemic amoxicillin and metronidazole in non-surgical treatment of generalized aggressive periodontitis: A randomized placebo-controlled clinical trial. *Journal of Clinical Periodontology*. https://doi.org/10.1111/j.1600-051X.2005.00814.x

Guo, Y., Nguyen, K. A., & Potempa, J. (2010). Dichotomy of gingipains action as virulence factors: From cleaving substrates with the precision of a surgeon's knife to a meat chopper-like brutal degradation of proteins. *Periodontology 2000*. https://doi.org/10.1111/j.1600-0757.2010.00377.x

Haines-menges, B. L., Whitaker, W. B., Lubin, J. B., & Boyd, E. F. (2015). Host Sialic Acids: A Delicacy for the Pathogen with Discerning Taste. In *Metabolism and Bacterial Pathogenesis*. https://doi.org/10.1128/microbiolspec.mbp-0005-2014

Hasebe, A., Yoshimura, A., Into, T., Kataoka, H., Tanaka, S., Arakawa, S., Ishikura, H., Golenbock, D. T., Sugaya, T., Tsuchida, N., Kawanami, M., Hara, Y., & Shibata, K. I. (2004). Biological Activities of *Bacteroides forsythus* Lipoproteins and Their Possible Pathological Roles in Periodontal Disease. *Infection and Immunity*. https://doi.org/10.1128/IAI.72.3.1318-1325.2004

Hashimoto, T., Kumazawa, S., Nanjo, F., Hara, Y., & Nakayama, T. (1999). Interaction of tea catechins with lipid bilayers investigated with liposome systems. *Bioscience, Biotechnology and Biochemistry*. https://doi.org/10.1271/bbb.63.2252

Hayashi, F., Smith, K. D., Ozinsky, A., Hawn, T. R., Yi, E. C., Goodlett, D. R., Eng, J. K., Akira, S., Underhill, D. M., & Aderem, A. (2001). The innate immune response to bacterial flagellin is mediated by Toll-like receptor 5. *Nature*. https://doi.org/10.1038/35074106

Hemmi, H., Takeuchi, O., Kawai, T., Kaisho, T., Sato, S., Sanjo, H., Matsumoto, M., Hoshino, K., Wagner, H., Takeda, K., & Akira, S. (2000). A Toll-like receptor recognizes bacterial DNA.[In Process Citation]. *Nature*.

Herath, T., Wang, Y., Seneviratne, C., Darveau, R., Wang, C., & Jin, L. (2011). Heterogeneous LPS of *Porphyromonas gingivalis* differentially modulate the innate immune response of human gingiva. *BMC Proceedings*. https://doi.org/10.1186/1753-6561-5-s1-p86

Holt, S. C., Kesavalu, L., Walker, S., & Genco, C. A. (1999). Virulence factors of *Porphyromonas gingivalis*. *Periodontology 2000*. https://doi.org/10.1111/j.1600-0757.1999.tb00162.x

Hong, J., Lu, H., Meng, X., Ryu, J. H., Hara, Y., & Yang, C. S. (2002). Stability, cellular uptake, biotransformation, and efflux of tea polyphenol (-)-epigallocatechin-3-gallate in HT-29 human colon adenocarcinoma cells. *Cancer Research*.

Honma, K., Mishima, E., & Sharma, A. (2011). Role of *Tannerella forsythia* nanh sialidase in epithelial cell attachment. *Infection and Immunity*, *79*(1), 393–401. https://doi.org/10.1128/IAI.00629-10

Honma, K., Ruscitto, A., & Sharma, A. (2018). ß-Glucanase activity of the oral bacterium *Tannerella forsythia* contributes to the growth of a partner species, *Fusobacterium nucleatum*, in cobiofilms. *Applied and Environmental Microbiology*. https://doi.org/10.1128/AEM.01759-17

How, K. Y., Song, K. P., & Chan, K. G. (2016). *Porphyromonas gingivalis*: An overview of periodontopathic pathogen below the gum line. In *Frontiers in Microbiology*. https://doi.org/10.3389/fmicb.2016.00053

Huang, Z., & Kraus, V. B. (2016). Does lipopolysaccharide-mediated inflammation have a role in OA? In *Nature Reviews Rheumatology*. https://doi.org/10.1038/nrrheum.2015.158

Hughes, C. V., Malki, G., Loo, C. Y., Tanner, A. C. R., & Ganeshkumar, N. (2003). Cloning and expression of α-D-glucosidase and N-acetyl-β -glucosaminidase from the periodontal pathogen, *Tannerella forsythensis* (*Bacteroides forsythus*). *Oral Microbiology and Immunology*. https://doi.org/10.1034/j.1399-302X.2003.00091.x

Hyeong-U, S., Eun-Kyeong, Y., Chi-Yeol, Y., Chul-Hong, P., Myung-Ae, B., Tae-Ho, K., Chang Hyung, L., Won Lee, K., Seo, H., Kyung-Jin, K., & Sang-Han, L. (2019). Effects of synergistic inhibition on α-glucosidase by phytoalexins in soybeans. *Biomolecules*. https://doi.org/10.3390/biom9120828

Iijima, R., Takahashi, H., Namme, R., Ikegami, S., & Yamazaki, M. (2004). Novel biological function of sialic acid (N-acetylneuraminic acid) as a hydrogen peroxide scavenger. *FEBS Letters*, *561*(1–3), 163–166. https://doi.org/10.1016/S0014-5793(04)00164-4

Inaba, H., Nomura, R., Kato, Y., Takeuchi, H., Amano, A., Asai, F., Nakano, K., Lamont, R. J., & Matsumoto-Nakano, M. (2019). Adhesion and invasion of gingival epithelial cells by *Porphyromonas gulae*. *PLoS ONE*, *14*(3), 1–16. https://doi.org/10.1371/journal.pone.0213309

Itzstein, M. Von, & Thomson, R. (2009). Anti-influenza drugs: The development of sialidase inhibitors. In *Handbook of Experimental Pharmacology*. https://doi.org/10.1007/978-3-540-79086-0_5

Iwaki, Y., Matsunaga, E., Takegawa, K., Sato, C., & Kitajima, K. (2020). Identification and characterization of a novel, versatile sialidase from a *Sphingobacterium* that can hydrolyze the glycosides of any sialic acid species at neutral pH. *Biochemical and Biophysical Research Communications*, *523*(2), 487–492. https://doi.org/10.1016/j.bbrc.2019.12.079

Iwasaki, M., Taylor, G. W., Awano, S., Yoshida, A., Kataoka, S., Ansai, T., & Nakamura, H. (2018). Periodontal disease and pneumonia mortality in haemodialysis patients: A 7-year cohort study. *Journal of Clinical Periodontology*. https://doi.org/10.1111/jcpe.12828

John W. Pelley (2012). Enzymes and Energetics. *Elsevier's Integrated Reviews Biochemistry (Second Edition)*.

Jotwani, R., & Cutler, C. W. (2004). Fimbriated *Porphyromonas gingivalis* Is More Efficient than Fimbria-Deficient *P. gingivalis* in Entering Human Dendritic Cells in Vitro and Induces An Inflammatory Th1 Effector Response. *Infection and Immunity*. https://doi.org/10.1128/IAI.72.3.1725-1732.2004

Jotwani, R., Eswaran, S. V. K., Moonga, S., & Cutler, C. W. (2010). MMP-9/TIMP-1 imbalance induced in human dendritic cells by *Porphyromonas gingivalis*. *FEMS Immunology and Medical Microbiology*. https://doi.org/10.1111/j.1574-695X.2009.00637.x

Juge, N., Tailford, L., & Owen, C. D. (2016). Sialidases from gut bacteria: A mini-review. *Biochemical Society Transactions*, *44*. https://doi.org/10.1042/BST20150226

Kaja, S., Payne, A. J., Singh, T., Ghuman, J. K., Sieck, E. G., & Koulen, P. (2015). An optimized lactate dehydrogenase release assay for screening of drug candidates in neuroscience. *Journal of Pharmacological and Toxicological Methods*, *73*, 1–6. https://doi.org/10.1016/j.vascn.2015.02.001

Karagodin, V. P., Sukhorukov, V. N., Myasoedova, V. A., Grechko, A. V., & Orekhov, A. N. (2018). Diagnostics and Therapy of Human Diseases - Focus on Sialidases. *Current Pharmaceutical Design*. https://doi.org/10.2174/1381612824666180910125051

Karhadkar, T. R., Pilling, D., Cox, N., & Gomer, R. H. (2017). Sialidase inhibitors attenuate pulmonary fibrosis in a mouse model. *Scientific Reports*. https://doi.org/10.1038/s41598-017-15198-8

Kariu, T., Nakao, R., Ikeda, T., Nakashima, K., Potempa, J., & Imamura, T. (2017). Inhibition of gingipains and *Porphyromonas gingivalis* growth and biofilm formation by prenyl flavonoids. *Journal of Periodontal Research*, *52*(1). https://doi.org/10.1111/jre.12372

Kawai, T., & Akira, S. (2010). The role of pattern-recognition receptors in innate immunity: Update on toll-like receptors. In *Nature Immunology*. https://doi.org/10.1038/ni.1863

Keil, J. M., Rafn, G. R., Turan, I. M., Aljohani, M. A., Sahebjam-Atabaki, R., & Sun, X. L. (2022). Sialidase Inhibitors with Different Mechanisms. *Journal of Medicinal Chemistry*. https://doi.org/10.1021/acs.jmedchem.2c01258

Khedri, Z., Li, Y., Cao, H., Qu, J., Yu, H., Muthana, M. M., & Chen, X. (2012). Synthesis of selective inhibitors against *V. cholerae* sialidase and human cytosolic sialidase NEU2. *Organic and Biomolecular Chemistry*. https://doi.org/10.1039/c2ob25335f

Kim, B. R., Park, J. Y., Jeong, H. J., Kwon, H. J., Park, S. J., Lee, I. C., Ryu, Y. B., & Lee, W. S. (2018). Design, synthesis, and evaluation of curcumin analogues as potential inhibitors of bacterial sialidase. *Journal of Enzyme Inhibition and Medicinal Chemistry*. https://doi.org/10.1080/14756366.2018.1488695

Kim, J. H., Ryu, Y. B., Lee, W. S., & Kim, Y. H. (2014). Neuraminidase inhibitory activities of quaternary isoquinoline alkaloids from Corydalis turtschaninovii rhizome. *Bioorganic and Medicinal Chemistry*. https://doi.org/10.1016/j.bmc.2014.09.004

Kumamoto, M., Sonda, T., Nagayama, K., & Tabata, M. (2001). Effects of pH and metal ions on antioxidative activities of catechins. *Bioscience, Biotechnology and Biochemistry*. https://doi.org/10.1271/bbb.65.126

Kumar, P., Nagarajan, A., & Uchil, P. D. (2018). Analysis of cell viability by the lactate dehydrogenase assay. *Cold Spring Harbor Protocols*, *2018*(6), 465–468. https://doi.org/10.1101/pdb.prot095497

Kuroiwa, A., Hisatsune, A., Isohama, Y., & Katsuki, H. (2009). Bacterial neuraminidase increases IL-8 production in lung epithelial cells via NF-κB-dependent pathway. *Biochemical and Biophysical Research Communications*, *379*(3). https://doi.org/10.1016/j.bbrc.2008.12.120

Lall, N., Henley-Smith, C. J., De Canha, M. N., Oosthuizen, C. B., & Berrington, D. (2013). Viability reagent, prestoblue, in comparison with other available reagents, utilized in cytotoxicity and antimicrobial assays. *International Journal of Microbiology*, *2013*, 1–5. https://doi.org/10.1155/2013/420601

Lamichhane, A., Azegami, T., & Kiyono, H. (2014). The mucosal immune system for vaccine development. In *Vaccine*. https://doi.org/10.1016/j.vaccine.2014.08.089

Lamont, R. J., Koo, H., & Hajishengallis, G. (2018). The oral microbiota: dynamic communities and host interactions. In *Nature Reviews Microbiology* (Vol. 16, Issue 12). https://doi.org/10.1038/s41579-018-0089-x

Larjava, H., Koivisto, L., Heino, J., & Häkkinen, L. (2014). Integrins in periodontal disease. In *Experimental Cell Research*. https://doi.org/10.1016/j.yexcr.2014.03.010

Latorre Uriza, C., Velosa-Porras, J., Roa, N. S., Quiñones Lara, S. M., Silva, J., Ruiz, A. J., & Escobar Arregoces, F. M. (2018). Periodontal Disease, Inflammatory Cytokines, and PGE2 in Pregnant Patients at Risk of Preterm Delivery: A Pilot Study. *Infectious Diseases in Obstetrics and Gynecology*, *2018*. https://doi.org/10.1155/2018/7027683

Lewis, A. L., & Lewis, W. G. (2012). Host sialoglycans and bacterial sialidases: a mucosal perspective. *Cellular microbiology*, *14*(8), 1174–1182. https://doi.org/10.1111/j.1462-5822.2012.01807.x

Li, C., Kurniyati, Hu, B., Bian, J., Sun, J., Zhang, W., Liu, J., Pan, Y., & Li, C. (2012). Abrogation of neuraminidase reduces biofilm formation, capsule biosynthesis, and virulence of *Porphyromonas gingivalis*. *Infection and Immunity*. https://doi.org/10.1128/IAI.05773-11

Li, J., & McClane, B. A. (2014). The sialidases of *Clostridium perfringens* type D strain CN3718 differ in their properties and sensitivities to inhibitors. *Applied and Environmental Microbiology*. https://doi.org/10.1128/AEM.03440-13

Li, W., Santra, A., Yu, H., Slack, T. J., Muthana, M. M., Shi, D., Liu, Y., & Chen, X. (2019). 9-Azido-9-deoxy-2,3-difluorosialic Acid as a Subnanomolar Inhibitor against Bacterial Sialidases. *Journal of Organic Chemistry*. https://doi.org/10.1021/acs.joc.9b00385

Li, X., Kolltveit, K. M., Tronstad, L., & Olsen, I. (2000). Systemic diseases caused by oral infection. In *Clinical Microbiology Reviews*. https://doi.org/10.1128/CMR.13.4.547-558.2000

Li, Y., & Chen, X. (2012). Sialic acid metabolism and sialyltransferases: Natural functions and applications. In *Applied Microbiology and Biotechnology*. https://doi.org/10.1007/s00253-012-4040-1

Liang, F., Seyrantepe, V., Landry, K., Ahmad, R., Ahmad, A., Stamatos, N. M., & Pshezhetsky, A. V. (2006). Monocyte differentiation up-regulates the expression of the lysosomal sialidase, Neu1, and triggers its targeting to the plasma membrane via major histocompatibility complex class II-positive compartments. *Journal of Biological Chemistry*. https://doi.org/10.1074/jbc.M605633200

Life Technologies Corporation. (2010). PrestoBlue™ Cell Viability Reagent Protocol. *Product Information Sheet*, *800*, 1–2. http://tools.thermofisher.com/content/sfs/manuals/PrestoBlue_Reagent_PIS_15Oct10.pdf

Lin, A., Giuliano, C. J., Palladino, A., John, K. M., Abramowicz, C., Yuan, M. Lou, Sausville, E. L., Lukow, D. A., Liu, L., Chait, A. R., Galluzzo, Z. C., Tucker, C., & Sheltzer, J. M. (2019). Off-target toxicity is a common mechanism of action of cancer drugs undergoing clinical trials. *Science Translational Medicine*, *11*(509). https://doi.org/10.1126/scitranslmed.aaw8412

Liu, Y., Ma, L., Chen, W. H., Park, H., Ke, Z., & Wang, B. (2013). Binding mechanism and synergetic effects of xanthone derivatives as noncompetitive α-glucosidase inhibitors: A theoretical and experimental study. *Journal of Physical Chemistry B*. https://doi.org/10.1021/jp4067235

Long, J., Song, J., Zhong, L., Liao, Y., Liu, L., & Li, X. (2019). Palmatine: A review of its pharmacology, toxicity and pharmacokinetics. *Biochimie*, *162*, 176–184. https://doi.org/10.1016/j.biochi.2019.04.008

Lund, J., Sato, A., Akira, S., Medzhitov, R., & Iwasaki, A. (2003). Toll-like receptor 9-mediated recognition of Herpes simplex virus-2 by plasmacytoid dendritic cells. *Journal of Experimental Medicine*. https://doi.org/10.1084/jem.20030162

Luo, Y., Li, S. C., Chou, M. Y., Li, Y. T., & Luo, M. (1998). The crystal structure of an intramolecular trans-sialidase with a NeuAcα2→3Gal specificity. *Structure*. https://doi.org/10.1016/S0969-2126(98)00053-7

MacAuley, M. S., Crocker, P. R., & Paulson, J. C. (2014). Siglec-mediated regulation of immune cell function in disease. In *Nature Reviews Immunology*. https://doi.org/10.1038/nri3737

Maekawa, T., Krauss, J. L., Abe, T., Jotwani, R., Triantafilou, M., Triantafilou, K., Hashim, A., Hoch, S., Curtis, M. A., Nussbaum, G., Lambris, J. D., & Hajishengallis, G. (2014). *Porphyromonas gingivalis* manipulates complement and TLR signaling to uncouple bacterial clearance from inflammation and promote dysbiosis. *Cell Host and Microbe*, *15*(6), 768–778. https://doi.org/10.1016/j.chom.2014.05.012

Malinowski, B., Węsierska, A., Zalewska, K., Sokołowska, M. M., Bursiewicz, W., Socha, M., Ozorowski, M., Pawlak-Osińska, K., & Wiciński, M. (2019). The role of *Tannerella forsythia*

and *Porphyromonas gingivalis* in pathogenesis of esophageal cancer. *Infectious Agents and Cancer*, *14*(1), 1–8. https://doi.org/10.1186/s13027-019-0220-2

Mantovani, A., Cassatella, M. A., Costantini, C., & Jaillon, S. (2011). Neutrophils in the activation and regulation of innate and adaptive immunity. In *Nature Reviews Immunology*. https://doi.org/10.1038/nri3024

Marsh, P. D., & Zaura, E. (2017). Dental biofilm: ecological interactions in health and disease. *Journal of Clinical Periodontology*, *44 Suppl 18*. https://doi.org/10.1111/jcpe.12679

McGuckin, M. A., Lindén, S. K., Sutton, P., & Florin, T. H. (2011). Mucin dynamics and enteric pathogens. *Nature Reviews Microbiology*. https://doi.org/10.1038/nrmicro2538

Medzhitov, R., Preston-Hurlburt, P., & Janeway, C. A. (1997). A human homologue of the Drosophila toll protein signals activation of adaptive immunity. *Nature*. https://doi.org/10.1038/41131

Megson, Z. A., Koerdt, A., Schuster, H., Ludwig, R., Janesch, B., Frey, A., Naylor, K., Wilson, I. B. H., Stafford, G. P., Messner, P., & Schäffer, C. (2015). Characterization of an α-L-fucosidase from the periodontal pathogen *Tannerella forsythia*. *Virulence*. https://doi.org/10.1080/21505594.2015.1010982

Meri, S., & Pangburn, M. K. (1990). A mechanism of activation of the alternative complement pathway by the classical pathway: protection of C3b from inactivation by covalent attachment to C4b. *European Journal of Immunology*. https://doi.org/10.1002/eji.1830201205

Mikuls, T. R., Payne, J. B., Yu, F., Thiele, G. M., Reynolds, R. J., Cannon, G. W., Markt, J., McGowan, D., Kerr, G. S., Redman, R. S., Reimold, A., Griffiths, G., Beatty, M., Gonzalez, S. M., Bergman, D. A., Hamilton, B. C., Erickson, A. R., Sokolove, J., Robinson, W. H., … O'Dell, J. R. (2014). Periodontitis and *Porphyromonas gingivalis* in patients with rheumatoid arthritis. *Arthritis and Rheumatology*. https://doi.org/10.1002/art.38348

Mira, A., Simon-Soro, A., & Curtis, M. A. (2017). Role of microbial communities in the pathogenesis of periodontal diseases and caries. *Journal of Clinical Periodontology*, *44*, S23–S38. https://doi.org/10.1111/jcpe.12671

Mishima, E., & Sharma, A. (2011). *Tannerella forsythia* invasion in oral epithelial cells requires phosphoinositide 3-Kinase activation and clathrin-mediated endocytosis. *Microbiology*. https://doi.org/10.1099/mic.0.048975-0

Miyagi, T. (2010). Mammalian sialidases and their functions. *Trends in Glycoscience and Glycotechnology*. https://doi.org/10.452/tigg.22.162

Monti, E., Bassi, M. T., Bresciani, R., Civini, S., Croci, G. L., Papini, N., Riboni, M., Zanchetti, G., Ballabio, A., Preti, A., Tettamanti, G., Venerando, B., & Borsani, G. (2004). Molecular cloning and characterization of NEU4, the fourth member of the human sialidase gene family. *Genomics*. https://doi.org/10.1016/j.ygeno.2003.08.019

Monti, Eugenio, Bonten, E., D'Azzo, A., Bresciani, R., Venerando, B., Borsani, G., Schauer, R., & Tettamanti, G. (2010). Sialidases in Vertebrates. A Family Of Enzymes Tailored For Several

Cell Functions. In *Advances in Carbohydrate Chemistry and Biochemistry*. https://doi.org/10.1016/S0065-2318(10)64007-3

Moustafa, I., Connaris, H., Taylor, M., Zaitsev, V., Wilson, J. C., Kiefel, M. J., Von Itzstein, M., & Taylor, G. (2004). Sialic acid recognition by *Vibrio cholerae* neuraminidase. *Journal of Biological Chemistry*. https://doi.org/10.1074/jbc.M404965200

Nagai T, Miyaichi Y, Tomimori T, Suzuki Y, Yamada H. (1990). Inhibition of influenza virus sialidase and anti-influenza virus activity by plant flavonoids. Chem Pharm Bull (Tokyo). 1990 May;38(5):1329-32. doi: 10.1248/cpb.38.1329. PMID: 2393958.

Nan, X., Carubelli, I., & Stamatos, N. M. (2007). Sialidase expression in activated human T lymphocytes influences production of IFN-γ. *Journal of Leukocyte Biology*. https://doi.org/10.1189/jlb.1105692

Newstead, S. L., Watson, J. N., Bennet, A. J., & Taylor, G. (2005). Galactose recognition by the carbohydrate-binding module of a bacterial sialidase. *Acta Crystallographica Section D: Biological Crystallography*. https://doi.org/10.1107/S0907444905026132

Newstead, S. L., Potter, J. A., Wilson, J. C., Xu, G., Chien, C. H., Watts, A. G., Withers, S. G., & Taylor, G. L. (2008). The structure of *Clostridium perfringens* NanI sialidase and its catalytic intermediates. *Journal of Biological Chemistry*. https://doi.org/10.1074/jbc.M710247200

Nisha, K. J., Suresh, A., Anilkumar, A., & Padmanabhan, S. (2018). MIP-1α and MCP-1 as salivary biomarkers in periodontal disease. *Saudi Dental Journal*, *30*(4), 292–298. https://doi.org/10.1016/j.sdentj.2018.07.002

Noris, M., & Remuzzi, G. (2013). Overview of complement activation and regulation. *Seminars in Nephrology*. https://doi.org/10.1016/j.semnephrol.2013.08.001

Parker, D., Soong, G., Planet, P., Brower, J., Ratner, A. J., & Prince, A. (2009). The NanA neuraminidase of *Streptococcus pneumoniae* is involved in biofilm formation. *Infection and Immunity*. https://doi.org/10.1128/IAI.00228-09

Paulson, J. C., MacAuley, M. S., & Kawasaki, N. (2012). Siglecs as sensors of self in innate and adaptive immune responses. In *Annals of the New York Academy of Sciences*. https://doi.org/10.1111/j.1749-6632.2011.06362.x

Philips, B. J., Coyle, C. H., Morrisroe, S. N., Chancellor, M. B., & Yoshimura, N. (2009). Induction of apoptosis in human bladder cancer cells by green tea catechins. *Biomedical Research*, *30*(4), 207–215. https://doi.org/10.2220/biomedres.30.207

Pillai, S., Netravali, I. A., Cariappa, A., & Mattoo, H. (2012). Siglecs and Immune Regulation. *Annual Review of Immunology*. https://doi.org/10.1146/annurev-immunol-020711-075018

Posch, G., Pabst, M., Brecker, L., Altmann, F., Messner, P., & Schäffer, C. (2011). Characterization and scope of S-layer protein O-glycosylation in *Tannerella forsythia*. *Journal of Biological Chemistry*. https://doi.org/10.1074/jbc.M111.284893

Pritchard, J. R., Bruno, P. M., Gilberta, L. A., Caprona, K. L., Lauffenburger, D. A., & Hemann, M. T. (2013). Defining principles of combination drug mechanisms of action. *Proceedings of the*

National Academy of Sciences of the United States of America, *110*(2). https://doi.org/10.1073/pnas.1210419110

Ram, S., Sharma, A. K., Simpson, S. D., Gulati, S., McQuillen, D. P., Pangburn, M. K., & Rice, P. A. (1998). A novel sialic acid binding site on factor H mediates serum resistance of sialylated *Neisseria gonorrhoeae*. *Journal of Experimental Medicine*. https://doi.org/10.1084/jem.187.5.743

Razani, B., & Lisanti, M. P. (2001). Caveolin-deficient mice: Insights into caveolar function and human disease. In *Journal of Clinical Investigation*. https://doi.org/10.1172/JCI200114611

Ricaldi, J. N., Matthias, M. A., Vinetz, J. M., & Lewis, A. L. (2012). Expression of sialic acids and other nonulosonic acids in *Leptospira. BMC Microbiology*. https://doi.org/10.1186/1471-2180-12-161

Richard A. McPherson (2022). Clinical Enzymology. *Henry's Clinical Diagnosis and Management by Laboratory Methods.*

Roy, S., Douglas, C. W. I., & Stafford, G. P. (2010). A novel sialic acid utilization and uptake system in the periodontal pathogen *Tannerella forsythia*. *Journal of Bacteriology*. https://doi.org/10.1128/JB.00079-10

Roy, S., Honma, K., Ian Douglas, C. W., Sharma, A., & Stafford, G. P. (2011). Role of sialidase in glycoprotein utilization by *Tannerella forsythia*. *Microbiology*, *157*(11), 3195–3202. https://doi.org/10.1099/mic.0.052498-0

Roy, S., Phansopa, C., Stafford, P., Honma, K., Douglas, C. W. I., Sharma, A., & Stafford, G. P. (2012). Beta-hexosaminidase activity of the oral pathogen *Tannerella forsythia* influences biofilm formation on glycoprotein substrates. *FEMS Immunology and Medical Microbiology*. https://doi.org/10.1111/j.1574-695X.2012.00933.x

Ruscitto, A., Hottmann, I., Stafford, G. P., Schäffer, C., Mayer, C., & Sharma, A. (2016). Identification of a novel N-acetylmuramic acid transporter in *Tannerella forsythia*. *Journal of Bacteriology*. https://doi.org/10.1128/JB.00473-16

Ryder, M. I. (2010). Comparison of neutrophil functions in aggressive and chronic periodontitis. *Periodontology 2000*, *53*(1), 124–137. https://doi.org/10.1111/j.1600-0757.2009.00327.x

Sakakibara, J., Nagano, K., Murakami, Y., Higuchi, N., Nakamura, H., Shimozato, K., & Yoshimura, F. (2007). Loss of adherence ability to human gingival epithelial cells in S-layer protein-deficient mutants of *Tannerella forsythensis*. *Microbiology*. https://doi.org/10.1099/mic.0.29275-0

Saleem, H. G. M., Seers, C. A., Sabri, A. N., & Reynolds, E. C. (2016). Dental plaque bacteria with reduced susceptibility to chlorhexidine are multidrug resistant. *BMC Microbiology*, *16*(1). https://doi.org/10.1186/s12866-016-0833-1

Satur, M. J., Urbanowicz, P. A., Spencer, D. I. R., Rafferty, J., & Stafford, G. P. (2022). Structural and functional characterisation of a stable, broad-specificity multimeric sialidase from the oral pathogen *Tannerella forsythia*. *The Biochemical Journal*, *479*(17), 1785–1806. https://doi.org/10.1042/BCJ20220244

Scannapieco, F. A., & Genco, R. J. (1999). Association of periodontal infections with atherosclerotic and pulmonary diseases. *Journal of Periodontal Research*. https://doi.org/10.1111/j.1600-0765.1999.tb02263.x

Schauer, R. (1985). Sialic acids and their role as biological masks. In *Trends in Biochemical Sciences*. https://doi.org/10.1016/0968-0004(85)90112-4

Schauer, R., & Kamerling, J. P. (2018). Exploration of the Sialic Acid World. In *Advances in Carbohydrate Chemistry and Biochemistry* (Vol. 75). https://doi.org/10.1016/bs.accb.2018.09.001

Schoenhofen, I. C., McNally, D. J., Brisson, J. R., & Logan, S. M. (2006). Elucidation of the CMP-pseudaminic acid pathway in *Helicobacter pylori*: Synthesis from UDP-N-acetylglucosamine by a single enzymatic reaction. *Glycobiology*. https://doi.org/10.1093/glycob/cwl010

Sekot, G., Posch, G., Messner, P., Matejka, M., Rausch-Fan, X., Andrukhov, O., & Schäffer, C. (2011). Potential of the *Tannerella forsythia* S-layer to delay the immune response. *Journal of Dental Research*. https://doi.org/10.1177/0022034510384622

Settem, R. P., Honma, K., Nakajima, T., Phansopa, C., Roy, S., Stafford, G. P., & Sharma, A. (2013). A bacterial glycan core linked to surface (S)-layer proteins modulates host immunity through Th17 suppression. *Mucosal Immunology*. https://doi.org/10.1038/mi.2012.85

Settem, R. P., Honma, K., Stafford, G. P., & Sharma, A. (2013). Protein-linked glycans in periodontal bacteria: prevalence and role at the immune interface. *Frontiers in Microbiology*, *4*(October), 1–6. https://doi.org/10.3389/fmicb.2013.00310

Severi, E., Hood, D. W., & Thomas, G. H. (2007). Sialic acid utilization by bacterial pathogens. In *Microbiology*. https://doi.org/10.1099/mic.0.2007/009480-0

Shen, B., Delaney, M. K., & Du, X. (2012). Inside-out, outside-in, and inside-outside-in: G protein signaling in integrin-mediated cell adhesion, spreading, and retraction. In *Current Opinion in Cell Biology*. https://doi.org/10.1016/j.ceb.2012.08.011

Shimizu, T., Ohtani, K., Hirakawa, H., Ohshima, K., Yamashita, A., Shiba, T., Ogasawara, N., Hattori, M., Kuhara, S., & Hayashi, H. (2002). Complete genome sequence of *Clostridium perfringens*, an anaerobic flesh-eater. *Proceedings of the National Academy of Sciences of the United States of America*. https://doi.org/10.1073/pnas.022493799

Silva, N., Abusleme, L., Bravo, D., Dutzan, N., Garcia-Sesnich, J., Vernal, R., Hernández, M., & Gamonal, J. (2015). Host response mechanisms in periodontal diseases. *Journal of Applied Oral Science*, *23*(3). https://doi.org/10.1590/1678-775720140259

Slack, T. J., Li, W., Shi, D., McArthur, J. B., Zhao, G., Li, Y., Xiao, A., Khedri, Z., Yu, H., Liu, Y., & Chen, X. (2018). Triazole-linked transition state analogs as selective inhibitors against *V. cholerae* sialidase. *Bioorganic and Medicinal Chemistry*. https://doi.org/10.1016/j.bmc.2018.10.028

Sochalska, M., & Potempa, J. (2017). Manipulation of Neutrophils by *Porphyromonas gingivalis* in the Development of Periodontitis. *Frontiers in Cellular and Infection Microbiology*, *7*. https://doi.org/10.3389/fcimb.2017.00197

Socransky, S. S., Haffajee, A. D., Cugini, M. A., Smith, C., & Kent, R. L. (1998). Microbial complexes in subgingival plaque. *Journal of Clinical Periodontology*. https://doi.org/10.1111/j.1600-051X.1998.tb02419.x

Sreedevi Chinthamani, Rajendra P Settem, Kiyonobu Honma, Graham P Stafford, Ashu Sharma. (2022). *Tannerella forsythia* strains differentially induce interferon gamma-induced protein 10 (IP-10) expression in macrophages due to lipopolysaccharide heterogeneity, *Pathogens and Disease*, Volume 80, Issue 1, 2022, ftac008, https://doi.org/10.1093/femspd/ftac008

Stafford, G., Roy, S., Honma, K., & Sharma, A. (2012). Sialic acid, periodontal pathogens and *Tannerella forsythia*: Stick around and enjoy the feast! In *Molecular Oral Microbiology*. https://doi.org/10.1111/j.2041-1014.2011.00630.x

Stamatos, N. M., Carubelli, I., van de Vlekkert, D., Bonten, E. J., Papini, N., Feng, C., Venerando, B., d'Azzo, A., Cross, A. S., Wang, L.-X., & Gomatos, P. J. (2010). LPS-induced cytokine production in human dendritic cells is regulated by sialidase activity. *Journal of Leukocyte Biology*. https://doi.org/10.1189/jlb.1209776

Stamatos, N. M., Curreli, S., Zella, D., & Cross, A. S. (2004). Desialylation of glycoconjugates on the surface of monocytes activates the extracellular signal-related kinases ERK 1/2 and results in enhanced production of specific cytokines. *Journal of leukocyte biology*, *75*(2), 307–313. https://doi.org/10.1189/jlb.0503241

Stamatos, N. M., Liang, F., Nan, X., Landry, K., Cross, A. S., Wang, L. X., & Pshezhetsky, A. V. (2005). Differential expression of endogenous sialidases of human monocytes during cellular differentiation into macrophages. *FEBS Journal*. https://doi.org/10.1111/j.1742-4658.2005.04679.x

Stathopoulou, P. G., Benakanakere, M. R., Galicia, J. C., & Kinane, D. F. (2010). Epithelial cell pro-inflammatory cytokine response differs across dental plaque bacterial species. *Journal of Clinical Periodontology*, *37*(1), 24–29. https://doi.org/10.1111/j.1600-051X.2009.01505.x

Stoddart, M. J. (2011). Cell viability assays: introduction. In *Methods in molecular biology (Clifton, N.J.)* (Vol. 740). https://doi.org/10.1007/978-1-61779-108-6_1

Streisinger, G., Walker, C., Dower, N., Knauber, D., & Singer, F. (1981). Production of clones of homozygous diploid zebra fish (Brachydanio rerio). *Nature*, *291*(5813), 293–296. https://doi.org/10.1038/291293a0

Sudhakara, P., Sellamuthu, I., & Aruni, A. W. (2019). Bacterial Sialoglycosidases in Virulence and Pathogenesis. *Pathogens*, *8*(1), 1–11. https://doi.org/10.3390/pathogens8010039

Sun, X. L., Kanie, Y., Guo, C. T., Kanie, O., Suzuki, Y., & Wong, C. H. (2000). Syntheses of C-3-modified sialylglycosides as selective inhibitors of influenza hemagglutinin and neuraminidase. *European Journal of Organic Chemistry*, *14*, 2643–2653. https://doi.org/10.1002/1099-0690(200007)2000:14<2643::aid-ejoc2643>3.0.co;2-1

Sun, J., Duffy, K. E., Ranjith-Kumar, C. T., Xiong, J., Lamb, R. J., Santos, J., Masarapu, H., Cunningham, M., Holzenburg, A., Sarisky, R. T., Mbow, M. L., & Kao, C. (2006). Structural and functional analyses of the human toll-like receptor 3: Role of glycosylation. *Journal of Biological Chemistry*. https://doi.org/10.1074/jbc.M510442200

Takahashi, N. (2015). Oral microbiome metabolism: From "who are they?" to "what are they doing?" In *Journal of Dental Research* (Vol. 94, Issue 12). https://doi.org/10.1177/0022034515606045

Tanner, M. E. (2005). The enzymes of sialic acid biosynthesis. In *Bioorganic Chemistry*. https://doi.org/10.1016/j.bioorg.2005.01.005

Telford, J. C., Yeung, J. H. F., Xu, G., Kiefel, M. J., Watts, A. G., Hader, S., Chan, J., Bennet, A. J., Moore, M. M., & Taylor, G. L. (2011). The *Aspergillus fumigatus* sialidase is a 3-deoxy-D-glycero-D-galacto-2- nonulosonic acid hydrolase (KDNase): Structural and mechanistic insights. *Journal of Biological Chemistry*, *286*(12), 10783–10792. https://doi.org/10.1074/jbc.M110.207043

Terrapon, N., Lombard, V., Drula, E., Coutinho, P. M., & Henrissat, B. (2017). The CAZy Database/the Carbohydrate-Active Enzyme (CAZy) Database: Principles and Usage Guidelines. In *A Practical Guide to Using Glycomics Databases*. https://doi.org/10.1007/978-4-431-56454-6_6

Teughels, W., Dhondt, R., Dekeyser, C., & Quirynen, M. (2014). Treatment of aggressive periodontitis. *Periodontology 2000*. https://doi.org/10.1111/prd.12020

Thakur, P., Chawla, R., Goel, R., Narula, A., Arora, R., & Sharma, R. K. (2016). Augmenting the potency of third-line antibiotics with *Berberis aristata*: In vitro synergistic activity against carbapenem-resistant *Escherichia coli. Journal of Global Antimicrobial Resistance*, *6*, 10–16. https://doi.org/10.1016/j.jgar.2016.01.015

Tomek, M. B., Maresch, D., Windwarder, M., Friedrich, V., Janesch, B., Fuchs, K., Neumann, L., Nimeth, I., Zwickl, N. F., Dohm, J. C., Everest-Dass, A., Kolarich, D., Himmelbauer, H., Altmann, F., & Schäffer, C. (2018). A general protein O-glycosylation gene cluster encodes the species-specific glycan of the oral pathogen *Tannerella forsythia*: O-glycan biosynthesis and immunological implications. *Frontiers in Microbiology*. https://doi.org/10.3389/fmicb.2018.02008

Traving, C., & Schauer, R. (1998). Structure, function and metabolism of sialic acids. In *Cellular and Molecular Life Sciences*. https://doi.org/10.1007/s000180050258

Tu, H. C., Chen, C. P., & Chan, W. H. (2010). Epicatechin gallate decreases the viability and subsequent embryonic development of mouse blastocysts. *Taiwanese Journal of Obstetrics and Gynecology*, *49*(2), 174–180. https://doi.org/10.1016/S1028-4559(10)60037-X

Turner, M. D., & Ship, J. A. (2007). Dry mouth and its effects on the oral health of elderly people. In *Journal of the American Dental Association*. https://doi.org/10.14219/jada.archive.2007.0358

Vajaria, B. N., Patel, K. R., Begum, R., & Patel, P. S. (2016). Sialylation: an Avenue to Target Cancer Cells. *Pathology oncology research : POR*, *22*(3), 443–447. https://doi.org/10.1007/s12253-015-0033-6

Vavricka, C. J., Muto, C., Hasunuma, T., Kimura, Y., Araki, M., Wu, Y., Gao, G. F., Ohrui, H., Izumi, M., & Kiyota, H. (2017). Synthesis of Sulfo-Sialic Acid Analogues: Potent

Neuraminidase Inhibitors in Regards to Anomeric Functionality. *Scientific Reports*. https://doi.org/10.1038/s41598-017-07836-y

Venkateswara, B., Sirisha, K., & Chava, V. K. (2011). Green tea extract for periodontal health. In *Journal of Indian Society of Periodontology*. https://doi.org/10.4103/0972-124X.82258

Vimr, E. R., Kalivoda, K. A., Deszo, E. L., & Steenbergen, S. M. (2004). Diversity of Microbial Sialic Acid Metabolism. *Microbiology and Molecular Biology Reviews*. https://doi.org/10.1128/mmbr.68.1.132-153.2004

Voigt, E. A., & Yin, J. (2015). Kinetic Differences and Synergistic Antiviral Effects Between Type I and Type III Interferon Signaling Indicate Pathway Independence. *Journal of Interferon and Cytokine Research*. https://doi.org/10.1089/jir.2015.0008

Wang, Q., Chang, B. J., & Riley, T. V. (2010). Erysipelothrix rhusiopathiae. *Veterinary Microbiology*, *140*(3–4), 405–417. https://doi.org/10.1016/j.vetmic.2009.08.012

Watts, A. G., Oppezzo, P., Withers, S. G., Alzari, P. M., & Buschiazzo, A. (2006). Structural and kinetic analysis of two covalent sialosyl-enzyme intermediates on Trypanosoma rangeli sialidase. *Journal of Biological Chemistry*, *281*(7), 4149–4155. https://doi.org/10.1074/jbc.M510677200

Wegner, N., Wait, R., Sroka, A., Eick, S., Nguyen, K. A., Lundberg, K., Kinloch, A., Culshaw, S., Potempa, J., & Venables, P. J. (2010). Peptidylarginine deiminase from *Porphyromonas gingivalis* citrullinates human fibrinogen and α-enolase: Implications for autoimmunity in rheumatoid Arthritis. *Arthritis and Rheumatism*. https://doi.org/10.1002/art.27552

Werts, C., Tapping, R. I., Mathison, J. C., Chuang, T. H., Kravchenko, V., Saint Girons, I., Haake, D. A., Godowski, P. J., Hayashi, F., Ozinsky, A., Underhill, D. M., Kirschning, C. J., Wagner, H., Aderem, A., Tobias, P. S., & Ulevitch, R. J. (2001). *Leptospiral* lipopolysaccharide activates cells through a TLR2-dependent mechanism. *Nature Immunology*. https://doi.org/10.1038/86354

Wu, Y., Li, J. Q., Kim, Y. J., Wu, J., Wang, Q., & Hao, Y. (2011). In vivo and in vitro antiviral effects of berberine on influenza virus. *Chinese Journal of Integrative Medicine*, *17*(6), 444–452. https://doi.org/10.1007/s11655-011-0640-3

Xu, W., Zhou, W., Wang, H., & Liang, S. (2020). Roles of *Porphyromonas gingivalis* and its virulence factors in periodontitis. *Advances in Protein Chemistry and Structural Biology*, *120*. https://doi.org/10.1016/bs.apcsb.2019.12.001

Yang, C. S., Maliakal, P., & Meng, X. (2002). Inhibition of carcinogenesis by tea. *Annu.Rev.Pharmacol.Toxicol.*

Ye, M., Fu, S., Pi, R., & He, F. (2009). Neuropharmacological and pharmacokinetic properties of berberine: a review of recent research. *Journal of Pharmacy and Pharmacology*, *61*(7), 831–837. https://doi.org/10.1211/jpp/61.07.0001

Yilmaz, Ö., Watanabe, K., & Lamont, R. J. (2002). Involvement of integrins in fimbriae-mediated binding and invasion by *Porphyromonas gingivalis*. *Cellular Microbiology*. https://doi.org/10.1046/j.1462-5822.2002.00192.x

Yu, S., Fan, J., Liu, L., Zhang, L., Wang, S., & Zhang, J. (2013). Caveolin-1 up-regulates integrin α2,6-sialylation to promote integrin α5β1-dependent hepatocarcinoma cell adhesion. *FEBS Letters*. https://doi.org/10.1016/j.febslet.2013.02.002

Yuk, J. M., & Jo, E. K. (2011). Toll-like receptors and innate immunity. In *Journal of Bacteriology and Virology*. https://doi.org/10.4167/jbv.2011.41.4.225

Zaric, S. S., Lappin, M. J., Fulton, C. R., Lundy, F. T., Coulter, W. A., & Irwin, C. R. (2017). Sialylation of *Porphyromonas gingivalis* LPS and its effect on bacterial-host interactions. *Innate Immunity*. https://doi.org/10.1177/1753425917694245

Zenobia, C., & Hajishengallis, G. (2015). *Porphyromonas gingivalis* virulence factors involved in subversion of leukocytes and microbial dysbiosis. In *Virulence* (Vol. 6, Issue 3). https://doi.org/10.1080/21505594.2014.999567

Zhang, L., Li, J., Ma, F., Yao, S., Li, N., Wang, J., Wang, Y., Wang, X., & Yao, Q. (2012). Synthesis and cytotoxicity evaluation of 13-n-alkyl berberine and palmatine analogues as anticancer agents. *Molecules*, *17*(10), 11294–11302. https://doi.org/10.3390/molecules171011294

Zhang, M. Y., Yu, Y. Y., Wang, S. F., Zhang, Q., Wu, H. W., Wei, J. Y., Yang, W., Li, S. Y., & Yang, H. J. (2018). Cardiotoxicity evaluation of nine alkaloids from rhizoma coptis. *Human and Experimental Toxicology*, *37*(2), 185–195. https://doi.org/10.1177/0960327117695633

Zhong, Y., Slade, G. D., Beck, J. D., & Offenbacher, S. (2007). Gingival crevicular fluid interleukin-1β, prostaglandin E2 and periodontal status in a community population. *Journal of Clinical Periodontology*, *34*(4), 285–293. https://doi.org/10.1111/j.1600-051X.2007.01057.x
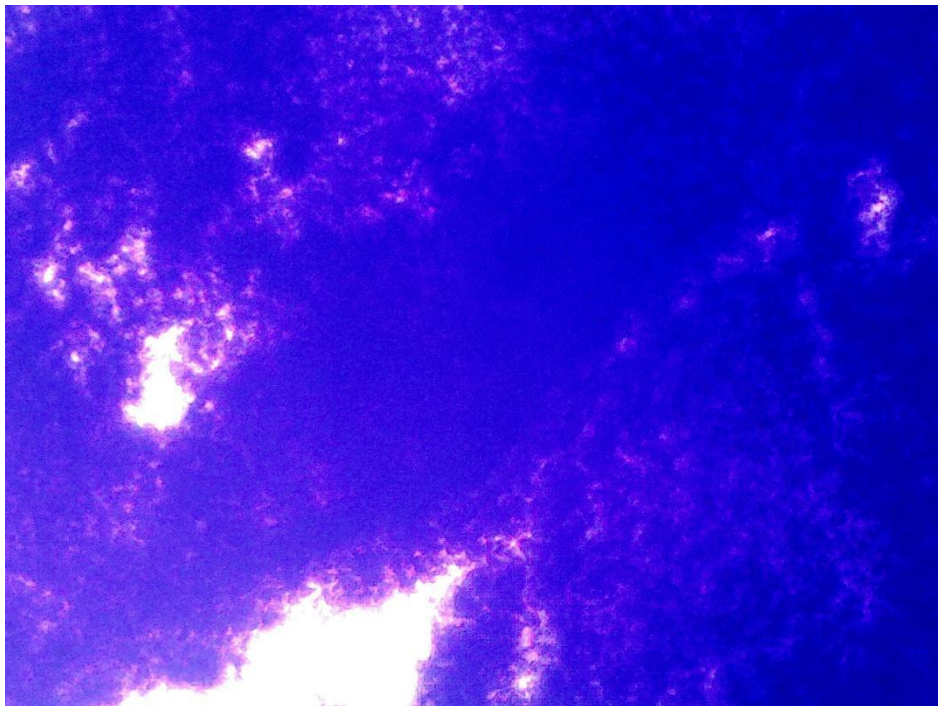
Appendices

Appendix 1: *Tannerella forsythia* **43037 growing on fastidious anaerobe (FA) plate supplemented with N-Acetylmuramic acid (NAM)**
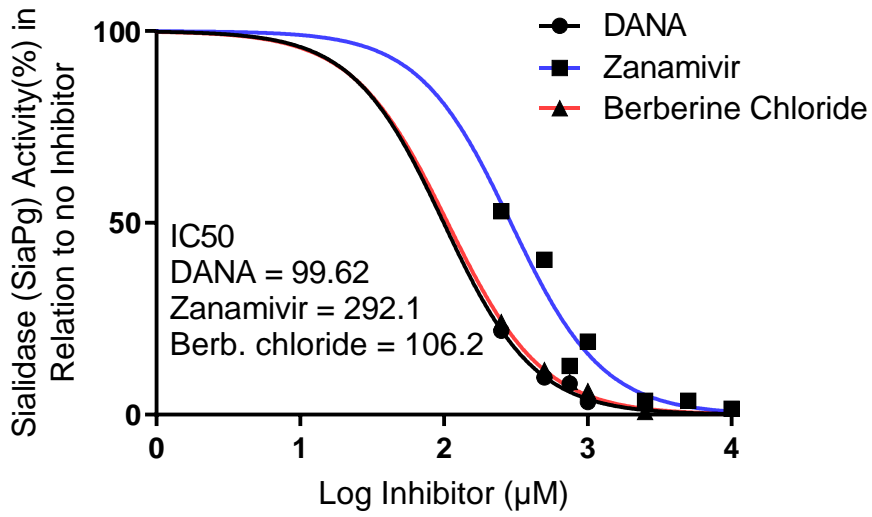

Appendix 2: *Porphyromonas gingivalis* **0381 growing on fastidious anaerobe (FA) plate**
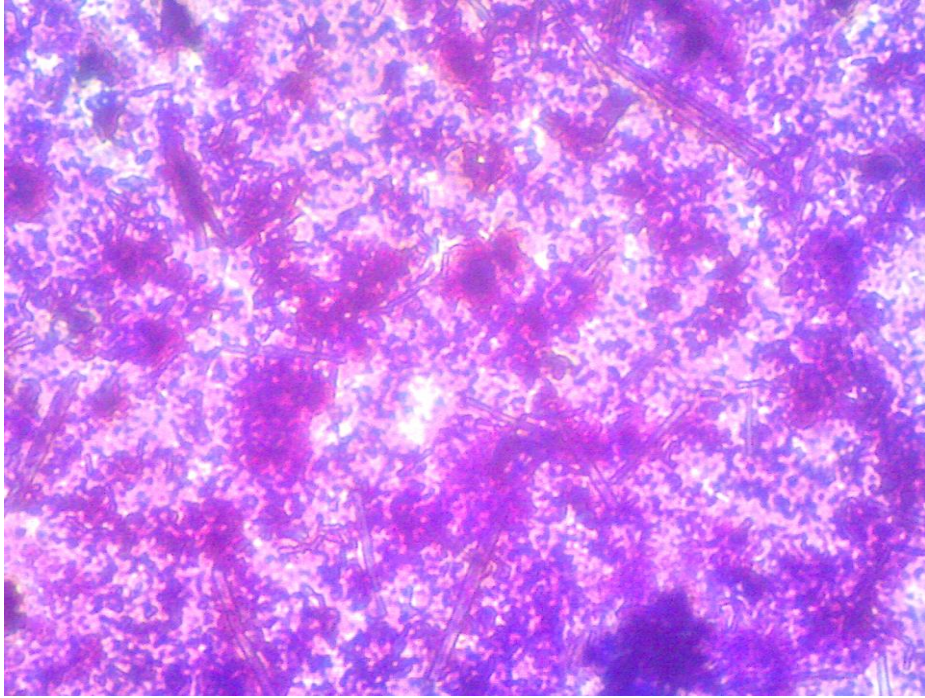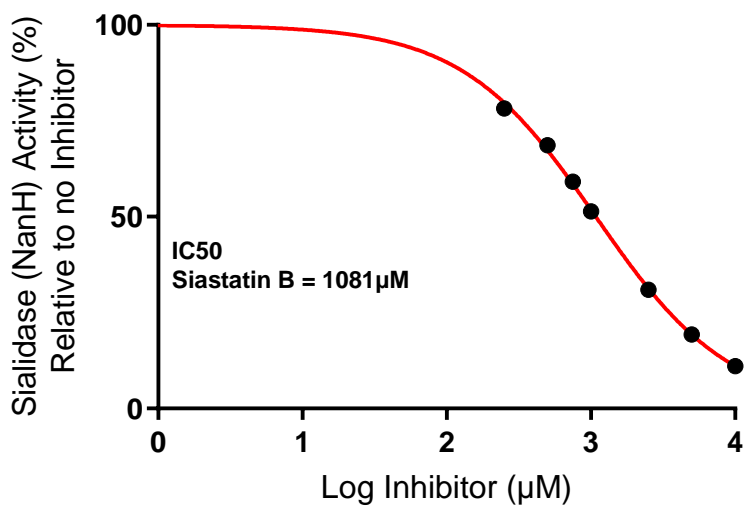
Appendix 3a: Wild type (Pg0381) Biofilm as seen under ToupView Digital Microscope
Camera SCMOS02000KPA

Appendix 3b: Mutant strain (ΔPg0381) Biofilm as seen under ToupView Digital Microscope
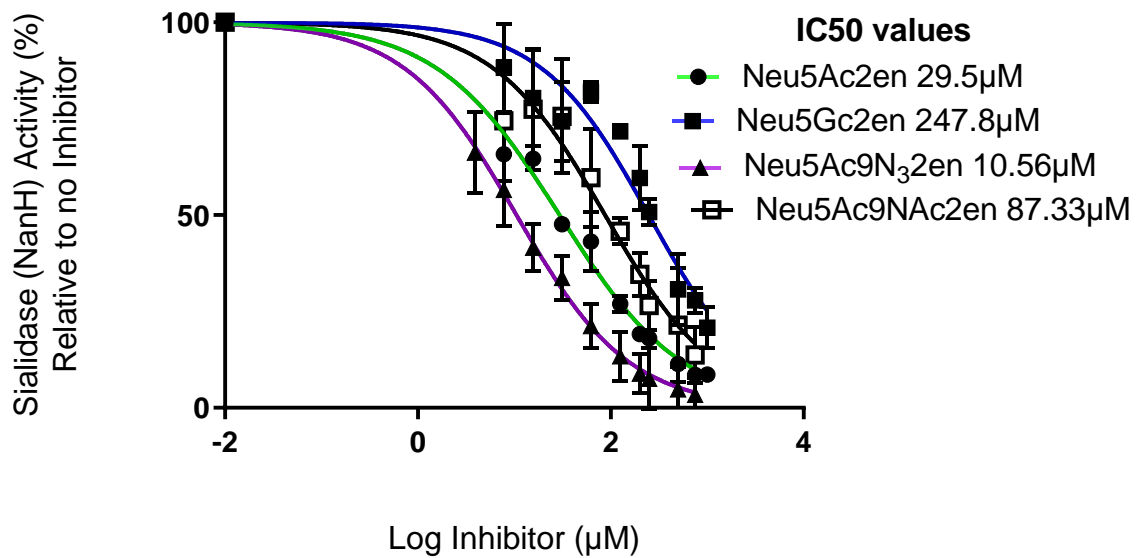Camera SCMOS02000KPA

Appendix4: Log[Inhibitor] against Percentage of sialidase (SiaPg) Activity

Appendix5: Log[Siastatin B] against Percentage of sialidase (NanH) Activity

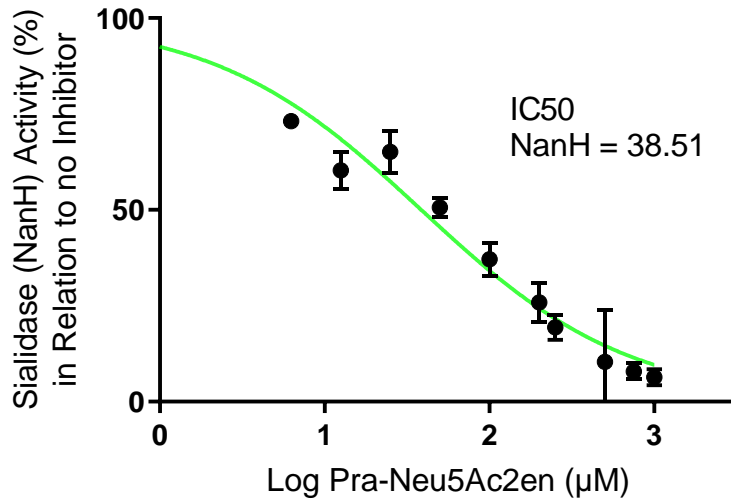**Appendix6: Log[Inhibitor] against Percentage of sialidase (NanH) Activity**
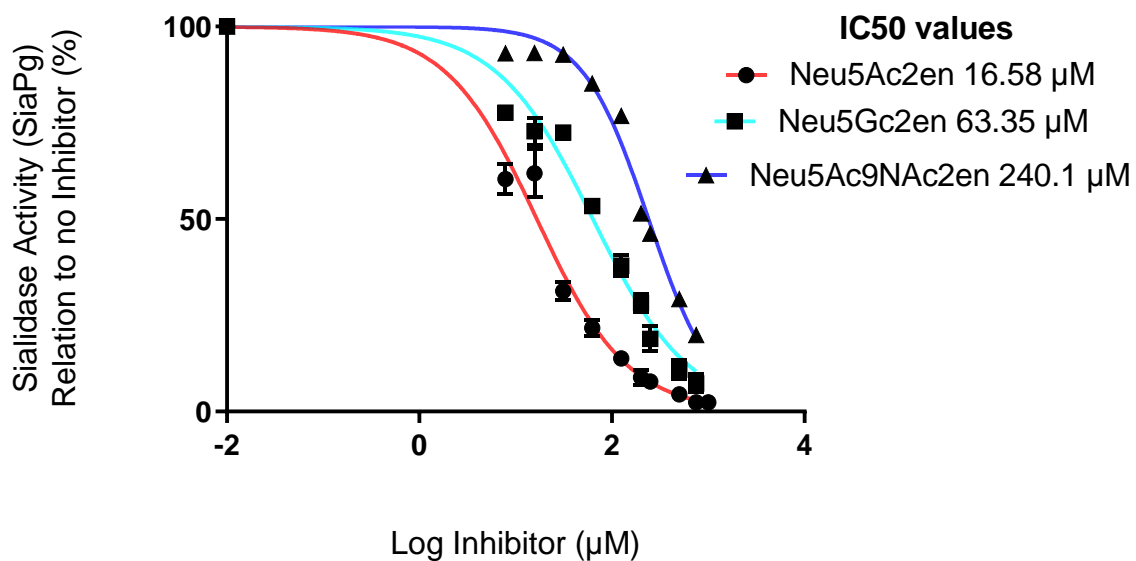
Appendix7: Log[Inhibitor] against Percentage of sialidase (SiaPg) Activity
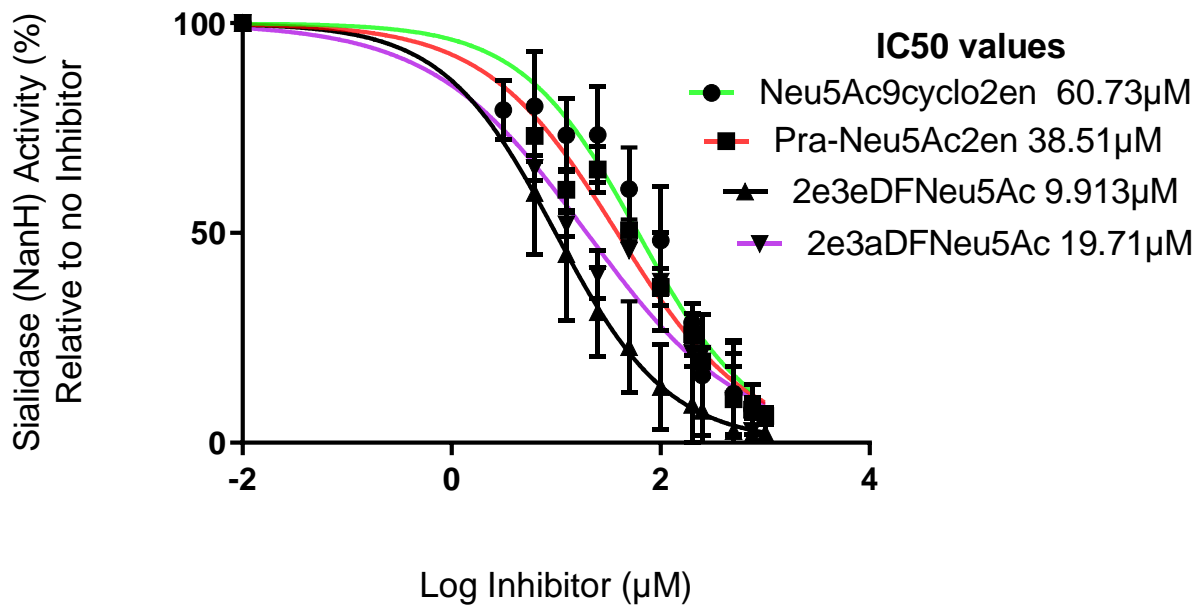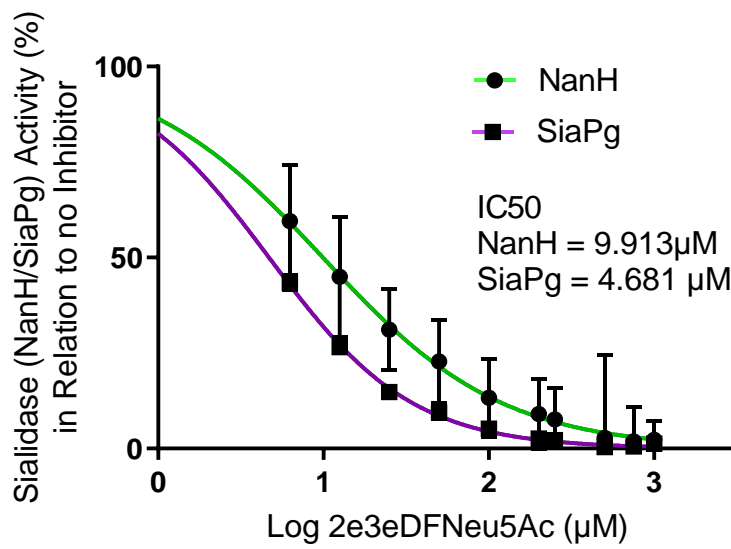
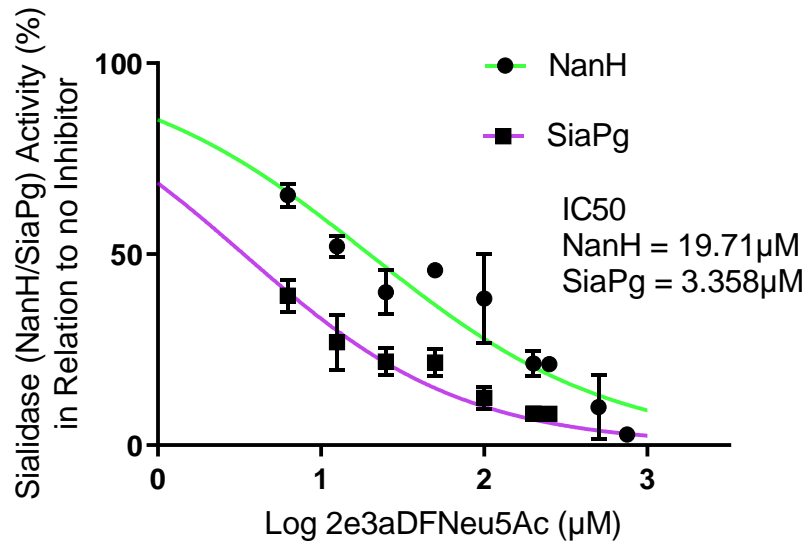**Appendix8: Log[Inhibitor] against Percentage of sialidase (NanH) Activity**
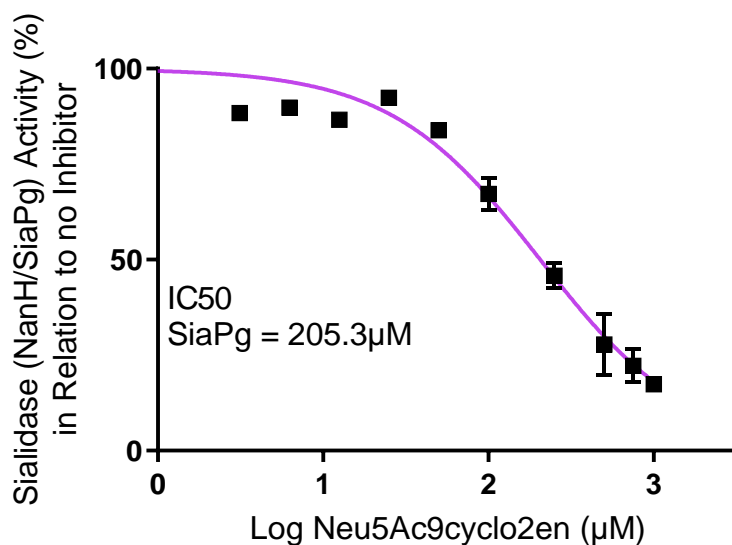
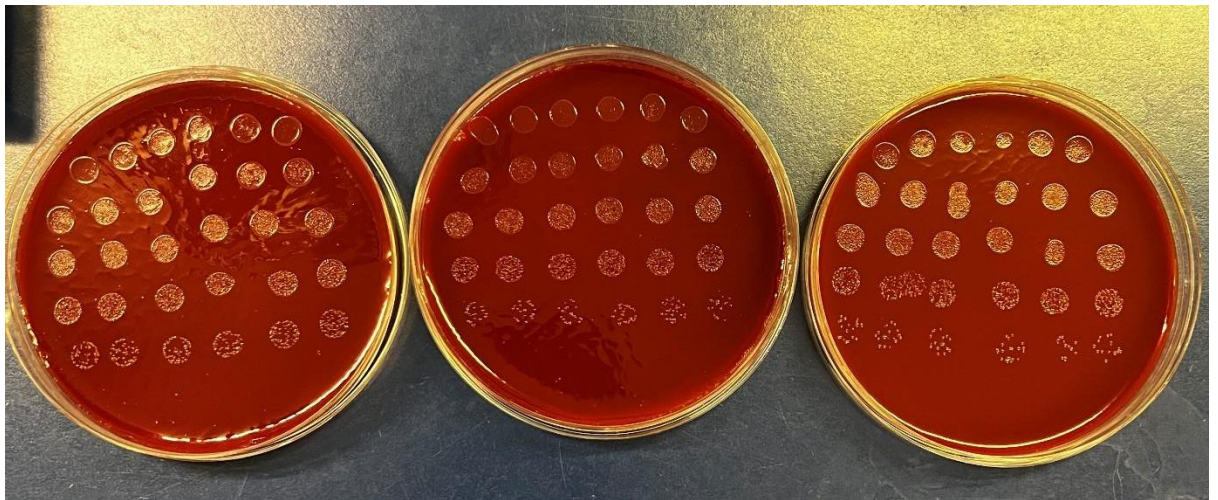**Appendix 9: Log[Inhibitor] against Percentage of sialidase (NanH/SiaPg) Activity**

Appendix10: Log[Inhibitor] against Percentage of sialidase (NanH) Activity

Appendix11: Log[Inhibitor] against Percentage of sialidase (NanH/SiaPg) Activity

Appendix12: Log[Inhibitor] against Percentage of sialidase (NanH/SiaPg) Activity

Appendix13: Antibiotic Protection Assay (plate layout = Viability, Total association and Invasion) + 1 μM 2e3aDFNeu5Ac9N3